the work of the

Rutherford Laboratory

1974

Swindon Press Ltd., Swindon, Wiltshire.

THE WORK OF THE RUTHERFORD LABORATORY IN 1974

Edited by
J R Smith and F M Telling

Science Research Council
Rutherford Laboratory
Chilton Didcot OX11 0QX
May 1975

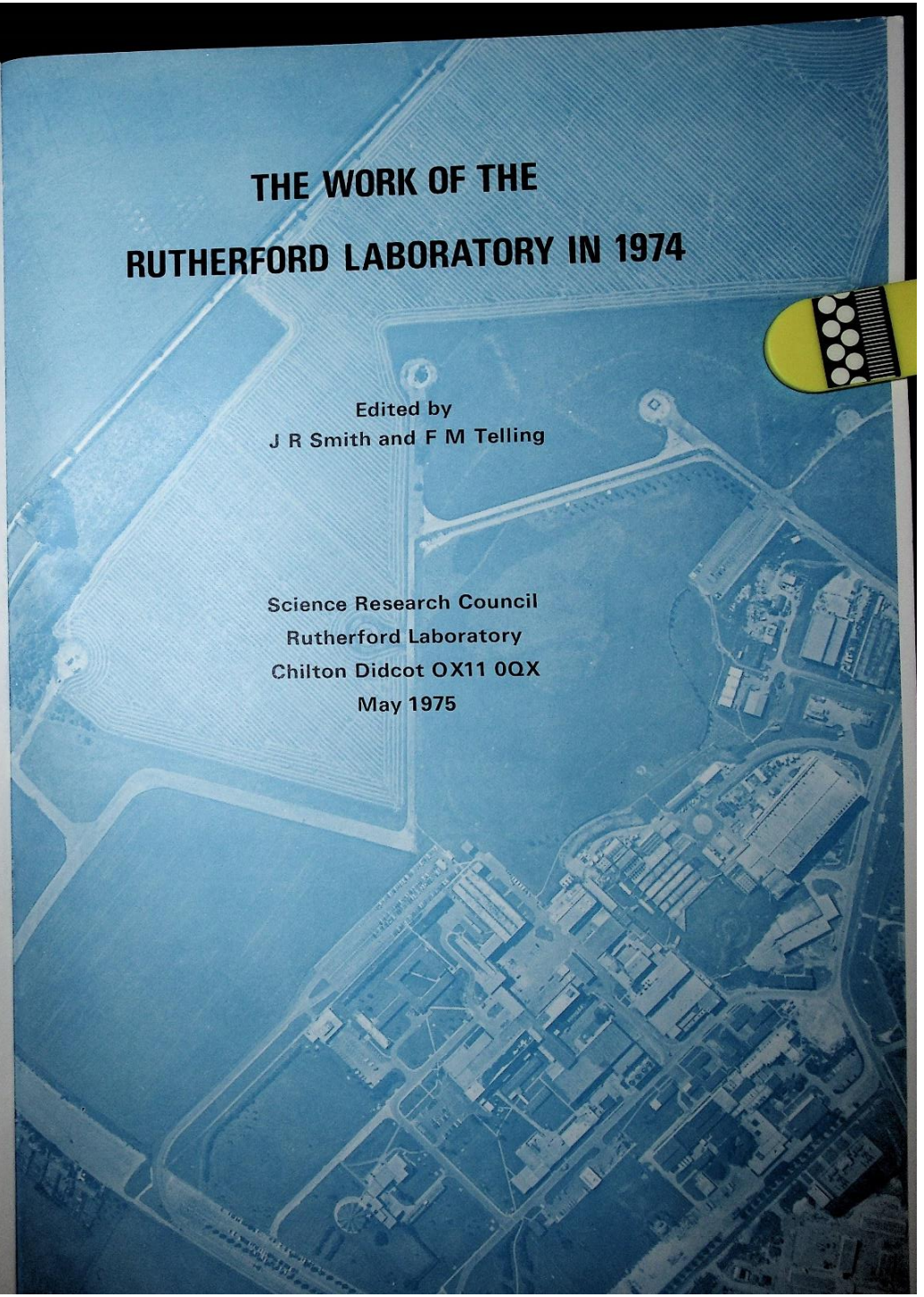

The Rutherford Laboratory was established in 1957 as the first Laboratory of the National Institute for Research in Nuclear Science to build and operate, for the common use by university scientists, that equipment which was required for the conduct of research in the nuclear sciences and which by its scale or cost was beyond the resources normally available to individual universities. In 1965 the Laboratory became part of the Science Research Council retaining a similar principal role.

Research programmes in particle physics, nuclear physics and radiobiology are based on the accelerator Nimrod, an 8 GeV proton synchrotron in the Laboratory. High energy physics experiments are also carried out at international research centres, particularly at CERN in Geneva. Other fields of research at the Laboratory include theoretical physics, accelerator physics and branches of experimental physics which may have relevance to the long-term development of high energy physics.

A Neutron Beam Research Unit was established at the Laboratory in 1971 to support the community of scientists who use neutrons generated in nuclear reactors as their principal research tool. The main European centre for this work is at the Institut Laue-Langevin in Grenoble.

The research and development programmes are supported by a computing system based on an IBM 370/195 computer which serves the requirements of the nuclear physicists and neutron beam users and also selected users in other fields.

There are 1160 staff employed by the Laboratory and 250 scientists in universities are associated with the nuclear physics programme. About 170 university scientists are involved in the SRC supported neutron beam research programme.

Contents

Laboratory Organisation (December 1974)

DIRECTOR: G. H. STAFFORD

ADMINISTRATION DIVISION
Personnel, finance, general and scientific administration.
DIVISION HEAD & LABORATORY SECRETARY: J. M. VALENTINE

APPLIED PHYSICS DIVISION
Superconducting magnet studies; magnet design; development of polarized targets; rapid cycling bubble chamber studies.
DIVISION HEAD: D. B. THOMAS

COMPUTING & AUTOMATION DIVISION
Operation and development of the central computer (IBM 370/195) and satellite computer system; computer applications for bubble chamber and spark chamber film analysis.
DIVISION HEAD: W. WALKINSHAW

ENGINEERING DIVISION
Design and manufacture of equipment for nuclear and applied physics research; department of engineering science; mechanical, electrical and building services; chemical technology; safety services.
DIVISION HEAD & CHIEF ENGINEER: P. J. BOWLES

ELECTRON PROTON INTERSECTING COMPLEX (EPIC) PROJECT
G. MANNING D.A. GRAY

HIGH ENERGY PHYSICS DIVISION
Experiments in particle physics and nuclear physics in collaboration with university groups; nuclear electronics.
DIVISION HEAD & DEPUTY DIRECTOR: G. MANNING

HIGH POWER LASER PROJECT
L. C. W. HOBBIS

NEUTRON BEAM RESEARCH UNIT
Support of research by universities using UK reactors and the reactor at the Institut Laue-Langevin, Grenoble; development of new instruments and techniques; study of new neutron sources; participation in experiments.
HEAD OF UNIT: L. C. W. HOBBIS

NIMROD DIVISION
Operation and development of Nimrod (8 GeV proton synchrotron accelerator); accelerator design; experimental area management; development of beam line components and cryogenic targets; radiation protection.
DIVISION HEAD: G. N. VENN

THEORY DIVISION
Studies in theoretical particle physics
DIVISION HEAD: R. J. N. PHILLIPS

HIGH ENERGY PHYSICS

Experimental Hall 3 of the Proton Synchrotron complex at the Rutherford Laboratory showing the experimental apparatus of K15A beam line (18773)

1. High Energy Physics

1974 has been a vintage year for high energy physics.

Particular experimental highlights have been the further verification of the discovery of a completely new class of weak interaction apparently mediated by a neutral current, the observation of a spectacular failure of simple quark-model predictions in electron-positron annihilation processes, and finally the dramatic discovery of the ψ (or J) particles. It is noteworthy that all three major discoveries were made by studying interactions involving leptons (electrons, muons or neutrinos). Leptons are proving to be particularly powerful probes of the structure of matter because their interactions are relatively simple and well understood, being mediated by the weak and electromagnetic currents acting (usually) at a single point.

Theoretically, great progress is continuing to be made in understanding and applying the unique properties of non-Abelian gauge theories. In consequence, it is becoming increasingly apparent that all the phenomenologically disparate "fundamental" interactions observed to occur between elementary particles (i.e. the strong, electromagnetic, weak and superweak interactions) may be describable by a single unified gauge theory. Such a unification would be comparable to the unification of electricity magnetism and optics in Maxwell's equations in the last century.

The first steps taken towards unification stemmed from the need to construct a renormalisable theory of weak interactions (i.e. a theory in which all processes are calculable with only a finite number of arbitrary constants and the divergences and violations of unitarity afflicting the standard theory are avoided). This was found to be possible within the framework of non-Abelian gauge theories. Because the existence of $W^{\pm}$ bosons (the supposed mediators of the weak interaction) created difficulties in the calculation of purely electromagnetic processes, it was natural in these theories to describe weak and electromagnetic processes in a unified way. In order to maintain their renormalisability, all such theories required the existence of either (i) a neutral W^{o} boson (in addition to the $W^{\pm}$ bosons) and therefore the existence of neutral current processes, or (ii) heavy leptons or (iii) both. The original Salam-Weinberg theory was unique in requiring only neutral currents.

There is no experimental evidence for heavy leptons, on which current neutrino experiments at FNAL are imposing increasingly stringent mass limits. The absence of neutral currents in strangeness-changing processes (e.g. K-meson decay) was exceedingly well established experimentally. This had led to a general expectation that no neutral currents existed even though stringent experimental tests in strangeness-conserving weak processes were extremely difficult. The unexpected experimental observation of strangeness-conserving neutral currents in neutrino reactions at a level in approximate agreement with the Salam-Weinberg theory, therefore caused great excitement and gave much additional impetus to this line of theoretical work.

In gauge theories, the absence of neutral currents in strangeness-changing processes requires changes to the simple quark model. This model is one of the main bases of our present understanding of the structure of hadrons (strongly interacting particles). The entire spectrum of hadron states currently known, excepting the recently discovered ψ particles, appears to be characterised by an approximate SU(3) group symmetry possibly corresponding to a basic structure of three different kinds of constituent (just as the SU(2) isospin symmetry characteristic of nuclear states corresponds to a basic structure of neutrons and protons). These three hypothetical basic constituents, each carrying spin ½ and (in the simplest model) fractional electric charge, are known as the n, p and λ "quarks". This simple three-quark model, despite fundamental paradoxes in its simplest formulation analogous to those in the original Bohr model of the atom, has had very remarkable success in correlating and predicting hadron properties. However it completely fails to account for the absence of neutral currents in strangeness-changing reactions. The simplest explanation requires the existence of a fourth type of quark, the p' or c quark carrying the additional quantum number of "charm".

Experiments on the highly inelastic scattering of leptons off nucleons clearly established the existence of point-like entities within the nucleon (in a manner analogous to the demonstration of the existence of heavy point-like nucleons inside the atom by Rutherford's classic experiment on the scattering of α-particles by a thin foil). These entities were christened "partons". Most recent and detailed results from such experiments are in impressive agreement with the hypothesis that these partons are in fact quarks.

It is paradoxical that in deep inelastic scattering experiments it appears that the basic constituents of strongly interacting particles behave like free point-like objects that do not interact with each other, particularly since they apparently never emerge as free particles. Non-Abelian gauge theories of the strong interaction, in which quark-quark interactions are mediated by massive vector "gluons", are apparently unique in possessing the property of "asymptotic freedom" necessary to explain this paradox – namely the property that the quark-quark interaction is very weak at close distances of approach but grows without limit as the quarks separate. This strongly suggests that gauge theoretical ideas should be extended to encompass the strong as well as the weak and electromagnetic interactions. This extension also appears necessary in order to preserve the renormalisability of even the weak interactions alone, in the presence of strong interactions.

Asymptotically free gauge theories predict small but characteristic deviations from the scaling predictions of the naive quark-parton model. Some preliminary experimental indications of such deviations were presented at the London Conference (July 1974). However the most characteristic effects are predicted to occur only at still higher energies than are currently available.

The great success of the quark-parton model predictions for inelastic lepton scattering contrasts strongly with their spectacular failure in the time-like four-momentum transfer region where an electron and positron annihilate into hadrons. Experiments recently performed at the CEA and SPEAR storage rings have shown that the $e^{+}e^{-}$ annihilation cross-section into hadrons is roughly constant instead of decreasing like $(\text{energy})^{-2}$ as predicted. There were equally spectacular theories proposed to explain this result, for example that leptons may acquire strong interactions at high energy or that quarks may carry additional as-yet-undetected quantum numbers and that in these experiments one is producing the new states of hadronic matter carrying them.

In fact there already existed very strong theoretical reasons for introducing new quark quantum numbers. That for introducing a fourth "charmed" quark has already been mentioned. The hypothesis that each of the three of four quarks exists in three different versions differing only by the (so far unobserved) quantum number of "colour" would explain several fundamental difficulties present in the simplest quark model of hadron structure. If these quantum numbers exist, there should be families of "charmed" and "coloured" hadrons with higher masses than the hadrons presently known. These would be unable to decay into "normal" hadrons via strong interactions. Consequently the least massive should have very narrow widths. The search for such states has therefore become a very important area for experimental investigation.

The new J or ψ particles discovered at Brookhaven and SPEAR at the end of 1974 do indeed have large masses and widths some two orders of magnitude narrower than one would expect for particles decaying via the strong interaction. At the time of writing, their most likely interpretation is that they are uncharmed vector mesons formed exclusively from charmed quarks. In that case a number of narrow charmed mesons decaying only via the weak interaction should exist with masses near 2 GeV. The latest report of a third ψ particle with a still higher mass of 4·1 GeV but a broad width, possibly decaying into such mesons, is consistent with this. Whether this particular interpretation is correct or not, it seems clear that a new form of matter has been discovered whose existence should hopefully shed light on a number of puzzles and paradoxes in our present theoretical understanding.

More experimental information, particularly from the electron-positron storage rings and from lepton-nucleon scattering experiments at FNAL and the CERN SPS, is eagerly awaited. Current theoretical ideas show exceptional promise but still involve an uncomfortably large number of as yet undetected objects (W-bosons, coloured and charmed hadron states, gluons etc). This remains true even if the ψ particles prove to be the first direct signal that some of these objects exist. Much experimental work clearly remains to be done in order to test these theoretical ideas thoroughly and allow the details to be filled in. It also seems increasingly clear that only the continued study of lepton-lepton and lepton-hadron collisions to higher energies than are currently available is likely to yield unambiguous answers to many of the presently outstanding questions. The situation augurs well for the fruitfulness of the physics programme that could be mounted at a machine such as the proposed electron-positron intersecting complex EPIC.

Electronics Experiments

29 experiments in all stages of progress from accepted proposals to practically completed experiments are reported in the following pages. The break down of this total into subject matter is approximately as follows:–

8 experiments on meson spectroscopy
6 experiments on baryon spectroscopy
1 quark search
4 experiments studying medium energy production mechanisms
6 experiments studying very high energy hadron interactions at the ISR or SPS
4 experiments studying weak or electro-magnetic interactions.

The predominance of spectroscopy experiments, though traditionally a strong field for this Laboratory, is slightly surprising in these days of 400 GeV physics. However, somewhat paradoxically, the study of low mass meson resonances is easier at high beam energies and two of the experiments proposed for the SPS are mainly concerned with this subject. The recent discovery of the narrow high mass states has added a further impetus to spectroscopy which has already recently passed through an extremely fruitful period with the great success of the $SU(6)_W$ symmetry scheme and the qualified success of the harmonic oscillator quark model. It is clear that whatever refinements in the way of charm etc. are required by the new discoveries these will remain as approximate descriptions of the low lying hadron states. The new data provided by the experiments described below on the inelastic and strange formation channels and on meson resonances will provide vital checks on these schemes.

Medium energy experiments are today more like the traditional formation experiments in that they are becoming detailed very high statistics studies of the production amplitudes for two body processes as a function of s and t. It is only by studying the amplitudes rather than the experimental observables, which are bi-linear combinations of the amplitudes, that detailed insight into the points of agreement and disagreement of the Regge description of two body scattering can be obtained and the reasons for the failure of this generally extremely successful model of particle interactions determined.

In the high energy region the emphasis of our experiments is on the study of the substructure of the hadrons either by probing them with the short range weak or electromagnetic interactions (ν or μ induced processes) or in the case of hadron-hadron interactions by studying the high transverse momentum phenomena which originate from highly localised processes. Present results show that hadrons seem to be made up of localised quark-like objects, providing a very satisfying link with the low energy region where the resonance spectrum also points to quark-like constituents.

Electronics Experiments

Experiment Number	Proposal Number	Title	Collaboration
Meson Resonances			
1	88	A study of neutral bosons using a neutron time-of-flight trigger	University of Birmingham Tel Aviv University Westfield College, London Rutherford Laboratory
2	75	Differential cross-sections for 2-body $\bar{p}p$ interactions	Queen Mary College, London University of Liverpool Daresbury Laboratory Rutherford Laboratory
3	103	Polarisation measurements for 2-body $\bar{p}p$ interactions	Queen Mary College, London Daresbury Laboratory Rutherford Laboratory
4	50, 99, 110, 128	Meson production cross-sections near threshold	Imperial College, London University of Southampton
5	145	Study of exclusive reactions in πp and Kp interactions in the energy range up to 100 GeV	CERN Max Planck Institute, Munich University of Amsterdam University of Oxford Rutherford Laboratory
6	93	Study of non-diffractive production of S=1 neutral resonances	University of Rome Rutherford Laboratory
7	142	K^+ interaction trigger experiment in the Omega spectrometer	DESY University of Birmingham University of Glasgow
8	158	Study of meson resonances decaying into strange particles in the Omega spectrometer at the SPS	University of Birmingham
Baryon Resonances			
9	43, 83, 105 120	$K^+, \bar{n}, \pi^-, K^-$-p elastic scattering differential cross-sections	University of Bristol University of Southampton Rutherford Laboratory
10	95	Coherent production of I=½ baryon states on helium	CERN University College, London University of Uppsala Rutherford Laboratory
11	81, 101	Differential cross-section and polarisation measurements in the charge exchange reactions $\pi^-p \to \pi^\circ n$ and $\eta^\circ n$	Rutherford Laboratory
12	87, 114	Differential cross-sections and polarisation in the reaction $\pi^-p \to K^\circ\Lambda$	University of Cambridge Rutherford Laboratory
13	73	$K^\pm n$ elastic and K^+n charge exchange differential cross-sections below 1 GeV/c	University of Birmingham Rutherford Laboratory
14	136	Polarisation in KN interactions	Queen Mary College, London Rutherford Laboratory
Quark Search			
15	144	Heavy particle experiment	University College, London AWRE Rutherford Laboratory

Experiment Number	Proposal Number	Title	Collaboration
Medium Energy Production Mechanisms			
16	126, 150	Study of exchange mechanisms in quasi two body final states in the RMS facility	University of Edinburgh Westfield College, London Rutherford Laboratory
17	100	Differential cross-sections and polarisations in the reactions $\pi^+ p \rightarrow K^+ \Sigma^+$ $K^- p \rightarrow \pi^- \Sigma^+$	University of Birmingham University of Genova University of Stockholm CERN Rutherford Laboratory
18	124	Spin rotation parameters in $\pi^- p \rightarrow K^0 \Lambda$	Imperial College, London University of Southampton ETH – Zurich CERN University of Helsinki
19	112	Spin dependence of inclusive reactions and low cross-section pp elastic scattering	CERN University of Paris-Sud University of Oxford
High Energy Experiments			
20	151	Study of exclusive hadronic processes at large p_T	CERN University College, London University of Genova University of Oslo University of Paris-Sud
21	129	Study of high transverse momentum behaviour at the ISR	University of Liverpool Daresbury Laboratory Rutherford Laboratory
22	130	Study of high transverse momentum phenoma in the Split Field Magnet at the ISR	University of Liverpool University of Paris-Sud Scandinavian Universities
23	72	Study of particles produced at large angles at the ISR	University of Bristol University of Liverpool University College, London Rutherford Laboratory University of Bergen University of Lund University of Copenhagen University of Stockholm CERN
24	131	Study of inclusive particle production at very low p_T and x=0	CERN University College, London University of Bristol Massachusetts Inst. Tech. Niels Bohr Institute University of Stockholm
25	146	ISR Solenoid experiment to study electron production	CERN Columbia University Rockefeller University University of Oxford
Weak and Electromagnetic Interactions			
26	141	Neutrino experiments at the SPS	CERN University of Hamburg University of Karlsruhe University of Oxford Westfield College, London Rutherford Laboratory
27	96	Muon-nucleon scattering	University of Chicago Harvard University University of Illinois University of Oxford
28	76	Search for C-violating decay $\eta \rightarrow \pi^0 e^+ e^-$	Westfield College, London Rutherford University
29	140	Experiments with high energy charged hyperons at the SPS	University of Bristol University of Geneva University of Heidelberg University of Lausanne Lab de l'Acc. Lin., Orsay Rutherford Laboratory CRN., Strasbourg-Cronenburg

EXPERIMENT 1

A study of neutral bosons using a neutron time of flight trigger

University of Birmingham
Tel Aviv University
Westfield College, London
Rutherford Laboratory

This experiment is studying the process

$$\pi^- + p \rightarrow n + X^0$$

using the Omega spectrometer facility at CERN. The charged decay products of X^0 are detected in the Omega spark chamber system. The neutron is detected in an array of scintillation counters and its time of flight measured. The angular acceptance of the neutron counter in the laboratory and the limits imposed on the time of flight lead to an acceptance for X^0 as shown in Fig. 1.1. Neutrons below 10 MeV are not detected and this produces our cut in t (4-momentum transfer squared between p and n) of 0·02 $(GeV/c^2)^2$.

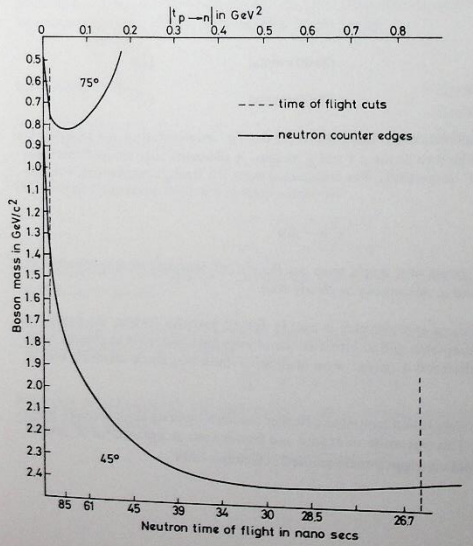

Figure 1.1. Plot of acceptance for neutral bosons determined by the angular acceptance of the neutron detector and limits imposed on the neutron time of flight: Experiment 1 (18556)

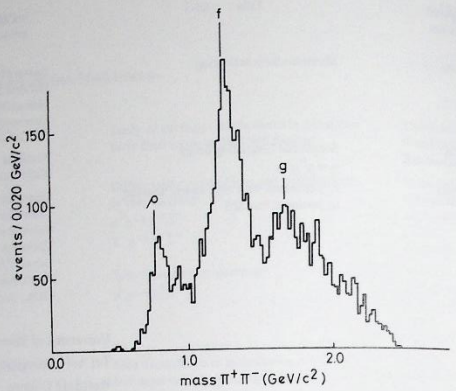

Figure 1.2. The two pion mass spectrum for the reaction $\pi^- p \to \pi^+\pi^- n$. Clear peaks can be seen for the ρ, f and g mesons: Experiment 1 (18563)

In December 1973 we completed data taking with a pion beam of momentum 12 GeV/c. Three million triggers were recorded on tape. A scan of some data revealed that in 15% of all triggers two charged particles could be seen in Omega and in 21% four charged particles could be seen. A preliminary analysis of a 20% sample of the two particle events has been made.

Events of the type

$$\pi^- p \to \pi^+\pi^- n \qquad \text{(8100 events)} \qquad (1)$$

and $$\pi^- p \to \pi^+\pi^-\pi^0 n \qquad \text{(10000 events)} \qquad (2)$$

were extracted using a kinematical fit. For channel (1) the $\pi^+\pi^-$ invariant mass plot is shown in Fig. 1.2. Clear peaks can be seen at the ρ f and g mesons. A moments analysis confirms these states to be 1^-, 2^+ and 3^- respectively. For channel (2) there is a strong contribution from the reactions

$$\pi^- p \to \Delta^0\rho^0 \qquad \pi^- p \to \Delta^+\rho^-$$

When this is removed by means of a simple mass cut the $\pi^+\pi^-\pi^0$ invariant mass spectrum is as shown in Fig. 1.3. The η and ω mesons can be clearly seen.

The acceptance of the Omega spectrometer is not 4π for all particles leaving the hydrogen target. The value of this acceptance and its effect on the physics distributions is at present being studied. When this is understood a partial wave analysis of both the above channels will be made.

In September 1974 the collaboration requested a further ten days' running at an incident beam momentum of 15 GeV/c. This was made to extend and improve our acceptance for X^0 masses up to 2·7 GeV/c². Three million triggers were recorded in October 1974.

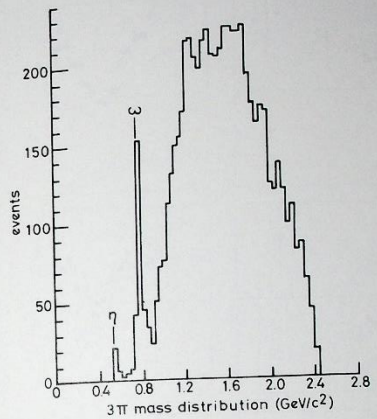

Figure 1.3. The three pion mass spectrum for the reaction $\pi^- p \to \pi^+\pi^-\pi^- n$ in which the peaks corresponding to the η and ω mesons can be seen: Experiment 1 (18564)

The final part of this experimental program, the measurement of the neutron detection efficiency of the neutron counter, is at present being set up at CERN. This requires the use of monoenergetic neutron beam incident on a hydrogen target. The elastically scattered proton is detected in an array of wire chambers and scintillation counters, and the neutron counter is positioned to intercept the scattered neutron. It is planned to measure the detection efficiency for neutrons between 10 MeV and 400 MeV kinetic energy.

EXPERIMENT 2

Differential cross-sections
for 2-body $\bar{p}p$ interactions

Queen Mary College, London
University of Liverpool
Daresbury Laboratory
Rutherford Laboratory

Differential cross-sections for the di-boson processes

(ref. 6, 47, 48, 49, 50, 51, 60)

(a) $\bar{p} + p \to \pi^- + \pi^+$

(b) $\bar{p} + p \to K^- + K^+$

were measured at 20 antiproton momenta from 0.79 to 2.43 GeV/c covering the angular range $-0{\cdot}95 \leqslant \cos\theta^* \leqslant 0{\cdot}95$.

An interesting comparison can be made between process (a) and an experiment carried out by a CERN-Munich group on the process

(c) $\pi^- + p \to \bar{p} + p + n$

Assuming this proceeds by one-pion-exchange the π^- scatters on a virtual pion target giving the inverse of (a), namely

(d) $\pi^- + \pi^+ \to \bar{p} + p$

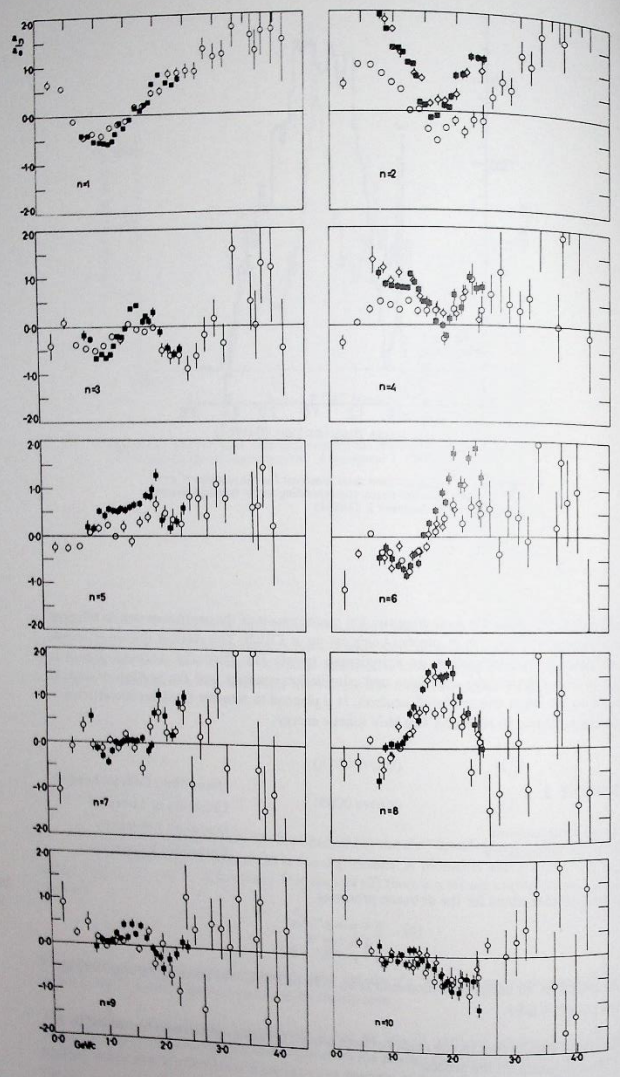

Figure 1.4. The Legendre coefficient derived from the angular distributions of $\bar{p}p \rightarrow \pi^- \pi^+$ expressed as a ratio to the A_0 coefficient. o CERN-Munich, – Cal. Tech.-Rochester-BNL (even coefficients only), – ■ - this experiment: Experiment 2 (17922)

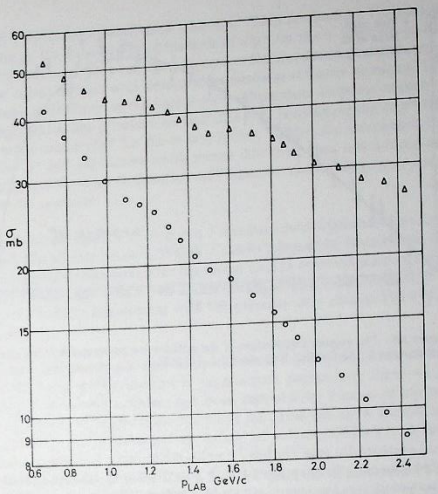

Figure 1.5. The total $\bar{p}p$ elastic cross section o – integrated over the measured angular range ($-0.95 \leqslant \cos\theta^* \leqslant 0.98$). Δ – extrapolated cross section – a correction has been applied to try to account for the unmeasured angular regions: Experiment 2 (18565)

Fig.1.4 shows the results of both experiments expressed as Legendre coefficients which represent fits to the angular distributions for (a) and (d). The agreement is reasonable thus supporting the assumption of one-pion-exchange in (c). Also shown are results from a Caltech-Rochester-BNL experiment on process (a) from which it was only possible to derive the even Legendre coefficients.

The elastic scattering of antiprotons or protons was measured simultaneously with (a) and (b) over approximately the same angular range, and results have been submitted for publication. Some results are shown in Fig.1.5. The elastic cross-section integrated over the measured angular range and also extrapolated to give the total channel cross-section are plotted as functions of beam momentum. Two small enhancements to the cross-section can be seen at values close to those found elsewhere in $\bar{p}p$ total cross-section measurements. Such bumps could be caused by the formation of heavy mesons in the $\bar{p}p$ system.

EXPERIMENT 3

Polarisation measurements for
2-body $\bar{p}p$ interactions

Queen Mary College, London
Daresbury Laboratory
Rutherford Laboratory

The angular distribution of the asymmetry has been measured in the reaction

$$\bar{p} + p \rightarrow \pi^- + \pi^+$$

using a polarised proton target (the apparatus and experimental layout is described in the 1972 Annual Report).

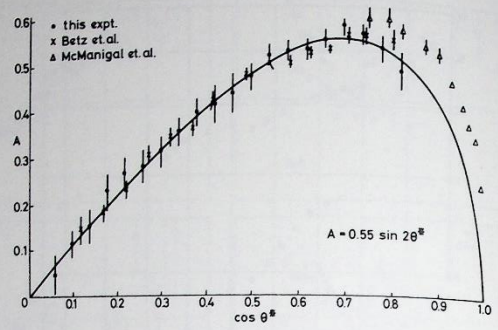

Figure 1.6. The angular distribution of the polarization parameter A in p-p elastic scattering at 1·385 GeV/c: Experiment 3 (18566)

Data collected at 11 momenta in the range 1·0 to 2·2 GeV/c was terminated in June 1974. The statistical accuracy of the measurements will be based on ∼ 5000 $\pi^-\pi^+$ events at each momentum.

In order to check the experimental apparatus and the analysis programmes, some data was collected on p–p elastic scattering where the asymmetry has been well determined from other experiments. This data has been analysed and a result for p–p at 1·385 GeV/c is shown in Fig.1.6, indicating good agreement over the range of cos θ^* covered. The analysis of the antiproton experiment will be completed by Spring 1975.

The results will be combined with the measurements of the differential cross-sections previously obtained by the group in an attempt to look for high mass meson resonances in a partial wave analysis. The mass range covered by the experiments is ∼ 2·0 GeV/c^2 to 2·5 Gev/c^2 where there is not yet a clearly identified resonant state.

EXPERIMENT 4

Experiments on mesons

Imperial College, London
University of Southampton

Meson Production Cross-Sections near Threshold (ref. RL-73-016, 18,42)

A series of experiments on mesons and their cross-sections have been carried out with a missing-mass spectrometer. The reaction used was π^- + p → missing-mass +n at incident momenta close to the appropriate production threshold and most of the results have already appeared in earlier reports. When the missing-mass was that of the ω meson it was found that the plot of σ/p* (where σ is the ω production cross-section and p* the final state momentum in the centre of mass) versus p* shows a pronounced dip below p* = 100 MeV/c. It is possible that this could result from an important P wave amplitude or alternatively that it might be associated with the relatively narrow width of the ω meson which ensures that most ω's in this region decay within a fermi of the neutron. There are however problems with both these explanations

A new result has come from the analysis of data on η' (958) production. This data was originally used to set limits on the η' width. The behaviour of σ/p* for the η' is shown on Fig.1.7. As the neutron counters were positioned near zero degrees to the beam only neutrons very forward and backward in the centre of mass were detected, particularly at higher momenta. In this mass region there is some uncertainty in the background subtraction. However neither of these problems is very important at low p* where we find that σ/p* is rising rapidly as p* falls. This is the same region of p* in which σ/p* for the ω was falling. No angular momentum barrier can explain a rise at low p* and the narrow width means that final state interactions in the η' decay cannot be significant. The result is therefore still a puzzle, and possibly may contain a clue to the behaviour of the ω meson.

Backward η production

Our measurements of the reaction π^- + p → η + n at backward angles are consistent with existing data. We find that all data below 1·05 GeV/c can be adequately described in terms of established s-channel poles and resonances. Our fits favour an S11 resonant mass of about 1515 MeV and amplitude at resonance of 0·38 ± 0·05 and confirm previous measurements of the D13 contribution. They are however inconsistent with the presence of a narrow P11 (1525) resonance of large amplitude.

Experiments on mesons near threshold (Imperial College Group)

A new missing-mass spectrometer is now in operation. It is being used in an attempt to answer some of the problems raised by the earlier experiments, particularly those on cross-sections. The original ring of 6 neutron counters has been replaced by a cross of up to 60 counters arranged to cover laboratory angles from 2 to 11 or 20°. This will allow the full meson production angular distributions to be measured up to a p* of at least 100 MeV/c. A subsidiary set of 12 small neutron counters will cover angles below 2° and will give information on cross-sections down to threshold. Secondly, the decay counters which previously surrounded the hydrogen target have been replaced by drift chambers. These are being used mainly to study the detailed behaviour of the elastic channel, π^- + p → π^- + p, across the meson thresholds.

The resolution of the momentum spectrometer has been improved and a new attempt will be made to measure the width of the η' meson. It is hoped to obtain an experimental resolution significantly below 1 MeV (f.w.h.m.).

Figure 1.7. A plot of cross section divided by centre of mass momentum for the reaction π^-p → ηn: Experiment 4 (18567)

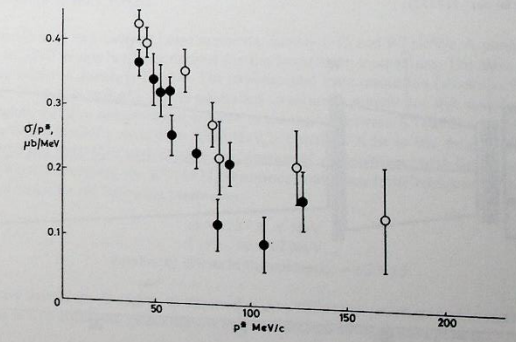

EXPERIMENT 5

CERN
Max Planck Inst., Munich
University of Amsterdam
University of Oxford
Rutherford Laboratory

Study of exclusive reactions
in πp and Kp interactions in
the energy range up to 100 GeV

We are currently preparing equipment for an experiment to be done on the SPS starting in 1976.

The equipment (Fig.1.8) consists of a multi-particle forward spectrometer of reasonably high resolution, particle identification via Cerenkov counters up to 100 GeV/c, and full solid angle coverage by lead-scintillator sandwich counters for γ ray rejection.

This technique should allow us to push the study of inelastic (mainly pion production) exclusive reactions up to 100 GeV/c. The resolution of the spectrometer is not adequate to separate the reactions of interest from backgrounds with π° production, e.g.

$$\pi^- p \to \pi^+ \pi^- n \qquad \text{versus} \qquad \pi^- p \to \pi^+ \pi^- \Delta^0 \;\big\downarrow\; n\pi^\circ$$

For this reason, the efficient π° rejection is necessary. The immediate aim of the experiment is a) to study the energy dependence of the cross-section for production of boson resonances, with a much larger lever arm in the energy than before, b) to search for high mass boson states (for mass up to 4 or 5 GeV), c) measurement of $\pi\pi$ and $K\pi$ phase shifts up to about 3 GeV mass. There are further possibilities for experiments, some involving future developments to the equipment. The main limitation is the worsening momentum resolution and lack of particle identification above 100 GeV/c. Solutions to these problems are expensive, and we prefer first to see what physics comes from the easily accessible energy range. We are particularly interested in using the spectrometer in studies of the recently discovered high-mass bosons, whose properties are suggestive of a new quantum number.

Figure 1.8. The apparatus for Experiment 5 consists of a target T, two spectrometer magnets M1 and M2, proportional chamber and scintillation counter trigger hodoscopes S, banks of spark chambers W, large multi-cell Cerenkov counters C, and lead-scintillator counters V, covering the full solid angle. Only some of these are shown on the layout: (18557)

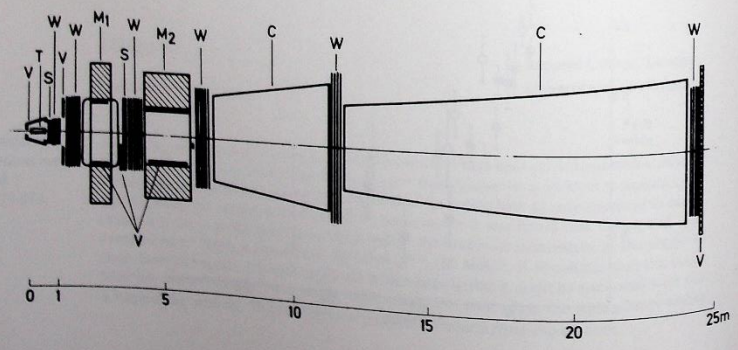

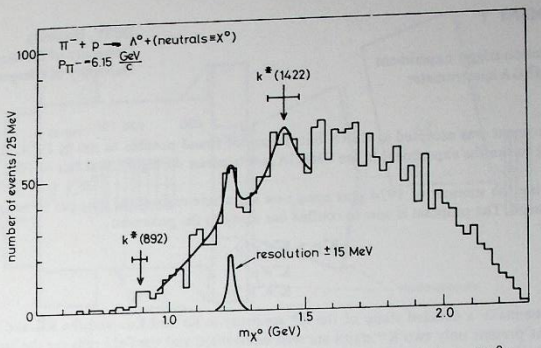

Figure 1.9. Mass spectrum of the missing mass, m_{X°, in the reaction $\pi^- + p \to \Lambda^\circ +$ (neutrals $\equiv X^\circ$). The solid line shows the result of the best fit described in the text: Experiment 6 (18568)

EXPERIMENT 6

University of Rome
Rutherford Laboratory

Study of non-diffractive
production of S=1 neutral
resonances

A counter experiment, using optical spark chambers, has been performed at the CERN Proton Synchroton, to study the mass spectrum of X° in the hypercharge exchange reaction.

$$\pi^- + p \to \Lambda^\circ + (\text{neutrals} \equiv X^\circ) \;\big\downarrow\; \pi^- + p$$

The mass interval covered by the experiment ranges from 1·0 to about 2·5 GeV. The Λ° identification is obtained from the measured directions of the decay π^- and proton, and from the observed proton and/or pion range, with the condition that both the decay particles be below threshold for Cerenkov radiation in a water Cerenkov counter. The film was digitised using the Rutherford Laboratory HPD 2.

Data was taken at two incident beam momenta, namely 6·15 and 9·7 GeV/c. A preliminary data sample of 2247 events has been derived for the lower beam momentum. The mass plot for the accepted events is shown in Fig.1.9. The experimental mass resolution (shown in the figure) is about ± 15 MeV (h.w.h.m.). As no significant structure is present for this sample in the high mass region, we have restricted our analysis to the region between K* (892) and the K* (1422) where a bump around a mass of $\sim$ 1200 MeV is observed. A fit to the data in the region between 950 and 1500 MeV with a linear combination of a Breit-Wigner with free mass and width, a Breit-Wigner describing the K* (1422) resonance, and a quadratic background, yields for the observed structure the following parameters:

$$m = 1227 \pm 6 \text{ MeV}$$
$$\Gamma = 46 \pm 17 \text{ MeV}$$
$$\text{number of events in the resonance} = 62 \pm 15$$

It appears that in the Q region, as observed in non-diffractive processes and in contrast to what happens in K^-p collisions, rather narrow and well defined structures are present.

EXPERIMENT 7

DESY, Hamburg
University of Birmingham
University of Glasgow

K^+ interaction trigger experiment
in the OMEGA spectrometer

The experiment was accepted at CERN but it was not found possible to run in 1974. We are proposing to run the experiment in the OMEGA spectrometer during the first half of 1975.

Tests during the summer of 1974 plus some new ideas have enabled the proposal to be refined and improved. The proposal is now to confine our study to the processes:

$$K^+p \rightarrow K^+\pi^+\pi^-p$$
$$K^\circ\pi^+p$$
$$K^+K^+K^-p$$

in order to make a detailed study of the K^* spectrum in $K\pi$ and $K\pi\pi$ and the $K\bar{K}$ and $KK\bar{K}$ spectra. At present only two K^* states are well understood and the field calls for the high acceptance high statistics study of this proposal.

The tests demonstrated that by using the multiwire proportional chambers in OMEGA we can select 4-prong and 2-prong V° topologies with good efficiency. We now propose to add a π° detector in anticoincidence downstream to exclude a large proportion of events containing π°s and enrich the sample of the above reactions.

The proposed arrangement will yield ~ 80 events/μb/day – a considerable improvement on the original proposal. We are requesting approximately 6 days running time to yield 500 to 600 events/μb in a total of 2×10^6 triggers.

EXPERIMENT 8

University of Birmingham

Study of meson resonances decaying
into strange particles in the Omega
spectrometer at the SPS

(ref. 41) It is known experimentally that mesons made of strange quark-antiquark pairs are produced much more copiously by incident K-mesons than by pions since the K itself contains a strange quark. Such a meson is the ϕ-meson and apart from this only one other the f′ (1514) is known to be in this class. Several more are expected and will be searched for using the Omega spectrometer and the RF separated beam at the SPS. Fluxes of K mesons in excess of 10^5 per pulse will be used and the mesons will be studied in the reactions

$$K^-p \rightarrow K^-K^+\Lambda^\circ$$
$$K^\pm p \rightarrow K^\pm K^+K^-p$$

at 18 and 32 GeV/c. In addition events including an extra π° will be recorded using the downstream γ-ray detector allowing mesons decaying into K^+K^- or $K^+K^-\pi^\circ$ to be studied. An outgoing K of opposite sign to the incident one will be detected by the two Cerenkov counters in order to provide the trigger for the spark chambers. The sensitivity of the experiment will be about 100 times that of a present day bubble chamber experiment.

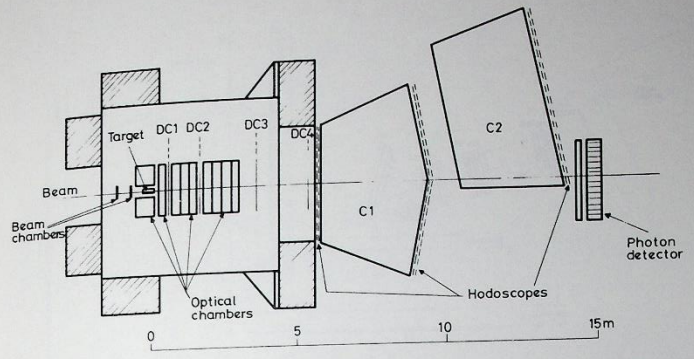

Figure 1.10. The proposed layout of the Omega spectrometer for 18 GeV/c incident K-mesons from the CERN SPS. DC1-4 are drift chamber planes and C1 and C2 are atmospheric pressure Cerenkov counters with respective π thresholds of 2·3 and 4·7 GeV/c and K thresholds of 8·2 and 16·7 GeV/c: Experiment 8 (18569)

EXPERIMENT 9

University of Bristol
University of Southampton
Rutherford Laboratory

K^+, π^+, π^-, K^--p elastic
scattering differential
cross-sections

K^+p scattering (ref. 25)

The differential cross-sections measured in the momentum range 0·7 to 1·5 GeV/c at the Rutherford Laboratory by the Bristol Group described in previous Annual Reports, have been used in an analysis by W. N. Cottingham *et al.* at Bristol University on the assumption that the cross-section is entirely due to particle exchange with no resonance formation. A good fit is obtained to the data. In the model the two pion exchange includes effects due to the exchange of the ϵ, ρ and ω mesons which contribute dominantly to forward scattering and of the Λ hyperon which dominates the exchange scattering in the backward direction. The fit gives values of the coupling constants to the K-meson and nucleon for these mesons which are in agreement with the predictions from the SU(3) unitary symmetry theory.

π^+, π^- p scattering

As described in the 1973 Annual Report sufficient data has been taken to give differential cross-sections continuously over the momentum range 0·4 to 2·20 GeV/c. We have approximately one million elastic events for π^+ and for π^-. The analysis is almost complete and the results will be used in phase shift analyses both at Bristol and Berkeley, USA.

K^-p scattering

Unlike the K^+p system where the data can be fitted without any resonances the K^-p system in the intermediate momentum range shows a large number of resonant states. To enable these to be resolved measurements of K^-p elastic differential cross-sections with a precision comparable to that available for the pion-nucleon system are required. Our apparatus has been completely redesigned and built to do this.

The beam line has been modified to include a lengthened electro-static particle separator to improve the ratio of K^- to π^- in the beam, and the magnets close to the target have been changed to increase the maximum momentum to 2·7 GeV/c.

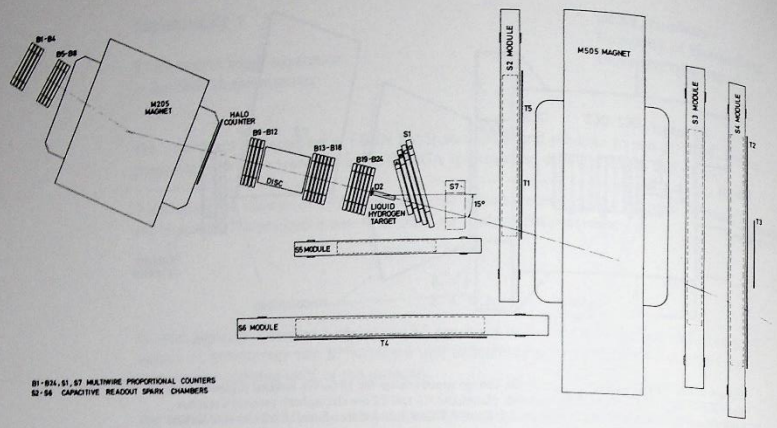

Figure 1.11. Diagram of the apparatus for Experiment 9 (18400)

As the yield of K^- mesons at momenta in the range of 1 to 2 GeV/c is relatively low a number of changes have been made to enable the full intensity available from Nimrod to be used. The sonic chambers used previously, limited the total particle flux which could be accepted. These are being replaced by proportional multiwire chambers to detect incoming beam tracks and by large area multiwire spark chambers with capacitive read-out to detect scattered particles.

The multiwire proportional chambers have been built by the Nuclear Physics Apparatus Group (NPAG) at the Laboratory. The electronics used with these chambers have been developed at Bristol University. Initial tests are encouraging. The capacitive read-out spark chambers, constructed by NPAG, use a modular system of read-out electronics provided by Bristol University. These electronic units have been tested by computer controlled spark chamber simulators. These chambers are being fired by a push-pull system which applies positive and negative voltages to the opposite plates of the chamber. This system gives a first order cancellation of the large voltage transients observed when a spark chamber fires, and which could harm the read-out electronics.

The apparatus shown diagrammatically in Fig.1.11, is now being installed and will be tested early in 1975.

EXPERIMENT 10

Coherent production of I=½ baryon states on helium

CERN
University College London
University of Uppsala
Rutherford Laboratory

The object of this experiment is to study the elastic and inelastic scattering of high energy protons on helium nuclei, under conditions where the alpha particle recoils coherently. The main inelastic channels being studied are the following:

$$p + {}^4He \rightarrow {}^4He\ (p\ \pi^+\ \pi^-)$$
$$\qquad\quad {}^4He\ (n\ \pi^+)$$
$$\qquad\quad {}^4He\ (p\ \pi^0)$$
$$\qquad\quad {}^4He\ (\Lambda\ K^+)$$
$$\qquad\qquad \hookrightarrow p\ \pi^-$$

Measurements of the decay distributions of the short lived I=½ states produced by diffraction disassociation of the incident proton will enable the spin and parity of such states to be investigated, free of any possible $I=\frac{3}{2}$ contamination. The comparison of elastic and inelastic data is, in addition, expected to provide information on the interaction of the produced states in nuclear matter.

The equipment is shown in outline in Fig.1.12. A represents a block of multiwire proportional chambers and a trigger counter to identify a beam particle well upstream of the equipment. B is a large veto counter with a small hole to reduce background caused by an unwanted halo around the beam. C is a further block of multiwire proportional chambers to determine the trajectory of a beam particle closer to the equipment. In order to minimise the stopping power for recoiling alpha particles, a high pressure helium gas target is used. This is situated on the axis of the recoil detector D which itself consists of a series of cylindrical wire spark chambers with current division and delay line read-out systems. The spark chambers are surrounded by a cylinder of scintillation counters which provide pulse height and time of flight information on the recoil particle, as well as a trigger signal. The spark chambers and scintillation counters operate in an atmosphere of helium and methyl alcohol at reduced pressure. There are no walls in the path of the recoiling particles other than that of the target. Momentum analysis of the fast forward charged particles is provided by the spectrometer magnet, K, together with magnetostrictive wire spark chambers, G, H and J as well as a bank of multiwire proportional chambers, E. Threshold Cerenkov counters, L, downstream of the equipment serve to help with the separation of π^+ from protons in the forward system.

All the data for this experiment has now been obtained, and the equipment has been dismantled. Analysis of the data is now well under way, and the results should be available by mid-1975.

Figure 1.12. Diagram of the apparatus for Experiment 10. A, C, E – Multiwire proportional planes, B – Halo veto counter, D – Recoil detector consisting of cylindrical wire spark chambers and surrounding scintillation counter, G, H, J – Magnetostrictive wire spark chambers, K – Spectrometer magnet, L – Threshold Cerenkov counters: (18570)

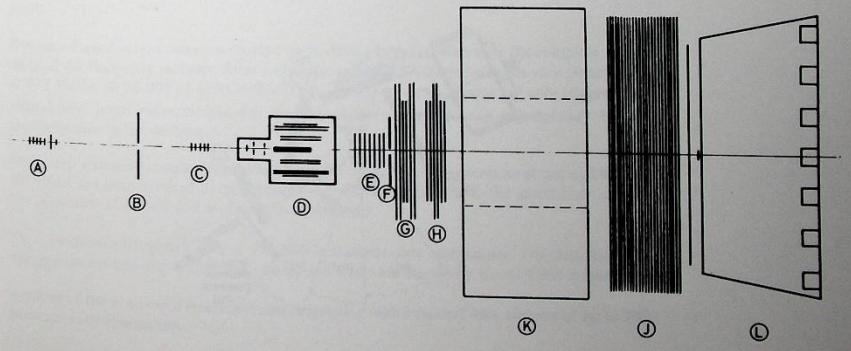

EXPERIMENT 11 **Rutherford Laboratory**

Differential cross-section and
polarisation measurements in the
charge exchange reactions
$\pi^- p \rightarrow \pi^0 n$ and $\eta^0 n$

As part of a continuing study of the pion-nucleon system, data has been taken to measure the charge exchange and $\eta^0 n$ differential cross-section at 23 momenta between 0·6 and 2·7 GeV/c. In addition the polarisation parameter is now being measured in the same momentum range. This experimental study will provide a powerful constraint to partial-wave analyses of the πN system. Existing differential cross-section and polarisation information in these channels have poor statistics, are widely spaced in momentum and are sparse at the higher momenta.

Polarisation Measurements. Data taking commenced in November 1974 and is expected to be completed by the end of January 1975. The experimental arrangement is shown in Fig.1.13. The polarised target is of the frozen spin type, designed to give maximum angular access. The counter arrays surrounding the target are designed to take full advantage of this solid angle. The polarised target consists of 20cm^3 of propanediol in the form of small spheres in a liquid He3 environment at an operating temperature below 0·5K.

In this experiment interactions yielding charged particles in the final state are rejected by placing veto scintillation counters around the target and in front of each of the neutron and γ-ray detectors. The neutrons produced in the charge exchange reactions are detected in a large array of liquid scintillator cells each one metre long, and viewed by a single photomultiplier. Large sheets of lead are used for converting the γ rays, resulting from π^0 or η^0 decay, into electron-positron showers. These are then detected by three planes of plastic scintillators placed behind the lead sheets. Earlier experimental studies of these channels have used optical spark chambers and consequently obtained lower rates than this experiment.

During the running of the experiment to date the average free proton polarisation, as measured by nuclear magnetic resonance technique, has been between 65 and 70%. To estimate the contribution of interactions with bound protons data has been taken from a dummy target which is similar to the polarised target but devoid of free hydrogen.

Figure 1.13. Diagram of apparatus for Experiment 11. The polarised target is of the frozen spin type designed to give maximum angular access. The surrounding arrays of scintillation counters are arranged to take advantage of the available solid angle: (18571)

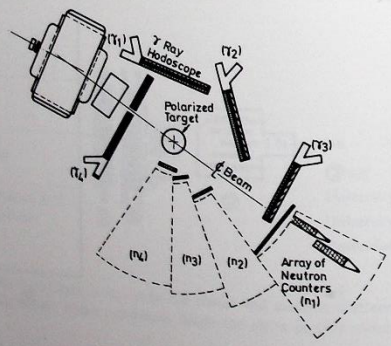

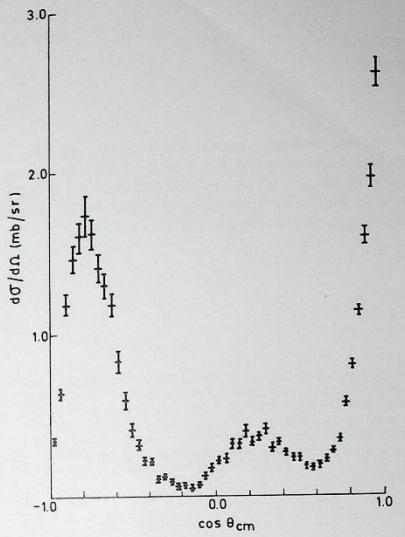

Figure 1.14. Cos θ_{cm} distribution (preliminary) at 977 MeV/c. Errors are limited by Monte Carlo statistics: Experiment 11 (18572)

A preliminary analysis of the data taken so far indicates that it should be possible to obtain between 10,000 and 50,000 charge exchange events off hydrogen, depending on the momentum. This should significantly constrain the number of acceptable phase-shift solutions in this momentum region.

Differential Cross-section Measurements. Data taken on this part of the experiment was completed in February 1973, and is currently in an advanced analysis stage. The experimental apparatus was similar to that shown in Fig.1.13, with a hydrogen target replacing the polarised target.

The use of scintillation counters enabled us to obtain high statistics over the complete angular range of the final state particles. After fitting the data, the final event samples vary from 70,000 at 677 MeV/c to 20,000 at 2730 MeV/c. Using data from a two gamma ray only trigger mode, substantially larger event samples are available at low momenta using a gamma-ray bisector approximation in the analysis.

Such large statistical samples necessitate a careful evaluation of systematic errors and substantial effort has been invested in minimising these effects. (Primarily in the gamma ray and neutron detection efficiency and aperture measurements.)

Fig.1.14 shows preliminary data at 977 MeV/c incident pion momentum. The data shown is a two gamma ray bisector distribution and quoted errors are limited by Monte Carlo statistics.

Analysis of the $\pi^- p \rightarrow \eta^0 n$ reaction is also progressing with expected data samples of up to 2000 events at each momentum.

EXPERIMENT 12

University of Cambridge
Rutherford Laboratory

Differential cross-sections and polarisation in the reaction $\pi^- p \rightarrow K^\circ \Lambda$

The object of the experiment is to identify resonances in the πN system in the mass range 1600 to 2150 MeV/c^2 and to determine their parameters. A study of this reaction ($\pi^- p \rightarrow K^\circ \Lambda^\circ$) is of particular interest since (a) the reaction is a pure isotopic spin channel, (b) high angular momentum waves are inhibited by centrifugal barriers near threshold and (c) polarisation data are obtained simultaneously from the decay asymmetry in $\Lambda^\circ \rightarrow p\pi^-$.

Figure 1.15. A diagram of the apparatus used in Experiment 12 in which the beam is entering from the left. The upstream magnet is situated between banks of multiwire proportional detectors. Further downstream and surrounded by veto counters is the liquid hydrogen target. Charged secondary particles emerging from the target enter a large magnetic spectrometer via further multiwire proportional detector planes. The spectrometer has large optical spark chambers at the entry side which are viewed by lead-oxide vidicon cameras. On the exit side there are more large spark chambers with magnetostrictive read-out which measure the energy of those particles within the magnet aperture. Wide angle particles are registered by a time-of-flight ring of counters 4m in diameter: (18374)

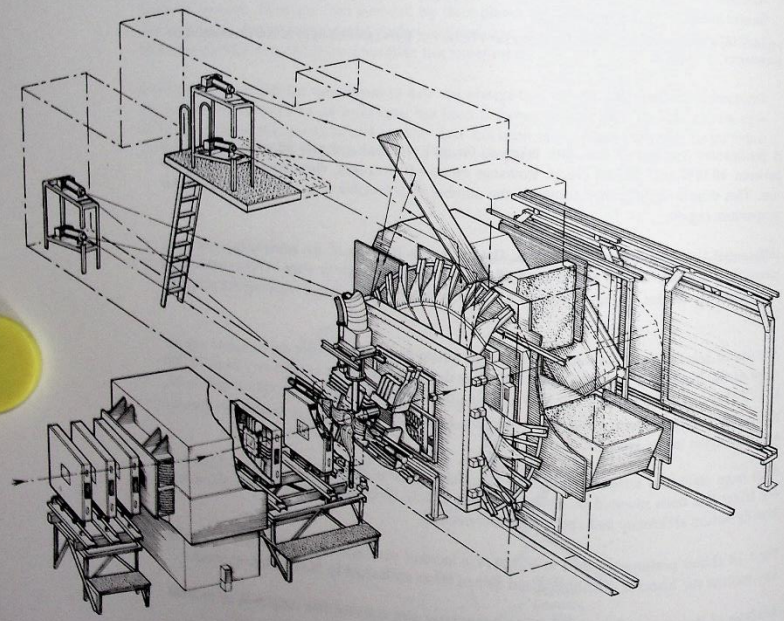

The first experiment (proposal 87) covered the mass range 1600 to 1850 MeV/c^2. Analysis of one million photographs of the detection spark chambers is nearly complete. About 3000 to 4000 events at 9 mass values are expected. In preparation for physics analysis of the data, a phase shift analysis has been made using the existing data in this channel. The Barrelet zero method was used and the results were presented at the 1974 International Conference in London. This analysis shows that the S11 (1700) and P11 (1780) resonances are definitely present and that the P13 and D13 waves also resonate. The F17 wave may be resonating near 2000 MeV.

A further experiment (proposal 114) has been set up to extend the mass range up to 2150 MeV/c^2. The apparatus is shown in Fig.1.15. The neutral particles, K° and Λ°, produced by the reaction are detected by observing their charged decay modes $K^\circ \rightarrow \pi^+\pi^-$ and $\Lambda^\circ \rightarrow p\pi^-$ giving the characteristic signature for the reaction of two vees. The charged secondary particles are observed in large optical spark chambers (1·20m x 1·20m and 2·20m x 2·20m sensitive areas) viewed by four lead oxide vidicon cameras on-line to a DDP516 computer. A double M5 spectrometer magnet followed by an array of magnetostrictive wire spark chambers downstream measures the energy of those particles within the magnet's 2·0m x 0·8m aperture. Wide angle particles are detected by a time-of-flight ring, 4m diameter, of 24 scintillation counters which, together with a set of 1·0m x 1·0m multiwire proportional chambers covering the magnet aperture, form the basis of the trigger for the detection system. The proportional chamber system comprises 2000 wires for triggering and 1000 wires for beam measurement.

The first experiment within this apparatus (proposal 114) is to measure the differential cross-section and Λ° polarisation at 10 beam energies between 1·4 and 2·0 GeV. In this mode of running the liquid hydrogen target is surrounded by 16 low mass magnetostrictive spark chambers arranged in 4 quadrants, top, bottom, left and right. This array permits the detection of large angle K° decays which is essential to cover the full centre of mass angular distribution of the reaction adequately. Data taking started during December 1974.

EXPERIMENT 13

University of Birmingham
Rutherford Laboratory

$K^\pm n$ elastic and $K^+ n$ charge exchange differential cross-section below 1 GeV/c

This experiment is a continuation of a systematic study of kaon-nucleon interactions below 1 GeV/c. The processes occurring when a kaon interacts with a deuteron

$$K^\pm n(p) \rightarrow K^\pm n(p)$$
$$K^+ n(p) \rightarrow K^\circ p(p)$$

where (p) represents the "spectator" particle (or non-interacting nucleon) were studied using a magnetic spectrometer system with sonic spark chambers and time-of-flight particle identification (1970 Annual Report). Data analysis is now completed. In Fig.1.16 and Fig.1.17 are shown some results for both $K^+ n$ reactions, together with other data at similar momenta. The results are a significant improvement over previous measurements.

A phase shift analysis has been performed by B Martin (UCL) using these and other data to determine the I = 0 amplitudes in $K^+ N$ scattering, where previously there have been suggestions of a resonant state (so called Z_0^*). This state could not be accommodated into the present spectrum of elementary particles, and indeed this phase shift analysis shows no strong evidence for resonant like behaviour for any I = 0 amplitude.

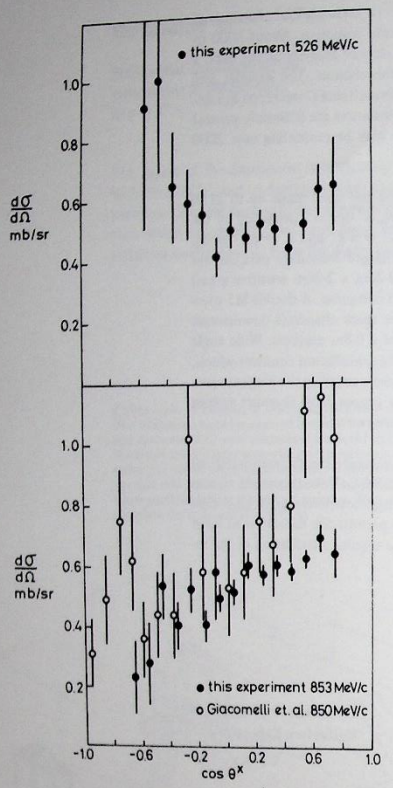

Figure 1.16. Differential cross sections for K^+n elastic scattering from Experiment 13 together with other data at similar momenta: (18573)

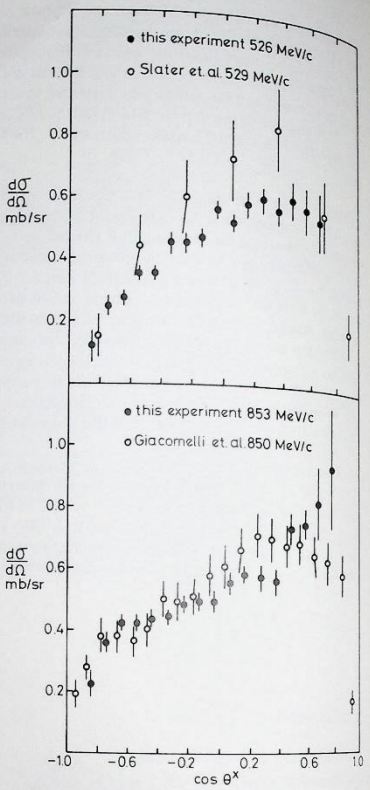

Figure 1.17. Differential cross sections for K^+n charge exchange scattering from Experiment 13 together with other data at similar momenta: (18574)

EXPERIMENT 14

Polarisation in KN interactions

Queen Mary College, London
Rutherford Laboratory

A Proposal is approved for a measurement of the angular distribution of the asymmetry parameter in the reactions

$$K^{\pm} + n \rightarrow K^{\pm} + n$$
$$K^{+} + n \rightarrow K^{o} + p$$
$$K^{-} + p \rightarrow K^{o} + n$$
$$K^{\pm} + p \rightarrow K^{\pm} + p$$

using a polarised target made from a deuterated hydrocarbon to provide the polarised neutrons. The estimate neutron polarisation is $\sim$ 25%.

In the initial phase the momentum range will be from 0·6 to 1·2 GeV/c. The data from the experiment will be combined with world data in an effort to improve the understanding of the KN system.

The experiment will commence setting up on Nimrod in October 1975.

EXPERIMENT 15

Heavy particle experiment

University College London
AWRE
Rutherford Laboratory

This experiment is designed to detect possible new stable or very long-lived heavy particles, with emphasis on the mass range 10 to 200 GeV. If such particles exist they would be expected to be present in ordinary matter in a very low natural or cosmic ray produced concentration. In particular, particles of charge +e would form heavy hydrogen-like atoms and (like natural tritium) become a constituent of terrestrial water. In this situation the concentration can be increased by a very large factor by means of the known separation techniques for hydrogen isotopes.

It is planned to process 10,000 litres of heavy water, in collaboration with AEE Winfrith and AERE Harwell, to produce final sample volumes in the region 1 to 10^{-3} ml, in which the concentration of any heavy particles will have been increased by a factor 10^{11} to 10^{13} relative to ordinary water. A counter array will be used to detect the high energy decay products of any unstable particles in the enriched samples and the presence of completely stable particles will be investigated by converting D_2O to D_2 gas which will be examined by a special mass spectrometry technique of enhanced sensitivity to hydrogen-like atoms. Work on the enrichment process began during 1974 and will continue throughout 1975. Some intermediate stage enriched samples will be used in preliminary heavy particle searches during 1975 with studies of full concentration scheduled for 1976.

EXPERIMENT 16

Study of exchange mechanisms in quasi two-body final states in the RMS facility

Edinburgh University
Westfield College, London
Rutherford Laboratory

Current approaches to hadronic reactions are largely phenomenological, with Regge exchange models successfully describing a broad spectrum of reactions. There are, however, significant failures which force the adoption of rather ad hoc modifications to the basic model. Further studies require that the amplitudes contributing to various processes can be extracted in a model independent fashion from the data alone. This, in turn, requires that the initial and outgoing particle spin states are known. With a polarised target the initial helicity state is defined, and the helicity states of the produced particles can be inferred from the joint angular distributions of the outgoing particles and their decay products. Quasi two-body channels have more final state observables, which is an advantage, but high statistics and good geometric detection efficiency are essential.

The Rutherford Multiparticle Spectrometer (RMS) is being built to allow the current systematic high statistics studies of two-body reactions to be extended to many-body, and in particular quasi two-body, processes. The RMS comprises the magnet of the 1·5 m Bubble Chamber suitably modified and reorientated, with an increased inter pole-face gap. Spark and wire proportional chamber detectors are utilised, with a large Cerenkov counter to distinguish pions from kaons (Fig.1.18). During 1976 a liquid hydrogen target will be used, but design work has started on a frozen spin polarised target, expected to be ready in 1977.

The first experiment of a continuing programme will be an examination of quasi two-body reactions involving either a $\Delta(1236)$ or a $\Sigma(1385)$ produced on a proton target. Initially 4 and 6 GeV/c π^+ beams will be used to provide $\sim$ 1000 events/μb on channels such as

$$\pi^+ p \to \eta, \omega, \rho\ \Delta^{++} \quad \text{and} \quad \pi^+ p \to K^+, K^{*+}\ \Sigma^+(1385),$$

with a hydrogen target. This will be followed up with K^+ and K^- beams, so that the analogous channels, including the crossed channels, can be studied.

The simple topology trigger, designed to select preferentially events with 4 particles in the final state, is based on 3 large proportional chambers surrounding the cylindrical spark chambers which in turn surround the target.

The data recorded for the study of exchange mechanisms will contain other channels of considerable interest. In particular, rare channels for which a specific trigger would be impossible to construct will be studied to see if they contain evidence for those elusive meson states predicted by the quark model.

Because some 35 million events are expected to be recorded in 1976, the computing-analysis load is likely to be exceptionally heavy. To alleviate this more efficient methods of pattern recognition have been examined, with encouraging results. Another solution to the problem of a heavy load on the central computer is to build hardware pattern recognition modules, and groups at the Rutherford Laboratory and at Edinburgh are actively pursuing this line of attack.

The RMS facility will be ready by the end of 1975. A significant saving in money and effort has been possible through the use of some of the capacitative read-out spark chambers previously used by Proposal 100 at CERN, and the loan to the Laboratory by CERN of the whole of the spark chamber read-out system used on that experiment.

Figure 1.18. Diagram of layout of Rutherford Multiparticle Spectrometer (RMS): Experiment 16 (18575)

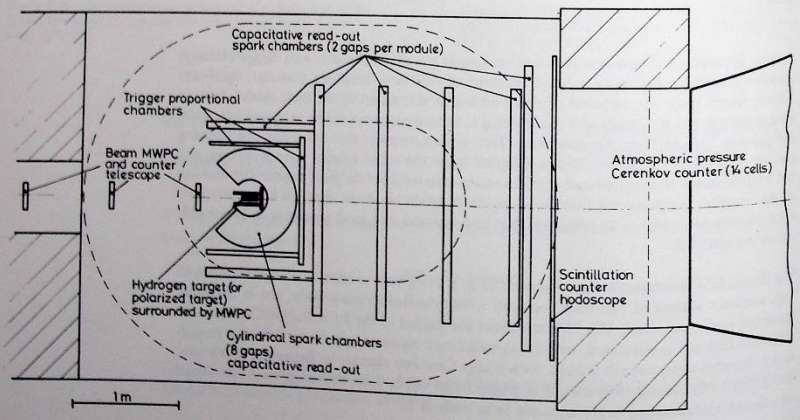

EXPERIMENT 17

Differential cross-sections and
polarisation in the reactions
$\pi^+ p \to K^+ \Sigma^+$
$K^- p \to \pi^- \Sigma^+$

University of Birmingham
University of Genova
University of Stockholm
CERN
Rutherford Laboratory

This experiment, which started taking data in December 1973, was completed in September 1974. In this time we have taken data to measure both the energy and t-dependence of the differential cross-sections for the two related reactions $\pi^+ p \to K^+ \Sigma^+$ and $K^- p \to \pi^- \Sigma^+$.

The set-up (already described in the 1973 Annual Report) consisted of a high resolution forward spectrometer, with very efficient particle identification, together with a spark chamber telescope for the recoil particle.

Initial results from the experiment are very satisfactory. The data from the single arm spectrometer (used to establish the differential cross-section at low t) is much cleaner than in any previous experiment (Fig.1.19). The virtual absence of a peak at the proton mass is a guarantee of no background under the Σ peak. This, plus the fact that we measure both reactions in the same set-up, ensures that we can make the long awaited reliable comparison of these reactions.

From the double arm spectrometer, we already have indications of the high t energy dependence, which shows promise of shrinkage of the differential cross-section as expected on a Regge model with K* exchange. Fig.1.20 shows a preliminary differential cross-section at 10 GeV/c, and Fig.1.21 shows the implied energy dependence vs t. If these results are borne out by the complete analysis, we may find that these hypercharge exchange reactions behave (in the differential cross-section) in a simple manner, as expected on the basis of a Regge pole model (but in a more complicated way as regards the polarisation, as with πp charge exchange).

Figure 1.19. a) shows the missing mass distribution for the final $\pi p \to K\Sigma$ data, and b) shows the corresponding distribution for the line reversed reaction: Experiment 17 (18558, 18559)

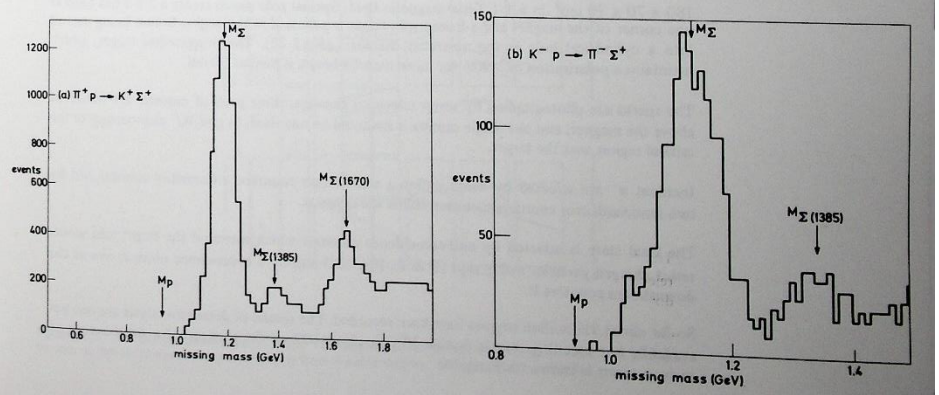

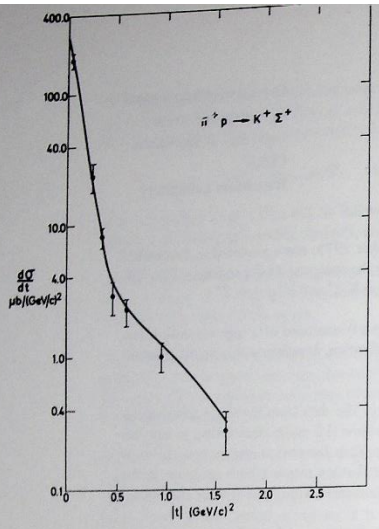

Figure 1.20. The preliminary differential cross-section at larger t values from a small sample of the 10 GeV/c data: Experiment 17 (18560)

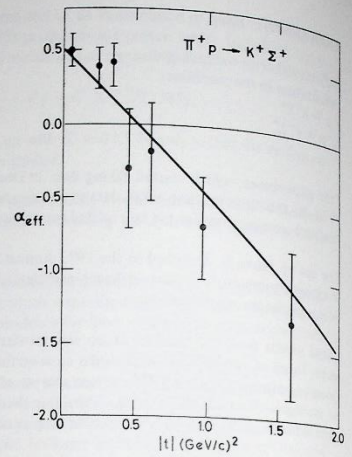

Figure 1.21. The implied energy dependence, represented by $\alpha_{eff}(t)$. The result is consistent with dominant K* exchange: Experiment 17 (18561)

EXPERIMENT 18

Spin rotation parameters in
$\pi^- p \rightarrow K^\circ \Lambda$

CERN
ETH, Zurich
University of Helsinki
Imperial College, London
University of Southampton

This experiment, to measure the P, A and R parameters in the reaction $\pi^- p \rightarrow K^\circ + \Lambda$ at 5 GeV/c has now been mounted at CERN. The apparatus comprises spark chambers covering 180 x 70 x 70 cm^3 in a 1·1 Tesla magnetic field. Special pole pieces create a 2·5 Tesla field at one corner of the magnet and a frozen spin target is polarised in this region before being moved into a cylindrical hole in the upstream chambers (Fig.1.22). The propanediol target, which maintains a polarisation of >90% for more than 24 hours, is held at 50 mK.

The sparks are photographed by seven television cameras; three pairs of cameras are mounted above the magnet; and one single camera is mounted on one flank to give 90° stereoscopy of the critical region near the target.

Incident π^- are selected by beam defining scintillation counters, a Cerenkov counter and by two semiconductor counters mounted inside the cryostat.

The final state is selected by anti-coincidence counters which surround the target and which reject charged particles and γ rays (F & R, Fig.1.22) and by a coincidence pulse in one of the downstream counters E.

So far about 1½ million triggers have been recorded. The results of detailed analysis are not yet available, but scanning reveals double V°s on about 10% of the photographs. An example of such an event is shown on Fig.1.23.

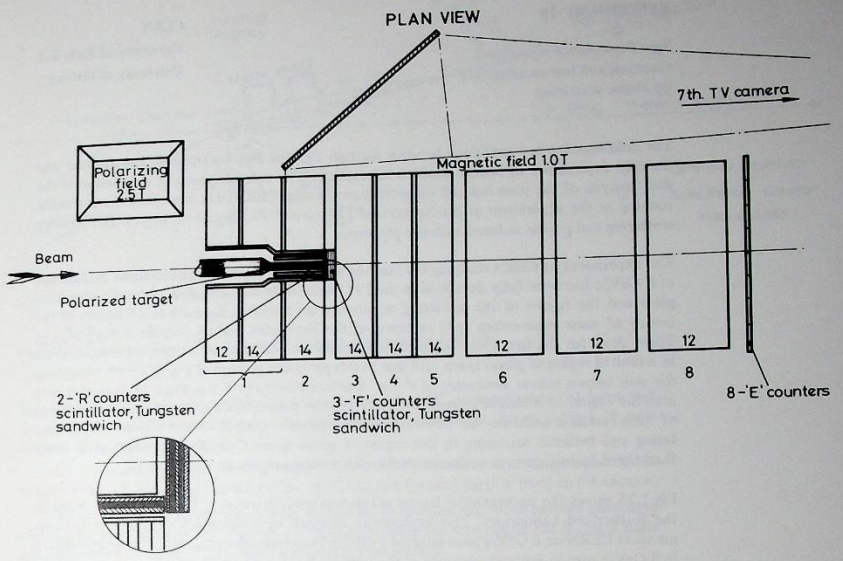

Figure 1.22. General view of the polarised target, spark chambers and counters for the study of the reaction $\pi^- + p \rightarrow K + \Lambda$. Optical chambers 1-8 are viewed by seven television cameras. Inset: details of the arrangement of veto counters and tungsten around the target: Experiment 18 (18576)

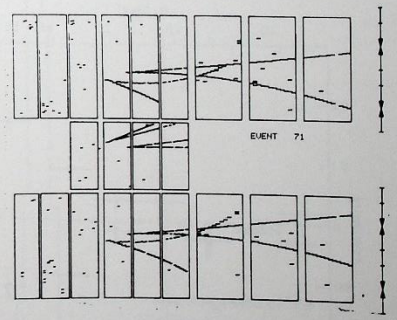

Figure 1.23. An example of a double V° event. The unseen pion enters the target from the left; two V°s can be seen on the three views, the central view is from the side camera: Experiment 18 (18380)

EXPERIMENT 19

Spin dependence of inclusive reactions and low cross-section pp elastic scattering

CERN
University of Paris-Sud
University of Oxford

The collaboration has continued to work through 1974 on its programme of investigation into the spin dependence of hadron induced interactions. The year has seen the completion of the data analysis of the pion induced inclusive experiment at CERN (d31 beam) and the successful running of the experiment at the Rutherford Laboratory (P81 beam) on large angle elastic pp scattering and proton induced inclusive processes.

The experiment at CERN studying the reaction $\pi^{\pm}p \to \pi^{\pm}$ + anything at an incident momentum of 8 GeV/c has been fully described in the 1973 Annual Report. The data analysis is now complete and the results of the scattering asymmetry are shown in Fig.1.24 as a function of the centre of mass momentum (p^*) in terms of the Feynmann scaling variable $x = p^*_{\parallel}/p^*_{MAX}$. These show for the first time that inclusive production processes can be spin dependent, albeit in a limited region of phase space, and that in this particular process of $\pi^{\pm}p(\uparrow) \to \pi^{\pm}$ + anything the well known mirror symmetry of $\pi^+ + \pi^-$ elastic scattering ($x \simeq 1$ in Fig.1.24) is carried over into the region of inclusively produced π's where the pion projectile fragments. Interpretation of these results is underway but obviously indicate an underlying similarity between elastic scattering and inelastic scattering in this region of phase space. Clearly the assumption in many theories of factorisation in exchange amplitudes is not borne out by this data.

Fig.1.25 shows the experimental layout which was used throughout 1974 in the P81 beam at the Rutherford Laboratory. This experiment, designed to complement the previous measurements at CERN on 8 GeV/c pion induced inclusive reactions, measured not only the asymmetry in 8 GeV/c proton induced reactions of the type $p + p(\uparrow) \to p$ + anything

$\to \pi^{\pm}$ + anything

but also the elastic polarisation parameter (P_0) in the region of four momentum transfer $|t| = 1{\cdot}0$ to $6{\cdot}0$ (GeV/c)^2. The full angular region extends to $|t| = 6{\cdot}6$ (GeV/c)^2 and hence for the first time at high energies the polarisation parameter has been measured over essentially the full angular range.

Figure 1.24. Polarisation asymmetry in the inclusive reaction $\pi^{\pm}p(\uparrow) \to \pi^{\pm}$ + anything at 8 GeV/c: Experiment 19 (18577)

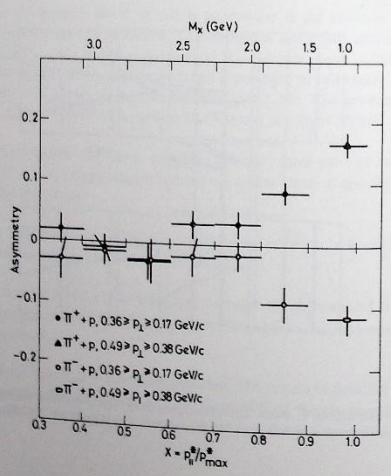

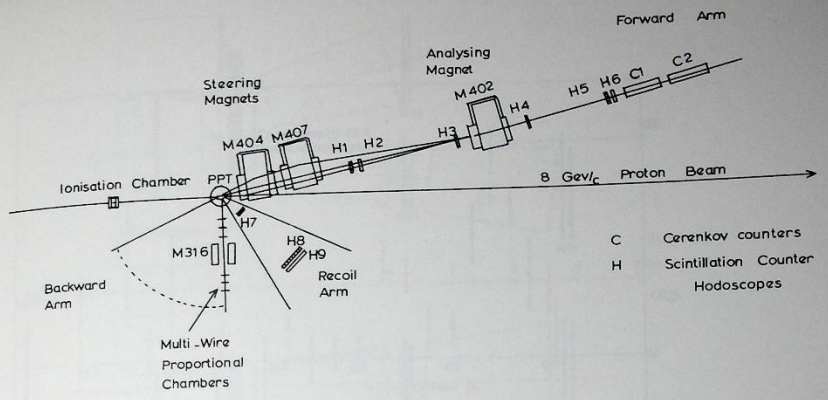

Figure 1.25. Layout of Experiment 19 at Rutherford Laboratory (P81): (15353)

The specially built high energy (7·9 GeV/c), high intensity (10^9 protons/pulse) P81 beam was described in the 1973 Annual Report. The experimental apparatus, as shown in Fig.1.25, consisted of three major sections:

(i) A forward arm with steering magnets M404 and M407 and an analysing magnet M402 to accept and measure using hodoscopes H_1 to H_6 the fast forward particle from an interaction;

(ii) A recoil arm with hodoscopes H_7 H_8 and H_9 to measure any recoil particle associated with the forward particles and through correlations between the recoil angle and forward angle and momentum to select out elastically scattered proton events;

(iii) A backward arm which detects and momentum analyses the fragmentation products of the polarised proton target.

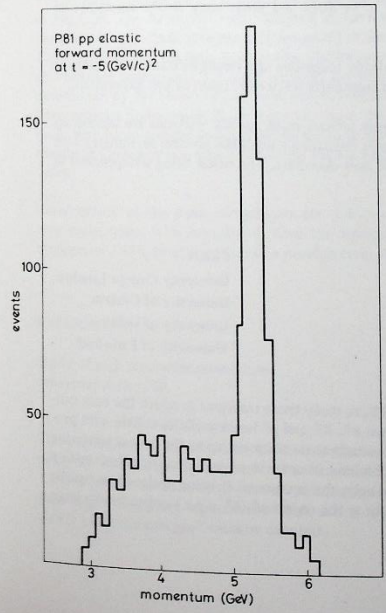

Figure 1.26. Distribution of forward momentum at t = 5·0 (Gev/c)^2: Experiment 19 (18578)

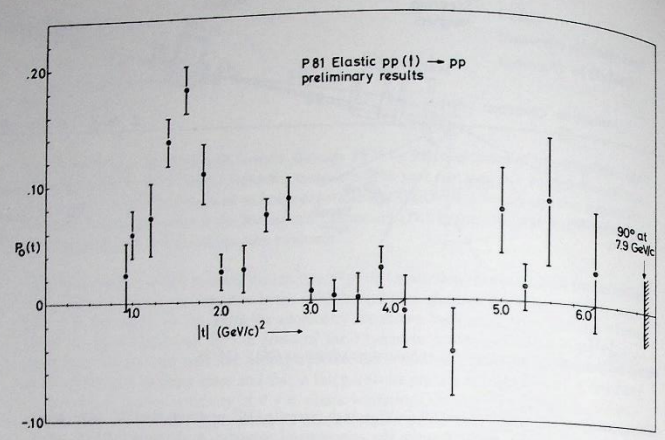

Figure 1.27. Preliminary results on the polarisation parameter (P_0) in 8 GeV/c proton proton elastic scattering: Experiment 19 (18579)

The analysis of the data taken is now under way and Fig.1.26 shows the quality of the elastic pp data taken with the distribution of the measured forward momentum at $|t| = 5{\cdot}0$ (GeV/c)^2 where the cross-section is very low ($< 1\mu b/(GeV/c)^2$). Similar distributions exist for the correlation between the forward and recoil angles. The distributions clearly show a narrow peak of events, coming from elastically scattered protons off the polarised protons in the target, above a smooth background of inelastic and quasi-elastic events. The quality of the data enables good measurements of the polarisation parameter to be made and preliminary results are shown in Fig.1.27.

The oscillatory nature of the asymmetry is clearly suggestive of a strong diffractive component to proton-proton elastic scattering even in the large angle scattering region of this experiment.

The analysis of the asymmetry in the scattering process when specific particles are inclusively produced is in progress with preliminary results indicating a small but positive asymmetry over all the region of projectile fragmentation and zero elsewhere. The result being independent of particle type.

EXPERIMENT 20

Study of exclusive hadronic processes at large p_T

CERN
University College London
University of Genova
University of Oslo
University of Paris-Sud

This is a proposal to be performed on the SPS, to study those reactions in which the only outgoing products are two charged particles, when $\pi^\pm$, $K^\pm$ and $p^\pm$ beam particles collide with protons. The primary intention of this project is to study these reactions up to the largest scattering angles at which significant statistics may be obtained, in order to try and observe effects arising from the inner structure of hadrons. Accordingly, the equipment is being designed to handle the highest feasible beam intensities (hopefully in the region of 10^8 p.p.s.) and to have a large acceptance up to $\Theta_{cm} = 90°$.

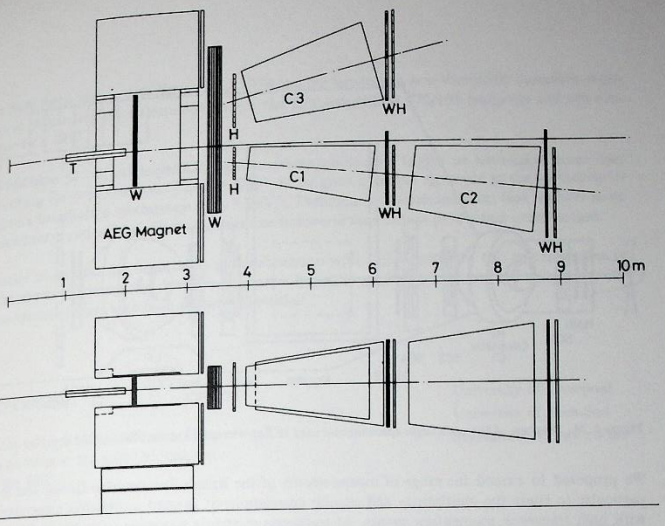

Figure 1.28. Proposed general arrangement for Experiment 20 at the SPS.
Key: T – liquid hydrogen target W – multiwire proportional detectors H – trigger scintillation counter hodoscope C – atmospheric pressure Cerenkov counters. (18580)

The equipment will be mounted in the West Hall, in the E1′/H1′ beam line. Particle momenta up to 80 GeV/c will be available in this beam. It is intended to obtain data at 20, 40, 60 and 80 GeV/c.

The proposed equipment, the details of which are still subject to slight modification, is shown in Fig.1.28. The beam has been designed to have relatively large transverse dimensions (8 x 8cm) and a very small divergence (0·03 mrad) at the target position. The hydrogen target, T, is 10cm diameter by 1m long. It protrudes slightly into a spectrometer magnet, in order to obtain an optimum acceptance. Scattered particles are momentum analysed and their trajectories are determined by the blocks of multiwire proportional chambers labelled W in the figure. Scintillation counters hodoscopes, H, are used to trigger the read-out system. These hodoscopes will require very loose angular correlation criteria to be satisfied by candidates. Atmospheric pressure threshold Cerenkov counters C1, C2 and C3 are installed in order to identify the outgoing particles.

Construction of the main components for this experiment has begun, although it is still at a very early stage. It is intended to have the equipment available on the beam line during the Summer of 1976, in anticipation of a possible early start of SPS operation.

EXPERIMENT 21

Study of high transverse momentum behaviour at the ISR

University of Liverpool
Daresbury Laboratory
Rutherford Laboratory

This experiment is an extension of the investigation begun by the British-Scandinavian Group using the Wide Angle Spectrometer at Intersection 2 of the CERN ISR. The Spectrometer (Fig. 1.29) is able to measure single-particle inclusive cross-sections between $\sim 35°$ and 90° centre of mass angle. Complete separation of π K and p is possible, in the momentum range 1·6 - 5·1 GeV/c using the two gas Cerenkov counters.

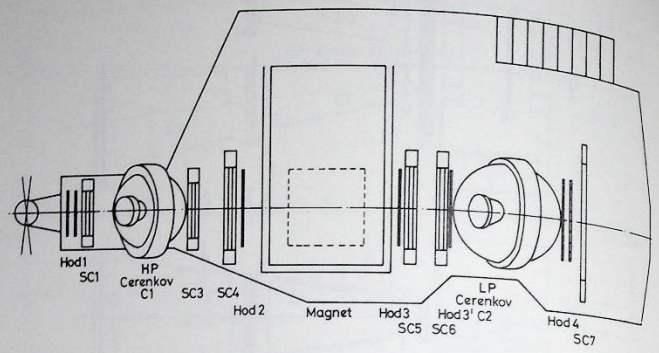

Figure 1.29. Diagram of the wide angle spectrometer used in Experiment 21 at the ISR: (18581)

We proposed to extend the range of measurements of the British-Scandinavian Group and in particular to study the multiplicity and angular correlations of charged secondaries associated with high transverse momentum events. At transverse momenta accessible to us the inclusive cross-section shows marked deviations which are not well understood from the low transverse momentum behaviour. With the additional multiplicity information and our ability to identify K and p secondaries it is hoped to improve on this situation.

The multiplicity detector (Fig.1.30), designed in consultation with the CERN-Holland-Lancaster-Manchester (CHLM) collaboration, whose experiment also makes use of the information it provides, was installed in the January 1974 shutdown. Its total solid angle coverage is $\sim 99\%$. The main detector is a barrel shaped assembly of scintillation counters surrounding the bicone. It is divided into eight "octants" of longitudinal strips and lateral hoops which provide detailed information on the polar and azimuthal distributions of secondaries. It is supplemented by counters covering the ends of the barrel and by large spark chambers on either side to resolve any particle jets in the central region.

Figure 1.30. The multiplicity detector used in Experiment 21. The main detector is a barrel-shaped arrangement of scintillation counters surrounding the intersection region bi-cone. The counters are arranged to provide detailed information on the polar and azimuthal distributions of secondary particles. The total solid angle coverage is ~99%: (18582)

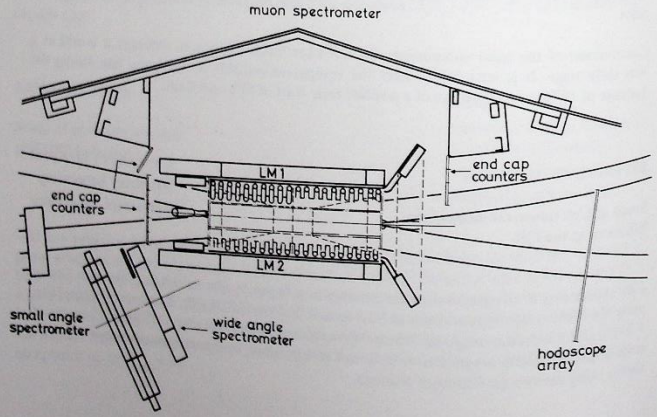

We have been taking data throughout 1974 and our program is now essentially complete. Analysis is proceeding via a telephone link to the Rutherford IBM 370/195 computer and will continue into 1975.

In addition to our single-particle high transverse momentum trigger we have taken some data searching for ϕ production. The $\phi \rightarrow K^+K^-$ decay gives a unique signature in the spectrometer above a threshold ϕ momentum of ~ 3 GeV/c. Preliminary analysis indicates that we have some ϕ candidates and will be able to measure the transverse momentum production cross-section.

Finally some data has been taken in collaboration with CHLM with the two spectrometers in coincidence. Although the data rate is low it is hoped to produce interesting and unique correlation measurements with both particles identified.

EXPERIMENT 22

University of Liverpool
University of Paris-Sud
Scandinavian Universities

Study of high transverse momentum phenomena in the split field magnet at the ISR

This experiment will study particle correlations associated with large transverse momenta events using the split field magnet (SFM) at the ISR.

The spectrometer currently being used at the ISR by the Daresbury-Liverpool-Rutherford collaboration will be used to trigger the SFM detectors in order to select the rare high P_T secondaries at 90°. This spectrometer can clearly separate pions, kaons and protons in the momentum range from 0·8 to 5·0 GeV/c. particle correlations associated with such triggers will be studied with the help of large solid angle counter hodoscopes around the SFM detector system. In particular with suitable arrangement of these hodoscopes it will be possible to look at the effective mass distribution for pairs including K and Λ, a search of considerable interest in view of the recent observation at Brookhaven and SPEAR of new heavy particles in the 3 to 4 GeV range.

During the year the compatibility of the spectrometer with the SFM and its detectors has been investigated in collaboration with the SFM group and ISR engineers. Parts for the modified system are presently being manufactured in the Liverpool workshops. The large hodoscopes have already been built for the MIT-Orsay-Scandinavian experiment at the SFM.

The experiment has been provisionally scheduled to run in the second half of 1975.

EXPERIMENT 23

University of Bristol
University of Liverpool
University College London
University of Bergen
University of Lund
University of Copenhagen
University of Stockholm
CERN
Rutherford Laboratory

Study of particles produced at large angles

The Wide Angle Spectrometer (ref. 3, 4)

The programme of measurements of inclusive single charged particle production at all ISR energies was completed by the end of 1973. The data covered the range of transverse momentum, 0·2 GeV/c $\leq P_T \leq$ 4·7 GeV/c and the range of centre of mass rapidity $0 \leq Y_{cms} \leq 1{\cdot}2$. The analysis of these data was completed in 1974.

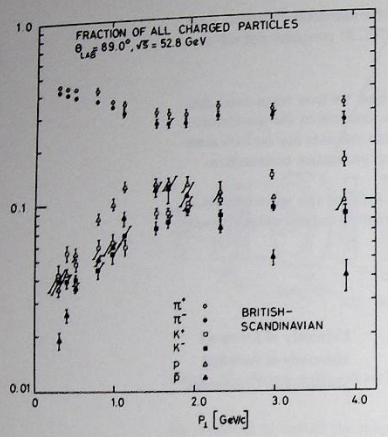

Figure 1.31. Variation of particle composition with transverse momentum in pp interactions: Experiment 23 (18551)

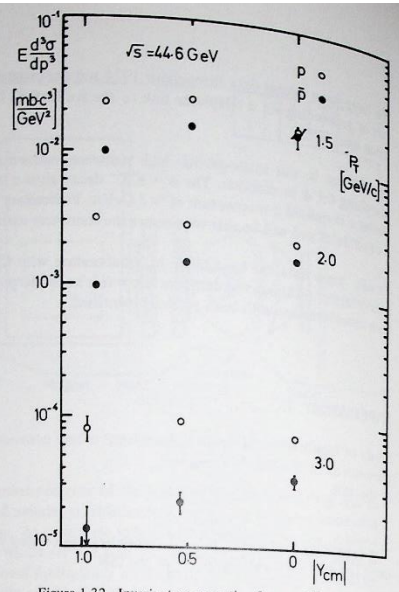

Figure 1.32. Invariant cross section for p and $\bar{p}$ versus rapidity: Experiment 23 (18562)

The main features of the variation of particle composition with transverse momentum can be seen in Fig.1.31. One of the striking features of the data is the rapid increase with P_T of the excess of K^+ over K^- and of p over $\bar{p}$ in the high P_T region. This effect is consistent with quark structure models of the protons but is inconsistent with those models where pair-production is the dominant mechanism contributing to high P_T events. The dependence of the invariant cross-section on rapidity (Y cms) is displayed in Fig.1.32, for p and $\bar{p}$. Here the ratio p:$\bar{p}$ is seen to increase rapidly with increasing Y cms as well as with P_T.

The analysis of correlation data taken with the spectrometer run in coincidence with the large solid angle magnetostrictive spark chambers of the muon detector has been completed. A linear increase with P_T of the associated multiplicity in the chamber opposite to the spectrometer particle was observed, whereas on the same side as the spectrometer the correlation was approximately independent of P_T and positive.

The Muon Detector

The experiment was performed to search for muons with high transverse momentum as evidence of the existence of a massive new particle (for example the Intermediate Boson) which has a muon decay. Other sources of muons at the ISR are from the decays of π and K mesons and from cosmic rays.

During 1973 the detector was improved to reduce the background muons from meson decay. The number of muons observed at low transverse momentum are in excellent agreement with the predictions of a Monte Carlo simulation of the experiment.

Care has been taken to eliminate background muons from cosmic rays and to date no signal from massive muon particles has been observed to a cross-section limit of

$$\frac{d\sigma}{d\Omega} \quad (pp \rightarrow \mu^{\pm} + \ldots) \leq 5 \times 10^{-36} \text{ cm}^2/\text{st. (90\% C.L.)}$$

This result can be used with theoretical models to set mass limits for the Intermediate Boson as seen in Fig.1.33.

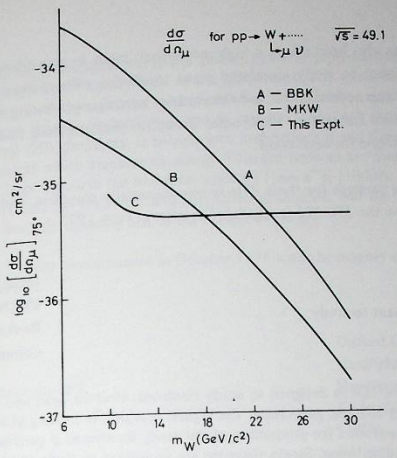

Figure 1.33. Limits on the mass of the postulated intermediate boson: Experiment 23 (18552)

EXPERIMENT 24

Study of inclusive particle production at very low p_T and x = 0

CERN
University College London
University of Bristol
Massachusetts Inst. Tech.
Niels Bohr Institute
University of Stockholm

The apparatus for proposal 131, consisting of a small magnetic spectrometer using multiwire proportional chambers (Fig.1.34), was installed in intersection 8 of the ISR at the beginning of 1974. Data were taken throughout 1974, and the experiment was dismantled at the beginning of 1975. At all five ISR energies, data have been obtained using the Terwilliger scheme to produce a short interaction diamond to match the acceptance of the spectrometer. These data will be used to extend the existing single charged particle inclusive cross-sections at x = 0 to low transverse momenta, normalisation being performed by using the total cross-section experiment of the Pisa-Stony Brook Collaboration as a monitor. During the non-Terwilliger runs, data have been obtained on π° production by detecting electron pairs.

Figure 1.34. Side view of the low p_T 90° spectrometer for Experiment 24: (18583)

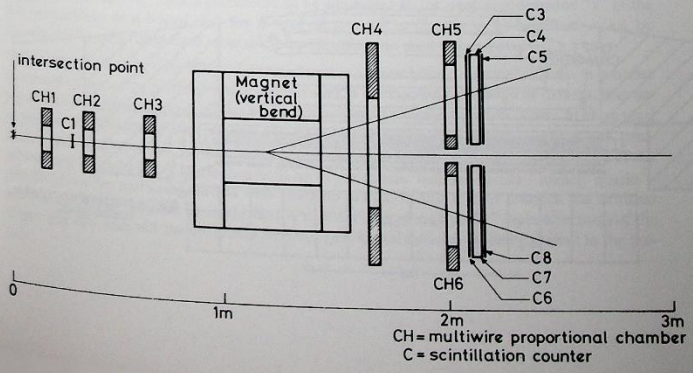

The spectrometer has also been run in a high momentum mode in coincidence with the Pisa-Stony Brook experiment to study correlated event topologies with charged particles at 90°. During the course of this collaboration, use was made of hardware processing equipment, developed by the Rutherford Laboratory Electronics Group, to perform track finding and momentum determination on-line for each event.

The analysis program package for these data is now essentially complete, and production running of the analysis on the 370/195 is scheduled to start in early 1975.

EXPERIMENT 25

ISR solenoid experiment to study electron production

Oxford University
CERN
Rockefeller University
Columbia University

This experiment at the ISR is designed to study electrons, electron pairs and π^0's produced in association with other charged particles at the highest energies. In looking at electron pairs, we can measure the cross-section for production of the newly discovered ψ particles and search for similar particles of higher mass. Single electrons are important to study because they may be associated with the production of other new particles such as the Intermediate Vector Boson or "charmed" particles. The apparatus is designed to measure the momentum of charged particles and the energy of π^0's and K^0's which accompany the electron. This electron-hadron signal will be a clear indication of the presence of new particles. We will also see events which are purely hadronic, and with these we will look for high transverse momentum correlations as are expected in parton models of the proton.

Figure 1.35. ISR solenoid experiment: horizontal section of the apparatus through the plane of the intersecting beams: Experiment 25 (18589)

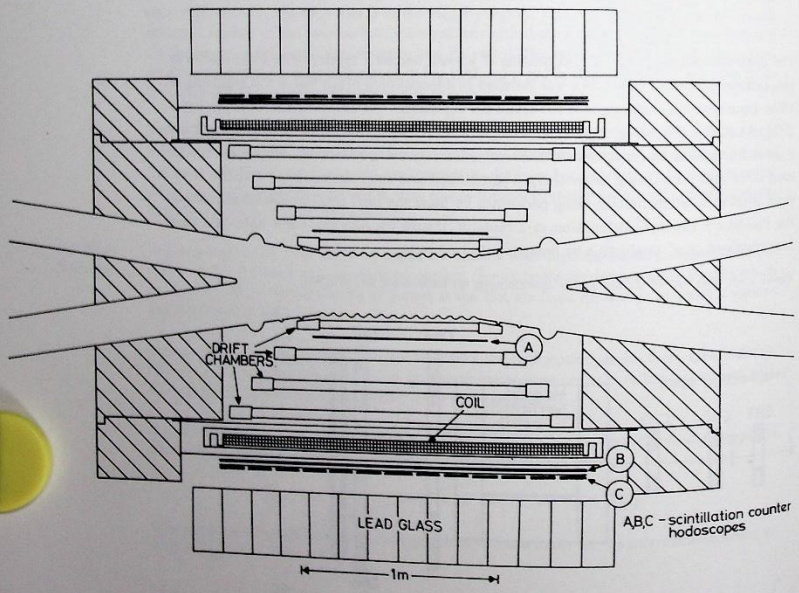

Fig.1.35 shows a section of the apparatus in the median plane. A superconducting solenoid surrounds a high luminosity intersection region of the ISR beams. The solenoid field is 1·5 T and is uniform to a few percent throughout a volume of 2·8 m^3. An electron emerging from the intersection region passes through hodoscope A and its trajectory through the field is measured by the four cylindrical drift chambers. It merges into hodoscopes B and C and finally showers in the lead glass counters which measure its energy. Charged hadrons are measured in the field but do not produce large signals in the lead glass while γ's from π^0's, produce showers. Counter A, the drift chambers, and the magnetic field cover the full azimuth, but the lead glass is arranged in two stacks, either side, covering half of the azimuthal range.

Installation at the ISR is due to commence in October 1976 with the magnet arriving during the 1976-77 winter shutdown.

EXPERIMENT 26

Neutrino experiments at the SPS

Oxford University
Westfield College, London
Hamburg University
Karlsruhe University
CERN
Rutherford Laboratory

From the start up of the SPS in Autumn 1976 it is planned to operate a neutrino facility in the West Hall. Two alternative ν beams will be available; a broad band horn focused beam, and a narrow band beam of special design. These beams, which will run alternatively down a single beam line, would serve all 4 planned neutrino experiments. The four detectors, 2 bubble chambers and 2 counter experiments, will lie one behind the other on the sloping "West area neutrino ramp". The beams pass through all 4 experiments and on into space. The neutrinos will therefore pass through several hundred tons of target and detector; such large target mass being essential in view of the smallness of the neutrino cross sections (10^{-38} cm^2/GeV). It would take some 100 earth diameters to interact out most of the neutrinos from a 100 GeV ν beam.

The very property of the neutrino which makes it so difficult to study – namely its tiny interaction cross-sections – also makes it a unique tool for high energy physics research. It is the only particle known to science, which undergoes only weak interactions (WI). All other known particles have electromagnetic and strong interactions with matter, and as these are many orders of magnitude stronger than the WI, the WI processes are normally masked although they are in fact occurring "underneath". The new intense neutrino beams will make it possible to study in some detail weak interaction scattering processes at very high energy (up to 300 GeV) and at very high momentum transfer (very small impact distances) up to q^2 of 500 $(GeV/c)^2$.

The subjects to be studied in this research would include:

a) Does the basic framework of the WI remain unchanged up to the highest value of E_ν and q^2?

b) The theory has for many years suggested that the WI may be carried (propagated) by a heavy boson particle the "W" this is considered to be equivalent to the photon propagator "γ" of the EM interactions. It is hoped that the W may be seen either directly or by implication (e.g. by causing the linearly rising total cross section with energy to start to bend over).

c) The neutrino having only WI can be considered as a "point-like projectile". This is in contrast to strongly interacting particles which are pictured as surrounded by a cloud of mesons, thus being diffuse and uncertain in both size and composition. Hence the neutrino is seen to be an ideal projectile for "X-raying" the internal structure of the sub-nuclear particles (proton and neutron). Thus the theoretical picture built up over the past decade of SU(3) symmetry and of the sub-nuclear particles being themselves built up of yet smaller building blocks – namely quarks – can be tested by scattering studies with neutrino beams. In this area of research the neutrino has the additional valuable property that it is sensitive to the "helicity" (spin direction) of the target and can thus tell the difference between quarks and anti-quarks being present in the proton.

d) It is possible that with the very high bombarding energies available new weakly interacting particles may be discovered, such as the proposed "heavy lepton". It is hoped that charmed particles may also be produced and studied in neutrino experiments.

e) A new type of weak interaction, "the neutral current process" has been discovered in the past year. It still remains to study this process in detail, even to determine whether it is parity violating or not. It is proposed to look in detail at neutral currents in the experiment discussed here.

The design of the apparatus for this experiment is shown in Fig.1.36.

Neutrinos can interact and be studied from two regions:

(i) Those that interact in the 5m long H_2/D_2 target;
(ii) Those that interact in the liquid Argon-Iron calorimeter/target.

The events of type (i) will be fewer in number by two order of magnitude but make it possible to study the individual processes $\bar{\nu}n$, νp and $\bar{\nu}n$ and $\bar{\nu}p$. This will be the first counter experiment to do this. The apparatus is designed to study two basic types of neutrino interaction namely charged currents, where the ν changes into a charged muon, and neutral currents, where it remains unchanged:

$$\nu + \text{Target} \rightarrow \text{Hadrons} + \mu$$

$$\nu + \text{Target} \rightarrow \text{Hadrons} + \nu$$

The concept of the experiment is similar in both cases, namely that the hadrons from the primary neutrino process are allowed to shower in the liquid Argon/Iron calorimeter. The calorimeter operates as a set of 1,600 separate ionization chambers, the ionization being collected from liquid Argon, as the medium, on to 3mm thick steel electrodes. The 3m x 3m cross-section is covered by sets of 3m x 10cm steel strips, the strips running in alternate layers vertically and horizontally to give spatial resolution for the device in these two dimensions. The hadronic showers will be typically 2m long. There will be 1,600 pulse height channels to record the energy deposited in each of the 1,600 independent calorimeter cells. The sum of the signals will give the energy that the neutrino transferred to the hadrons to an accuracy of a few percent. From the pattern of energy deposited in the various cells the hadron shower direction can be determined. Large angle muons from the charged current process can be recognised by the hit pattern they make in some of the 1,600 calorimeter cells. Muons of intermediate and small angle pass through a number of calorimeter tanks and on into the solid iron muon spectrometer magnet (to be built by the CERN/Saclay/Dortmund/Heidelberg group). Their direction is obtained from the drift chambers in between calorimeter tanks and their momentum from the muon spectrometer.

Part of the time the apparatus will receive the "narrow band" (NB) or "dichromatic" beam that has been designed to have a high intensity and good ν energy definitions. Event rates of 100,000 for a 100-day run have been predicted for a NB neutrino beam. Part of the time the broad band beam will be run, giving event rates of $\sim$ 100 times higher. Because the neutrino energy is not known for each individual event in a broad band beam, the experiments become much more difficult.

In the case of the charged currents sufficient quantities are measured in the apparatus (θ_H, E_H, θ_μ and P_μ) to make it possible to calculate the unknown neutrino energy (E_ν) and to fully constrain the events kinematically. Therefore useful work can be done in the broad band beam. In the case of the NB beam, there is a good knowledge of E_ν from the beam itself, and so a stringent energy cross check can be made $E_\nu = E_H + E_\mu$ thus making the NB experiments more reliable.

The neutral current experiment is much more difficult; a neutrino comes out from the interaction with neither its energy nor its direction measured. Hence the only quantities known are: E_H and θ_H, plus E_ν for a NB experiment. Thus only in the case of a NB experiment can the

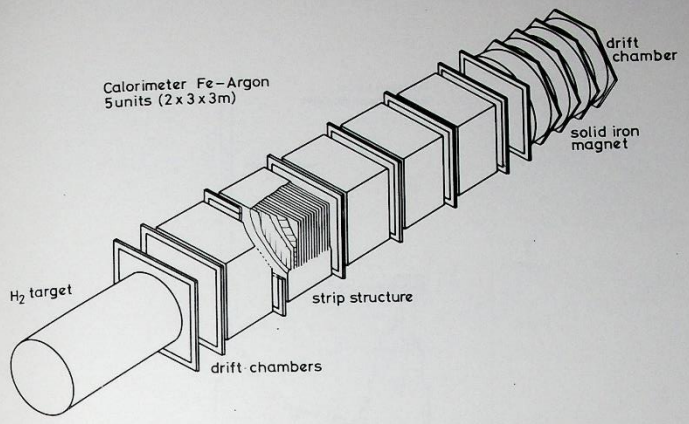

Figure 1.36. Isometric view of the proposed apparatus to study neutrino interactions at the SPS showing 5 units of a fine grain calorimeter, drift chambers and a solid iron magnet: Experiment 26 (18584)

kinematics of the neutral current process be determined, and even then with no spare measured quantity to allow a cross check. The "fine grain" calorimeter made possible by this new liquid Argon ionization technique offers the best hope for a detailed study of the neutral current process.

EXPERIMENT 27

Muon-nucleon scattering

University of Chicago
Harvard University
University of Illinois
University of Oxford

This experiment attempts to probe the internal structure of the nucleon by scattering high energy muons off protons and neutrons. The electromagnetic interaction between charged leptons (muons or electrons) and nucleons is mediated by virtual photons whose mass, energy and polarisation can be varied by the choice of scattering angle and energy. Thus muon scattering permits the separation and measurement of the nucleon structure functions.

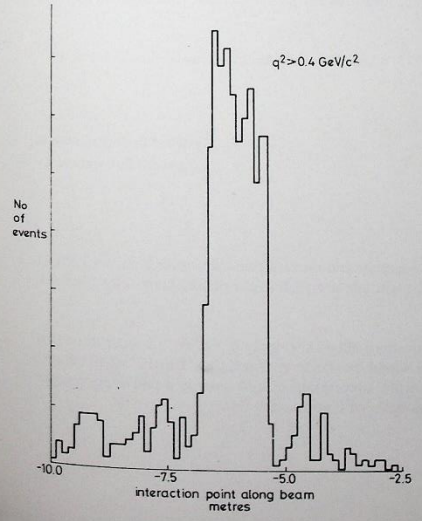

Figure 1.37. Interaction point distribution along the beam direction for $\mu + p \rightarrow \mu +$ anything. The position of the hydrogen target is clearly visible: Experiment 27 (18585)

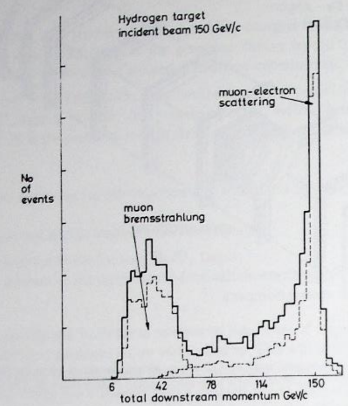

Figure 1.38. Total spectrometer momentum for $\mu + p \rightarrow \mu$ + anything. Dashed lines show the contributions from muon bremsstrahlung and muon-electron scattering. The solid line is the sum of all contributions: Experiment 27 (18586)

The building of the muon scattering facility was completed in 1973 and, with continuous improvements to the FNAL muon beam, two high intensity data-taking runs were made in 1974 with muon beams of 150 GeV and 5 to 8 x 10^5 muons per pulse. The first run in May used a liquid hydrogen target while the second run in July used deuterium. Some 500,000 triggers were recorded and this should yield 50,000 nucleon scatters.

The analysis of the data is in an advanced state. Fig.1.37 shows the interaction point distribution along the beam direction. The hydrogen target is clearly visible. Fig.1.38 shows the sum of the momenta of all particles accepted by the spectrometer. The principal interactions seen are muon bremsstrahlung, muon electron and muon nucleon scattering.

The first results from this analysis are expected in 1975 and will give information on the nucleon structure functions, some detailed measurements of the inclusive hadron behaviour and rho production.

Further data-taking is expected in 1975 when the muon beam intensity should reach 10^6 muons per pulse.

EXPERIMENT 28

Westfield College, London
Rutherford Laboratory

Search for the C-violating decay
$\eta \rightarrow \pi^\circ e^+ e^-$

(ref. 70) The final analysis of the data is almost complete and the result should provide an upper limit to the decay rate $\eta \rightarrow \pi^\circ e^+ e^-$ an order of magnitude smaller than the present limit of less than 4 x 10^{-4}.

C invariance (particle-antiparticle substitution) allows the decay $\eta \rightarrow \pi^\circ e^+ e^-$ to occur through a two photon exchange process, but this would be at a level of less than 1 in 10^9 of all decays, well below the level of current experiments. Observation of such a decay would imply a single photon exchange process and hence a violation of C invariance.

EXPERIMENT 29

University of Bristol
University of Geneva
University of Heidelberg
University of Lausanne
Lab. de L'Acc. Lin., Orsay
Rutherford University
CRN, Strasbourg-Cronenburg

Experiments with high energy charged hyperons at the SPS

A special compact beam line has been designed for the West Area at CERN in order to study the interaction and decay properties of the short lived charged hyperons, Σ^+, Σ^-, Ξ^- and Ω^-. The first stage of the programme which is a study of the weak leptonic decays:

(i) $\Xi^- \rightarrow \Lambda e^- \bar{\nu}$, $\Lambda \rightarrow p\pi^-$

(ii) $\Xi^- \rightarrow \Sigma^\circ e^- \bar{\nu}$, $\Sigma^\circ \rightarrow \Lambda\gamma$, $\Lambda \rightarrow p\pi^-$

(iii) $\Sigma^- \rightarrow \Lambda e^- \bar{\nu}$, $\Lambda \rightarrow p\pi^-$

and if possible

(iv) $\Sigma^+ \rightarrow \Lambda e^+ \nu$, $\Lambda \rightarrow p\pi^-$

has already been approved. Thus the target of the charged hyperon beam will be one of the first to receive 200 GeV protons when the CERN SPS comes into operation in 1976.

The Cabibbo theory has been remarkably successful in fitting with three free parameters all the existing data on the leptonic decay transitions between the states of the baryon octet. However, there is still a strong demand for more accurate measurements in order to check thoroughly the validity of the Cabibbo theory, in particular the absence of second class currents. In view of the large SU(3) breaking effects observed in strong interactions it will be extremely interesting to discover at what level and in what way the Cabibbo description fails for the baryon leptonic decay.

Studies of decays (i) and (ii) are particularly attractive since the Λ and Σ° polarisations can be measured via their parity violating decays. This allows both the magnitude and the sign of the form factor ratio g_A/g_V to be measured for each of the decays.

It is expected that it will be possible to perform experiments with the beam tuned for positive particles although it is difficult to calculate the proton background in this case. We hope to make a direct comparison of decays (iii) and (iv) to test for the presence of second class currents. It is possible that the presence of second class currents would not lead to an anomalous ratio between the decay rates but that they might be detected in polarisation measurements. Again the parity violating decay of the final state Λ makes such measurements straightforward in the proposed beam.

The mean lifetimes of the charged hyperons are all in the region of 10^{-10} seconds. Thus for example at 100 GeV/c a Ξ^- travels only 5 metres on average before decaying. The basic problem in designing a charged hyperon beam is to make it as short as possible and still provide adequate shielding against the background radiation produced by the target and the proton beam dump.

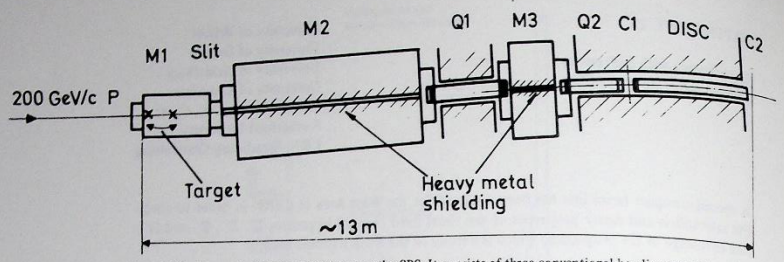

Figure 1.39. Layout of the hyperon beam at the SPS. It consists of three conventional bending magnets and two superconducting quadrupoles. It is designed to select the momentum of secondary particles up to 150 GeV/c and also to sweep away muons which penetrate the shielding: Experiment 29 (18587)

A layout of the beam is shown in Fig.1.39. It consists of three conventional bending magnets and two superconducting quadrupoles. The bending magnets are designed not only to select the momentum of secondary particles up to 150 GeV/c but also to sweep away from the apparatus muons which penetrate the shielding. The narrow beam channel in the magnets is surrounded by high density lead, tungsten and uranium shielding. The quardupoles serve to make the beam parallel as it emerges from the channel allowing identification of the various particle types with a DISC counter.

Expected particle fluxes for 10^9 protons interacting in the target are shown in the Table. In addition there should be usuable numbers of $\bar{\Omega}^-$'s.

Table: Expected particle fluxes per 10^9 protons interacting in the target

Particle	π^-	π^+	$\bar{p}$	p	Σ^-	Σ^+	Ξ^-
150 GeV/c; 3 mrad prod. beam length: 12·9 m	3×10^4	7×10^4	10	4×10^6	$2{\cdot}8\times10^3$	$2{\cdot}75\times10^3$	3·1
75 GeV/c; 6 mrad prod. beam length: 11·9 m	2×10^5	5×10^5	$2{\cdot}2\times10^3$	5×10^5	$1{\cdot}7\times10^2$	3·3	2·7

Figure 1.40 300 GeV hyperon beam experimental set-up: Experiment 29 (18588)

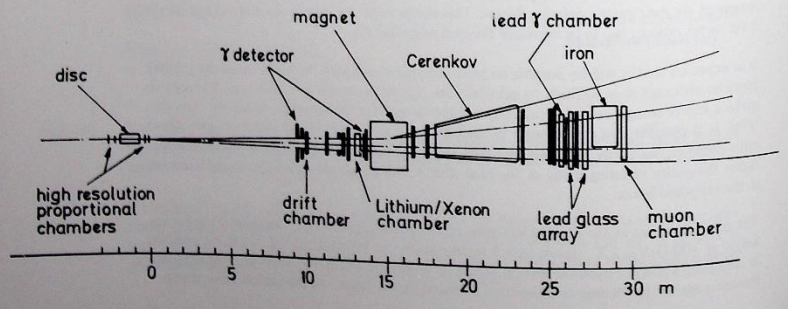

A schematic plan of the experiment is shown in Fig.1.40. It basically consists of a magnetic spectrometer with drift proportional chambers to measure the momentum and direction of the hyperon decay products. The most difficult problem is to separate the rare electronic decays from the non leptonic decays which occur roughly a thousand times more frequently. Electrons are identified in a large lead glass array, a large threshold gas Cerenkov counter and a lithium foil-xenon gas proportional chamber assembly which detects transition radiation. Gamma rays from Σ° decays in process (ii) are detected in the lead glass array and in three lead-scintillator hodoscopes.

The momenta and directions of particles in the beam are measured with very high resolution wire proportional chambers situated before and after the DISC counter.

The Rutherford Laboratory and Bristol University are supplying the large lead glass array, the gas Cerenkov counter, the gamma-ray hodoscope together with associated electronics, the lithium foil stack for the transition radiation detector and the on-line computer for the experiment.

Bubble Chamber Experiments

The distinction between bubble chamber experiments and counter experiments becomes less clear each year. 1974 saw the successful operation of two hybrid systems at SLAC, combining the advantages of the two techniques. At the Laboratory, the Rapid Cycling Vertex Detector (RCVD) is expected to come into operation in 1975. However, the major effort of many bubble chamber groups is still concentrated on the conventional bubble chamber experiments.

Track sensitive targets

The technique of using a track sensitive target (TST) has proved successful for studying certain classes of events that are very difficult to observe by other techniques. The TST consists of a perspex walled target filled with liquid hydrogen situated inside the bubble chamber containing a neon-hydrogen mixture. Both regions are sensitive to charged tracks. Beam particles introduced into the target interact with free protons, then their reaction products in general pass into the neon-hydrogen mixture, which serves as an efficient detector of γ rays (e.g. from π°, η° or Σ°).

The Laboratory has been collaborating on installing a TST in the 12 foot chamber at the Argonne National Laboratory. Preliminary tests of this system have been successful and physics runs are expected during 1975. The Laboratory group has proposed a $\bar{p}$ experiment in this chamber, and also a neutrino experiment in a TST in the BEBC chamber at CERN. The use of much larger chambers leads to higher conversion probabilities and secondary interaction rates, making the system much more useful for the detection and reconstruction of multi-π° events.

Rapid Cycling Vertex Detector

The major limitation of many bubble chamber experiments has been the lack of statistics in rarer reactions. To overcome this problem, but retain the major advantages of the bubble chamber technique – good spatial resolution and essentially 100% track detection efficiency in all directions – hybrid systems have been developed. One such system is a rapid cycling bubble chamber as the target and near vertex track detector, with electronic detectors to trigger the photographing of the desired events and to provide additional track information. The system being built at the Laboratory consists of a cylindrical bubble chamber 30 cm in diameter, which will be expanded at the rate of 60 cycles/second. The amount of matter immediately surrounding the chamber is kept to a minimum to facilitate the detection of particles outside the chamber. The whole system will operate inside the magnetic field of some 20 kG (provided by the magnet of the old Helium Bubble Chamber). This technique will make possible experiments at the statistical load of 500 events/μb (compared with some 30 events/μb from a large experiment in a conventional bubble chamber).

The first experiment in the chamber (see Experiment 42), which will study the production of S = −2 resonances, is planned to run in late 1975 and the special beam line and triggering electronics to control photography are under construction. Later experiments will include the external information as part of the experimental data.

Conventional B.C. Experiments

During the past year two high statistics "second generation" conventional bubble chamber experiments have produced interesting new results on N* and Y* resonance formation. The IC-Westfield low energy π^+p experiment (Experiment 32) has completed isobar model partial wave analyses of the N$\pi\pi$ reactions, complementing the recent results from the SLAC-Berkeley analyses. The RL-IC low energy K$^-$p experiment (Experiment 38) have performed energy dependent partial wave analyses of the two body reactions over a wide range, including their new data in the 1775-1960 MeV cm energy range. Analysis is also commencing on the K^0_L p data (Experiment 36), which will provide useful constraints on the S = −1 partial wave solutions, together with interesting information on the S =+1 (Z*) amplitudes.

The amplitude analysis technique of analysing three meson systems (Ascoli analysis) has been successfully applied in several experiments. In the 4 GeV π^+d experiment (Experiment 30) analysis of ρ production of 2π systems and detailed analysis of the ω° production in 3π systems have used this technique. Similarly the K$\pi\pi$ systems have been analysed in the K$^+$d experiment at 2 to 3 GeV/c (Experiment 34) and the 14 GeV/c K$^-$p experiment (Experiment 39). All these have illustrated the power of this analysis method when good high statistics data are available.

The 14 GeV/c K$^-$p experiment has also produced much new data on various inclusive reactions, providing tests of scaling and triple Regge models. Intensive searches have been made for narrow resonances in the light of recent discoveries, but these have proved unproductive.

The Cambridge group is currently analysing experiments using a high energy Λ° beam (Experiment 33) and a medium energy neutron beam (Experiment 35) in the CERN 2m chamber.

Data Processing

On the data processing side, major developments have taken place in two areas. An improved fitting procedure has been developed taking into account the non-linearity of the constraint equations. This has been implemented in the KINEMATICS program. A new post-Kinematics program operating under the CERN HYDRA system has been written, offering versatile selection methods. This program, ORACLE, is being used in place of the old JUDGE program.

BEBC

The big bubble chamber (BEBC) has suffered delays but the group should receive film from this chamber in 1975: three scan tables now set up for the BEBC film.

Bubble Chamber Experiments

Experiment Number	Proposal Number	Beam and Chamber	Collaboration
30	36	π^+; 4 GeV/c : CERN 2m (D_2)	University of Birmingham University of Durham Rutherford Laboratory
31	38	K$^-$; 2·1 GeV/c : RL, Heavy liq.	Free University of Brussels CERN Tufts University, USA University College, London Rutherford Laboratory
32	39, 86	π^+ ; 0·8 to 1·6 GeV/c ; RL 1·5m(H_2), Saclay 80 cm (H_2)	University of Cambridge Imperial College, London Westfield College, London
33	49, 82	Λ ; 0 to 2·33 GeV/c : CERN 2m (H_2)	University of Cambridge
34	56	K^+ ; 2 to 3 GeV/c ; RL 1·5m (D_2)	Imperial College, London Westfield College, London
35	85	n ; 1 to 3·5 GeV/c ; CERN 2m (H_2)	University of Cambridge
36	89	K°_L ; 0·4 to 0·8 GeV/c ; CERN 2m (H_2)	University of Bologna University of Edinburgh University of Glasgow University of Pisa Rutherford Laboratory
37	91	π^+ ; 4 GeV/c ; RL/TST (H_2,Ne)	CERN Lawrence Berkeley Lab. University of Turin Rutherford Laboratory
38	108, 159	K$^-$; 0·45 to 1·40 GeV/c ; CERN 2m (H_2)	Imperial College, London Rutherford Laboratory
39	109	K$^-$; 14·3 GeV/c ; CERN 2m (H_2)	Ecole Polytechnique, Paris CEN, Saclay Rutherford Laboratory
40	115	$\bar{p}$; 2 GeV/c ; RL/TST (H_2,Ne)	Tata Institute, Bombay University of Melbourne
41	117	K$^-$; 0 to 0·58 GeV/c ; RL/TST (H_2,Ne)	University College, London Free University of Brussels University of Durham University of Birmingham
42	119	K$^-$; 2·9 GeV/c ; RL/RCVD (H_2)	University of Oxford University of Rome CEN, Saclay College de France, Paris Rutherford Laboratory
43	122	Σ^- ; 50, 100 GeV/c ; FNAL 15 ft (H_2)	University of Cambridge
	127	π^+, K$^\pm$; 50 to 200 GeV/c ; FNAL 15 ft (H_2)	University of Cambridge
44	147	π^+, K$^-$; 6·7 GeV/c ; SLAC Hybrid Facility (H_2)	Imperial College, London
Experiments Proposed			
	162	$\bar{p}$; 2·6, 5·7 GeV/c ; ANL/TST (H_2,Ne)	Argonne National Lab., USA University of Melbourne Carnegie-Mellon University, USA Rutherford Laboratory
	134	π^- ; 22 GeV/c ; BEBC (H_2)	University of Oxford University of Pisa Rutherford Laboratory
	161	K$^-$; 45,65 GeV/c ; BEBC (H_2)	University of Glasgow CEN, Saclay Rutherford Laboratory
	160	$\nu, \bar{\nu}$; ∼30 to 70 GeV/c Wide Band; BEBC/TST (H_2,Ne)	University of Bari Free University of Brussels University College, London Rutherford Laboratory

EXPERIMENT 30

π^+d interactions at 4 GeV/c

University of Birmingham
University of Durham
Rutherford Laboratory

(ref. RL-74-106, RL-74-107, 26, 52, 53, 54, 55)

Altogether 735,000 pictures were taken in this experiment and the measurement of most of the film is now complete. Large data samples have been obtained for the charge exchange reactions

$$\pi^+ d \rightarrow pp\,\pi^+\pi^-$$

and $\pi^+ d \rightarrow pp\,\pi^+\pi^-\pi^\circ$

and significant samples are now available in many more channels.

Figure 1.41. Comparison of vector meson production data of Experiment 30 (solid circles) with photoproduction data (open circles) obtained at electron accelerators. The results are derived from two different solutions of an amplitude analysis of the ρ data: (18435)

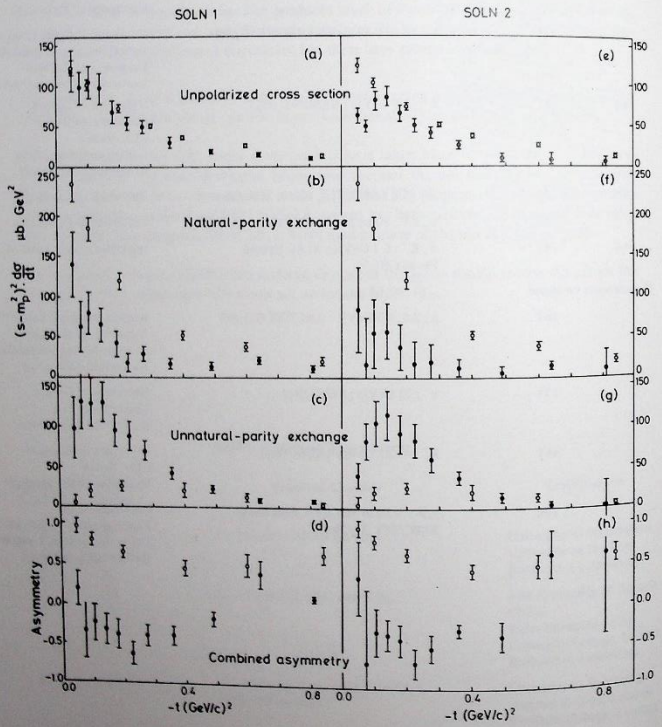

The study of boson resonance production, which is the main aim of this experiment, is continuing with a systematic study of 41,000 events corresponding to the second of these reactions. A detailed study of ω° production is nearing completion, while the recently-developed techniques of phase shift analysis of three pion systems are being applied to investigate the spin-parity content and the production mechanism over the whole $\pi^+\pi^-\pi^\circ$ mass range.

The availability of high statistics data from the above reactions together with an accurate knowledge of the relative normalization of these two channels, has made possible a comparison of the production of the vector mesons ρ° and ω° with the predictions of the vector dominance model, in which it is postulated that the photon, also a vector particle, couples to the strong interactions through these vector mesons. The results of a comparison of our vector meson production data with photoproduction data obtained in experiments at electron accelerators are shown in Fig.1.41. It is seen that there is agreement between the total cross-sections for the two processes, but that the agreement is not maintained when considering the separate contributions to the total cross-section from natural and unnatural parity exchanges.

The methods of three pion phase shift analysis, mentioned above, have been applied to the coherent reaction $\pi^+ d \rightarrow d\,\pi^+\pi^+\pi^-$, and the spin-parity content of the $\pi^+\pi^+\pi^-$ system determined. In other experiments the charged 3π system has been analysed in production both off free protons and off heavier nuclei, and, together with the deuteron data from this experiment, a consistent picture of this process is emerging.

A topic of current interest is the possibility that the deuteron, which is normally considered as a pn bound state, consists for some fraction of the time as a $\Delta(1236)$ $\Delta(1236)$ state. A contribution to the discussion of this possibility has been made using a data sample of 42,000 events from our experiment, and an upper limit of 0·8% has been determined for the $\Delta\Delta$ component of the deuteron.

EXPERIMENT 31

2·2 GeV/c K^- interactions in a heavy liquid bubble chamber

Free University of Brussels
CERN
Rutherford Laboratory
Tufts University, USA
University College, London

The film for this experiment was originally scanned for Ξ hyperons produced on complex nuclei. During the data analysis about 350 events were found with both a K^+ or K° and two Λ-hyperons produced. Some structure was found in the invariant mass spectrum of these Λ pairs. This led to a rescan of the entire film to find the remaining Λ pairs with no detected K^+ or K°. This rescan has been done and all the candidates have been measured. A total sample of 878 Λ pairs was obtained and these events have been carefully studied. No significant structure has been found in the final $\Lambda\Lambda$ mass spectra. This experiment is now completed. *(ref. 110)*

EXPERIMENT 32

π^+p interactions in the range 0·8 to 1·5 GeV/c

University of Cambridge
Imperial College, London
Westfield College, London

Film taken in the 80 cm and 1·5 m hydrogen bubble chambers at the Laboratory is being used to study π^+p interactions in the centre of mass energy range 1560 - 1930 MeV. The experiment has a total of 150,000 events at 14 energy points within this region. The data reduction is almost complete, with re-measurements at 4 of the momenta remaining. *(ref. 7)*

As outlined in last year's annual report, the main effort of this experiment has been on performing an isobar model partial wave analysis of the two single pion production channels $p\pi^-\pi^\circ$ and $n\pi^+\pi^0$ which dominate the inelastic cross section at these energies. Part of this data is particularly important because it lies within the infamous gap in the energy distribution of the Berkeley–SLAC collaboration analysis which led to solution ambiguities. The data at 1612 MeV which is at the centre of the gap agrees well with extrapolations of the Berkeley–SLAC solution B and disagrees with their solution A. Solution B is the one which is favoured by the theoretical predictions of ℓ-broken SU(6) and Melosh Transformations. This result has formed the subject of a SLAC–Berkeley–Imperial College–Westfield Collaboration paper which has been submitted for publication.

It is important to pursue an analysis independent of that of Berkeley–SLAC because experience with the elastic channel has shown that confidence in the results only comes as separate analyses converge on similar solutions. Our analysis differs in some respects from that made by the Berkeley–SLAC collaboration. An independent fitting program, written at Imperial College and based on the formalism of Deler and Valladas, has been used. Also the $n\pi^+\pi^+$ final state, ignored by Berkeley–SLAC, is fitted. In order to do so it was found necessary to introduce a $I = \frac{1}{2}$ isobar the $P_{11}(1470)$. Results obtained at three energies, 1612, 1641 and 1669 MeV were presented at the London International Conference. We have since analysed a further energy, 1694 MeV, and found results that follow the general trend of the first three energies. Our preliminary conclusions are that introducing the new isobar and fitting the $n\pi^+\pi^+$ channel do not change significantly the relative phases of the partial waves from those in solution B. Hence the agreement with $SU(6)_w$ is preserved. However significant differences from solution B are observed in the magnitudes of the partial waves.

A K-matrix program has been written at Imperial College to investigate the energy dependence between the energy independent solutions, and also to tie the results to the well known elastic partial wave solutions. Further analysis awaits more energy independent solutions at different energy values.

Doubts have been raised recently on the validity of the Isobar Model formalism. In particular it has been suggested that the constraints of three-body unitarity might invalidate the basic assumption that isobar couplings are constant across the Dalitz plot. An investigation into the magnitude of these effects in our data is under way.

EXPERIMENT 33 **University of Cambridge**

Hyperon proton interaction up to
24 GeV/c

Most of the stages in the processing of this experiment, are now finalised. The first stage yielded 22,000 Λ° decays, and 17,000 K°_s decays, and the association scan, identifying the sources of these decays, is now complete. All neutral induced source events are being measured as candidates for $\Lambda^\circ p$ interactions, and $np \rightarrow$ strange exclusive channels. Approximately 17,000 such events have been measured, and only a small amount of remeasuring remains to be done.

For possible $\Lambda^\circ p$ events, fits have been attempted in the channels

$$\Lambda p \rightarrow \Lambda p$$
$$\Lambda p \rightarrow \Lambda p\pi^+\pi^-$$
$$\Lambda p \rightarrow K^\circ_s pp\pi^-$$

trying both beam and non-beam hypotheses. In the case of non beam fits, a further association scan is being done, in order to find the sources of the Λ°s, thus enabling a 3 constraint fit to be carried out. Such associations have been found, and seem to indicate that 1C fits may be reliable in the case of the elastic channel, and possibly in the inelastic channels at low energies. In this case, about 100 elastic and 50 inelastic events will be obtained.

Fits have been attempted to $np \rightarrow$ strange exclusive channels with from 3 to 9 particles in the final state.

Some rough preliminary cross-section calculations, using the beam flux from the tagged neutron experiment, show the cross-sections for 3 and 4 body YK production channels to be fairly constant with energy (e.g. $\sim 30\mu$b for the $\Lambda pK^+\pi^-$ channel), while those for the higher topologies are rising rapidly with energy, and are now of similar magnitude. Cross-section for $K\overline{K}$ production, in contrast, are rising rapidly even in lower topologies. Ultimately the statistics in this experiment will be ~ 10 events/μb, corresponding to about 150 events in the best channels.

Events have also been found in the channel $np \rightarrow \Sigma^- K^+ p$ among the three-prong measured in the $np \rightarrow pp\pi^-$ experiment. So far, 109 fits have been obtained with momenta above 6 GeV, corresponding to a cross-section of $\sim 18\pm3\mu$b at 17 GeV. The events divide clearly into those with the $\Sigma^- K^+$ system produced backwards and forwards in the centre-of-mass frame; the cross-section for the former category seems to be falling with energy, whereas for the latter it is nearly constant.

Data on inclusive $pCu \rightarrow \Lambda^\circ X$ and $\pi^\circ X$ at the target is being obtained from the beam Λ° decays in the chamber, and the fast electron pairs which were measured with the Λ° decays. Some results for Λ and n production are shown in Fig.1.42.

Inclusive $np \rightarrow \Lambda^\circ X$ can be studied in the chamber for neutron and Λ° momenta above 10 GeV/c where the neutron spectrum is relatively uncontaminated.

Figure 1.42. Momentum distribution for n and Λ produced near 0° from inclusive data at 24 GeV/c. Experiment 33 (18702)

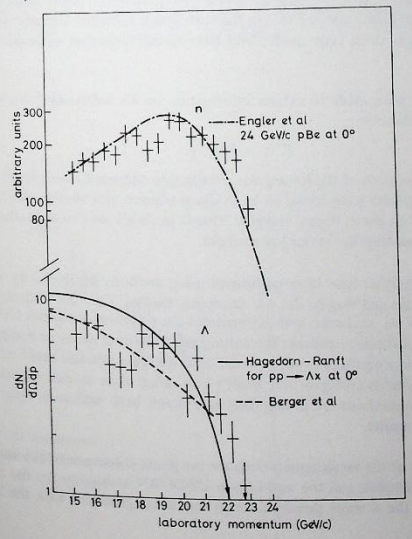

EXPERIMENT 34

Imperial College, London
Westfield College, London

K^+d interactions in the 2 to 3 GeV/c region

This experiment used the deuterium filled 1·5m bubble chamber at Nimrod. Final data summary tapes are now completed and detailed analyses of several channels has begun.

An "Ascoli" type partial wave analysis has been made of the $K\pi\pi$ system in the reactions

$$K^+n \rightarrow K^+\pi^+\pi^- n \quad (1)$$
$$\rightarrow K^0\pi^+\pi^- p \quad (2)$$
$$\rightarrow K^+\pi^-\pi^0 p \quad (3)$$

involving both charge exchange and non-charge exchange, at energies not much above Q threshold.

The charge exchange reactions have a slightly smaller forward slope for $d\sigma/dt$ than the non-charge exchange (slopes 3·1, 2·6 and 2·3 $(GeV/c)^{-2}$ for reactions 1, 2 and 3). In our data, the cross-sections rise with p_{beam}, but above p_{beam} = 2·7 GeV/c the cross-sections seem to go as p_{beam}^n with n = −1·1, −0·85 and −1·0 for reactions 1, 2 and 3 respectively.

$N\pi$ mass cuts to remove Δ production leave about 1000 events for each reaction. Only a few principal amplitudes and their variations with $K\pi\pi$ mass are well determined by the fits.

The total amount of unnatural parity final states (∼70%) is the same in both charge exchange and non-charge exchange reactions and this is also about the same as that found in corresponding reactions at much higher energies. However in the charge exchange reactions, the amount of 0^- (J^P) relative to 1^+ is about 3 to 1. This ratio is not very well determined, but is consistent between different mass bins and channels. In the non-charge exchange reactions, this ratio is about 1 to 1, compared with about 1 to 2 in the corresponding higher energy experiments. The predictions of a simple Deck type model have been found consistent with the results of this analysis.

Three attempts have been made to extract information on $K\pi$ scattering from approximately 15,000 events in the reaction

$$K^+n \rightarrow K^+\pi^- p$$

Firstly a linear extrapolation of the $K\pi$ angular distribution t-channel moments to the pion pole was performed. The results were found to be in disagreement with similar results from the reaction $K^+p \rightarrow K^+\pi^-\Delta^{++}$ at much higher energies. This is probably due to the failure of the pion exchange dominance assumption at our low energies.

Two $K\pi$ amplitude analyses have been performed using methods developed by 1) Estabrooks and Martin and 2) Ochs and Wagner for π-π scattering studies. The first of these makes the assumption of negligible A_1 exchange and extrapolates the s-channel moments to the pion pole. The second method additionally assumes the natural and unnatural parity exchange helicity one amplitudes are equal in magnitude, and, in order to investigate possible rapid mass variations, uses the t-channel moments averaged over small t-bins rather than an extrapolation. It is satisfactory that these two methods are in excellent agreement, both with each other and with the earlier $K^+p \rightarrow K^+\pi^-\Delta^{++}$ results.

The principal features of the resulting solutions are the phase coherence of the unnatural parity exchange P-wave amplitudes, and the well-known UP-DOWN ambiguity for the S wave at the K*(890) mass. Also, the S wave threshold behaviour is in agreement with the Weinberg soft meson theory.

In conclusion, the agreement of our low energy analysis of the reaction $K^+n \rightarrow K^+\pi^-p$ with the high energy $K^+p \rightarrow K^+\pi^-\Delta^{++}$ shows that these pion exchange models are in excellent shape and one can consider large statistics experiments of this type for the new multiparticle spectrometers such as Omega or RMS.

Analysis has also been completed on the full data of the K^+n charge exchange channel

$$K^+n \rightarrow K^0p$$

The additional data has reinforced earlier conclusions about the lack of acceptable models to explain simultaneously this and other $0^-\frac{1}{2}^+$ scattering in this s range. The full data gives no hints of any Z*.

Also being studied currently are the events with the deuteron in the final state, and a closer analysis of s-channel effects in the single pion production channels.

EXPERIMENT 35

University of Cambridge

"Tagged neutron" experiments

Two experiments have been carried out on existing neutron beam film, at 3 GeV and at 10 to 24 GeV, with the primary purpose of determining absolutely the beam flux. This has been done by finding events in which a beam neutron scattered elastically from a proton, and the outgoing neutron induced a secondary interaction in the chamber. In particular, the elastic cross-section is determined (see Fig.1.43) from the number of secondary elastic scatters, so that the number of primary elastic scatters may then be used to determine the beam flux. Approximately 250 and 450 events of this type were found in the two experiments, enabling the beam to be normalized to about 15%.

In addition, it has been possible to examine the differential elastic cross-section down to momentum transfer $|t| = 0.02$ GeV^2, and to measure a number of cross-sections for other processes at the secondary vertex. In the 10 to 24 GeV experiment, the charge multiplicity distributions and inclusive distributions for production of p and π^- have been investigated, and found to be explicable in terms of analogous quantities in pp interactions.

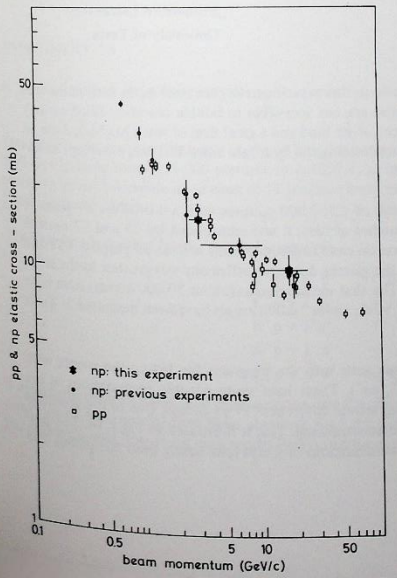

Figure 1.43 pp and np elastic cross sections: Experiment 35 (18703)

EXPERIMENT 36

University of Bologna
University of Edinburgh
University of Glasgow
University of Pisa
Rutherford Laboratory

$K^\circ_L p$ interactions in the range 400 to 800 MeV/c; Parameters of the τ and semi-leptonic decays of K°_L

The original exposure consisted of 520,000 pictures in the 2m chamber at CERN. This film has now all been scanned and measured, and the data is on data summary tapes and in the process of being analysed. The data from the extension taken August - September 1974 consisted of about 500,000 pictures in a new monoenergetic K°_L beam to the 2m chamber designed by the RL group. A K°_L flux increase of about a factor of 2 compared to the previous exposure was achieved despite using only 3 instead of 5 bunches from the proton synchrotron. This film is being currently scanned and measured. The main purpose of the experiment is to examine the strong interaction channels:

$$K^\circ_L p \rightarrow \Lambda^\circ \pi^+ \quad (1)$$
$$\rightarrow \Sigma^\circ \pi^+ \quad (2)$$
$$\rightarrow K^\circ_S p \quad (3)$$

Apart from covering the entire momentum range, film in the second exposure was also taken in fine energy intervals in the region of 1580cm energy where evidence for a narrow resonance in the $\Lambda\pi^\circ$ channel from K^-p interactions has been reported. The interest in channel (2) is in that it is a pure isospin state (I = 1) in contrast to the mixed isospin in $K^-p \rightarrow \Sigma^\pm\pi^\mp$. Thus the differential cross-section (and polarization) measurements will help to unravel the partial wave amplitudes in the $\Sigma\pi$ channel. Channel (3) is of interest since it contains the interference between S = -1 and S = +1 amplitudes and it is being studied to yield information concerning the Z* question.

The weak interaction part of the experiment is concerned with the decays $K^\circ_L \rightarrow \pi e\nu$, $\pi\mu\nu$ and $\pi^+\pi^-\pi^\circ$. These are being studied in their own right and also as a means of normalizing the strong interaction channels.

EXPERIMENT 37

CERN
Lawrence Berkeley Laboratory
Rutherford Laboratory
University of Turin

4 GeV/c π^+p in a track sensitive target

(ref. RL-74-035, 33, 56)

The track sensitive target (TST) was used in this experiment so that final states with more than one neutral could be studied. Such states are not accessible to bubble chambers filled entirely with hydrogen. It is the first experiment of its kind and a great deal of work has been done on the data analysis system so that the tracks leaving the hydrogen filled TST and entering the surrounding neon can be correctly treated.

The data was taken in 1972 with a total of 1,362,000 pictures with a 4·0 GeV/c π^+ beam. A steel framed TST was used for two batches of film; it was surrounded by 73 and 77 mole % neon concentration. A further batch was taken (516,000 pictures) with an all purpose TST and 80 mole % neon concentration. Since the gamma detection efficiency was greatest in the latter exposure, we have analysed this first. The first measurements (about 30,000 events) have been completed at the Laboratory and LBL, while about 10,000 events have been measured at Turin and CERN.

During this year considerable effort has gone into the programs for fitting the events with several neutral particles, ($\pi^\circ\pi^\circ\pi^\circ$, $\pi^\circ\pi^\circ$, $n\pi^\circ$). These have many possible permutations of the observed gamma rays thus reconstructing several different $\pi^\circ \rightarrow \gamma\gamma$ decays. One of the problems in selecting events is the presence of bremsstrahlung. This is illustrated in Fig.1.44. The programs for extracting the most probable combinations of γ rays have nearly been completed. The

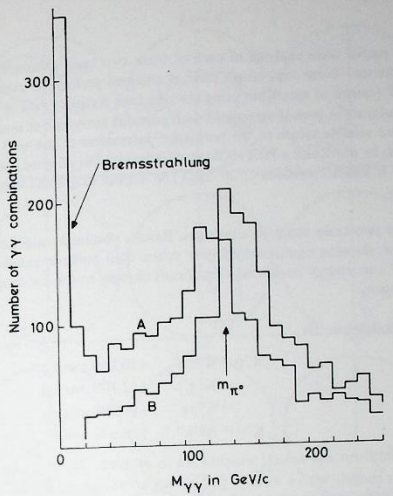

Figure 1.44. The $\gamma\gamma$ mass distribution. Curve A is all $\gamma\gamma$ candidates from 2,000 measured events. Curve B is the remaining $\gamma\gamma$ combinations after all bremsstrahlung γ have been measured: Experiment 37 (18547)

new program, ORACLE is being used to select events. It is anticipated that the data will be available shortly for a study of the reaction $\pi^+p \rightarrow \Delta^{++}\pi^\circ\pi^\circ$; the remeasures of events that failed in their first pass through. The program should be completed during 1975.

Preliminary results from the measurement of events on the HPD are encouraging. The events can be reconstructed with mean measurement errors on film of 2·5 μm, better than in typical experiments in the 2m bubble chamber. This confirms that any optical distortions due to the TST are indeed negligible.

EXPERIMENT 38

Rutherford Laboratory
Imperial College, London

K^-p interactions in the 1 GeV/c region

0·96 to 1·40 GeV/c
(ref. 29, 30, 107)

This experiment is a high statistics study of K^-p interactions in the momentum range 0·96 to 1·40 GeV/c using some 415,000 pictures from CERN 2m hydrogen bubble chamber. The data, averaging about 1·4 events/μb at each of 11 incident beam momenta increase the data in this region by a factor of two.

The final data reduction for the two body reactions

$K^-p \rightarrow K^-p$	(102,418 events)
$K^-p \rightarrow \bar{K}^\circ n$	(12,928 events)
$K^-p \rightarrow \Sigma^+\pi^-$	(7,634 events)
$K^-p \rightarrow \Sigma^-\pi^+$	(9,842 events)
$K^-p \rightarrow \Lambda^\circ\pi^\circ$	(18,454 events)

is essentially complete and final cross-sections, angular distributions and polarisation distributions (where appropriate) have been obtained. Fig.1.45 shows the values of A_0 ($= \sigma/4\pi\lambda^2$) for the elastic channel, compared with results from previous experiments.

Energy dependent partial wave analyses of each of these two body channels were presented at the London Conference. These were single channel analyses performed over the energy range 1540 to 2170 MeV (centre of mass) but using our new high statistics data in the range 1775 to 1960 MeV. The results are in general agreement with previous analyses but several states are now confirmed and more reliable values of the resonance parameters of the well established states have been obtained. In particular a P03(1905) state is required in all good solutions for the $\bar{K}N$ channel. This state is also accommodated in $\Sigma\pi$. (The Argand diagrams for the $\bar{K}N$ channel are shown in Fig.1.46).

The analysis of the two body channels continues. Results obtained since London Conference for $\Sigma\pi$ cross-section, showing significantly higher values than previous results in the region of 1800 to 1850 MeV c.m. energy could make significant changes to the $\Sigma\pi$ couplings of D05 and F05 states in this region.

Data for the three-body channels

$$\begin{aligned} K^-p \to K^-p\pi^\circ \quad & (10{,}166 \text{ events}) \\ \to K^-\pi^+n \quad & (12{,}709 \text{ events}) \\ \to K^\circ p\pi^- \quad & (14{,}080 \text{ events}) \\ K^-p \to \Lambda\pi^+\pi^- \quad & (36{,}639 \text{ events}) \end{aligned}$$

are now in their final form and several analyses are in progress. These channels are being analysed using an Isobar model, with a view to performing an energy dependent partial wave analysis of the contributing quasi two body channels, in particular the $\Lambda(1520)\,\pi^\circ$ and K(890)N from the KNπ channels and the $\Sigma(1385)\pi$ from the $\Lambda\pi\pi$ channel.

A new measurement of the Λ° lifetime of $(2{\cdot}611 \pm 0{\cdot}020) \times 10^{-10}$ s has been obtained from 34,000 Λ° events with two prong vee zero topology. This is in good agreement with another recent result of Poulard et al but differs significantly from the previous world average $[(2{\cdot}51 \pm 0{\cdot}02) \times 10^{-10}\,\text{s}]$.

In the main experiment only some 50% of the two prong topology events were measured. The rest of the two prong events have been measured recently and should be on DST in the near future. This will increase the statistics on all the above three body channels and in the K^-p elastic by a considerable factor.

Figure 1.45. A_0 values for $K^-p \to K^-p$ as a function of K^- momentum, showing results from Experiment 38 and from CERN-Heidelberg-Munich (CHM), CERN-Heidelberg-Saclay (CHS), and Chicago-Heidelberg (CH): (18546)

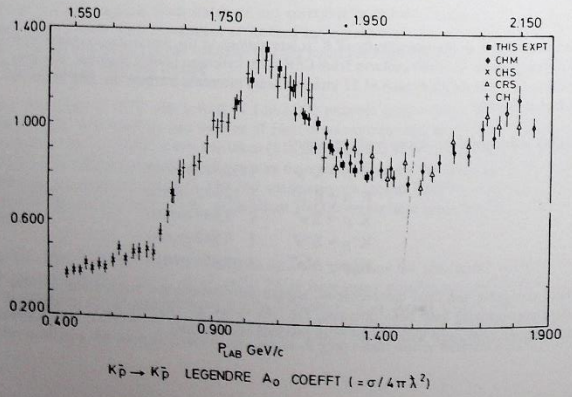

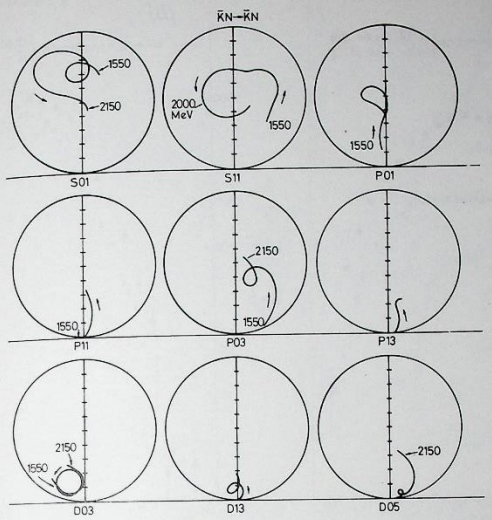

Figure 1.46 Argand diagram for the partial waves S01 and D05 from the analysis of $K^-p \to \bar{K}N$: Experiment 38 (18704)

As an extension to this experiment, 310,000 pictures have been taken in the CERN 2m HBC at 4 incident K^- momenta between 0·92 and 1·04 GeV/c; some 210,000 of these pictures are at 1·00 GeV/c K^- momentum, to provide one very high statistics data point. The first measurement of all this film is complete, and the data will be processed using a revised version of the kinematics program and the group's new post kinematics program, ORACLE.

0·92 to 1·04 GeV/c

In order to extend our high statistics studies of the formation of S = −1 baryon resonances, we have proposed an exposure of 5×10^5 pictures in CERN 2m HBC of K^- at 8 momenta, between 450 and 100 MeV/c. These data together with some existing film from Heidleberg-Munich which we are now measuring will yield statistics at the level of 1800 ev/mb/25 MeV/c K^- momentum range, representing an increase of about a factor of 10 over existing data in this range. Hopefully this will improve the partial wave solutions enabling us to answer the many specific problems already known in this energy range.

0·45 to 0·90 GeV/c

Further it means that there will be high statistics over the complete range 450 MeV/c to 1800 MeV/c just from two collaborations – CERN-Heidleberg, and RL-IC. These data should be taken late in 1975.

EXPERIMENT 39

K^-p interactions at 14 GeV/c

Ecole Polytechnique, Paris
CEN, Saclay
Rutherford Laboratory

In October this year the final measurements on the Laboratory's part of the 14 GeV/c K^-p film were completed and put on data summary tapes. 1974 has seen the continued accumulation of data and the publication of many results.

(ref. RL-74-017, RL-74-073, 8, 9, 19, 39, 40, 43, 44, 45, 86, 93, 105)

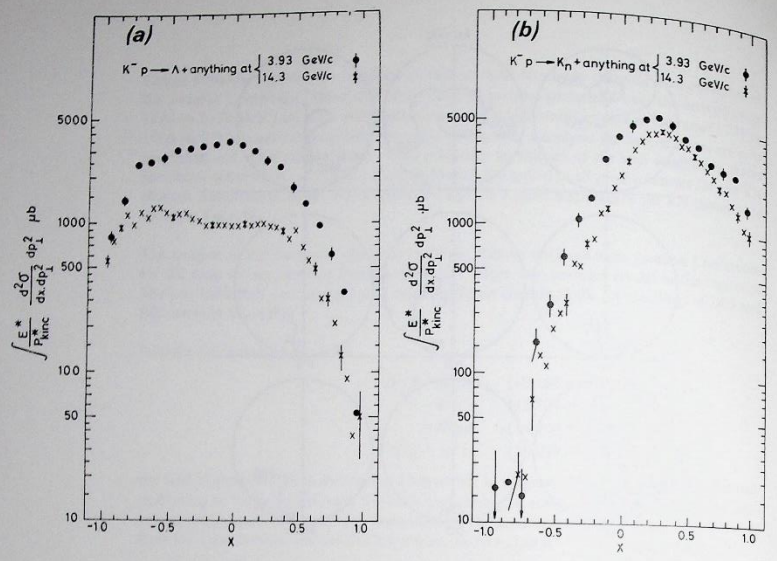

Figure 1.47. Values of the structure function as a function of x for the reactions (a) $K^-p \to \Lambda + X$, (b) $K^-p \to K^\circ + X$ Experiment 39 (18705, 18706)

The analysis has proceeded both for inclusive and exclusive reactions.

The main studies are described below:

a) **Inclusive reactions**

(i) **Λ and Neutral Kaon production**

The reactions analysed were:

$$K^-p \to \Lambda + X \qquad (1)$$

and $$K^-p \to (\bar{K}^\circ, K^\circ) + X \qquad (2)$$

The results on reaction (1) showed that (in the energy range $4 < p_{lab} < 14{\cdot}3$ GeV/c) the Λ inclusive cross-section decreases with energy as $p_{lab}^{-0{\cdot}45}$. In addition the values of the scaling function $(E\frac{d^3\sigma}{dp^3})$ decrease with energy and its shape as a function of x $(p_L/p_L\,(\max))$ changes with energy. These latter two features can be seen from Fig.1.47a. In contrast reaction (2) (Fig. 1.47b) shows no variation of the inclusive cross-section with energy and the energy variation of the shape and magnitude of the scaling function is much smaller than in reaction (1). It was found that the cross-section for $\Lambda K\bar{K}$ production increased from 360 μb at 3·93 GeV/c to 725 μb at 14·3 GeV/c.

(ii) **Charged and Neutral Σ production**

The reactions studied were:

$$K^-p \to \Sigma^\circ + X^\circ \qquad (3)$$

and $$K^-p \to \Sigma^\pm + X^\mp \qquad (4)$$

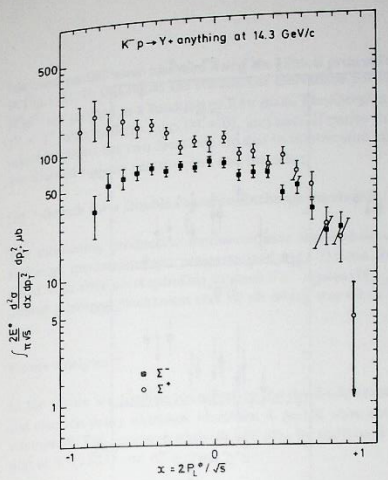

Figure 1.48. Values of the structure function as a function of x for the reactions $K^-p \to \Sigma^- + X^\circ$ and $K^-p \to \Sigma^+ + X^-$. Experiment 39 (18545)

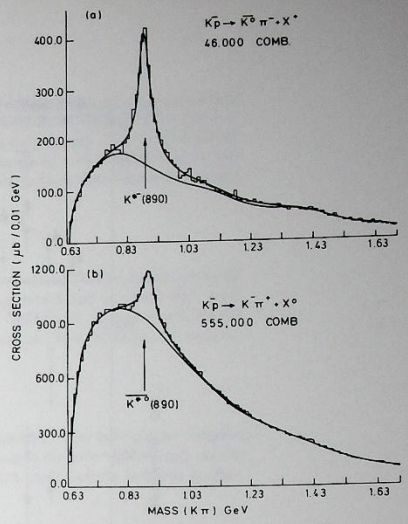

Figure 1.49. Kπ mass spectra for the reactions (a) $K^-p \to \bar{K}^0\pi^- + X^+$ and (b) $K^-p \to K^-\pi^+ + X^\circ$. Experiment 39 (18544)

This analysis found that the inclusive cross-sections for Σ's and Λ's are approximately equal i.e.

$$\sigma(K^-p \to \Sigma^\circ + X^\circ) + \sigma(K^-p \to \Sigma^+ + X^-) + \sigma(K^-p \to \Sigma^- + X^+) = \sigma(K^-p \to \Lambda + X)$$

$$\text{also } \sigma(K^-p \to \Sigma^\circ + X^\circ) = \tfrac{1}{3}\sigma(K^-p \to \Lambda + X) = \tfrac{1}{2}[\sigma(K^-p \to \Sigma^+ + X^-) + \sigma(K^-p \to \Sigma^- + X^+)]$$

The shapes of the structure functions, which are shown in Fig.1.48, depend on the charge of the hyperon. A comparison with the reactions $pp \to \Sigma^\pm + X$ which gives the scaling limit in the proton fragmentation region of reactions (3) and (4) showed that a large non-scaling component exists in reaction (4) at 14·3 GeV/c.

Figure 1.50. Values of the ratio of the unnatural parity exchange, σ^-, to natural parity exchange, σ^+, as a function of m_X^2/s for the reactions: (a) $K^-p \to K^{*-}(890) + X^+$ and (b) $K^-p \to K^{*\circ}(890) + X^\circ$. Experiment 39 (18711)

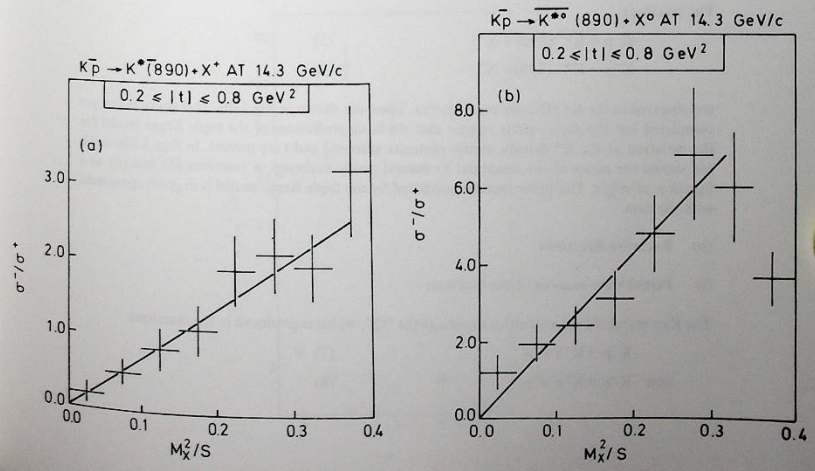

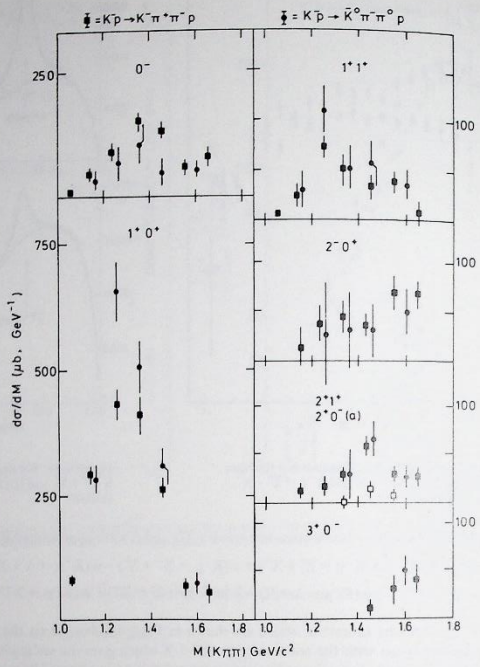

Figure 1.51. Values of the intensity of the various partial wave states J^PM^η as a function of $K\pi\pi$ mass in the reactions: $K^-p \to K^-\pi^+\pi^-p$ and $K^-p \to \bar{K}^0\pi^-\pi^0 p$. Experiment 39 (18543)

(iii) Inclusive K*(890) production

The reactions:

$$K^-p \to \overline{K^{*0}}(890) + X^0 \qquad (5)$$

$$K^-p \to K^{*-}(890) + X^+ \qquad (6)$$

are observed in the $K\pi$ effective mass spectra. These are shown in Fig.1.49. This study is not yet completed but the main results suggest that the basic predictions of the triple Regge model for the variation of the K* density matrix elements with m_X^2 and t are correct. In Figs.1.50a and b are shown the ratios of the unnatural to natural parity exchange in reactions (5) and (6) as a function of m_X^2/s. The linear increase predicted by the triple Regge model is in good agreement with the data.

(b) Exclusive Reactions

(i) Partial Wave analysis of the Q-system

The $K\pi\pi$ threshold enhancement, known as the "Q", which is produced in the reactions:

$$K^-p \to K^-\pi^+\pi^-p \qquad (7)$$

and $$K^-p \to \bar{K}^0\pi^-\pi^0 p \qquad (8)$$

has been partial wave analysed using the Illinois program of Ascoli. The main results are shown in Fig.1.51. In this figure the amounts of the various partial wave states defined by the values of J^PM^η are plotted as a function of $K\pi\pi$ mass. The Q-region ($1{\cdot}0 < M(K\pi\pi) < 1{\cdot}5$ GeV) is mainly $J^P = 1^+$ with helicity zero (M = 0), and natural parity exchange ($\eta = +$). The differences that occur between the two reactions are due to interference effects between the decay modes which are allowed for one reaction and not the other.

(ii) Search for a Double-Pomeron-Exchange mechanism

The interesting production mechanism was searched for in reaction (7). The double pomeron exchange mechanism was parameterized by a Double Regge Model and its predictions compared with data corresponding to small $\pi^+\pi^-$ masses ($M_{\pi^+\pi^-} < 0{\cdot}6$ GeV). An upper limit for the double pomeron mechanism was 10 μb which was 4% of reaction (7) in the same $\pi^+\pi^-$ mass region.

Future Analyses

In the future we propose to re-analyse the two-body reactions which now have greater statistics and also the many exchange channels. A partial wave analysis of the $p\pi^+\pi^-$ system may also be attempted. The inclusive analyses will also be continued with studies of the inclusive production of Y*(1385) and Δ^{++} states.

EXPERIMENT 40

Tata Institute, Bombay
University of Melbourne

2 GeV/c $\bar{p}p$ annihilations in a neon-hydrogen track sensitive target

A total of 200,000 pictures with a 2 GeV/c $\bar{p}$ beam were taken in October 1972 in the 1·5m Bubble Chamber with a track sensitive hydrogen target. 60,000 frames have been scanned, 23,000 for all events and the remaining 37,000 for only those events with two or more associated gammas, or one or more associated V°. All film has been scanned twice, giving a scanning efficiency of 0·99 for all events. A total of 58,300 events and 24,300 gammas have been recorded in these 60,000 pictures. *(ref. 27)*

Figure 1.52. The inclusive π^0 cross section, $\sigma_n(\pi^0)$, as a function of the negatively charged multiplicity (n^-). Experiment 40 (18542)

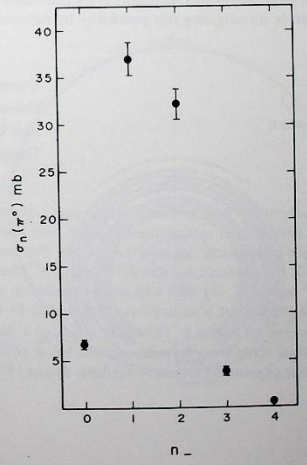

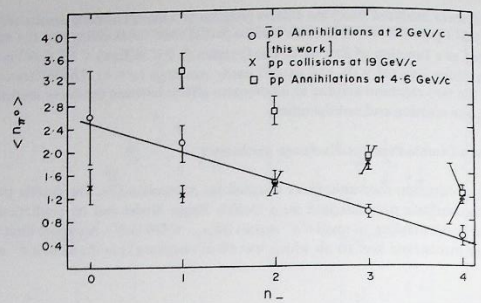

Figure 1.53. The average π° multiplicity $<n\pi^\circ>$, as a function of the negatively charged multiplicity from this experiment compared with $\bar{p}p$ annihilations at 4·6 GeV/c and pp collisions at 19 GeV/c.
Experiment 40 (18541)

Preliminary topological cross-sections $[\sigma_n]$ have been calculated together with inclusive π° cross-sections $[\sigma_n(\pi^\circ)]$, and average π° multiplicity $< n_{\pi^\circ} >$ as a function of charged particle multiplicity. To obtain the average number of π° the average gamma conversion probability $P\gamma$ is required for each topology. This was estimated as $P\gamma = 0{\cdot}30$ essentially independent of the number of π°s in the final state, assuming that the momentum and angular distributions of pions are determined by phase space.

The inclusive π° cross-section is shown in Fig.1.52. It may be noted that the dominant production takes place in 2 and 4 prong topologies. Fig.1.53 shows $< n_{\pi^\circ} >$ as a function of n^-, the negatively charged multiplicity. The line is simply a fit of the form $< n_{\pi^\circ} > = \alpha\, n^- + \beta$, with $\alpha = -0{\cdot}50 \pm 0{\cdot}08$ and $\beta = 2{\cdot}48 \pm {\cdot}07$. In this figure we also compare our results with those of pp interactions at 19 GeV/c, (for which the c.m. energy radiated into particle production is close to that of the $\bar{p}p$ annihilations at 2·0 GeV/c). This indicates that the processes responsible for π° production in $\bar{p}p$ annihilations are different from those of pp reactions. Fig.1.53 also shows the data for $\bar{p}p$ annihilations at 4·6 GeV/c for $n^- > 1$. An attractive possibility to explain a negative α in $\bar{p}p$ annihilations at low energies is the dominance of ρ meson production, but this fails to explain the high value of $< n_{\pi^\circ} >$ for zero prong points. The final explanation may lie in the narrowness of the total pion multiplicity distribution for annihilation as compared to the pp interactions. We are currently investigating this possibility by determining the total multiplicity distribution.

EXPERIMENT 41

Interactions of slow and stopped K^- mesons

University College, London
University of Birmingham
Free University of Brussels
University of Durham

Scanning has continued throughout the year, and some momentum regions have been completely scanned. All laboratories have started measurement. Events have been passed through the geometry programs and simple kinematical fits have been made. Differential and total cross-sections and polarizations will be measured for the $\Lambda^\circ\pi^\circ$ and $\Sigma^\circ\pi^\circ$ channels over the whole momentum range. The $\Sigma^-\pi^+$ and $\Sigma^+\pi^-$ channels will also be studied in some momentum regions. The general aim of the experiment is to improve the K-matrix fit to low-energy $\bar{K}N$ reactions. Theoretical and experimental results in 1974 have indicated a definite need for more data on the $\Lambda^\circ\pi^\circ$ and $\Sigma^\circ\pi^\circ$ final states from K^-p interactions below 600 MeV/c. The first results on these channels from this experiment should be available during 1975.

EXPERIMENT 42

The study of the S = −2 baryon resonances using the rapid cycling bubble chamber

University of Oxford
University of Rome
CEN, Saclay
College de France, Paris
Rutherford Laboratory

The experiment is designed to study the S = −2 resonances in the mass region $> 2{\cdot}0$ GeV/c^2. These states are characterised by many strange particle decays and hence high final state multiplicities. The rapid cycling bubble chamber with a charge multiplicity trigger is therefore well suited to this study. A diagram of the proposed chamber and trigger configuration is shown in Fig.1.54. The main component of the multiplicity trigger will be provided by four cylindrical wire spark chambers using capacity read-out. The four independent spark chamber multiplicities will be combined with additional scintillator information to provide the bubble chamber flash trigger. The spark chambers will themselves be triggered by a pre-trigger scintillator array.

The bubble chamber has diameter 30 cm, depth 20 cm and is designed to cycle at $\geqslant 60$ cps. The chamber is mounted vertically with the electromagnetic vibrator at the bottom. The whole is contained in a magnet which provides a field of 2·2T. The beam line has to provide 40 fully separated K^- fast spills during the Nimrod flat top. The beam (K 18) has been designed and installation has started.

A run of 5 cycles ($\sim$ 100 days) should yield 10^3 events/μb before geometrical efficiency factors are included. Monte Carlo estimates of the expected yield correspond to 500 events/μb for the S = −2 events.

Figure 1.54 (a) Plan view of the Rapid Cycling Vertex Detector: Experiment 42 (18549)

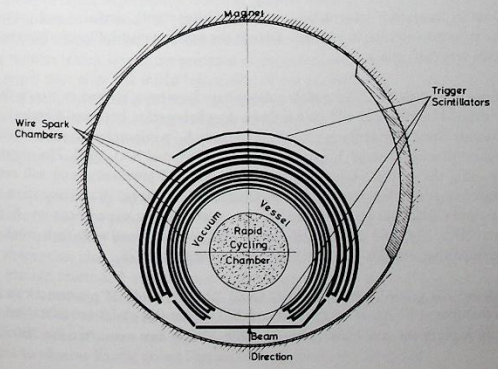

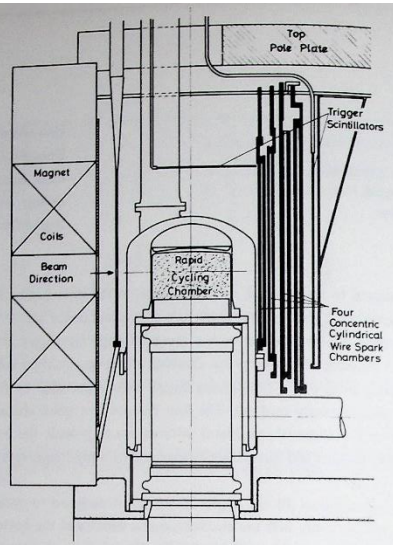

Figure 1.54 (b) Elevation of the Rapid Cycling Vertex Detector, showing the counter arrays proposed for the trigger in Experiment 42 (18550)

EXPERIMENT 43

University of Cambridge and collaborators

Experiments using special beams at Fermi Lab.

Considerable advances have been made during 1974 in developing the techniques required for special high energy beams at FNAL. A definite experimental programme has now emerged.

$\bar{p}p$ interactions at 100 GeV/c. A proposal (NAL 311) from Cambridge, FNAL, and Michigan State University to study $\bar{p}p$ interactions at 100 GeV/c using the 30" hydrogen bubble chamber and downstream wide-gap spark chamber hybrid system has recently been submitted and accepted at FNAL. The exposure of 100k pictures is scheduled for January 1975. The required beam (which contains 50% $\bar{p}$'s) will be made using a "target halo" technique; this technique has already been successfully tested.

We expect that cross-section information and comparisons with similar π and proton experiments will be of great interest; in addition there is the exciting possibility of observing $\bar{p}p$ annihilations at this very high energy.

K^-p interactions at 200 GeV/c. Two collaborations have now been formed to attack the physics programme outlined in Proposal 127 (NAL 213). A collaboration between Birmingham, Cambridge and Florida State University is proposing to study K^-p interactions in the 15 foot chamber at the highest practical energy, hopefully 200 GeV (Proposal NAL 333). The required beam will be made using the multiple-targetting technique outlined previously, and will employ the high field pulsed quadrupoles developed at Rutherford Laboratory. A collaboration including Aachen, Bonn and CERN has been formed to carry out a similar experiment on K^+p interactions (Proposal NAL 334) and close collaboration will be maintained with their work. It seems reasonable to hope that film for these studies could be taken in 1975.

Σ^-p interactions. The group's proposal P-122 (NAL 214) to study Σ^-p interactions in the 15 foot bubble chamber at FNAL at energies 50 and 200 GeV is still under consideration. It is possible that this experiment could take place in 1976, and in any case after the 200 GeV/c $K^\pm$ runs.

Imperial College, London

EXPERIMENT 44

Y^* production from π + p and K^-p incident states at 6·7 GeV/c using the SLAC Hybrid Facility

A proposal by the Imperial College bubble chamber group to study Y^* production from 6·7 GeV/c π^+p interactions in the SLAC 40 inch hybrid chamber was accepted by the SLAC Program Advisory Committee in April, 1974. This chamber runs at 12 cps and can be triggered using data from a downstream system of 3 proportional wire chambers and a large threshold Cerenkov counter. For this experiment, the trigger will be a heavy particle (K or p) with momentum greater than 2 GeV/c through the Cerenkov. During the Summer, a team from Imperial College joined groups from SLAC and Purdue University in the preparation of the counters and attendant software system. We expect to take film in the Summer and Autumn of 1975.

A second part of the proposal considers Y^* production via the line reversed reaction using a K^- beam and a π trigger. For this part efficient triggering demands a muon veto to eliminate K^- decays and this we hope to construct and test at the Laboratory.

Nuclear Physics Experiments

One of the features of pion-nucleus interactions which has been studied at several laboratories during the past year has been the measurement of γ-ray spectra from the residual nucleus formed after the pion has interacted. Of particular interest has been the strong production of γ-rays corresponding to the nucleus with 2 protons and 2 neutrons (an "α" particle) less than the target nucleus. Strong production of γ-rays corresponding to nuclei with 2 and 3 "α"-particles less has also been observed. Similar results have been obtained in an experiment with stopping K-mesons.

The interpretation of these experiments is not at present clear. It could be argued that the incoming particle interacts with an "α" particle in the nuclear surface, knocking it out, and so leaving the residual nuclei which have been observed. Such an interpretation could support those nuclear models which favour the presence of α-clusters in the nuclear surface. Alternative explanations argue that after the initial interaction of the incident particle the nucleus is left in a highly excited state and that α-particles are emitted in the subsequent evaporation process. Clearly to distinguish between these various interpretations further experimental data is required and comparisons between experiments using stopping pions or kaons and higher energy pions or protons should prove valuable.

An experiment using stopping kaons is described in the following reports. The γ-ray data should also help in interpreting the process by which the nuclear capture of the kaon takes place. This interaction is complicated by the presence of the Y_0^* (1405) resonance in the K^-p interaction. The nuclear absorption also gives rise to a broadening and shifting of the energy levels of the lowest kaon atomic orbits and a consequent broadening, shifting and attenuation of the final observed X-ray transition. Measurements of these effects in a range of nuclei are reported. Broadening of the X-ray lines can also occur in some cases due to the hyperfine interaction with the nuclear quadrupole moment and this has been observed for the first time in kaonic atoms. An experiment to observe kaonic atoms formed in hydrogen is also included.

The interest in the interactions of pions with nuclei has been considerably stimulated by the construction of the "pion-factories" at LAMPF (Los Alamos), SIN (Zurich) and TRIUMF (Vancouver). Initial programmes of experiments at the first two laboratories are now well under way and in the last few days of 1974 the successful operation of the 500 MeV H^- facility at TRIUMF was reported. One of the first experiments to be carried out on this machine will be by a collaboration which includes several British physicists with support from the Rutherford Laboratory. A progress report on this work is included.

A further new facility which has become available to British nuclear physicists is the reactor at I.L.L. Grenoble. There are a number of valuable experiments which can be carried out using the very intense neutron beams available from this reactor: an experiment to measure the electric dipole moment of the neutron to considerably improved accuracy has been proposed and is briefly reported; an experiment to test for parity violation in strong interactions is described. In the latter case an experiment carried out in the USSR using apparatus placed near the core of a reactor has shown a small but significant effect. The high intensity beams available at I.L.L. will enable the experiment to be repeated under much more favourable conditions. The availability of polarised neutron beams also allows symmetry tests for T-violation to be made.

The accelerators at AERE continue to be used by several experimental teams supported by the Rutherford Laboratory. Measurements of the n-p total cross-sections to search for possible structure in the variation as a function of energy have been made using the synchrocyclotron. Alpha and ^{3}He beams from the Variable Energy Cyclotron have been used in a number of studies of elastic and inelastic scattering from a range of nuclei and for measurements on the (^{3}He, α) reaction. Experiments of this type are normally analysed using the optical model and distorted wave approximations. Experiments on collective nuclei can show the need for further modifications of these basically simple models and are likely to yield new information.

Nuclear Physics Experiments

Experiment Number	Experiment ; Location	Collaboration
45	Experiments with stopping kaons; K17 beam Nimrod	University of Birmingham University of Surrey Rutherford Laboratory
46	Study of X-rays from K^--p atoms; K17 beam Nimrod	University of Birmingham University of Surrey Rutherford Laboratory
47	Measurement of triple scattering parameters in n-p scattering; 500 MeV H^- cyclotron TRIUMF, Vancouver	Bedford College, London AERE, Harwell University of Surrey Queen Mary College, London University of British Columbia University of Victoria
48	Search for the electric dipole moment of the neutron using bottled neutrons; Reactor, ILL, Grenoble	University of Sussex Harvard University Oak Ridge National Laboratory Technical University, Munich University of Oxford ILL, Grenoble CENG, Grenoble
49	Symmetry tests for P-violation; Reactor, ILL, Grenoble	University of Sussex Harvard University University of Glasgow ILL, Grenoble
50	Symmetry tests for T-violation; Reactor, ILL, Grenoble	University of Sussex ILL, Grenoble

Experiment Number	Experiment : Location	Collaboration
51	Measurement of n-p total cross-sections; Synchrocyclotron, AERE, Harwell	Queen Mary College, London University of Surrey University of Birmingham AERE, Harwell
52	Studies of inelastic scattering from collective nuclei; Variable Energy Cyclotron, AERE, Harwell	Kings College, London Queens University, Belfast
53	Elastic scattering of ^{3}He beams at 53 MeV; Variable Energy Cyclotron, AERE, Harwell	Kings College, London Bedford College, London Oak Ridge National Laboratory
54	The ^{56}Fe (h, α) reaction at 83 MeV; Variable Energy Cyclotron, AERE, Harwell	Kings College, London
55	The n-d break-up process between 100 and 155 MeV	Queen Mary College, London Bedford College, London AERE, Harwell
56	Elastic Scattering of polarised neutrons from deuterons	Queen Mary College, London Bedford College, London AERE, Harwell

EXPERIMENT 45

Experiments with stopping kaons

University of Birmingham
University of Surrey
Rutherford Laboratory

(ref. RL-74-033)

A slow negative kaon travelling through matter will be captured by a nucleus into an atomic state of fairly high principal quantum number; following this the kaon then cascades through the atomic energy levels by a mixture of radiative and auger transitions until the strong interaction between the kaon and the nucleus competes with these processes. The final observable radiative transition is frequently broadened, shifted and attenuated as a result of this interaction. Because this process takes place in the region where the nuclear density is about 10% of its central value, the study of kaonic atoms is expected to yield information about the surface of the nucleus. However, before this hope can be realised, it is necessary to understand the kaon-nucleus interaction in much greater detail than our present knowledge will allow. The study of the products from the absorption of the kaon might help in this task.

X-rays from the atomic cascade of the kaon and γ-rays produced following its absorption by the nucleus have been detected for a number of elements (C, Aℓ, S, Ni, Co, Ag, Cd, In, Sn, Yb, Hf, Ta, Pb) using a lithium drifted germanium detector of 16% relative efficiency with an in-beam resolution of 1·75 keV at 1·33 MeV and 750 ev at 122 keV. The preamplifier has been specially modified to cope with the very high effective counting rates experienced in the experimental environment. Examples of the spectra are shown in Figs.1.55 and 1.56. In almost all the spectra the broadening, shifting and attenuation of the final observed transition is clearly evident.

In addition, for two elements in the rare-earth region, Ytterbium, and Tantalum, hyperfine splitting due to the quadrupole moment of the nucleus has been observed. γ-rays have been observed following kaon capture in aluminium; these measurements have been made as a function of target thickness in order to separate possible two step processes. Final state nuclei corresponding to the observed γ-rays have been identified. Further calculations using this data must be made before detailed conclusions can be drawn.

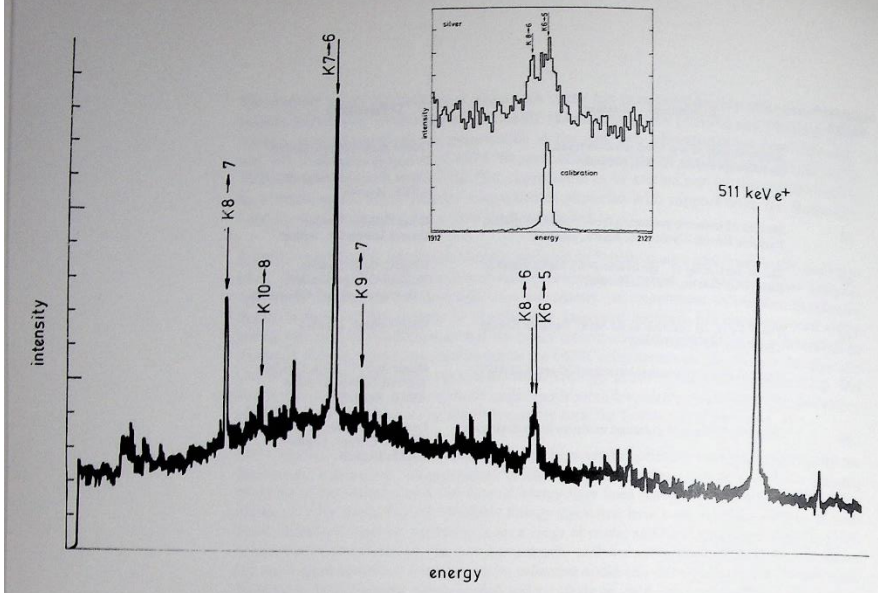

Figure 1.55. X-ray spectrum observed from kaons stopping in a silver target. The energies of X-rays corresponding in transitions between various atomic levels are indicated. Also shown in detail is the n = 6 → 5 transition which is broadened and attenuated by the nuclear absorption, together with a calibration line showing the overall energy resolution: Experiment 45 (18709)

Figure 1.56. X-ray spectrum observed from kaons stopping in an ytterbium target. The energies of X-rays corresponding to transitions between various atomic levels are indicated. Also shown in detail is the n = 7 → 6 transition which is broadened by the hyperfine interaction with the nuclear quadrupole moment, together with a calibration line showing the overall energy resolution: Experiment 45 (18707)

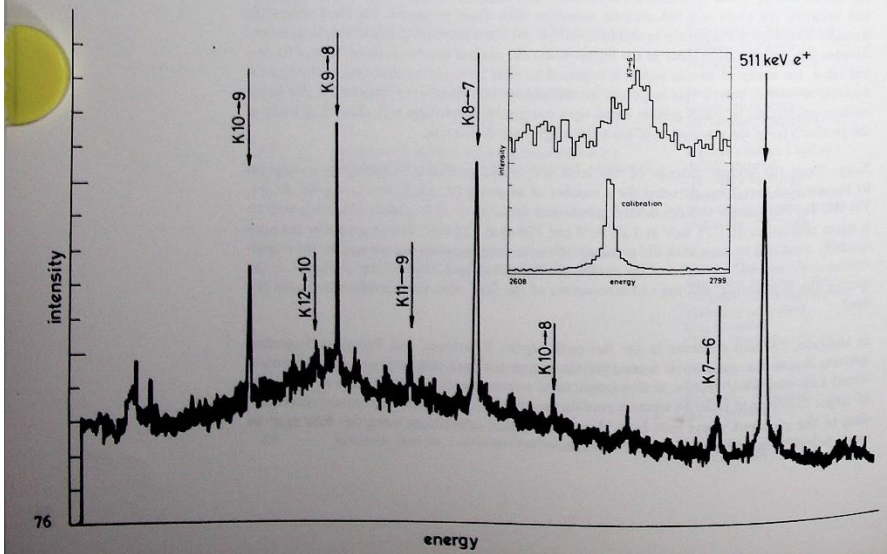

EXPERIMENT 46

Study of X-rays from K^-–p atoms

University of Birmingham
University of Surrey
Rutherford Laboratory

Several analyses of low energy K^-–p scattering have been made but, owing to a general lack of scattering data for momenta below 100 MeV/c, there are considerable difficulties in obtaining values for the S-wave scattering length. The situation is complicated by the presence of the Y_0^* (1405) resonance just below threshold (1432 MeV) and the fact that the $\Sigma\pi$ and $\Lambda\pi$ channels are open so that the scattering lengths are complex.

Direct information about the scattering lengths can come from measurements on the X-rays from K^-–p atoms. Measurements of the shift and width of the lowest level are then directly proportional to the real and imaginary parts of the complex scattering length. For the K^-–p system it is expected that due to the strong interaction the 2P - 1S transition (X-ray energy 6·5 keV) should be shifted by about 300 eV and should have a natural line width of about 500 eV. It is uncertain as to whether the 2P - 1S transition can be observed owing to the existence of Stark mixing. Since the K^-–p atoms are electrically neutral and relatively small in size they can approach closely the neighbouring positively charged nuclei where they will be exposed to strong electric fields. The resulting "Stark-mixing" can give rise to a high probability of the kaon-proton system making a transition to an S-state of large principal quantum number n. Since the K^-–p S-state interaction is very strong the atomic cascade may never reach the 1S-state.

The principal aim of the present experiment is to see if 2P - 1S X-rays from the K^-–p system can be observed using a hydrogen gas target whose density can be varied and to make measurements of the width and shift to check that these are at least consistent with predictions from present determinations of the scattering length.

The apparatus consists of a large vessel containing hydrogen at 10 atmospheres pressure. Eight large thin window proportional counters mounted inside the vessel are used to detect the 5 to 6 keV X-rays. Eight scintillation counters mounted outside the vessel are used to detect and veto charged particles passing through the proportional counters.

Experiments with the apparatus in the beam line have indicated severe background problems due to low energy charged particles and due to neutrons or gamma-rays which interact in the proportional counters or surrounding materials. It will be necessary to extensively redesign the apparatus to overcome these problems and to improve the trigger signal for kaons stopping in the hydrogen gas.

EXPERIMENT 47

Measurements of triple scattering parameters in n-p scattering

Bedford College, London
AERE, Harwell
University of Surrey
Queen Mary College, London
University of British Columbia
University of Victoria

This project at the TRIUMF accelerator, located in Vancouver, Canada, started with the delivery from Britain in early Summer of a polarimeter consisting of arrays of multiwire proportional chambers (MWPC's) and scintillators, neutron counters and a superconducting solenoid. All items have subsequently been shown to be operating satisfactorily.

During the Summer and Autumn effort has been concentrated on construction of the beam line and provision of shielding, cabling and services. Detectors, electronics and computer programs have also been brought to a state of readiness.

On 15 December 1974 a 500 MeV extracted unpolarised beam was obtained from the TRIUMF accelerator and it is hoped that by early Spring 1975 reliable operation with extracted currents of tens of nano-amps can be achieved. Polarised beam injection should be available by early Summer 1975. This should coincide with assembly at TRIUMF of a liquid deuterium neutron production target (being built at University of Victoria) and a liquid hydrogen target (being built at University of British Columbia). Both projects are well under way. The programme of n-p triple scattering measurements should commence in Summer 1975.

EXPERIMENT 48

Search for the electric dipole moment of the neutron using bottled neutrons

University of Sussex
Harvard University
Oak Ridge Nat. Lab., USA
Technical University, Munich
University of Oxford
ILL, Grenoble
CENG, Grenoble

Several measurements of the lower limit for the electric dipole moment (EDM) of the neutron have already been made and current work at Grenoble by an American group suggests that the neutron EDM is equal to eX, where e is the electron charge and X is essentially zero with a standard deviation of approximately 10^{-24} cm. We are proposing to reduce the standard deviation to 10^{-26} cm with the possibility of further reduction to 10^{-27} cm.

The existence of a neutron EDM would imply both P and T violation and it is possible to estimate a range of X values for each of the various weak interaction theories. Values of X less than 10^{-23} cm, for example, rule out electromagnetic CP violation; milliweak theories imply X in the range 10^{-23} cm to 10^{-25} cm and superweak theories predict values of X less than 10^{-27} cm. If X is found to lie in the range 10^{-24} to 10^{-26} cm, the superweak theory will be ruled out.

The experiment will be carried out in the ILL reactor at Grenoble using ultra-cold polarised neutrons (energy $<10^{-7}$ eV) stored in a cavity for a time of the order 30 seconds. The neutron spins precess slowly about a local weak magnetic field of 10 milligauss and any change in precession angle which can be correlated with the application of an additional strong electric field of 30 kV.cm^{-1} is assumed to be due to the interaction of the neutron EDM with the electric field.

The lower limit of 10^{-26} cm should be reached after a data collection time of three months using the room temperature ultra-cold neutron source proposed at ILL. Design work has been carried out at the ILL with the collaboration of Munich and Sussex in the past year. Some decrease in the lower limit will be possible if the source is subsequently cooled and the resultant increase in beam intensity will also facilitate the study of systematic errors, thus significantly reducing the overall running time.

The factors most likely to limit the sensitivity, apart from counting statistics, are the uniformity and stability of the magnetic field. We are proposing to use a mu-metal shield unless further study leads to the conclusion that the limit of 10^{-26} cm cannot be realised without using a superconducting shield. Such a shield will almost certainly be necessary if the limit is to be lowered to 10^{-27} cm. This work will be carried out at Sussex, together with the construction and development of the storage vessel, the high voltage system and the computer control. We would expect to move the apparatus to Grenoble after a building time of 1½ to 2 years.

EXPERIMENT 49

Symmetry tests for P-violation

University of Sussex
Harvard University
University of Glasgow
ILL, Grenoble

The aim of this experiment is to establish the extent to which the radiation following the p(n; γ)d reaction is circularly polarized. The presence of circular polarization is indicative of parity violation and the upper level of theoretical predictions are approximately an order of magnitude smaller than the result of Lobashov et al who obtained $P_\gamma = (1{\cdot}30 \pm 0{\cdot}45) \times 10^{-6}$. It is important to carry out an experiment of at least comparable accuracy either to verify the result of the Leningrad group or to show how it may be in error.

The IH2 beam at ILL has been selected for this experiment. It provides a neutron flux of 3·3 x 10^{10} n cm^{-2} sec^{-1} over a circular area of 12 cm^2 and is the greatest external integrated neutron intensity that is available at the reactor. A hydrocarbon target will be used for the p(n; γ)d reaction. This has some advantages over a water target as the small but nevertheless significant capture by oxygen may give rise to unwanted β-decay processes. The circular polarization will be measured by searching for an asymmetry in the intensity of radiation transmitted through magnetised iron when the direction of magnetisation is reversed. A cylindrical magnet with two analysing sections (illustrated in Fig.1.57) encloses the target. A set of detectors around the analyser magnet will be used to record the light level rather than individual pulses – count rates of $\sim 10^{10}$/sec are expected.

At present measurements are under way on different target configurations and we are examining the effect of cooling the target to 4K and the neutron distribution within it. This will permit the target geometry to be optimised so that the large majority of captures occur in regions which are opposite the most sensitive parts of the analysing magnet.

Simple transmission magnets have been made and these are being used in measurements on circular polarized radiation in order to assess effects due to multiple scattering. Radiation of a known polarization is produced by using A(n ; γ)B reactions in which a beam of polarized neutrons is used. In these measurements a Ge(Li) detector records the transmitted spectra under good and poor geometry conditions. Such measurements should give us confidence that we can adequately take account of multiple scattering in the final experimental magnet.

Figure 1.57. The form of the analysing magnet. In neighbouring sections the field direction is opposite and may be reversed upon reversing current direction: Experiment 49 (18540)

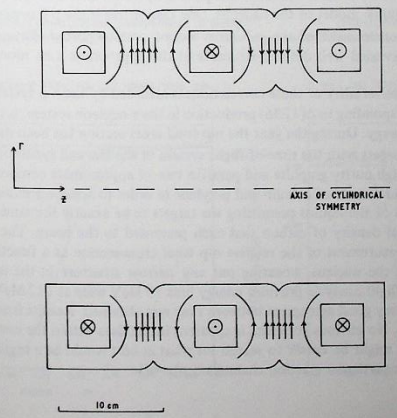

EXPERIMENT 50

University of Sussex
ILL, Grenoble

Symmetry tests for T-violation

The basis of T-violation tests is to measure a quantity which depends on a term similar to **J** (**k**(1) x **k**(2)) (**J**. **k**(1)) where **J** is an axial vector and **k** are polar vectors.

Ensembles of polarized nuclei may be produced by the capture of polarized neutrons. At the ILL the polarized neutron beam has an intensity of 5×10^8 n sec^{-1} on a 0·5 x 6·0 cm^2 area and a polarization of 70%. This is substantially greater than beams that are available elsewhere and for a target with a moderate cross-section and dimensions of typically several cm long by 0·4 mm diameter the statistical accuracy is not a significant limitation to the overall accuracy.

The first measurement will examine a β-γ correlation from a polarized source. A Fluorine target will most probably be used and this will be maintained at liquid helium temperature in a magnetic field in order to preserve the polarization; the half-life is 10 sec. A helium cryostat has been obtained and the chamber containing the target and detector parts has been designed together with the coil that provides splitting of magnetic substates. In addition magnetic shielding from this field is provided by a superconductor layer on the helium shield.

The decay information on Fluorine-20 still contains some gaps, but this source appears to be one of the more promising of several possible ones. In particular, ensembles of polarized ^{20}F nuclei have been prepared successfully by a method similar to the one that will be used in the present experiment.

EXPERIMENT 51

Queen Mary College, London
University of Surrey
University of Birmingham
AERE, Harwell

Measurement of n-p total cross-sections

In an unpublished preprint (RPP/H103) Astbury drew attention to correlations between the structure seen in various hadron-nucleon total cross-sections. It was noted that "bumps" appear whenever the c.m. momentum reaches a value at which, in the π-nucleon system, production of nucleon isobars can occur in the S-channel. This peculiarity could have a simple explanation, on the basis of a naive quark model of the hadrons. One test of this is the p-$\bar{p}$ system and, early in 1974, results of a measurement of the p-$\bar{p}$ cross-section were reported (Phys. Rev. Lett. 32 (1974) 247). These revealed well defined structure at the appropriate c.m. momentum.

Another test of the universality of these correlations is afforded by the n-p system in which the c.m. momentum corresponding to $\Delta(1236)$ production in the π-nucleon system, is reached at 112 MeV Lab. neutron energy. During the year the n-p total cross-section has been measured in two runs using different targets with the time-of-flight system of the Harwell synchrocyclotron. The first used targets of high purity graphite and paraffin wax of approximate composition $(CH_2)_n$. The second used liquid targets of dekalin and p-xylene in order to achieve a more accurate subtraction, the densities of the liquids permitting the targets to be exactly the same length, whilst still matching the areal density of carbon that each presented to the beam. The object was to perform a precise measurement of the relative n-p total cross-section as a function of energy; Fermi motion within the nucleus, smearing out any narrow structure in the n-C total cross-section. The time-of-flight analysis provides energy bins 10 MeV wide at 112 MeV with relative errors of about 1%. Very good agreement between runs was obtained. Results from the first run are shown in Fig.1.58. No obvious structure is apparent in the data within the energy resolution of the experiment. It might be better to search for what at best would be a small effect on the total cross-section in a particular reaction channel e.g. np→dγ.

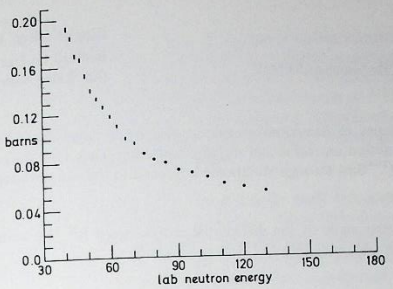

Figure 1.58. Measured values of the n-p total cross-section as a function of energy: Experiment 51, (18701)

EXPERIMENT 52

King's College, London
Queen's University, Belfast

Studies of inelastic scattering from collective nuclei

A set of experiments has been completed to study the interference of the Coulomb and nuclear contributions to forward angle inelastic scattering of 15, 16, 17, 18 and 19 MeV alpha particles from Cr^{52}, Fe^{56}, Ni^{60} and Zn^{64}.

The cross-sections in the interference region are sensitive to the shape of the form-factors and are being used to test the folding approach to the calculation of the nuclear inelastic form-factors for collective nuclei in which a deformed nuclear density is folded with the nucleon interaction. Typical results obtained by this method for proton scattering from Mg^{24} at 20, 40 and 80 MeV are shown in Fig.1.59 for L = 2 and L = 6 transitions.

Work has also continued on a more microscopic approach to inelastic scattering using the R P A which has been incorporated into a coupled channels program, and applied to the scattering of deuterons from C^{12} as part of a study of the two step processes in the transfer reaction C^{12} (d, He^3) B^{11}.

Figure 1.59. Inelastic scattering form-factors for 20, 40 and 80 MeV protons off Mg^{24} : Experiment 52 (18537, 18538)
———— direct contribution (independent of energy) ; – – – exchange contribution 20 MeV, ; – – – – – – exchange contrjbution 40 MeV, ; . . . . . exchange contribution 80 MeV.

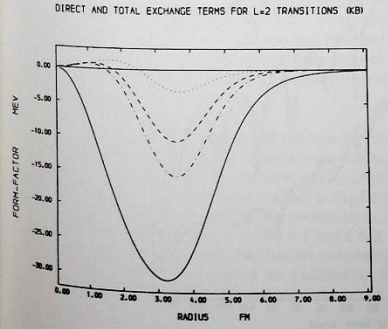

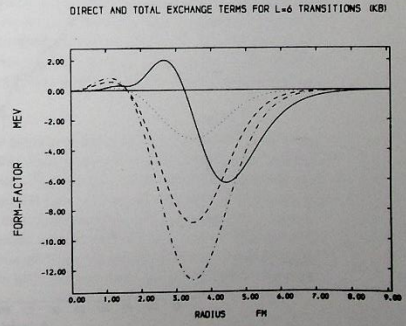

EXPERIMENT 53

King's College, London
Bedford College, London
Oak Ridge National Laboratory

Elastic scattering of ^{3}He beams at 53 MeV

(ref. 64) The stable even isotopes of Samarium provide an interesting target group for studying the effects of collective motion on elastic and inelastic scattering. They span the transition from a closed neutron shell (^{144}Sm) through vibrational isotopes into the rare earth region of permanent deformation.

Measurements have been made of the differential cross-sections for ^{3}He scattering from the Samarium isotopes Sm 144, 148, 150, 152, 154 at 53·4 MeV.

Figure 1.60. Elastic scattering cross-sections for 53·4 MeV helions on the even samarium isotopes. The fits correspond to the simple optical model with volume integrals per particle pair for the real potential equal to 240 and 300 MeV. fm^{3} : Experiment 53 (18700)

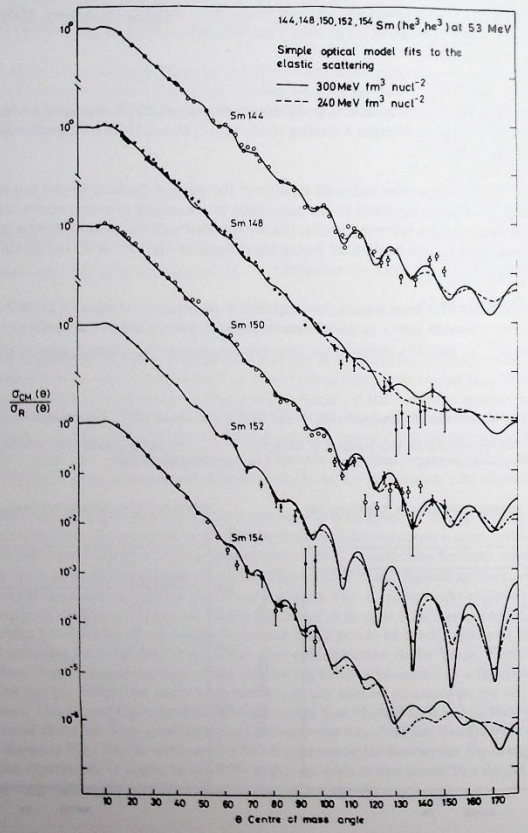

The measurements on ^{148}Sm and ^{150}Sm were performed on the Variable Energy Cyclotron, at AERE, Harwell. The beam intensity (up to 1800 nA on target) permitted the data to be extended to 150°, where the cross-sections are extremely small. To separate the first excited state, a resolution of less than 80 KeV was needed for the measurements on ^{152}Sm and ^{154}Sm. Consequently the broad range magnetic spectrograph at the Oak Ridge Isochronous Cyclotron, was used for these measurements. Angular distributions of elastic scattering and inelastic scattering to the first 2^{+} level were measured for each target.

These measurements complement similar studies already made with proton and alpha beams at the same energy. The discrete ambiguity problem of helion optical model parameters can be solved by measurements at sufficiently high energy and over a large enough angular range. At this energy several sets of parameters are acceptable but the set characterized by a real potential with a volume integral per particle pair of 300 MeV. fm^{3} corresponds to the set preferred at higher energies. The optical model fits for two sets are shown in Fig.1.60.

No combination of volume imaginary and surface imaginary potentials gave a better fit than pure surface imaginary terms. There was no evidence for a spin orbit depth of greater than zero.

The envelope of the cross-sections plotted as a ratio to the Rutherford cross-section shows an exponential decrease with angle. The proton and alpha data showed the same basic feature but there was evidence of differences between the isotopes. In the 50 MeV alpha data, the oscillatory structure was more pronounced than for the ^{3}He case but the structure decreased for the rotational isotopes ^{152}Sm and ^{154}Sm. In the proton data, the slope of the cross-section envelope increased for the rotational isotopes. This feature was even more pronounced in the inelastic proton cross-sections. The ^{3}He data shown here are interesting insofar that the cross-sections are so similar for all the isotopes, the largest difference being between ^{144}Sm, ^{148}Sm. In the parameter sets obtained so far, the large values of a_l for ^{148}Sm, ^{150}Sm, ^{152}Sm and ^{154}Sm, compare well with the value obtained by Woollam et al, in their coupled channel calculations on ^{144}Sm using the strong coupling approximation.

They do not however agree with the value of a_l in the regular optical model analysis of ^{144}Sm. A complete coupled channel calculation for the elastic and inelastic scattering cross-sections will be necessary before any valid conclusions can be drawn. The validity for deformed nuclei of recent reformulations of the optical model may then be ascertained.

EXPERIMENT 54 **King's College, London**

The ^{56}Fe (h, α) reaction at 83 MeV

Measurements of helion elastic scattering at 83 MeV on ^{56}Fe have demonstrated that unique optical model parameter sets could be obtained with sufficiently extensive high energy data. In order to analyse the (h, α) reaction measurements taken at the same time, the elastic scattering of 85·7 MeV alpha particles was also measured to simulate the conditions of the outgoing channel. Although an unambiguous potential was not possible for the alpha elastic scattering the data was easily fitted with the simple optical model and both the helion and alpha data and fits are shown in Fig.1.61.

With a unique helion potential and an acceptable alpha potential the limitations of conventional DWBA under momentum mismatch conditions should be observed in the (h, α) reaction. Several states corresponding to neutron pickup from the $f^{7}/_{2}$ and $p^{3}/_{2}$ states were observed and the DWBA fits are shown with the data in Fig.1.62 as full lines. The structural features of the cross-sections can be observed in the predictions but the overall envelope of the distributions cannot. This feature occurs for both $\ell = 1$ and $\ell = 3$ states even though the momentum mis-match is less for the latter case. The data are consistently larger than the predictions at backward angles, although this feature must be qualified by the fact that the data was normalized at forward angles and not by known spectroscopic factors.

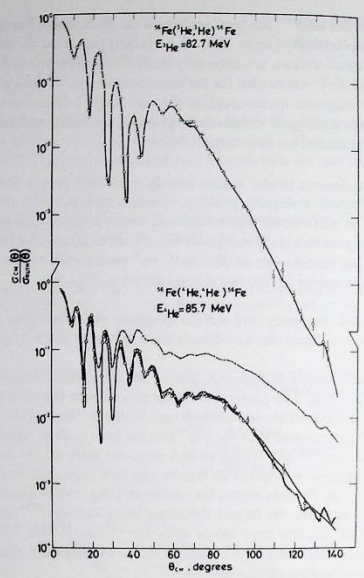

Figure 1.61. Elastic scattering cross-sections for 82·7 MeV ^{3}He and 85·7 MeV ^{4}He on ^{56}Fe. The continuous lines are the optical model fits for potentials with $J_{RS}/A_P A_T$ = 333 MeV. fm^3 for ^{3}He and 422 MeV. fm^3 for ^{4}He. The dotted line is the fit for $J_{RS}/A_P A_T$ = 530 MeV. fm^3 and the dot dash line is the fit obtained when r_I for the ^{4}He channel is reduced by 10% from the 422 MeV. fm^3 set values. Experiment 54 (18548)

Many attempts have been made to improve on conventional DWBA under conditions of momentum mis-match. In this analysis the form factor was calculated using a conventional Saxon Woods potential for the bound state neutron without correction for finite range or non locality. Variation of the form of the bound state wave function has shown primarily that the form factor affects the spectroscopic factors but not the general shape of the angular distributions.

Kunz et al have shown that collective effects can be included by changing the radius parameters of the distorted wave potentials. Further, Dodd and Greider have used the "three body problem" approach of Fadeev to derive additional terms in the DWBA, the importance of which can be minimised by suitable choice of the optical potentials. Following this approach but still keeping the unique optical potential for the incident ^{3}He, the parameters of the ^{4}He optical potential were allowed to vary. It was noticed that the only change of parameter to give any improvement was a 10% decrease in r_I for the alpha channel. The fits to the $\ell = 3$ states were then greatly improved and are shown as dotted lines in Fig.1.62. However, the fits to the $\ell = 1$ states still leave much to be desired. This improvement of the angular distributions for the (h, α) reaction could only be produced at the expense of the fit to the alpha elastic cross-sections as shown on Fig.1.61.

It is worth noting that the momentum mis-match is much greater for the $\ell = 1$ states which are still poorly fitted by DWBA. It is evident that this reaction forms a stringent test of conventional DWBA and a number of improvements to take into account second order processes are being considered.

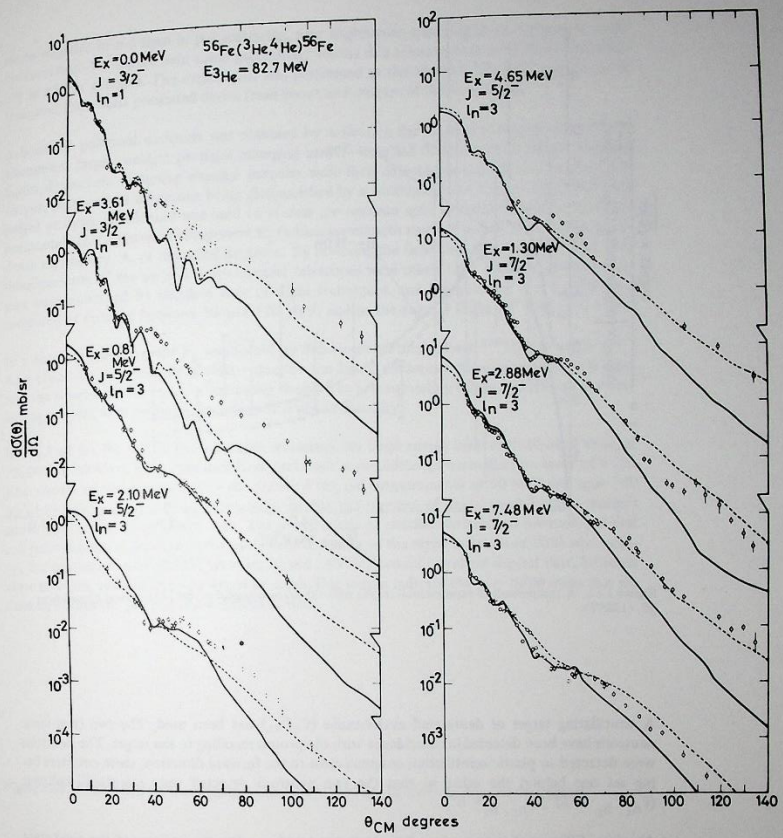

Figure 1.62. Angular distributions for the ^{56}Fe (^{3}He, ^{4}He) reaction at 82·7 MeV. The continuous curves show the DWBA predictions for the potentials which fit the elastic scattering data (shown as continuous lines on Fig.1.61). The dotted lines are the predictions when the r_I of the ^{4}He potential is reduced by 10%. Experiment 54 (18698)

EXPERIMENT 55

The n-d break-up process between 100 and 155 MeV

Queen Mary College, London
Bedford College, London
AERE, Harwell

The reaction n+d → n+n+p has been studied in a kinematical region where very little interference is expected between processes giving a strong n-n final state interaction and those responsible for nn and np quasi-free scattering. Kinematically complete data have been obtained over a range of incident neutron energies from 100 to 155 MeV.

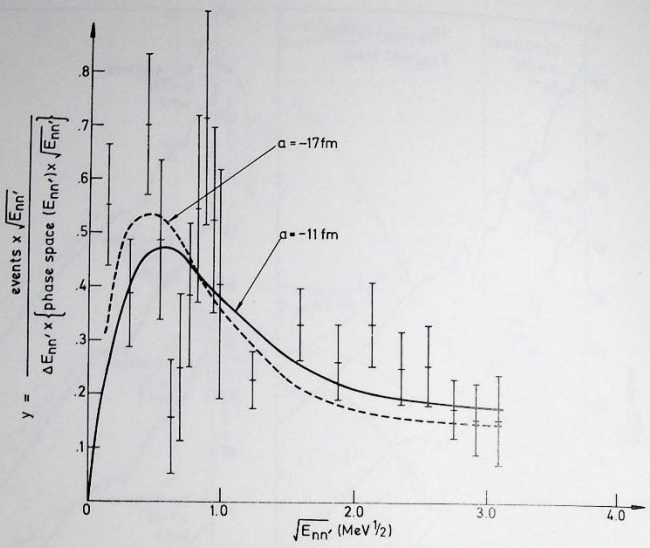

Figure 1.63. A comparison of experimental results with the Watson-Migdal model predictions: Experiment 55 (18697)

A scintillating target of deuterated cyclohexane (C_6D_{12}) has been used. The two final state neutrons have been detected in coincidence with the proton recoiling in the target. The neutrons were detected in plastic scintillation counters close to the forward direction, these counters being set one behind the other so that the two neutrons detected were essentially colinear ($\theta_{n_1, n_2} = 30°$, $\phi_{n_1, n_2} = 0°$).

Absolute differential cross-sections have been extracted as a function of one of the final state neutron energies for incident energies between 100 and 155 MeV. A simple model based on Watson-Migdal theory for the final state interaction was used to fit the data obtained in this experiment as shown in Fig.1.63 and the value $a_{nn} = -11\ ^{+4.5}_{-3}$ fm. extracted for the neutron-neutron scattering length.

EXPERIMENT 56

Elastic scattering of polarised neutrons from Deuterium

Queen Mary College, London
Bedford College, London
AERE, Harwell

There are few reported measurements of the polarisation P(Θ) in n-d elastic scattering, to complement the extensive p-d data. What comparison of the two systems has been made, near 23 MeV and at 35 MeV, seems to indicate systematic discrepancies with P(Θ) being significantly more negative in n-d than in p-d scattering, near angles corresponding to the minimum in the cross-section. We report here some preliminary results of a measurement of P(Θ) in n-d scattering at higher energies. The experiment was performed at the Harwell 160 MeV synchrocyclotron, and the results presented derive from about one quarter of the data taken.

A beam of polarised neutrons was obtained by deflecting the internal proton beam on to an aluminium target; neutral particles emerging at 47° travelled 50m before striking a target of liquid deuterium. Outgoing charged particles were then detected in scintillation counter telescopes, protons and deuterons being distinguished by a combination of time of flight and pulse height analysis. A solenoid was used to precess the neutron spin, initially vertical, towards the horizontal. This horizontal component P_n (which varied with neutron energy) resulted in an up-down asymmetry, A, of the recoil deuteron. By reversing the field direction, the effects of small misalignments of the up and down counter telescopes were minimised. Incident neutron energies were measured by standard time of flight techniques, and the quantity $A = P_n\ P(\Theta)$ was measured at energies between 50 and 120 MeV, and in the angular range $70° < \Theta_{cm} < 170°$.

In a separate measurement P_n was found by Schwinger scattering from ^{238}U at an angle of 1°. As a check on the methods of data reduction the liquid deuterium was replaced by hydrogen, and the asymmetry in free n-p scattering found. The corresponding values of P(Θ) are in excellent agreement with previous determinations of this quantity.

In Fig.1.64 we show P(Θ) for n-d elastic scattering, for three energy bins, each 10 MeV wide, at 70, 80 and 90 MeV. Errors are statistical, and there is an additional normalisation error of ± 7%. Also shown are lines representing the trend of the p-d measurements at 50 MeV and near 140 MeV. Future analysis will approximately double the number of angles, and include energies above and below those shown here. The implications of possible differences between n-d and p-d polarisations at lower energies are ascribed mainly to the rapid variation of P(Θ) with energy; the near-constancy of P(Θ) between 50 and 140 MeV would therefore suggest that, between these energies, such differences would be small. Our results indicate that any differences that do exist lie within the present experimental errors.

Figure 1.64. Polarisation P(θ) in n-d elastic scattering at 70, 80 and 90 MeV: Experiment 56 (18699)

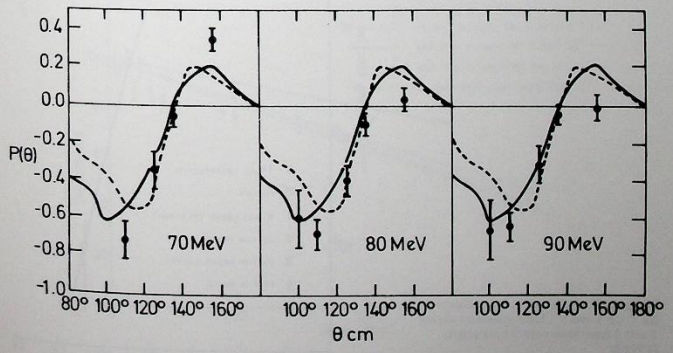

Radiological Experiments

π^- mesons (pions) are potentially superior to γ and X-rays for radiotherapy. The basic properties which are important in this application are (i) the well defined range, for mesons of a definite momentum, with most of the energy being given up at the end of the range and (ii) the nuclear absorption process of stopped mesons; the resulting heavily ionizing products can cause local damage even to oxygen starved cancerous tissue.

π11 Beam Line

Over the past four years the π11 beam from Nimrod has been used in an attempt to determine how far these theoretical advantages are realized in practice. During this period the available dose rate over a small volume of 10cc has been increased from 0·3 rad min^{-1} in 1971 to 3 rad min^{-1} in 1974. Towards the end of 1975, when the new injector is operational, we look forward to a dose rate of 15 rad min^{-1} over the same small volume.

During the four year programme of radiobiological experiments various biological systems have been studied using cultured cancer cells, human lymphocytes, bean roots and mice. A great deal of interesting, but often contradictory, biological information has been obtained. The answer to the basic question concerning the efficacy of a beam of π^- mesons as a radiotherapeutic agent remains in doubt.

The current timetable for construction of the proposed EPIC machine calls for the closure of Nimrod in 1979. This would not leave sufficient time for experimental work to be done using the large aperture beam line which was described in last year's annual report. This project is therefore not being pursued at present.

The results from the work carried out in 1974 are presented in the following reports.

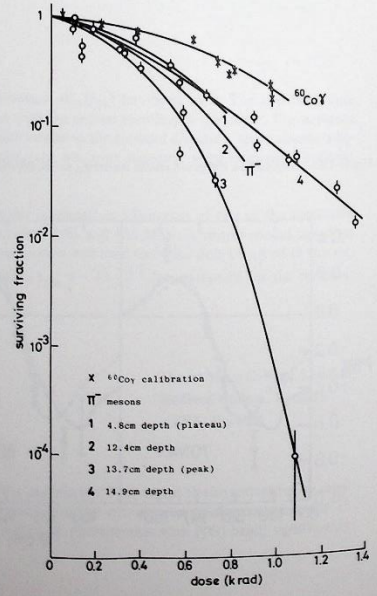

Figure 1.65. HeLa cell survival curves for ^{60}Co γ and π^-. Data points on curves 1 and 2 have been omitted for clarity: (18712)

Experiments with cultured human cancer (HeLa) cells

Medical College of St Bartholomew's Hospital, London

During 1974 there were several successful runs each lasting 1-2 days. These runs used a 10 cm Tungsten target in the X3 beam, and dose rates up to 160 rad h^{-1} were obtained. HeLa cells were irradiated at 4 depths in a Perspex phantom – 4·8 cm (in the plateau), 12·4 cm, 13·7 cm, and 14·9 cm (all in the peak region). The relative dose rates at these four depths were in the ratio 0·96 : 1·19 : 1·35 : 1·22. The results are shown in Fig.1.65. At the 20% survival level, the Relative Biological Effectiveness (RBE) peak-to-plateau is ~ 1·4. The RBE in the peak compared to ^{60}Co gamma rays is 2·1. Further experiments are planned to investigate the depth-survival profile of the beam for both aerobic and hypoxic cells.

Thymic weight loss

Medical College of St Bartholomew's Hospital, London

Earlier results on thymic weight loss in 2½ week old mice irradiated with π^- mesons at dose < 50 rad and at a dose rate of 10 to 12·5 and 50 rad h^{-1} suggested a relatively high RBE for pions compared to 220 KVp X-rays at a similar dose rate. Recent thymic weight loss data at doses up to 100 rad and at a dose rate of 100 rad h^{-1} given in Fig.1.66 together with the old data, do not support such a high value – although π^- mesons seem to be slightly more effective (RBE = 1·3) than comparable dose rate 250 KVp X-rays. We do not find any significant difference in this system for a given dose of radiation at the π peak or plateau.

(ref. 32)

Figure 1.66. Thymic weight loss in 2½ week old SAS/4 mice as a percentage of sham irradiated controls and as a function of dose for peak and plateau π^- mesons and other radiation sources: (18713)

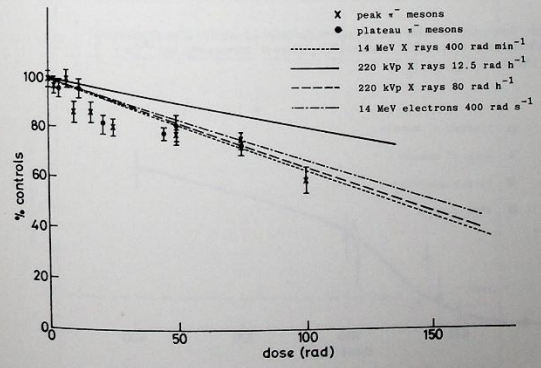

Lens opacities

Medical College of St Bartholomew's Hospital, London

Following the preliminary experiments in 1973 on the induction of lens opacities in mice irradiated at 1 day old, further irradiations have been performed to strengthen the low dose groups. Fig.1.67a shows the incidence of opacities in mice 12 months after irradiation as a function of dose and indicates no peak to plateau differences. Over 80% of the lens opacities observed were minute and only 19% were gross, occupying > 50% of the lens. Fig.1.67b shows the % of mice with such gross opacities induced by pions plotted together with similar data for high dose rate 14 MeV X-rays.

Figure 1.67a. Percentage of mice with lens opacities 12 months after irradiation to the head only at 1 day old: (18715)

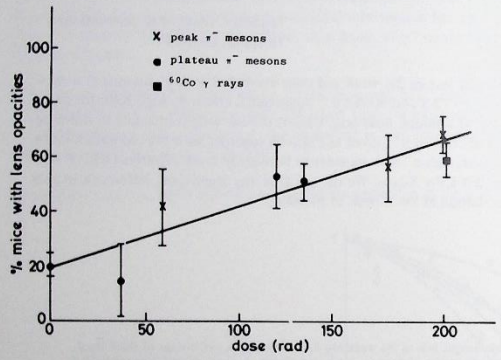

Figure 1·67b. Percentage of mice with gross lens opacities 12 months after irradiation with 14 MeV electrons (O); peak π^- mesons (X); plateau π^- mesons (●); and ^{60}Co γ rays (■) : (18714)

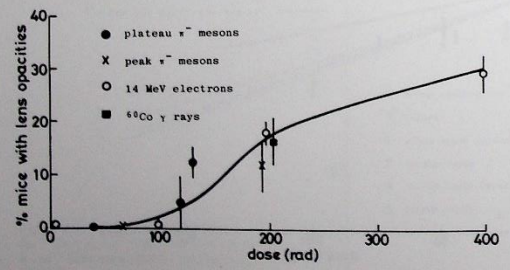

Experiments with frozen HeLa cells

Glasgow Institute of Radiotherapeutics Rutherford Laboratory

During 1974 cells have been irradiated to obtain a complete depth response curve of about 1g cm^{-2} spacing together with some off axis positions, and to obtain dose response curves at selected positions in the plateau, over the peak and in the tail. The cells have been assayed at Glasgow and the data are being analysed. Further exposures are planned.

Experiments with Human Lymphocytes

National Radiological Protection Board Rutherford Laboratory

Fractionation Study (ref. RL-74-150)

Microscope analysis has been completed for a dose fractionation experiment. The aim of the study was to determine whether pion dose fractionation, which will ultimately be used in any radiotherapy regime, affects the peak to plateau chromosome damage ratio as this could result in additional sparing of healthy tissues outside the peak. The irradiated lymphocytes were examined for dicentric and acentric aberrations which together are responsible for much of the cell death during the initial post-irradiation divisions. It can be seen in Fig.1.68 that the combined yield per cell of these aberrations remained approximately constant in the 2 positions when plotted against the time interval between fractions. There is consequently no significant change in peak to plateau ratio from that obtained for the unsplit control doses.

It is interesting to consider the aberration types separately. A reduction in dicentric yield of 26% in the peak and 41% in the plateau was reported last year for a 24 hour interval. Subsequent analysis has shown a similar effect with a 6 hour interval and confirms the improvement in the peak to plateau ratio for this type of aberration. A reduction in dicentric yield is characteristic of split dose low Linear Energy Transfer (LET) radiation. At high LET however the 2 hits needed to produce dicentrics mostly result from single ionizing tracks so that there is little chance of repair before the damaged sites interact and no fractionation effects are observed. The dicentric data are therefore consistent with the fact that the dose in the plateau region has a greater low LET component. However with increased fractionation intervals the plateau yield for acentric aberrations rose with respect to the peak. As an acentric is equally deleterious to the cell this response counterbalances any advantage obtained with the dicentrics. Presumably the additional acentrics, a proportion of which are single-hit aberrations, are formed from the lesions which would otherwise have interacted to produce dicentrics.

Figure 1.68. The relationship of the yield of aberrations per cell to the time interval between two exposures to a pion beam, each of 63 rad at the plateau and 100 rad at the peak: (18717)

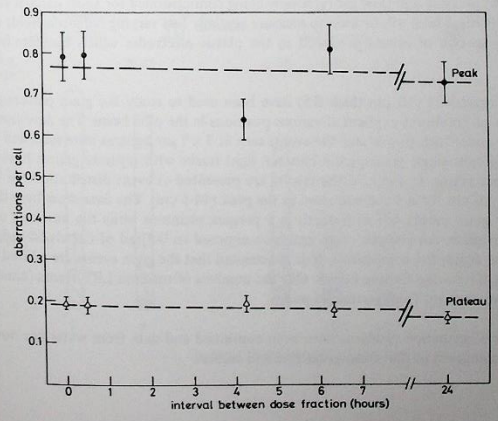

Broad Peak Experiment

Irradiation of solid tumours will require a beam in which the peak to plateau ratio has been partially sacrificed in order to obtain a broad flat-topped peak. An attempt has been made to generate a biological profile for chromosome aberrations which meets this requirement by irradiation with pions of three different energies: 50, 64 and 80 MeV as opposed to the single energy of 75 MeV used in previous experiments. Blood samples have been exposed in a water phantom for 25 cm along the axis of the beam. A dose of 150 rad measured in the peak was delivered in 3 cycles of the 3 energies. The resultant dose rate using a 10 cm Cu target was about 75 rad per hour. The irradiated cells have been successfully cultured, microscope slides prepared, and analysis started.

Physics Experiments

Medical College of St Bartholomew's Hospital, London
University of Leeds
Rutherford Laboratory

Following the successful operation of the 2nd harmonic RF cavity in Nimrod we have obtained a dose rate of 3 rad min^{-1} from a 10 cm Tungsten target with $1{\cdot}8 \times 10^{12}$ protons per pulse. The X3 extracted proton beam and $\pi 11$ were realigned during the 1973/4 winter shutdown. Subsequent beam studies have shown that the $\pi 11$ beam now has a slightly larger spot with the same relative intensity. The opportunity was taken to explore some new modes of running the beam including one which resulted in a better defined momentum and reduced spot size with equal peak dose. This mode was adapted to produce a trial flat biological peak between 7 and 18 cm depth for the lymphocyte experiment mentioned above.

We have investigated how the pion dose is dependent on the absorber. Similar 0·2 cc ion chambers, one 'air equivalent' (AE) and one 'tissue equivalent' (TE) have shown no relative change of response over the region of the pion field with a dose $\geqslant$ 10% of the peak value to an accuracy of 7%. The absolute ratios TE/AE at the plateau and peak, assuming unity for ^{60}Co γ rays, are 0·99 ± ·01 and 0·98 ± ·01. In order to observe the different doses from Carbon and Oxygen bearing absorbers, spheres of polythene were placed about an ion chamber within a water bath. The stopping power of the polythene was 3·5% less per cm than water, and the total depth was adjusted to keep the ion chamber at the dose peak to within 0·5mm. The results shown in Fig. 1.69 indicate no significant effect to the order of 1%.

Our biological results do not show a higher RBE just behind the dose peak as would be expected. We have not been able to resolve this. A new thin parallel plate ion chamber that will enable us to measure the shape of the ionization peak is planned.

A new constant pressure and flow gas rig is now being commissioned for small parallel plate proportional chambers. These will be used to measure spatially fast varying radiation fields and also obtain energy spectra of events produced in the plastic electrodes which simulate bone and other tissue.

(ref. 72)

Thin nuclear emulsions (10 μm thick K5) have been used to study the grain patterns seen in small volumes of emulsions exposed at various positions in the pion beam. The developed slides were scanned under high power and the events seen in 7 x 7 μm squares were recorded under 4 arbitrary categories: single grains; grain clusters; light tracks with separate grains; heavy tracks with continuous grains. In Fig.1.70 the results are presented as event distributions in 100 volumes 7 x 7 x 10 μm for a 1 rad exposure at the peak (14·5 cm). The data show how the numbers of single grain events fall with depth in a perspex phantom while the numbers of heavy track events increase. An analysis of an emulsion exposed to 0·3 rad of Cobalt-60 radiation is included in the figure for comparison. If it is accepted that the grain events are related to LET then the most interesting finding here is that the numbers of medium LET events (clusters and light tracks) are constant from plateau to peak.

Measurements of spallation products have been continued and data from water are now being analysed and compared to that from polythene and carbon.

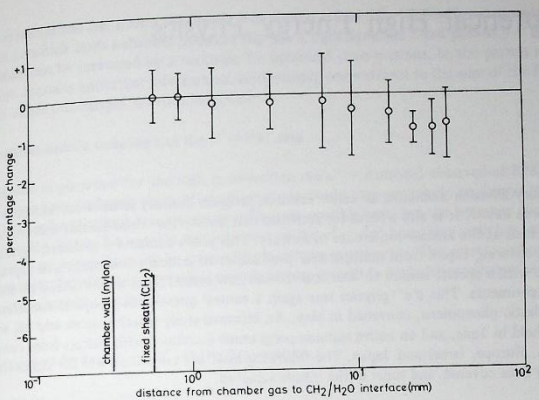

Figure 1.69. Effect on air equivalent ion chamber by replacing oxygen by carbon (H_2O by CH_2) : (18716)

Figure 1.70. Event distributions in thin nuclear emulsions exposed at several positions in a perspex phantom to a pion beam: (18816)

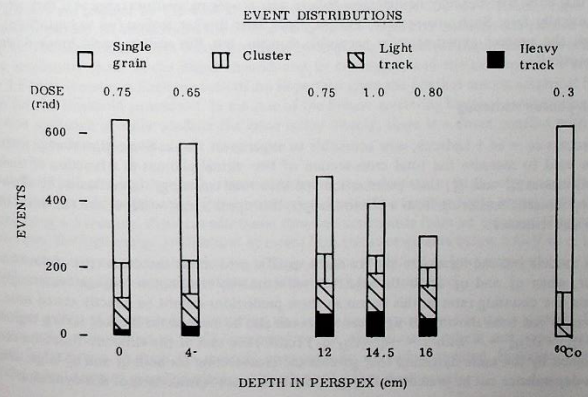

Theoretical High Energy Physics

The Theory Division maintains an active research program in many areas of current interest, as can be seen below. It is also a focus for activities that involve the whole British university community, such as the annual conference in January. This year's conference included eight review lectures, covering topics from multiparticle production to critical phenomena and asymptotic freedom, with a special session to hear and discuss new results from the SPEAR e^+e^- colliding beam experiments. This e^+e^- physics was again a central question at a topical conference on deep inelastic phenomena, convened in May. An informal study meeting on $\pi\pi$ and πK scattering was held in June, and an active summer programme continued with visitors from centres in the USA, Europe, Israel and Japan. The following brief accounts illustrate the research areas that have been covered, and some of the results achieved.

Bjorken scaling and massive gauge theories

(ref. 94) A very important phenomenon in inelastic lepton-nucleon scattering is Bjorken scaling: when the inelasticity and momentum transfer are both large, the inclusive cross-section behaves as if the lepton were scattering from a pointlike object. This is surprising since strong interactions were expected to give a diffuse structure to the nucleon and its constituents. It seems as if the strong interactions are somehow switching off in this region.

There is a possible theoretical explanation in the fact that a class of field theories based on non-abelian gauge groups have this kind of property. If g is the gauge coupling constant, the point $g = 0$ is an ultraviolet fixed point of the renormalization group. Such theories are "asymptotically free", and predict Bjorken scaling within logarithmic factors. However, these theories contain massless vector fields that cause severe problems; experimentally they are not seen and theoretically they give infra-red singularities. A solution is to give these fields mass by the Higgs mechanism, but this in turn may change the UV behaviour and spoil scaling.

The gauge group SU(n) has been studied as an example, introducing Higgs scalars such that all the vector bosons acquire masses. It is found that this theory is not UV stable. However, it appears that such theories may nevertheless behave over a wide momentum range as if they were asymtotically free. Such quasi-stable theories could have Bjorken scaling (up to logarithms) through the present experimentally accessible domain, but this scaling would break down asymptotically.

Photon-photon scattering

(Ref. 112, 113) The process ee → ee + hadrons, now accessible to experiment thanks to electron storage rings, can be used to measure the total cross-section of two virtual photons as a function of their squared masses q_1^2 and q_2^2, their polarization and their total cm energy. In particular, by allowing deep inelastic scattering from a photon target, this opens a new window into the world of subnuclear structure.

Parton models and the light-cone algebra make specific predictions about the cross-section behaviour, when q_1^2 and q_2^2 are both large, but unfortunately the photon propagators strongly suppress the counting rates in this region so these predictions cannot be directly tested soon. However, it has been shown that significant tests can also be made in the Bjorken scaling region where $q_1^2 \simeq 0$, $q_2^2 \to \infty$ with $x = -q_2^2/(2q_1 \cdot q_2)$ fixed. Here two of the structure functions are determined by the same dynamics that governs the cross-section for both q_1^2 and q_2^2 large, and their x-dependence can be predicted; they provide much more feasible tests of this dynamics.

Another investigation has shown that when one photon is real ($q_1^2 = 0$), the forward scattering amplitude in which both s-channel helicities flip has a right-signature fixed pole at $J = 0$. The pole residue can be measured by a sum rule for polarized cross-sections. In the parton model this residue contains important information, being simply proportional to the sum of the fourth powers of all parton charges, independent of q_2^2.

Direct electron-hadron coupling and the $\pi^\circ \to e^+e^-$ rate

One suggested explanation for the high cross-section $\sigma(e^+e^- \to \text{hadrons})$ observed at SPEAR is that electrons have hadronic cores. If so, these cores would also contribute to decays such as $\pi^\circ \to e^+e^-$. Pseudoscalar and axial vector couplings are possible here, but the latter are suppressed by a helicity factor. No specific measurement of the $\pi^\circ \to e^+e^-$ branching ratio has yet been reported, but an upper limit can be inferred from certain experiments. The corresponding limit on the pseudoscalar coupling strength is already strong enough to exclude some hypotheses for direct electron-hadron couplings. *(ref. 38)*

η_{+-} measurement from $e^+e^- \to K^+K^-$ at the ϕ resonance

The magnitude of the CP-violating ratio

$$\eta_{+-} = \text{Amplitude}\,(K_L \to \pi^+\pi^-)/\text{Amplitude}\,(K_S \to \pi^+\pi^-)$$ *(ref. 36)*

is an important and still open question. A recent redetermination differed by about 20% from previous values, and some authors have interpreted this discrepancy to question the theoretical formalism. Older determinations required the combining of four different experimental ratios. The recent remeasurement used a single experiment, on the time distribution of $\pi^+\pi^-$ decays from an initial K°-$\bar{K}^\circ$ mixture, but fitted five parameters simultaneously and depended crucially on the K_L-K_S interference term in this distribution. A new procedure is proposed, namely to measure the time-distribution of $\pi^+\pi^-$ kaon decays, within a specified angular cone, from the reaction $e^+e^- \to K^\circ\bar{K}^\circ$ at the ϕ resonance. The analysis requires fitting only two parameters and avoids complications and uncertainties from the interference term, which is now suppressed by a factor of about 1000.

Pion-pion scattering

The special situation of $\pi\pi$ scattering with its theoretical simplicity and incomplete data has continued to stimulate theoretical effort. Exploiting the constraints from analyticity, crossing and unitarity remains a major concern. One question is what correlations among low energy $\pi\pi$ parameters are implied by the data at higher energies, say about 600 MeV. Results have previously depended on complicated fits to data using fixed-t dispersion relations and related techniques. The same results have been reproduced by imposing two simple requirements, weak exotic amplitudes (both in the direct channel and in exchange), and the existence of a strong $I = 1$ P-wave resonance. Such predictions are important given the conflict among empirical findings for the threshold parameters. In the case of the P-wave scattering length, for which the dispersion approach actually predicts the value rather closely, there is a direct conflict with the present experimental result. *(ref. RL-74-068, RL-74-079, RL-74-128, 80, 81, 82, 87)*

Analyticity and crossing also imply relations between the behaviour at high energies and at the lower energies where data exist. For $\pi\pi$ scattering, beside the familiar finite energy sum rules embodying s-u crossing, there are additional sum-rule constraints from s-t crossing. Using such sum rules, the high-energy implications of recent high statistics $\pi\pi$ data below 2 GeV have been evaluated. An important result is that the ρ Regge residue is required to have a zero at $t \simeq -0{\cdot}44$ GeV^2, suggesting that absorption effects are rather weak in $\pi\pi$ scattering.

Another aspect of meson-meson scattering which has been brought out is the low value of the exotic total cross-section σ_t $(\pi^+\pi^+)$, compared to the plateau value which one would expect from factorization. Perhaps the inelastic cross-sections are underestimated. However, explicit model calculations of several particular channels yield rather small results.

There are rather few well attested meson supermultiplets, and this is a handicap in evaluating the success of classification schemes like the L-excitation quark model. In general, the natural parity sector is best studied in the appropriate 0^-0^- channels, $\pi\pi$, $K\pi$ etc. Of the predicted levels, the lowest lying which has proved difficult to assign has been the 0^{++} family, the natural parity companions of the 2^{++} tensors in the quark model L = 1 band. There is no shortage of candidates for the 0^+ nonet. Besides a full quota K(1250) and δ(970) for I = ½ and I = 1, three possibilities have at various times been considered for the two I = 0 members, the ϵ(900), S* (1000) and ϵ'(1250) effects. A new interpretation of the I = 0 phenomena has now been offered. Firstly, a resonance description is proposed for the S*(1000) (which couples strongly to $\pi\pi$ and KK) involving poles on two of the nearby unphysical sheets; this enables effective decay coupling constants to be defined. Secondly, it is suggested that the S* contribution to the I = 0 channel should be removed by subtracting the corresponding $\pi\pi$ phase shifts to isolate the remaining dynamics. This causes the two elastic ϵ and ϵ' effects to coalesce, yielding one broad elastic resonance of mass 1100 MeV or more. The fit has been extended to all the $0^+ \to 0^-0^-$ resonance decays and shown to admit a solution consistent with SU(3).

Any such fit is characterized by the mixing angle θ, the ratio λ of singlet to octet coupling, and the overall strength. It is natural to compare the results for the scalar decays with those of the associated supermultiplets, in the present instance the tensors. For the latter, as for the vectors, the observed pattern of decays approximately corresponds to 'ideal mixing', $\cot\theta = \sqrt{3}$, and "Zweig's rule" $\lambda = \sqrt{3}$. For the scalars, the mixing is far from ideal, but λ is rather similar to that for the tensors. If upheld, this would suggest an interesting systematics with mixing varying from supermultiplet to supermultiplet, but "Zweig's rule" (decay going according to quark content) extending over the whole band. Further confirmation of the 0^+ assignments is to be sought, especially in the $K\bar{K}$ channel.

Geometrical scaling and the Pomeron

(ref. RL-74-034, 12)

Recent measurements of pp scattering at very high momenta ($p_{LAB} \geqslant 100$ GeV/c) have an intriguingly simple property. The energy dependence of the inelastic and total cross-sections, and of the elastic angular distribution, can all be described and correlated just by a scale change in the interaction radius. This geometrical scaling (GS) is apparently a property of Pomeron exchange (alias diffraction) that dominates pp scattering. It is important to discover if GS is really a general Pomeron feature or just a local accident, and also to pursue its theoretical implications.

It turns out that almost none of the Pomeron mechanisms usually proposed can predict or even accommodate GS. A possible prescription has been found, using a Regge dipole, that has GS but lacks a fundamental basis. Alternatively, a Regge pole exchange with intercept greater than unity can be adjusted to give approximate GS through a limited energy range; there is theoretical support for such a mechanism, as the first term in a perturbation series, but GS then emerges as an accident.

If GS is a general property, it should appear in other reactions too. The πN and KN data above 100 GeV/c are still sparse but nevertheless consistent with GS. One then wonders whether the GS idea can be generalized to describe not just one process at a time, but to unify the Pomeron contributions in different reactions. Indeed it can be generalized, but the prescription is not unique, and the present data are consistent with a whole range of possibilities. More extensive πN and KN angular distributions will clarify these questions soon.

Finally, the experimental implications of GS have been pursued, to show that it puts strong constraints on the real part of the Pomeron amplitude, and on polarization effects. Its predictions can also be extended to hyperon-nucleon scattering, using SU(3) symmetry, and to inclusive reactions.

Pomeron factorization tests in $\gamma N \to \phi N$

(ref. 37)

ϕ-photoproduction is a good place to study the Pomeron mechanism, since other contributions seem to decouple here. Tests for factorization have been investigated, for arbitrary initial polarizations.

Factorization for parity-conserving two-body reactions implies M-purity, that corresponds asymptotically to purely natural or unnatural parity exchanges. Present $\gamma N \to \phi N$ data do already indicate M-purity, with natural parity for the Pomeron. In principle the ϕ density matrix contains information that can independently test (a) factorization, (b) M-purity and (c) relative reality of amplitudes (expected if the Pomeron is a Regge pole). These tests require polarization of the beam and/or target, but not target polarization in the reaction plane. Unfortunately the tests that distinguish factorization from M-purity are hard to perform accurately, since they depend on s-channel helicity-flip amplitudes that appear to be small experimentally.

Derivative rule for spin-dependence

(ref. 13)

Several authors have recently proposed a rule for high-energy two-body reactions at small angles, whereby the s-channel helicity-flip amplitude is directly proportional to the derivative of the non-flip amplitude, with respect to momentum transfer. An empirical rule similar to this is already familiar in low-energy nuclear physics; if true, it would greatly simplify high-energy amplitude analyses. This rule has been tested by careful comparison with a simple and well-measured reaction, namely $\pi^- p \to \pi^0 n$. Here it is extremely plausible that helicity-flip is described by a single Regge-pole mechanism, and the combined assumptions are very strong. Although most of the data can be fitted quite well, the derivative rule is found to predict a pronounced deepening of the dip in the differential cross-section, contrary to experiment. This casts doubt on the rule, as an exact condition.

Multiparticle production

(ref. RL- 74-046, RL-74-118 RL-74-119 RL-74-155, 67, 68, 88, 89, 90, 97)

It is generally accepted that high-energy multiparticle production processes have two components, corresponding to diffraction and a multi-peripheral type of mechanism. The Rutherford Laboratory group has continued to study the detailed structure of each component, and has pushed forward an ambitious programme for calculating the diffractive part from a dual description of the multiperipheral part, through the unitarity relation.

The non-diffractive component appears most clearly in the central region, where double Regge pole exchange in the Mueller-Regge framework is supposed to describe inclusive production. However, a detailed analysis of the π^+-π^- cross-section difference shows that this picture is valid only for $p_T \geqslant 0{\cdot}7$ GeV/c, and that estimates of the central vertex from different energy regions are inconsistent. A more profitable approach has been to consider specific models for exclusive n-particle production, and from them to construct explicit predictions for inclusive, semi-inclusive and exclusive distributions. In the limit where transverse momenta are neglected, closed form expressions can be obtained for the distributions predicted by standard models; these can be used to analyze semi-inclusive correlations and hence to learn the nature of cluster production, for example.

The diffractive component has been studied by analyzing the world data on $pp \to pX$ in terms of the triple-Regge formalism. The results show that diffractive scattering is dominated by the triple-Pomeron term, which furthermore shows no tendency to vanish at t = 0, contrary to some theoretical expectations. This result implies that the total diffractive cross-section rises by 3·3 mb between 200 and 2000 GeV/c, i.e. that most of the observed rise in the inelastic pp cross-section can be attributed to this component. The picture has therefore changed considerably from the original simple view, that diffraction would provide a constant cross-section with a fixed low multiplicity distribution.

A programme was started last year (see 1973 Annual Report) to calculate diffractive scattering from a dual model input, using multiparticle unitarity; it has now been carried several stages further. The basic assumptions include Regge asymptotic behaviour, semilocal duality and exchange degeneracy. The scheme provides a practical way to calculate the unitarity sum over multiparticle states, and from this several important properties of elastic scattering can be deduced. The energy dependence and forward slopes of pp, $\pi^{\pm}p$ and $K^{\pm}p$ scattering are all completely determined; the results are all consistent with experiment and furthermore the output Regge parameters agree with the input values. The scheme contains only one free parameter that can be fixed by inclusive data; the scheme is presently being extended so that this parameter too can be determined by a unitarity sum, giving a "reggeon bootstrap".

Another application of multiparticle unitarity allows the ratios of electromagnetic form factors of the pion, kaon and nucleon to be computed. The process $\gamma \to h\bar{h}$ (where h is the relevant hadron) receives contributions from intermediate n-particle states. By considering the mismatch between these states in $\gamma \to n$ and $h\bar{h} \to n$, due to local conservation of quantum numbers in rapidity, one is led to results such as $F_\pi(t)/F_K(t) \sim |t|^{\alpha_\rho - \alpha_{K^*}}$ for large t.

Finally, the two-component idea has been used in an analysis of the pp inelastic overlap function. This overlap function can be deduced from high energy elastic data; its form does not immediately suggest two components, but does indicate that absorption is important. When absorption is allowed for in a plausible way, the results strongly suggest the presence of two components, that can be separated. An interesting conclusion is that diffractive scattering resembles elastic scattering, in that it is concentrated at small impact parameters.

Unitarity in the Glauber model

(ref. RL-74-121)

The Glauber model is a simple prescription for calculating high energy scattering from a compound target, such as an atomic nucleus, that has been widely used. Nevertheless, it is only an approximation, and a systematic investigation of its properties has therefore been formulated. The first result is that the model in fact violates unitarity slightly; this happens because it assumes impact parameter conservation, that is not strictly true for inelastic processes.

Nucleon-nucleon cross-sections and extensive air showers

(ref. RL-74-156)

All two-body cross-sections seem to be rising, at the highest energies accessible to accelerators, and this is believed to be the start of an asymptotic regime. There is great interest therefore in exploiting cosmic rays, to attain still higher energies, to confirm and quantify this phenomenon more fully, and to compare with various theoretical predictions. For example, the altitude dependence of unaccompanied hadron spectra has been used to estimate the N–N total cross-section σ up to 3×10^4 GeV/c. To go higher still, one must resort to extensive air showers (EAS), and there have been recent attempts to extract σ from the zenith angle dependence of EAS. This question has been reanalyzed. It is concluded that these EAS data cannot determine σ quantitatively without additional assumptions, such as the energy dependence of the inelastic N–N cross-section, for which there is no solid justification.

Computer aided theory

Effects of strong potentials

Studies have continued on vacuum polarisation effects in very strong finite range potentials, in particular the phenomena associated with the critical potential for which bound states are drawn into the negative energy continuum. Apart from its interest as a relatively unexplored area of quantum electrodynamics, these critical potential phenomena exhibit features analogous to the behaviour of lepton currents in weak interactions, and offer a possible interpretation of the apparent conversion of leptons from a state of observable charge to a state of unobservable charge, as an extreme vacuum polarisation effect. The study of short range vacuum polarisation effects is also relevant to the interpretation of electron scattering from possible point-like subunits in the nucleon, in particular to the possibility of localised regions of fractional observed charge.

Two techniques are being used; the first involves a lengthy computer summation of positive and negative energy continuum solutions of the Dirac equation to obtain the induced charge for specific source potentials, and the second involves re-expressing this sum as a Green's function contour integral and computing this numerically. The two methods of computation have been shown to be in numerical agreement, at least for situations free from divergences, and are being applied to the study of the localised vacuum polarisation charge distribution produced by short range potentials.

Effects of an internal velocity distribution for partons

The above work has provided an instructive example of the use of the computer "experimentally" to discover new features of the theory which would have been difficult or impossible to achieve by purely analytical means. As a second example of this, computer models have been set up to explore the effect of an internal parton velocity distribution on the structure function distribution for electron-nucleon scattering, by numerically transforming the former into the latter using off-mass-shell kinematics analogous to those of Fermi motion in a nucleus. One immediate result is that with a finite velocity distribution, slight departures from scaling occur, the x distribution undergoing small changes with increasing energy and scattering angle. Also, since not all internal momenta yield a kinematically allowed final state, the structure function integral can be less than unity, thus offering an alternative interpretation of this familiar experimental result, normally attributed to a hypothetical sharing of the 4-momentum with neutral "gluons".

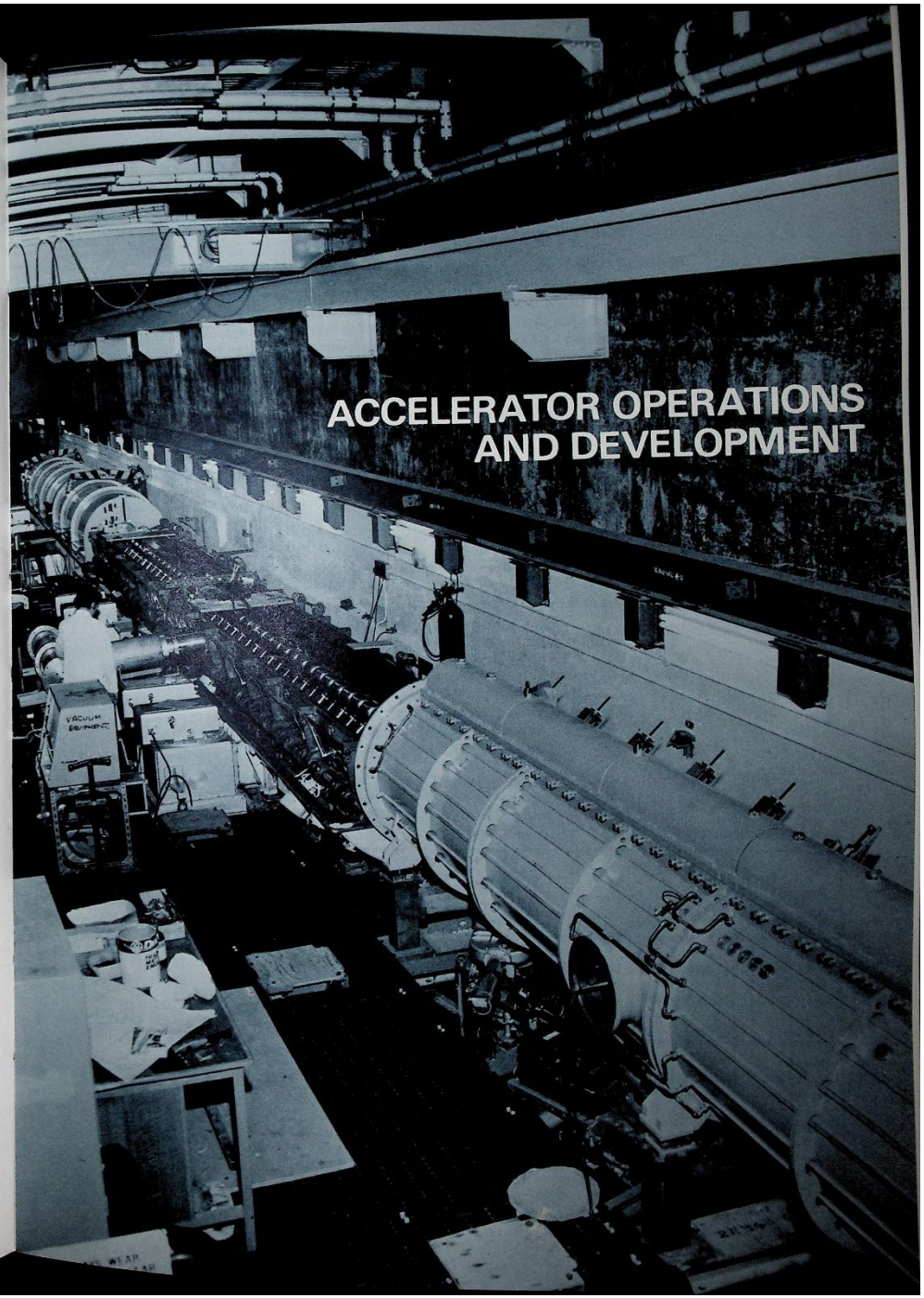

ACCELERATOR OPERATIONS AND DEVELOPMENT

Assembly of the 70 MeV injector

2. Accelerator Operations and Development

OPERATION OF NIMROD

(ref.RL-74-148) Nimrod, the 8 GeV/c proton synchrotron, has been operated in a continuing 21 day cycle. Usually in each cycle about 17½ days were allocated to high energy physics research and the remainder accounted for by accelerator development, maintenance and start up. The Winter shutdown, which started in December 1973, was phased in with the requirements of the new 70 MeV injector building programme. This shutdown continued until mid-April when Nimrod restarted operation, on schedule. The first cycle was wholly devoted to recommissioning Nimrod and the extracted proton beam lines. The subsequent eleven cycles largely followed the pattern outlined above.

The operations record is summarised as follows:–

High Energy Physics Research	Hours
Scheduled time	4557
Good beam time	3913

i.e. "beam on" for 85·9% of scheduled physics research time.

The remainder of the year is accounted for as follows:–

	Hours
Machine physics and start-up	1177
Routine maintenance and minor modifications at 21 day intervals	350
Shutdown periods for major modifications and maintenance, and also including the Christmas Holiday	2676

The total number of protons accelerated to full energy was about $17{\cdot}3 \times 10^{18}$. Machine pulses, with beam, totalled $5{\cdot}72 \times 10^{6}$.

Nimrod Operations 1974

Hours / Date From To	Clock	Shut-down	Maint.	HEP Research Sched.	Beam On	Exp. Off	Nimrod Off	Nimrod Avail.	Machine Physics and Development Sched.	Beam On	Exp. Off	Nimrod Off:	Nimrod Avail.
Jan 1 Mar 31	2159·00	2159·00											
Apl 1 June 30	2184·00	368·00	110·76	1021·03	851·65	1·22	168·16	852·87	684·21	390·26	119·21	174·74	509·47
Jul 1 Sep 30	2208·00		107·45	1789·17	1549·76	0·13	239·28	1549·89	311·38	194·75	19·89	96·74	214·64
Oct 1 Dec 31	2209·00	149·00	132·07	1746·48	1511·52	0·27	234·69	1511·79	181·45	83·76	23·32	74·37	107·08
Totals	8760·00	2676·00	350·28	4556·68	3912·93	1·62	642·13	3914·55	1177·04	668·77	162·42	345·85	831·19
Percent Clock Time	100·00	30·54	4·00	52·02					13·44				
Percent HEP Scheduled Time				100·00	85·87	0·04	14·09	85·91					
Percent MP Scheduled Time									100·00				70·62

Analysis of Nimrod Off Time during Scheduled Operating Time in 1974

Scheduled Operating Time 5733·72 hours
Off Time 987·98 hours

	Beam Time Lost Hours	% of Scheduled Op Time	% of Nimrod Off Time
1. **Faults and Routine Inspections**			
Vacuum Systems	185·58	3·24	18·78
Synchrotron RF/Beam Control/TV/ Diagnostics	175·86	3·07	17·80
Nimrod Magnet Power Supply	(131·30)	(2·29)	(13·29)
(a) Rotating Plant	66·14	1·15	6·70
(b) Converter Plant	39·55	0·69	4·00
(c) Ripple Filter Plant	25·61	0·45	2·59
Straight Section 1 Environment Problem	96·47	1·68	9·77
Extraction Systems	(85·64)	(1·49)	(8·67)
(a) Plunging Mechanisms	50·57	0·88	5·12
(b) Power Supplies	31·57	0·55	3·20
(c) Magnets	3·50	0·06	0·35
Injector	78·68	1·37	7·96
Coolant Systems	77·91	1·36	7·89
Nimrod Magnet	16·52	0·29	1·67
Inflector System	3·80	0·07	0·38
Miscellaneous	57·68	1·01	5·84
2. **Other Reasons**			
Start-up	66·75	1·16	6·76
Public Electricity Supply	11·79	0·20	1·19
	987·98	17·23	100·00

Figures for Vacuum and Extraction Systems include routine inspection time. The Pole Face Winding Systems and Targets and Target Mechanisms areas were virtually trouble free in 1974, with off time totals of less than 0·5 hours each. They are included in the Miscellaneous figure. The Miscellaneous total also includes 24 hours of lost time, in one incident, due to the failure of a beam line element, and its replacement, in the Nimrod machine area.

Figure 2.1. Nimrod operation record for high energy physics during 1974: (18782)

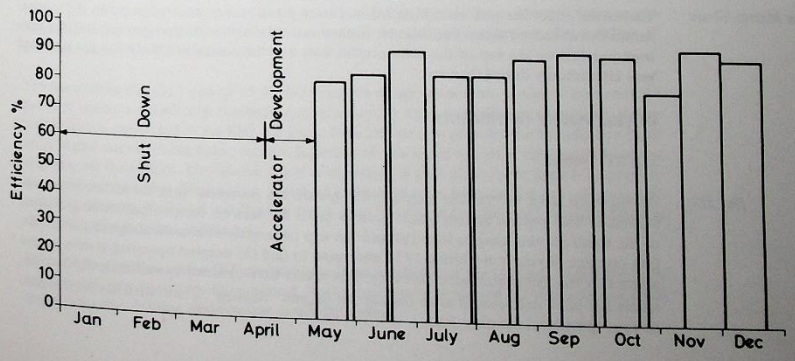

Magnet Power Supplies and Ancillary Plant

The Nimrod magnet has been pulsed throughout the year with the complete power supply plant and overall performance continues to be good. The arc-back rate on the converter plant has continued at a low level and the ripple filter installations have given good service.

Operating statistics for the year are as follows:–

Machine running time	5,545 hrs
Machine pulsing time	5,285 hrs
Total pulses	6,450,140

Fatigue testing on a number of V coil support bolts was carried out during the year. As a direct result of these tests, it was agreed that the service life of these bolts could be safely increased to 60×10^6 pulses and hence no bolts will have to be changed until 1978 or later.

Excitation Rectifiers With the ending of the manufacturer's reconditioning service for the mercury-arc rectifiers, which are currently in use, alternative thyristors have been built and tested under normal operational conditions. The results of these tests show that the use of thyristors in the excitation circuitry of alternators subjected to pulsed load conditions is feasible. However, since the mercury-arc rectifiers have caused little lost operating time, have a greater over-load capacity and are more tolerant of voltage transients than thyristors, it has been decided to continue their use for as long as possible.

Drive Motors The advantage of having a spare drive motor was emphasised when a fault occurred in September which necessitated the removal of No 1 motor from service. The spare motor was installed and operational within 4 days. As this period was mainly scheduled for machine physics and maintenance, the effect on the HEP research programme was only slight.

The fault was due to overheating of connections at the slip-ring end of the rotor where a conductor leaves the winding interconnection region on its way to the slip-ring. Routine checks on the motor prior to its return to the manufacturer's works revealed a stator winding fault. During the repairs the design of the conductors between the slip rings and the winding connections was modified to eliminate one of the joints which had failed. The repairs have now been completed.

Converter Grid Control Gear Silicon transistors have been successfully used in place of germanium-type transistors in the converter grid control gear to end the intermittent mal-function, during periods of high ambient temperature, of some components, in particular the printed circuits which are responsible for the timing and generation of the grid impulse. All ninety-six operational printed circuits of this type on the plant have been converted.

New Master Timer The master timer has now been installed in a more permanent position adjacent to the original Brown-Boveri master timer. Facilities for control and indication of the programme settings have been installed on the top of the main control desk and the complete installation has operated very satisfactorily during the year.

DEVELOPMENT OF NIMROD

2nd RF System

(ref.58) Development work on the 2nd harmonic RF system has continued with the addition of a new automatic level control system which allows a faster RF turn-on. Minor modifications of some of the signal limiting circuits have reduced the trip occurrence rate to an acceptable level. The first machine physics runs during 1974 were used to find the simplest operating system to give optimum extracted proton beam intensity. Best results were obtained by switching the 2nd harmonic RF off 4 milliseconds after the start of magnet "flat-top". The system has been in continuous operational use since June.

During the year the intensity of the extracted proton beam into Hall 3 was increased, with 1·8 $\times 10^{12}$ protons per pulse on average and peak pulses of about 2×10^{12} ppp. Prior to the introduction of the 2nd RF system, the extracted proton beam to Hall 3 was normally $1{\cdot}2 \times 10^{12}$ ppp. About 40% of the increase may be attributed to the 2nd RF accelerating system and the remainder is accounted for by improved beam steering in the upstream end of the beam line. This latter improvement was assisted by the installation of additional diagnostic facilities in the extracted proton beam line to Hall 3.

Development of Vacuum Switches For Radiation Environments

Further tests have been carried out on a new type of vacuum switch incorporating Field Effect Transistors (FET) to overcome the problem of rapid deterioration of conventional switches due to radiation damage. The tests have proved successful. The life of the FET model is a factor of ten better than that of the junction transistor models. The vacuum switches in the Magnet Hall will now be progressively replaced by the new model.

Cryopump Fitted to Aid Localised Pump Down

Improved operation of the electrostatic inflector, which guides the protons from the linear accelerator into the Nimrod magnet ring, has been achieved by installing a cryopump in the local vacuum system. With its high pumping speed for water vapour (50,000 l/s) and hydrocarbons the level of these contaminants has been reduced by a factor of about 20.

70 MeV INJECTOR FOR NIMROD

The new injector building constructed adjacent to the existing 15 MeV injector hall was completed during the year and all the required mechanical and electrical services were installed. Earth mounding was replaced over the tunnel linking the injector building to the synchrotron hall to provide adequate radiation shielding. Most of the pre-injector equipment has been installed in the EHT area. The power supply is based on a 5-stage Cockcroft-Walton generator with a 0·01μF reservoir capacitor.

The initial setting of pre-injector d.c. gun voltage and control of long term stability is achieved by the normal controls of the Cockcroft-Walton generator; rapid short term fluctuations in d.c. gun voltage resulting from beam loading of the EHT coupling network is compensated to within $\pm$0·2% by a bouncer stabiliser (Fig.2.2).

The bouncer, which has been developed at the Laboratory, cancels short term voltage variations in the EHT system by applying an appropriate offset voltage to the low voltage plate of the reservoir capacitor. Although the voltage excursion at the bouncer output has been restricted to 15kV, the coupling network needed to protect the accelerating tube from damage places exceptional bandwith demands upon the stabiliser system. A pulse transformer coupled stabiliser of the single hard valve pattern is used.

The bouncer is initially rated at 15 kV 0·5A and its design allows two modes of operation. In the first mode, a closed loop feedback system accepting error signals for an ac coupled potential divider is connected to the EHT platform. Facilities are also provided for the addition of an error signal derived from beam current. Injection of this signal improves the overall transient response of the system. The second mode of operation is that of a simple open loop pre-programmed compensator. Closed loop testing of the bouncer has been carried out using a model coupling network. Full load stabilities of better than $\pm$0·05% under simulated beam loading conditions have been obtained (Fig.2.3).

Three of the four linac tanks (RF cavities) have been installed over the trench in which the main vacuum diffusion pumps are being housed. Drift tubes have been aligned in the second and third tanks and a start is being made on low power RF testing.

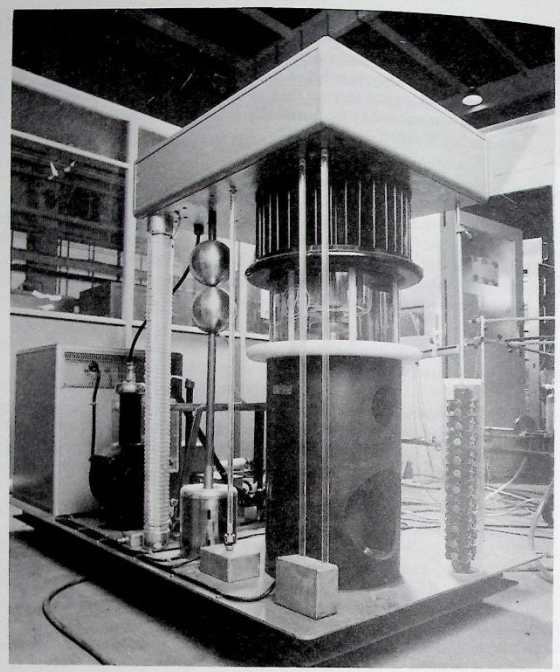

Figure 2.2. The bouncer stabiliser which is designed to cancel short term voltage fluctuations resulting from beam loading in the initial d.c. acceleration stage of the 70 MeV injector: (18055)

Work has proceeded on the manufacture of four pulse modulators which supply the main RF power valves. Each modulator has a 15 section delay line charged to 32 kV and provides an output, via a pulse transformer, of 80 MW at 40 kV with a flat top time of 800 microseconds, and a pulse repetition rate of up to one per second. Tests on the first modulator have been completed successfully and work on the remaining units is well advanced.

The two power amplifiers which form the final stages of the first of four RF systems (one for each tank) have been successfully tested into a matched dummy load to their full design output power levels of 0·5 MW and 4 MW. A start has been made on installing the RF equipment in the new building.

The beam transport elements required for the transfer of the beam to Nimrod have been manufactured and tested. Models of the electrostatic inflector assembly incorporating the two alternative types of septa (a thin magnesium aluminium sheet or an array of molybdenum grid wires) have been tested. The final choice from these alternatives based on the test results will be made in 1975. Modifications to the straight section box for the inflector components are complete.

The CAMAC control system has been on test with a simplified version of the final programme. The pre-injector and EHT platform link for control and data transfer has been tested in its working position in the EHT platform test rig.

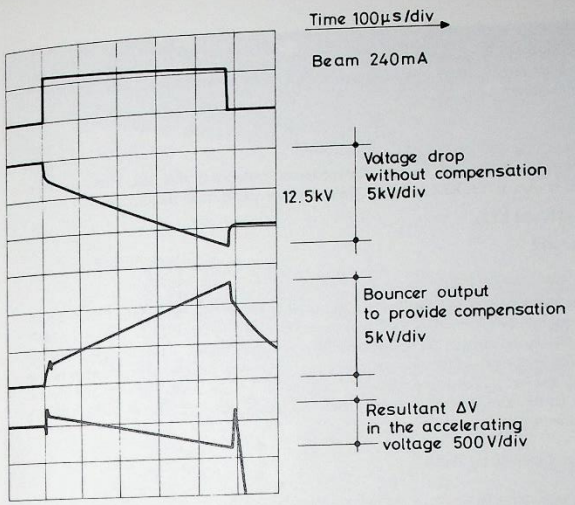

Figure 2.3. Bouncer, beam and accelerating voltage waveforms: (18783)

Beam currents and beam losses will be measured by current transformers. The transverse properties of beams will be investigated using multi-wire profile monitors which monitor the secondary emission from thin tungsten wires (0·025mm dia). A prototype system has been evaluated on the present 15 MeV injector under conditions which closely match the expected 70 MeV conditions.

Beam stops, threshold foils, and slits are being prepared for use on the injector. The beam stops will be used as beam dumps during part of the commissioning period and special shielding and handling arrangements are being made taking account of the high levels of induced radio-activity expected. The threshold foils will be used in the determination of the onset of acceleration of the respective tanks and a slit used with the sector magnet will constitute a spectrometer for energy measurements.

All of the diagnostic equipment will eventually work under the control of the Nimrod GEC 4080 computer. Computer software for the measurement modes required is under development.

EXPERIMENTAL AREAS AND EXTERNAL BEAMS

Hall 1

P71, a scattered-out beam, and parasitic on the machine Piccioni X3 target, was operational as a test beam until October.

P81, a low-emittance full energy beam, which peels off some of the X3 protons before extraction from Nimrod, continued operation until early December.

Both of these beams, P71 and P81, have now been dismantled to clear the area for installation of the new Hall 1 complex of beams (see below).

Hall 2

The Hall has been used throughout the year as an equipment assembly area in connection with the new 70 MeV injector.

Hall 3

The extracted proton beam, X3, services all experiments installed in this Hall. There are three target stations known as X3, X3X and X3Y. Secondary beams off these stations are:–

X3 – π8a, π11, and K15a

X3X – π9 and π12

X3Y – K17

The beams in Hall 3 continued largely unchanged from 1973 with the exception of π8 and K15 which were extensively modified and are now known as K15a and π8a. K15a is now a 3-tank electrostatically separated beam, with a production angle of 7°, for K^-p to cover the momentum range 1·0 to 2·7 GeV/c. π8a beam was designed for π^-, covering the momentum range of 0·6 to 2·0 GeV/c, and has a production angle of 7°. A feature of this beam is the use of a precise spectrometer to measure the momentum of individual particles to ± 1 part in 4000, within a momentum bite of 0·8% $\Delta P/P$.

The New Beam Complex for Hall 1

In the new beam complex currently being installed in Hall 1, the extracted proton beam (EPB) X1 is divided into three branches initially to feed K18, K20 and π13 secondary beams. The arrangement allows considerable freedom in the design of secondary beams, in particular the selection of optimum targetting conditions and zero production angle, and flexibility to accommodate changes in the secondary beam lay-out (Fig.2.4).

One of the major items of the new beam complex is the shielding bridge which forms part of the new X1 blockhouse. The bridge, containing 800 tonnes of reinforced concrete, cast in situ using pumped techniques, was completed early in November. Headroom under the bridge is 3·7m; span is 10·8m and roof thickness 2·7m, with wall thickness of 1·2m. The cooling water, electrical and ventilation services to the beam line components under the bridge will be supported from the roof in order to facilitate handling of units. Fig.2.5 shows some of the components being installed in the new shield bridge area.

Figure 2.4. Hall 1 beam lay-out, Phase I: (18781)

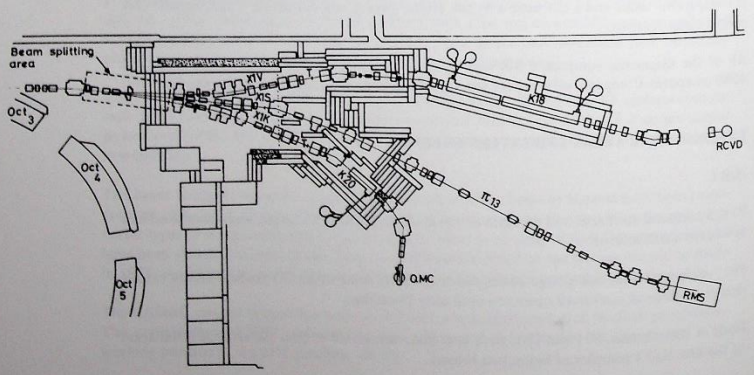

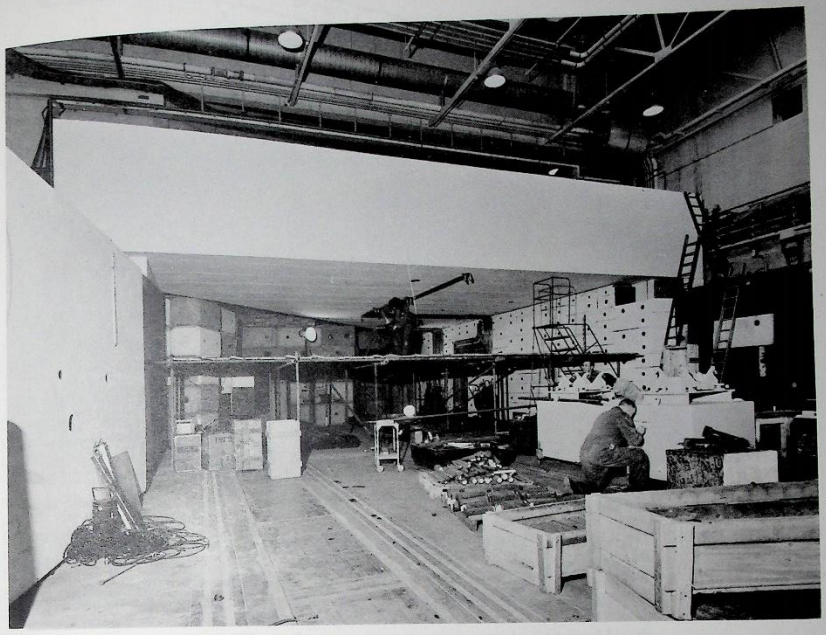

Figure 2.5. The new shield bridge in Hall 1: (18369)

The EPB System

In Hall 1 the emphasis will be on kaon physics, which places restrictions on secondary beam length due to the in-flight decay of kaons, and the use of large fixed facilities such as the Rapid Cycling Vertex Detector and the Multiparticle Spectrometer.

For additional flexibility, the optics of the EPB are chosen to be the 'parallel' transmission mode which is comparatively insensitive to large changes in length and moderate variations of directions.

An important part of the EPB complex is a means of sharing protons between the three branches. To accommodate the required special magnets an optical insert has been introduced at the front end of the EPB which allows variation of beam sizes. The beam sharing system is to be introduced in stages.

Beam Sharing Phase I (ref.RL-74-023)

Phase I consists of a pair of switching magnets capable of having their field polarity reversed during the time between successive NIMROD beam spills. This means successive spills may be diverted to any one of three secondary beam targets. The switching magnets are modified extraction magnets which have had their pole faces altered to give better field uniformity. The beam is matched to the magnet aperture by forming a double waist between them. To run the Rapid Cycling Vertex Detector (RCVD) experiments, fast spills will have to be generated along flat top to give 0·5 ms bursts of beam at 60Hz.

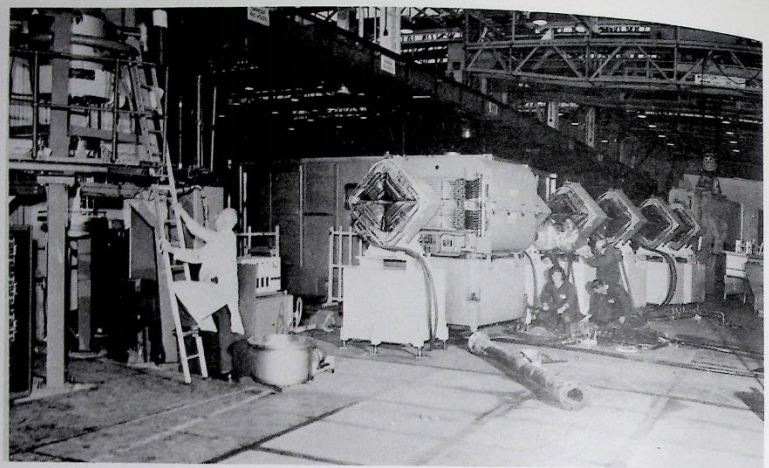

Figure 2.6. Construction of the K18 beam line in Hall 1. The Rapid Cycling Vertex Detector construction is on the left: (18267)

K18 beam for Rapid Cycling Vertex Detector

The K18 beam (Proposal No.119, to study S = −2 baryon resonances) is required to give a high flux of 2·8 GeV/c K^- and with good purity. A single-stage electrostatically-separated beam line is being built. A K^- flux of 750 to 1000 per 10^{12} protons is satisfactory when the protons are delivered in 40 bursts of 0·5ms duration, each containing 2·5 x 10^{10} protons. Contamination is predicted to be $< 5\%$ for pions and $\sim 30\%$ for muons. With some minor changes the beam should be capable of transmitting momenta up to 4 GeV/c (Fig.2.6).

π13 beam for Rutherford Multi-particle Spectrometer

The π13 beam (Proposal 150 to study exchange mechanisms in quasi two-body final states) is unseparated and for momenta up to 6 GeV/c. A production angle of 70mrad is used to allow separation of the 6 GeV/c positive secondary particles from the non-interacting portion of the EPB. Operation will be for positive particles at two momenta (4 and 6 GeV/c). The acceptance is 1msr% Δp/p and total beam length 62m. The detector rate limitations of RMS, restrict the total flux to 4 x 10^5 particles per burst. Particle fluxes in this total are 700K^+, 4 x 10^4 π^+ and 3·6 x 10^5 protons at 4 GeV/c and 150K^+, 3·3 x 10^3 π^+ and 3·97 x 10^5 protons at 6 GeV/c. Particle identification is by means of Cerenkov counters at the downstream end of the beam.

K20 Beam

The K20 beam (Proposal 136, polarisation measurements in K-nucleon elastic and charge exchange scattering) is a two stage design incorporating a single tank electrostatic separator in the first stage, and is for the momentum range 0·7 to 1·4 GeV/c. The total length is 23m. Flux is a strong function of momentum due to variation of target yield (factor of 3), acceptance for separation (factor of 1/3) and decay loss (factor of 9) over the required range, and will depend on the reciprocal third to fifth power of momentum. Predicted K^+ fluxes at the experiment are 7 x 10^3 at 0·7 GeV/c rising to 6 x 10^4 at 1·4 GeV/c.

Figure 2.7. The bi-speed kicking system for beam sharing: (18780)

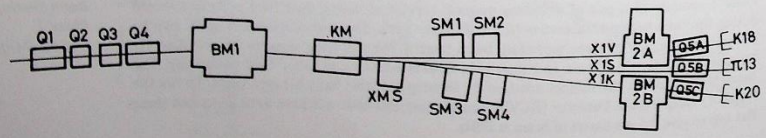

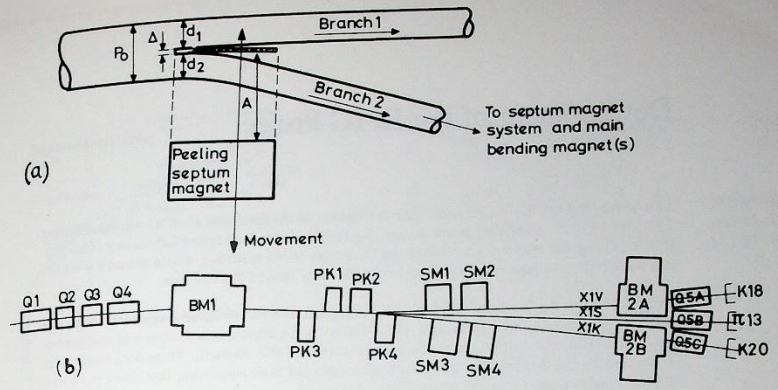

Figure 2.8. The d.c. splitting system for beam sharing. (a) schematic of peeling septum magnet, (b) beam line arrangement: (18779)

Beam Sharing Phase II

Design work is in progress on an improved beam sharing arrangement and a scheme consisting of two independent but interchangeable methods is under consideration. One alternative is based on kicker magnets and the other is a 3-way d.c. split. A major design consideration has been to minimise the rebuilding of the EPB complex, and this has been limited to the splitting region shown in Fig.2.4 in both methods. For Scheme A, a magnet system as shown in Fig.2.7 consisting of a fast switching magnet (KM) and a medium speed switching magnet XSM is used. The fast switch (KM) kicks the beam out of the aperture of XSM and hence to K18 beam target and RCVD. This magnet is synchronised with the chamber expansion cycle and the fast spill from NIMROD. Two 10mm septum magnets SM1 and SM2, are used to match the total splitting angle to the Phase I layout geometry. XSM is used to switch beam on a pulse by pulse basis to either π13 or K20. The narrow beam in the splitting region of Phase I is retained to minimise the aperture of KM.

The principle of the d.c. split used in Scheme B is shown in Fig.2.8a and the magnet layout for use in Hall 1 in Fig.2.8b. The splitting region optics are modified to produce an 110mm wide horizontal beam at the splitting magnet septum to minimise beam loss and hence radiation levels. PM1 and PM2 peel off a fraction of the spill and divert it into SM1 and SM2 and hence to K18, similarly PM3, PM4, SM3 and SM4 provide beam for K20. The beam left over goes on to π13 target. The splitting magnets are mounted on traversing tables so that the beam fraction in each branch may be varied.

Liquid Hydrogen Targets

Three liquid hydrogen targets were installed and tested in Hall 3 for the start of the operational year. Two of the targets in the π8a and π12 beams have operated continuously since installation. The one in the K15a beam line has had only limited use, dictated by the team's operational requirements. Two further targets for π12 (Phase 2) and π13 are under construction.

Electrostatic Separators

Two separators have been in operation in beam lines during 1974, a single tank unit in K17 and a three tank unit in K15a. Both are of the standard flattened tube electrode construction and have operated satisfactorily during the year. Each has operated with a 100 mm gap and has maintained an electric field strength of 6·6 kV/mm. Three separators for the proposed Hall 1 beam lines are currently being built: a single tank unit for K20 and a two tank unit and a three tank unit for K18. The latter is on test and is operating successfully at 6·4 kV/mm with a 100 mm gap.

Development of the EPIC Project

(ref.RL-74-078, RL-74-100, RL-74-124)

Last year's Annual Report carried a full description of the feasibility studies completed during 1973 for EPIC, – a colliding beam storage ring facility at the Rutherford Laboratory. This project, replacing the Rutherford Nimrod and Daresbury NINA machines, would ensure a continuing contribution to high energy physics in the UK from about 1980 onwards.

During 1974 these feasibility studies were embodied in a comprehensive report detailing the scientific justification for the project, (RL-74-124); and a shorter presentation was also prepared, summarizing the main lines of the argument, (RL-74-078 Revised). These documents were submitted to the Nuclear Physics Board, who endorsed their conclusion that there is an outstanding physics case for constructing EPIC.

As a result, the Nuclear Physics Board presented a formal request to Council for EPIC Stage I as their only new major project in the 1974/75 Five Year Forward Look, [NP1 (74)]. To amplify this request, a detailed description of the proposed machine was prepared, together with an outline of its programme requirements in terms of cost and manpower: this is the "Proposal to build a 14 GeV Electron-Positron Colliding-Beam Facility, – EPIC", (RL-74-100).

The Proposal concerns a Stage I single-ring machine to store and collide counter-rotating electron and positron beams, each of 14 GeV energy. The estimated cost for capital equipment is £25·7 million, and the construction time extends over about 5½ years. With early approval, the project would be ready for commissioning in 1980. The machine design allows the possibility of future extension to give electron-proton interactions, by means of a second storage ring for protons installed in the same tunnel. This "Stage II" EPIC is a long-term development possibility, and no request for its approval has been made at this stage.

Figure 2.9. Aerial View of the Rutherford Laboratory showing an outline of the proposed EPIC main ring location: (17850)

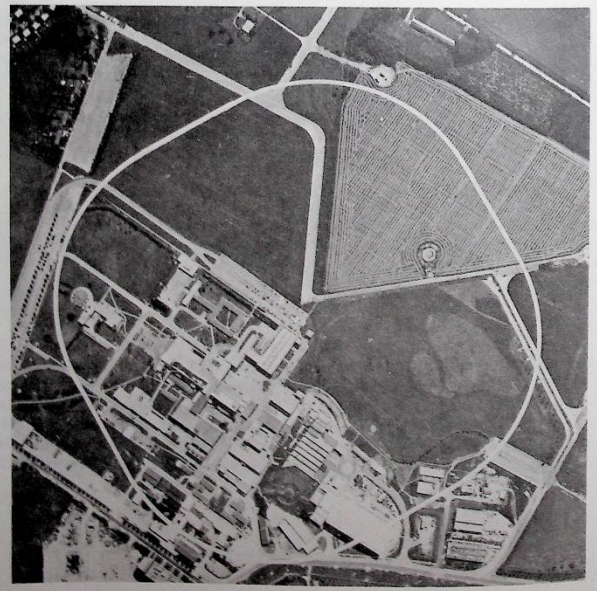

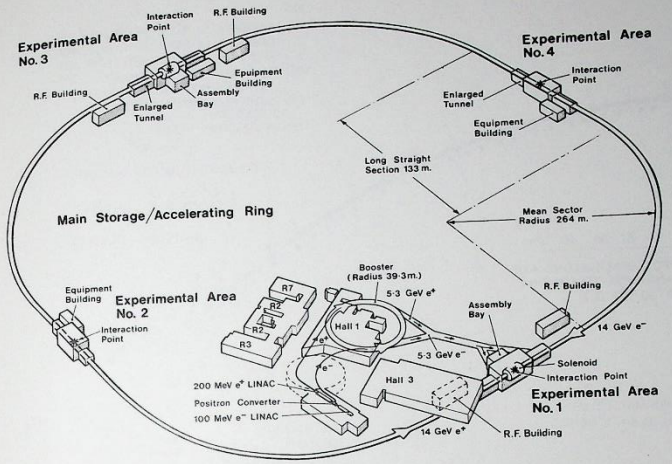

Figure 2.10 EPIC (Stage 1). Principle of proposed 14 GeV e^+e^- Storage Ring Machine: (18436)

At its meeting in November 1974, the Science Research Council endorsed the strong scientific case for EPIC. However, they deferred giving full approval to the project in view of uncertainty regarding financial resources during the next few years. In the meantime, they encouraged continuation of basic design research and development studies for EPIC, and invited exploration of possible financial support, for any part of the project, on an international basis. They likewise invited the Engineering Board of the Council to consider the possibility of financing University participation in the programme. As a result of this encouragement, the Laboratory is continuing to pursue the EPIC studies, and exploratory talks are proceeding along the suggested lines.

The recent discovery of heavy particles, in which the 4·5 GeV electron-positron storage-ring SPEAR at SLAC played a major part, has further stimulated interest in the EPIC project. These new particles are evidenced by narrow pronounced resonance peaks in the hadron production cross-section. So far, particles of mass 3·1 GeV, 3·7 GeV and 4·1 GeV have been identified with no simple theoretical explanation for their existence. These particle states are now being intensively studied; access to higher mass regions must await the construction of storage rings such as EPIC.

The Machine Design

Fig.2.9 shows an outline of the EPIC main ring layout, superimposed on an aerial view of the Rutherford Laboratory, and the Fig.2.10 perspective sketch illustrates the complete machine complex.

The injector system for the electrons and positrons involves linear accelerators and a booster synchrotron to accelerate pulses of these particles to about 5·3 GeV. The booster consists of the Daresbury NINA machine, re-assembled in a modified configuration and operating at a repetition rate of about 8 pulses per second.

From the booster, alternate pulses of electrons and positrons are transferred to the EPIC main ring, where they are each stored as two short intense bunches circulating in opposite directions, but are not yet allowed to collide. Sufficient intensity in the main ring is built up during a filling time of about five minutes. They are then accelerated to the desired operating energy, brought into collision, and allowed to collide during a storage time of several hours.

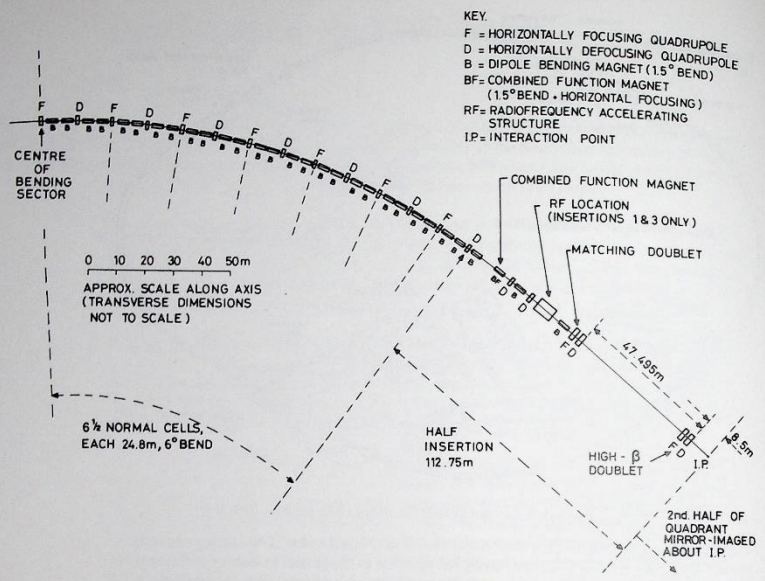

Figure 2.11. Layout of the main elements in EPIC half quadrant: (18778)

Although the EPIC design is optimised for 14 GeV operation, experiments can be carried out over the approximate range 5 to 17 GeV, and future improvements could give a further increase in energy.

The main ring has fourfold symmetry, each quadrant consisting of a bending sector and a special "insertion" containing a long straight section. The quadrants have mirror-symmetry about their centre; Fig.2.11 illustrates the arrangement of different magnetic elements in a half-quadrant. A special arrangement of quadrupole magnets reduces the beam size to tiny dimensions at the centres of the insertions, – the "interaction points", – and it is only at these four points that the beams collide.

The "luminosity" L is an important figure of merit for colliding-beam machines, being defined as the ratio of the rate R for some particular interaction event in the collision to the cross-section σ for that event: $R = L\sigma$. In EPIC, the luminosity value is about 3×10^{31} cm^{-2} sec^{-1} for each interaction point at the 14 GeV design energy, and Fig.2.12 shows how L varies as the operating energy is changed. (These curves assume a conservative value for the limit imposed by the focussing effect of one beam on the other at the interaction point : $\Delta Q = 0{\cdot}04$).

The main ring would be installed in a tunnel of about 4 m diameter, bored in the hard chalk of the Rutherford Laboratory site: part of the ring would be excavated from the surface by the "cut-and-fill" method. Fig.2.13 illustrates a tunnel cross-section at one of the main dipole bending magnet locations. Sufficient height is available above the electron-positron ring for the future addition of a proton ring.

Preliminary specification of all the necessary hardware has been completed in detail, – magnets, RF system, vacuum system, computer control, etc, – and, where appropriate, prototype elements will be constructed for laboratory testing and development.

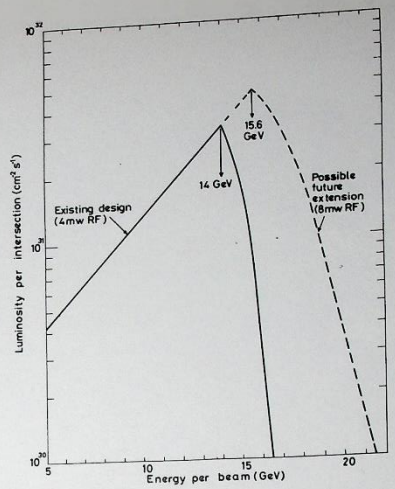

Figure 2.12. EPIC luminosity assuming linear beam-beam tune shift $\Delta Q = 0{\cdot}05$: (18777)

The main ring contains 240 dipole bending magnets, including 8 combined function elements: each is 4·5 m long and operates at 0·27 T field for 14 GeV. There are 156 quadrupole magnets, of which the majority are just over 1 m long, giving 5 T/m field gradient at 14 GeV. Other elements include about 144 sextupole magnets for chromaticity correction, and about the same number of small correction dipoles for control of the closed orbit.

The RF accelerating system consists of 8 separate structures, each 5·22 m long, operating at a radiofrequency of 402·72 MHz with a peak accelerating voltage of about 30 MV. The total available DC power is 4 MW peak for the highest operating energies, supplied by 16 klystrons: of this power, 1·4 MW at 14 GeV goes to overcome the radiation emitted by the circulating electron and positron beams. As shown on Fig.2.10, the RF structures are located symmetrically each side of Interaction Regions 1 and 3.

The EPIC complex has been carefully designed to make the fullest possible use of existing equipment at the Rutherford and Daresbury Laboratories, and to exploit existing Rutherford site facilities to the best possible advantage. The total effort involved, including commissioning of the machine, is estimated to be about 2166 man-years, of which 30% is support effort at the Laboratory, not directly employed on the project.

Figure 2.13. Cross-section of main ring tunnel at dipole locations: (18776)

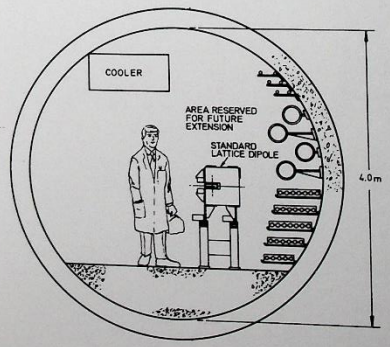

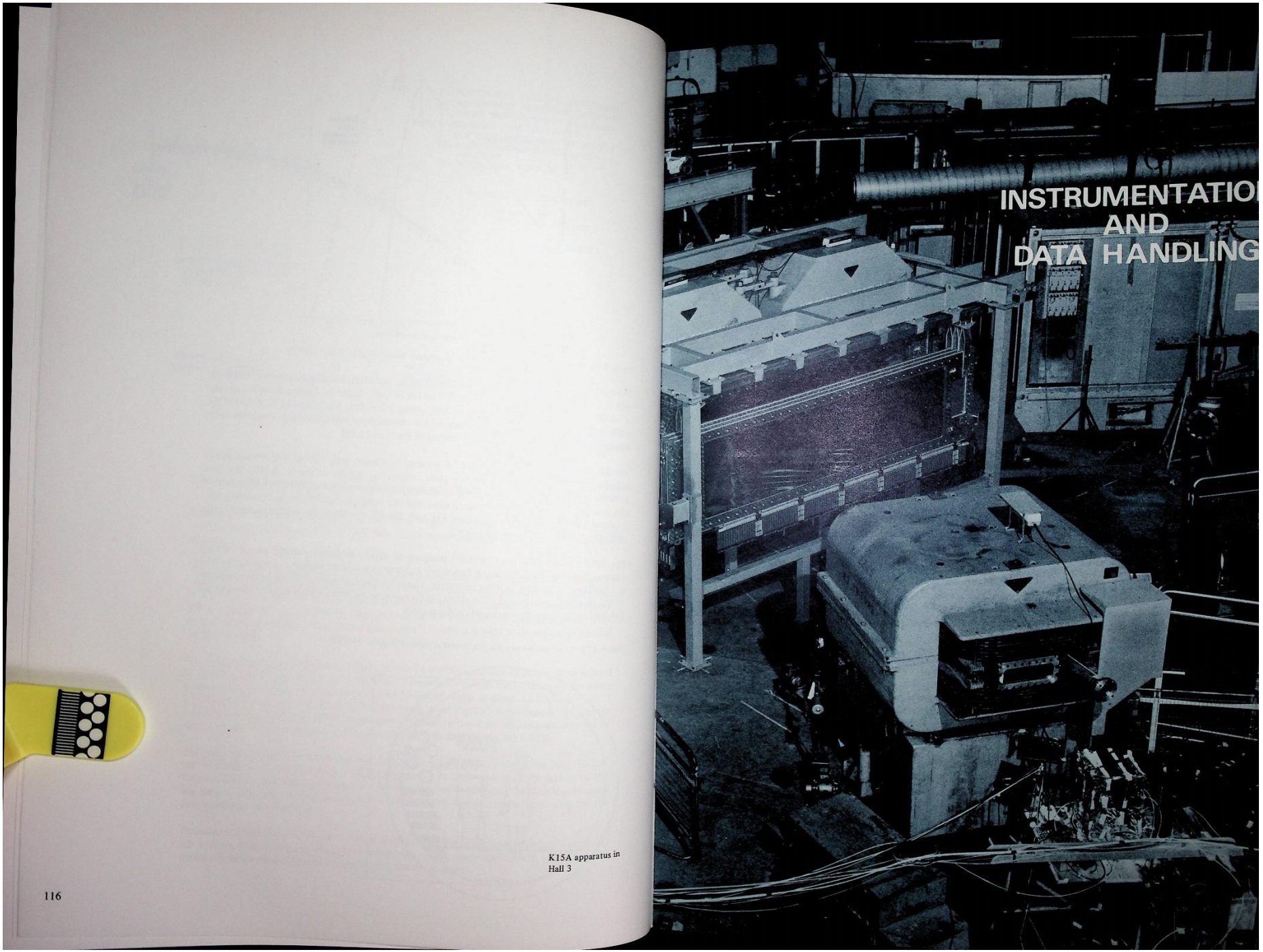

K15A apparatus in Hall 3

3. Instrumentation and Data Handling

DETECTORS

Drift Chambers

Drift chambers have considerable potential for achieving high spatial resolution in the measurement of particle trajectories. In this type of detector the basic principle is to measure the time taken for electrons, produced by a charged particle passing through a chamber gas, to drift to a collector wire (anode) under the influence of an electric field. Chambers with drift distances of 30 mm have been built to study drift time measurement techniques. Using a 1 GeV/c π^+ beam measurements show good time/space linearity and spatial resolution of 0·44 mm f.w.h.m (Fig. 3.1). Single wire chambers with drift distances of 10 mm were used to monitor particle trajectories. As a further development, two chambers measuring in orthogonal directions (ie x and y coordinates) have been operated with a separation between centres of 25 mm without any interference effects being observed. The bi-filar wire technique to identify left and right drift regions has also been verified.

On the basis of this work, a large 1m x 1m drift chamber is being produced to test out the techniques on a scale more suited to current high energy physics experiments.

Compared with multi-wire proportional chambers, drift chambers have many fewer electronic channels for a given detector area. However the electronics associated with each drift chamber channel is much more complex and it is necessary in some applications to effect a saving by multiplexing several chamber wires into one set of measuring electronics. A unit is being developed which will accept signals from 8 wires and be capable of measuring up to 16 signals per event, distributed over the 8 wires and recording them together with their wire identification information.

Multiwire Proportional Chambers (MWPC) (ref.RL-74-018) RL-74-080)

Much interest currently attaches to the possible application of the logarithmic rise in the energy loss of relativistic charged particles in gases to detect very fast particles. This would require the use of large volume MWPC's in strictly proportional mode and leads to a new set of problems such as gain uniformity and gain stability. A detector capable of giving useful dE/dx pulses has been built. The chamber has an active area of 18 cm diameter and total gas path for particles of 22 cm. Promising results have been obtained in a study of the resolution on the dE/dx signal and chamber stability.

A photographic technique for testing MWPC's, using glow discharge, has been introduced to give rapid and positive fault checking on large chambers as their manufacture is completed. The chambers are filled with high purity nitrogen and subjected to a current of about 300 μA to produce a glow discharge. Faults such as slack or open circuit wires, continuation and mis-alignment of planes are revealed on the photographic exposures.

Other advances in the operation of multiwire proportional chambers have been made with the development of read-out systems, a gas mixture monitor with rapid response, and a stabilised power supply (0 to 9kV) with interlock circuitry.

A Multiwire Proportional Chamber X-ray Detector

The use of MWPC's in the detection of X-rays is of increasing interest to many users in both Bio-medical applications and Radiological experiments. A detector system of this type employing a delay line read-out system has been built for evaluation in several possible applications in these fields. The detector has an active area of 20 x 20 cm with both cathode and anode wire planes wound on a 2 mm pitch. The outer cathode wire planes are wound at 90 degrees to each other and the centre anode plane wires are wound at 45 degrees to both cathode planes. The complete detector system including the delay lines is housed in a gas-tight vessel 570 mm diameter and 75 mm deep with a 20 cm diameter window in one face through which the X-rays can reach the active region of the detector.

The system has operated successfully in obtaining X-ray absorption pictures using X-ray energies up to 22 keV with various gas mixtures at atmospheric pressure. It is planned to increase the energy range by providing a pressurised gas system and to incorporate collimation facilities in the window structure.

Beam Current Monitors for the 70 MeV Injector

The manufacture of equipment for the beam current monitor system is now almost completed. Sixteen toroid current transformer units are ready for assembly in the beam line installation. The production of electronic equipment is also well advanced: commissioning and calibration tests have been completed on the toroid current transformers and associated head amplifier electronics. The functions of the various units incorporated in the signal processing electronics have been checked and the operation of the first control station electronic system tested.

Beam Chopper for Low Energy X-rays

A beam chopper has been developed for operation with channel plate multipliers used as detectors of X-rays in the 6 to 40 keV range. Beam chopping is a particularly valuable technique for improving signal to noise ratios in detectors. Basically, the chopper is a slotted disc mounted on the shaft of an electric motor, with a top speed of 2,800 r.p.m. and chopping rate of up to 470 times per second. The device incorporates beam timing electronics.

Figure 3.1. The spatial resolution (beam profile) obtained with a drift chamber in a 1 GeV/c π^+ beam. The chamber is displaced by 4 mm for calibration: (18843)

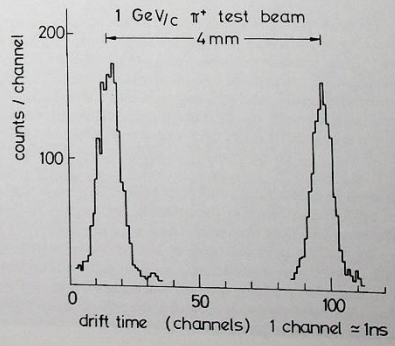

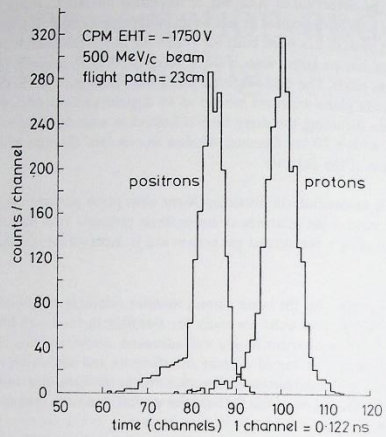

Figure 3.2. Time of flight spectra of e^+ and p under identical conditions at 500 MeV/c derived from a channel plate multiplier and a timing scintillation counter placed 23 cm apart: (18844)

Channel Plate Multipliers

Channel plate electron multipliers (CPM) have attractive properties but so far have not found any definite application in high energy physics. Development work has proceeded along two lines:

(a) Direct use of CPM's in particle beams. Calculation showed that the number of secondary electrons liberated in the CPM by a minimum ionising particle traversing a CPM of 25 cm is adequate to give ∼100% detection efficiency. Fig.3.2 shows the time of flight spectra obtained between a scintillation timing counter and a CPM with e^+ and p particles over a flight path of 23 cm at 500 MeV/c. Sub-nanosecond (∼0·75ns fwhm) resolution is achieved. It is anticipated that this can be reduced substantially with further development in view of the intrinsically fast response of the devices.

(b) Development of CPM-based photomultiplier tube. The CPM has two properties of particular value to high energy physics viz, it can operate in high magnetic fields and has a very short transit time (∼2ns). It has been shown that a cascade of two CPM's yields electron multiplication factors of 10^7 as required in a photomultiplier tube for high energy physics. In collaboration with Instrument Technology Ltd. a CPM-based photomultiplier tube of 20 mm active window diameter has been developed. Preliminary results show that the device can operate in a magnetic field of 0·1T with a loss of 5% and a shift in the timing distribution of $< 0{\cdot}5$ ns.

Apparatus for Experiment 9 (K15 beam line)

Construction and installation of detectors to study K^-p differential cross-sections neared completion during the year. Fig.3.3 shows some of the fifteen large capacitive read-out wire spark chambers installed in the beam line. Each have active areas in the order of 2·5m x 1·0m and the whole system comprises approximately 72,000 wires of 1mm pitch orientated at 0° ± 15° and ± 30° to the vertical axis. Twenty four beam defining proportional chambers of active area 20 cm x 20cm with wires at 2mm pitch are being installed. Six larger proportional chambers totalling 1500 sense plane wires are currently being produced and will be used to identify the forward going scattered particles from beam particles.

Optical Spark Chamber for Experiment 12 (π12 beam line)

An optical spark chamber, the largest multi-plane optical chamber to be built in the Laboratory with an active area of 2·25 metres square, is being used in the experiment to study associated production. The chamber consists of eight pairs of foil planes mounted in a gas-tight envelope, with transparent sides of perspex. Performance in the beam line has been good with high efficiences, clear and precise sparks and reference fiducials.

The Rutherford Multiparticle Spectrometer Detector System

The detector system consists of an array of cylindrical shaped, capacitive read-out, spark chambers up to 1 m diameter and height and six circular flat chambers concentrated around a hydrogen or polarised target (Fig.3.4). In addition ten large flat plane capacitive read-out chambers are to be installed between the poles of the large magnet. Other items to be provided for on this facility will include a large Cerenkov counter, disc counters, beam proportional counters, numerous scintillation counters, and gas systems. An overall design has been prepared and the necessary techniques to be employed in manufacturing the cylindrical capacitive read-out spark chambers, as well as the other chambers in the system, have been established.

A low mass structure is being used for the cylindrical spark chambers, consisting of beryllium-copper wires spaced at 1 mm and based on a polyester film (Melinex). The bonding of the wire to the polyester film is such that on curing, the upper surface of the wire is left bare, thus enabling the wire to be "sparked". Small spark chambers have already been constructed using this technique and successfully tested over long periods.

Figure 3.3. Capacitive read-out wire spark chambers being installed in K15 beam line: Experiment 9 (17967)

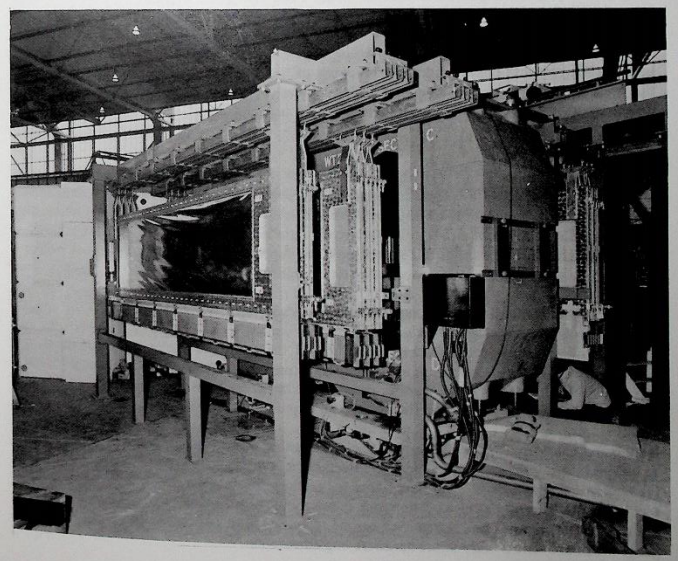

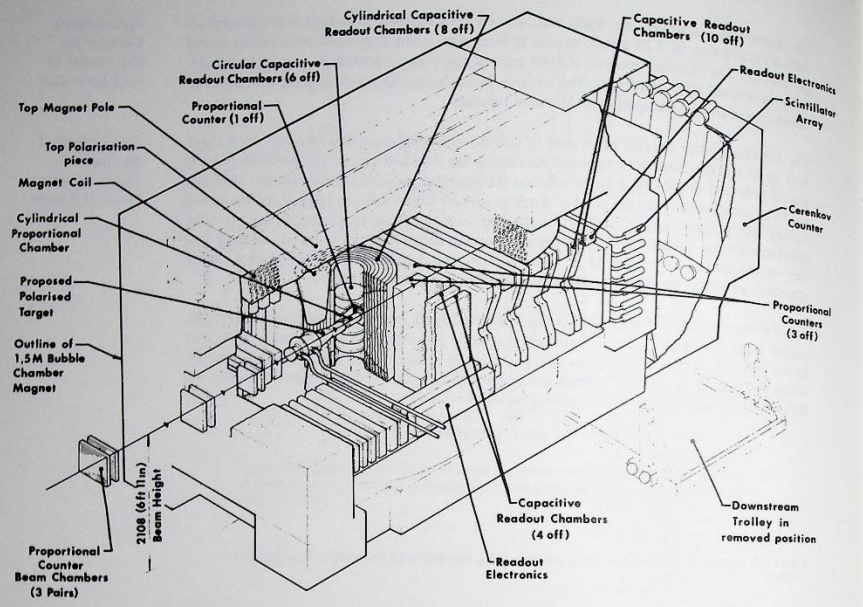

Figure 3.4. Design of the detector system for the Rutherford Multiparticle Spectrometer: (18536)

This wire-on-film design has the advantage that it can be used to effect a continuous connection between the read-out boards and the active wires of the chamber thus bypassing the need for the usual large number of soldered connections in wire chamber systems. The technique makes maximum use of active area relative to overall size of the chambers.

ELECTRONICS

T.V. Camera Systems

More than 20 precision T V camera channels are now being used with various particle detectors. Most of them are used with spark chambers but this year the Laboratory has supplied two cameras for reading data from a flash-tube hodoscope installed on the e–p storage rings (ADONE) at Frascati. The development of this system led to an improvement in signal to noise ratio which in turn will enable increased efficiency to be obtained in the spark chamber applications.

Special Purpose Computing Hardware

Special purpose computing hardware was used successfully in Experiment 24.

Hopefully this will speed the further application of these ideas to the reduction of the data handling load implicit in most high energy physics experiments. The development has provided a technological base from which further progress can be made. It has also indicated that a careful balance between efficiency and flexibility is an important factor in system design.

Now being considered is the problem of track-recognition which is inherent in the use of RMS, as well as in many other particle detector systems. This is a field where special purpose computing equipment would be of great importance in matching the data acquisition rates of these detectors to the currently available computing power. Some of the software algorithms already in use for the purpose of track recognition can be rephrased in an associative data processing language which can have a fairly direct hardware implementation.

Other Developments

One factor limiting the accuracy when measuring the energy of particles in nuclear and high energy physics is the statistical spread of the energy loss in a detector. This spread can often be reduced by using several detectors instead of one and computing a more accurate average figure. A prototype unit which calculates the geometric mean of 4 signals has been designed and evaluated. It provides the expected spectrum width reduction and has an accuracy and stability which shows that the technique can be extended. A new unit capable of modular expansion has been designed which can calculate the geometric mean of 8 signals in about one microsecond.

In connection with the Laboratory program on polarized targets a signal enhancer is being developed which will improve the signal to noise ratio in NMR spectrometers and enable cross checks to be made on the polarization level in the target. The technique of signal enhancement, or noise reduction, is applicable to any repetitive signal. Successive copies of the waveform are added together, resulting in the coherent signal component increasing faster than the incoherent noise component.

The development of electronics for beam position and profile monitoring has made steady progress during the year. The present sensitivity is such that a signal of $1{\cdot}5 \times 10^7$ ions per channel will give a signal equal to the noise level. This sensitivity is accompanied with an integration limit of 20 milliseconds. It is expected that this time constant will be considerably increased as a result of continuing development.

Additional to this more specific work is the normal sustained effort of development, commissioning and servicing. The major part is in support of the high energy physics program, the remainder being special support for the new injector and for the polarized target development program.

Data Handling for Electronic Experiments

Whereas in the past, data acquisition software for on-line computers was written specially for each experiment with a resultant duplication of effort and inefficiency, most experiments are now controlled by DDP516 computers and a highly modular multiprogramming operating system has been written for these machines. Important features of the system are the ease with which software for a new experiment may be configured, the optimisation of data acquisition functions and the handling of all input/output operations. A number of GEC 4080 computers are also to be used for data acquisition and a similar package is being developed for them. The first version is currently operational on the K17 experiment and includes significant additions to the manufacturer's software. Important experience has been gained in the use of this advanced and complex computer.

Support continues for the MIDAS Graphics Computer which provides experimenters with the ability to examine large display files independently of the central IBM370. The MIDAS computer also has powerful facilities for the development and documentation of software for all DDP 516 computers.

The advent of experiments in which volumes of data in excess of 10^6 events are to be recorded has led to an examination of techniques for reducing the corresponding load on the analysis computer. The special computing hardware described earlier constitutes one method for achieving this. Work is in progress on efficient software algorithms to associate sparks into particle tracks for the RMS project.

Electronics Services

Track Analysis Machines

Development work has been continued to improve the production efficiency and throughput of some 30 scanning and digitising machines. Particular projects were: an automatic frame advance system, provision of a 3-view scanning facility for spark chamber film and the adaption of visual display units for communication between digitisers and computers instead of electric typewriters. A third BESSY machine has been added and assistance has continued with the commissioning of the CRYSTAL computer/Vanguard system and with the HPD Tandem Project.

Design and Manufacture

During the year 92 new designs of printed circuit boards were produced representing 314 drawings in total with the trend continuing to greater component density, function and complexity in each board (50% done off site). Manufacturing work was completed to the value of £200,000 including component costs (over 70% done off site). The in-house effort totalled 26,750 man-hours, a reduction from previous years due to the difficulties in recruiting electronic craftsmen. The training and use of part time women workers has been increased to overcome this deficiency. Over 2700 items were handled for repair, calibration, servicing and "on-call" breakdown investigation with 20% of this total being dealt with by specialist firms. The problems and difficulties again reflect the trend towards greater complexity and sophistication of the equipments in use.

The Instrument Loan Pool continued to function as a viable site service with 467 issues from the 570 instruments in the Pool. An up to date catalogue has been issued enabling the operation of service by the stores organisation to be very effective.

INFRA-RED RADIOMETERS FOR ATMOSPHERIC SOUNDING

University of Oxford
Rutherford Laboratory

The selective chopper radiometer is now in its third year of operation in orbit and is still successfully providing synoptic data of the atmosphere's temperature profile. The flight spare unit of this radiometer with special command and interface units was successfully commissioned on a Canberra research aircraft of the Meteorological Office and a series of experiments are in progress.

Pressure Modulated Radiometer (PMR) Nimbus 'F'

The pressure modulated radiometer has completed its tests on the spacecraft and is now awaiting launch from NASA's Western Test Range.

Stratospheric and Mesospheric Sounder (SAMS) Nimbus 'G'

The SAMS radiometer for temperature and composition remote sounding has been funded by means of an SRC Grant to the Department of Atmospheric Physics, Oxford University. The Laboratory will be providing the pressure modulators, scanning mirror and other mechanisms and the various detector assemblies plus all the test equipment, including the spacecraft simulator.

The final scheme is shown in Fig.3.5. There are 7 pressure modulators feeding 6 detectors, the principal one being cooled by a 2-stage passive radiant cooler.

A prototype pressure modulator has been made and tested and so has a scanning mirror system proving also that position measurement can be made to the specified accuracy of 2 arc seconds. The pressure modulator cell geometry allows compression ratios of the gases from 2 to 4 and the mean pressure is set by molecular sieve techniques and may cover a 20 to 1 range in 5 controlled temperature levels.

Commercial molecular sieve materials have been identified and tested to cover the pressure range required for the gases CO, CO_2, CH_4, NO, N_2O and water vapour within the limitations of 5 grams of material and a 70°C temperature band. The compatibility of the materials and adhesives used with these gases has been investigated.

A pressure modulator designed by the Laboratory is shown in Fig.3.6. This unit will be supplied to the Jet Propulsion Laboratory of Californian Institute of Technology to be launched on a Pioneer spacecraft in 1978 to orbit the planet Venus. It is very similar to the SAMS pressure modulators.

A balloon experiment as a forerunner to the SAMS experiment was successfully flown from France last year. This carried three pressure modulated radiometers, designed and manufactured at the Laboratory together with the gondola.

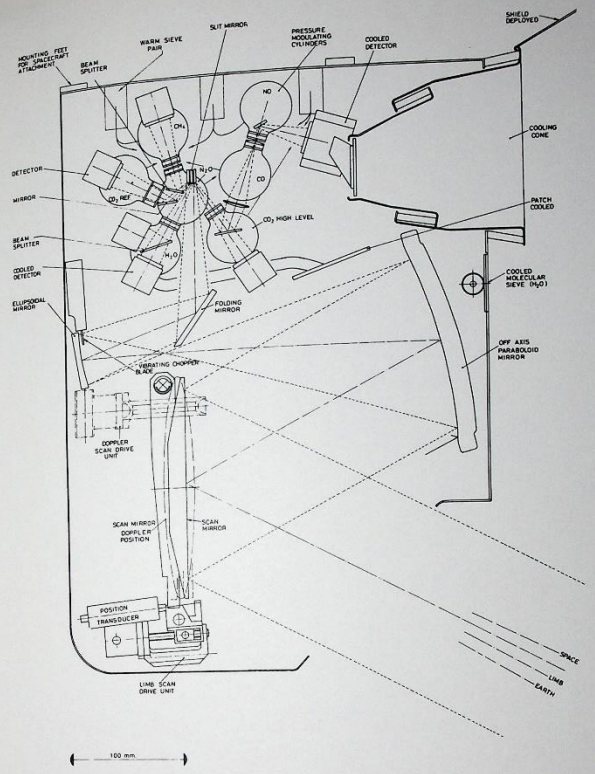

Figure 3.5. The design for the chopped pressure-modulated radiometer for temperature and composition sounding of the stratosphere and mesosphere: (18799)

Figure 3.6. Design for a pressure modulator unit: (18798)

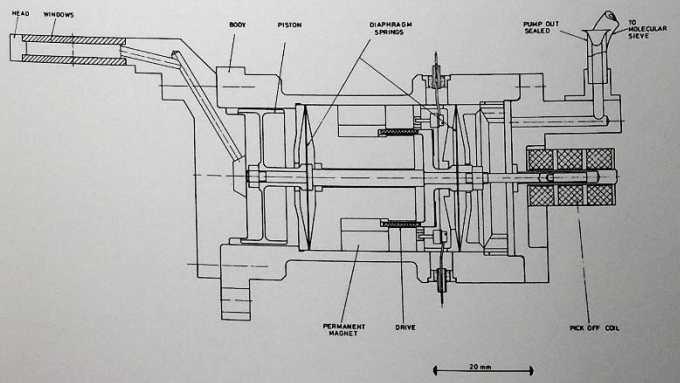

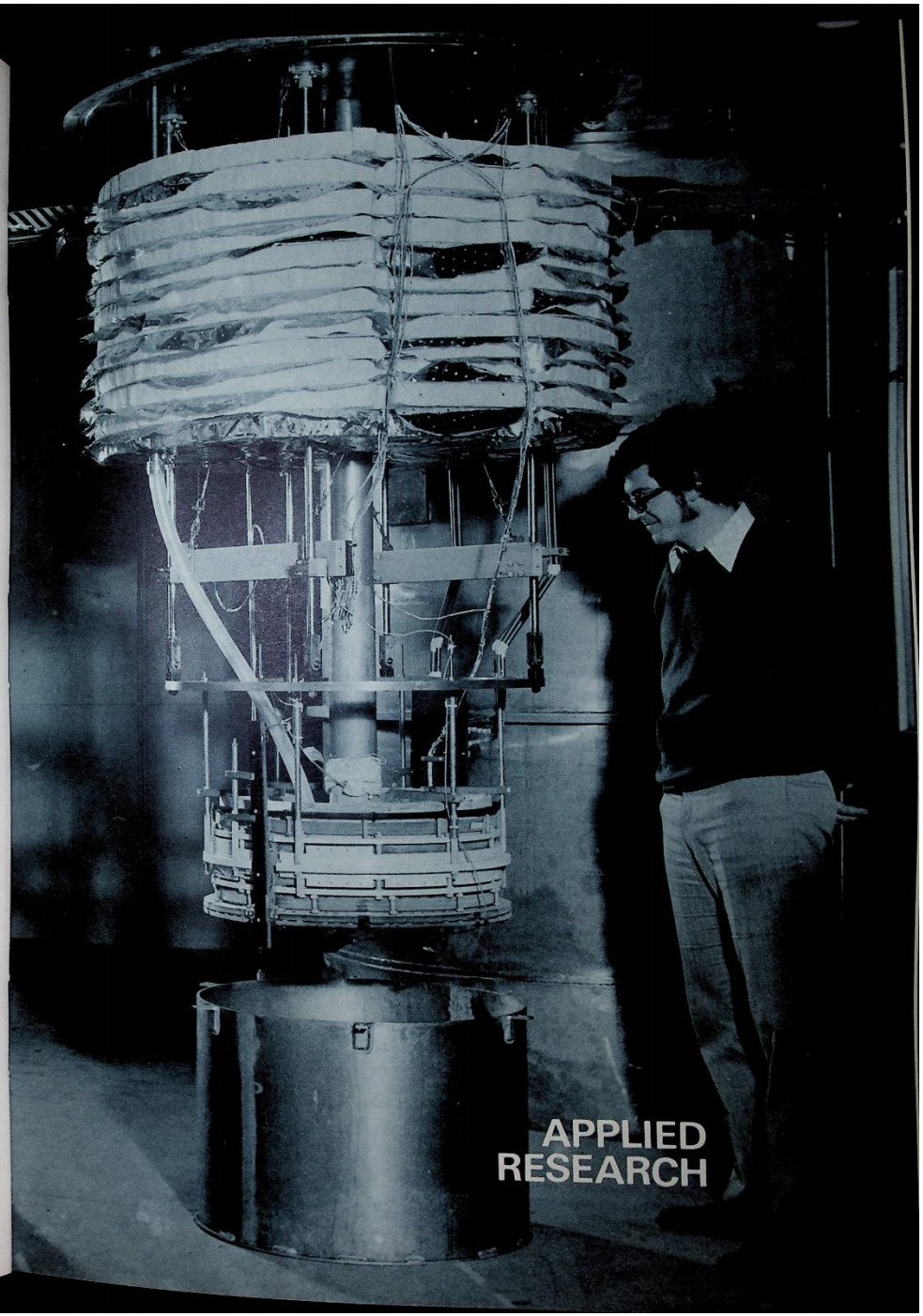

APPLIED RESEARCH

The coil system of the superconducting magnet for polarized target PT55 assembled for testing

4. Applied Research

MAGNET DESIGN AND MANUFACTURE

Pulsed superconducting dipole magnet AC5 (ref.35)

The final design for the pulsed dipole magnet AC5 was established during the year, after completion of the basic R & D work in 1973. For a model coil, or test winding of four layers, it proved possible to 'pot' the tightly packed assembly as a single piece, yet form subsequently the regular network of annular helium cooling channels between all the layers.

The benefits from achieving a high density winding are a more uniform current density in the 'window area' together with a much reduced thermal contraction on cooling, sufficient to allow the use of pre-shrunk stainless steel support rings. These in turn allow the coil to be shrunk into a whole-iron yoke, built as a bonded stack of laminations.

Manufacture of the magnet is well advanced. The flat-helix conductor from 15 x 1 mm NbTi wires was formed and braided 'in house' to closely specified dimensions. The coil winding, which uses many accurate but different spacer pieces cast in highly filled resin for low thermal contraction, has gone well. In the work of achieving a suitable low thermal contraction material a valuable contribution has been made by the resin laboratory.

It is a feature of the design that the winding may be tightened by using oversize wedges without noticeable detriment to the uniformity of the magnetic field. It has further proved possible to find a layout for the end turns of this 'saddle type' winding which, whilst furnishing a good axial integral of field, does not as a concommitant cause an increase of field at the conductor.

A comprehensive programme of testing, similar to that for AC4 (Proc. IEE 121 (1974) 771), will be carried out in the first half of next year subject to the availability of liquid helium in sufficient quantity.

Superconducting hexapole magnet for Neutron Beam Research

The design for a 1 m long prototype hexapole magnet is in progress, and if the design specification is achieved it should provide a useful aid to neutron beam research by focussing and polarising a beam of slow neutrons. This will be the first superconducting hexapole winding to be made and the design is somewhat different from the dipole magnets built to date. The windings will be around iron poles, which though highly "saturated" help to reduce the peak field experienced by the superconductor as well as contribute to the useful field.

Superconducting solenoid magnet for TRIUMF (ref.RL-74-104)

A superconducting solenoid magnet has been completed during the year and sent to the TRIUMF accelerator in Canada where it will be used in Experiment 47 to precess the spin axis of a beam of polarised protons. The team mounting this experiment is a collaboration between Canadian and British Universities together with AERE Harwell and Rutherford Laboratory.

Before shipment the solenoid was thoroughly tested at the Laboratory. After a small amount of "training" the magnet produced a field of 6·75 tesla, comfortably exceeding the design specification of 6·0 T, in a room temperature bore 1 metre long and 100 mm diameter. In the final tests the magnet was run continuously for three weeks at various fields up to the design maximum of 6 T. It was found to be completely reliable and require minimal attention at intervals of up to 30 hours. The liquid helium consumption, when running at 6 T is 1·5 litres per hour.

After installation in the beam line at TRIUMF, the magnet and ancilliary equipment were again tested and found to be in good working order. The experiment will start as soon as polarised protons are available from the accelerator.

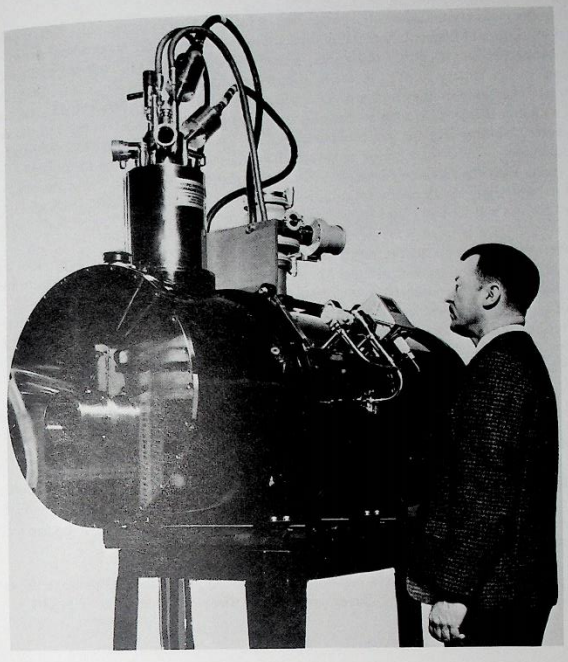

Figure 4.1. The 6 tesla solenoid magnet, 1 metre long, in use at the TRIUMF accelerator in Canada: (15544)

"Training" Research (ref.RL-74-137)

Work is now well advanced on the construction of a superconducting d.c. dipole magnet, intended as a large scale 'training' experiment. The windings of this magnet will be put into a strong pressure vessel and then impregnated at high pressure (20×10^6 N m^{-2}) with an epoxy resin which is then cured at the same high pressure. The pressure vessel will remain in place throughout the life of the magnet, serving also to support the magnetic field forces; the impregnating resin will thus be kept permanently under hydrostatic pressure. In this way it is hoped to reduce "training", an effect which degrades the performance of superconducting magnets and which is thought to be caused by the local release of energy in the winding under the action of magnetic forces by means of small movements, friction, slippage and cracking.

A programme of development of pressure impregnation techniques has been completed. Many samples of magnet winding and a full scale model of the magnet have been impregnated at high pressure. It has been found that, although some of the pressure may disappear after thermal cycling between ambient and low temperature, most of the initial pre-compression (∼70%) is retained indefinitely.

Several new techniques have been adopted in winding the magnet, notably the use of a thermoplastic coating on the conductor to hold it in place during winding, the use of 'constant perimeter' end turns and a semi automatic two axis winding machine. One pole of the two is complete and the other is in hand.

Superconducting composites (ref.RL-74-135, RL-74-136)

The Laboratory has continued to collaborate with AERE Harwell in the development, production and utilization of filamentary niobium tin composites. Niobium tin has excellent superconducting properties but its brittle mechanical properties have made it difficult to produce the compound in filamentary form or to use it in high field magnets. These difficulties have now been largely overcome by means of a process whereby the conductor is fabricated in the form of pure niobium filaments in a tin bronze matrix. A heat-proof insulation is applied to the conductor before winding into the magnet. The complete magnet is then heated to a temperature of approximately 700°C for a period of several days, during which time the tin of the bronze matrix reacts with the niobium filaments to form filamentary niobium tin. After reaction the magnet is impregnated with epoxy resin. Solenoids of this type have produced fields of 11 T in a bore of 55 mm and 12 T in a bore of 30 mm.

Even after reaction, sufficient tin unfortunately remains in the bronze matrix to produce a resistivity at low temperature which is more than 100 times that of pure copper. The electromagnetic stability of the composite can therefore be greatly improved by including several large filaments of high purity copper as shown in Fig.4.2. This copper also serves to protect the magnet from over-heating or voltage breakdown when it quenches. In order to maintain the purity of the copper filaments, they must be surrounded by a diffusion barrier which keeps out the tin during the reaction heat treatment.

Further work is now aimed at the optimization of current density, improvement of diffusion barriers and the development of insulation and coil winding technologies. Work has also started on the design of a small niobium tin hexapole.

The collaborative programme with Imperial Metal Industries Limited on filamentary niobium titanium has continued at a lower level throughout the year. A new process involving hydrostatic extrusion has been investigated and shows promise for the production of composites with improved current density and lower hysteresis loss.

Flux Pump (ref. RL-74-134)

Further detailed improvements have increased the power output of the flux pump to 38 watts at 1500 A. A high power version is under construction with a design output of 500 watts.

Figure 4.2. Cross section of a filamentary niobium tin superconducting composite, showing fine filaments of Nb_3Sn and large filaments of copper, protected by diffusion barriers (magnification x 70; courtesy of AERE Harwell)

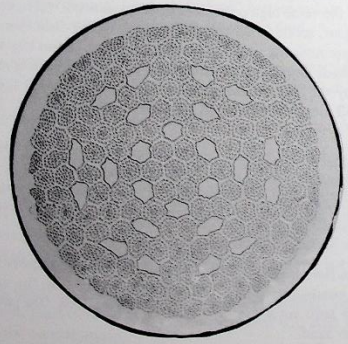

Magnet Computation (ref.RL-74-132, RL-74-133)

The interactive graphics technique for two and three dimensional magnetic field calculation has been applied to several design projects. These include the following superconducting magnets: test coils for conductor research and "training" experiments, the design of a quadrupole for the ISR at CERN, the polarized target magnet PT 55 and a sextupole for neutron beam research. Also design work has been carried out for the following conventional magnets: sextupoles and quadrupoles for the EPIC design study, the Rutherford Multiparticle Spectrometer magnet, PEM polarized target magnet and the Rapid Cycling Vertex Detector magnet.

In addition to these internal projects the following organisations have consulted the Laboratory on various aspects of magnet computations: Daresbury Laboratory, Liverpool University, CERN, Thor Cryogenics, Perkin Elmer, Oxford Instruments, University of Sussex, Ferranti, Hammersmith Hospital, Chalk River, Oxford University, Culham Laboratory, LRL Berkeley, and ANL Argonne. Because of the wide interest shown in the magnet computer programs it was decided to make the system available under licence. In particular an agreement has been completed with NV Philips Gloelampenfabrieken enabling the program to be used at their laboratories.

A design study was also carried out on behalf of Daresbury Laboratory to optimise and cost a 'Wiggler Magnet' for insertion into a straight section of the proposed Synchrotron Radiation Facility. This magnet has to provide a localised region of high field causing the electron beam to perform oscillations and thereby generating radiation at a wavelength considerably shorter than that produced at other points in the machine. Fig.4.3 shows the geometry and graphs of magnetic fields for this design with electron beam trajectories.

Figure 4.3. (a) The wiggler magnet: predicted field distribution in the plane of symmetry along the beam path: (18852)

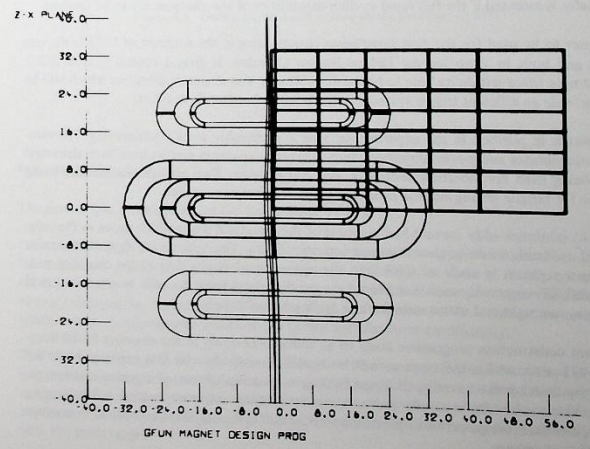

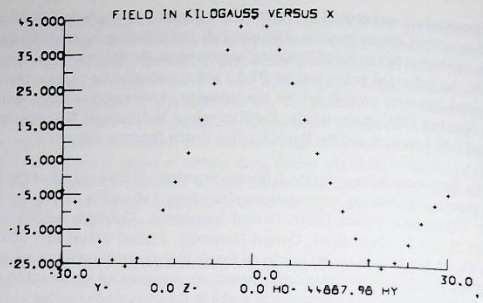

Figure 4.3. (b) Computer generated picture showing the projection of the geometry and electron trajectories in the z - x plane for the wiggler magnet: (18853)

A joint project with Culham Laboratory has been the development of a package of computer programs for use in connection with the Tokamak fusion experiments. The program will calculate the fields and forces in a toroidal system of either circular or 'dee' shaped coils. A modified version of the Swansea FINESSE program is used to carry out the stress analysis. A program has been written to compute the optimum 'dee' shape for the toroidal coils for minimum shear stress within the conductor.

RAPID CYCLING VERTEX DETECTOR

During the year emphasis has moved from development work to the building phase. The design of the chamber is now virtually complete and has incorporated changes which have been made in the light of experience gained in carrying out the development work. The most significant change is in the basic layout which is shown in Fig.4.4. The large optical window is now at the bottom and the mirror surface at the top. This layout gives more efficient heat transfer to the refrigerant hydrogen which is contained in a separate dished end welded on at the top. Good heat transfer is essential if the full rapid cycling capabilities of the chamber are to be realised.

The magnet to be used for the first experiment commencing in the Autumn of 1975 is the one designed and built in 1966 for the Helium Bubble Chamber. It gives a central field of 2·2 T and has ample space within its bore to house downstream wire chamber detectors which will be used to provide an efficient trigger system for the bubble chamber flash tubes.

The magnet is in position in the experimental area and assembly work is proceeding. The electromagnetic vibrator and power amplifier which drive the expansion system have been delivered and are being used for vibration testing of key components. Two chamber bodies are being made, one for fatigue testing and the other for use in the first experiment.

In order to minimise eddy current heating most of the structural items which move in the magnetic field are being made in glass reinforced plastic (GRP). The optics cartridge which is also the expansion piston is made of GRP with the optical window glued in at the chamber end. Considerable development work has been done on this glued joint in order to produce a seal which is vacuum tight and withstands thermal cycling and vibration.

The current construction programme leads to an initial cool-down in the chamber in the Summer of 1975 after which the cameras will be installed ready for the first experiment in the Autumn. By limiting the quantity of liquid hydrogen, making full use of a gaseous helium refrigerator which is bought as a fully proven commercial item and incorporating a data logging computer, the basic design permits operations with a small operating team compared to conventional bubble chambers.

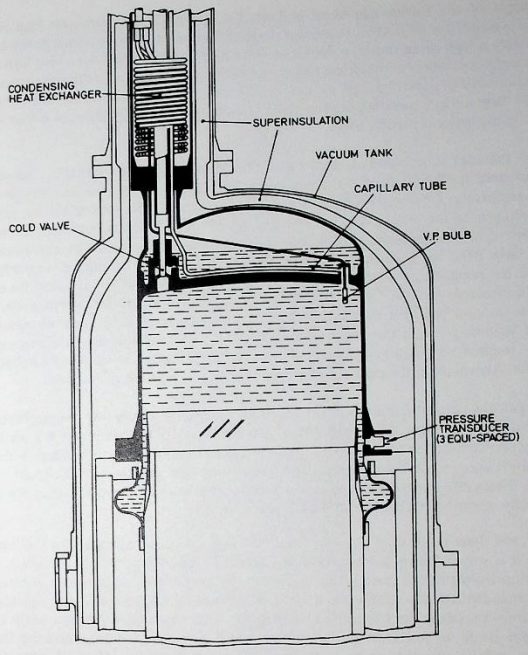

Figure 4.4. Design for the rapid cycling vertex detector: (18624)

POLARIZED TARGETS

The frozen spin polarized target for Experiment 11 (π9)

Commissioning of the frozen spin polarized proton target was completed in October 1974 and the target was immediately used in the successful collection of data in the charge exchange experiment $\pi^- p \rightarrow \pi^0 n, \eta n$. Although the development of the frozen spin target (FST) had been severely delayed by technical problems the final performance of the target when used in the charge exchange experiment exceeded the design specifications significantly.

The target is of novel design and successfully incorporates several new features not previously employed in polarized proton targets. It is the first target using the separated function principle to complete a physics experiment; it makes the first use of superconducting magnets in an HEP experiment at the Rutherford Laboratory and the first use of a dummy target interchangeable with the main target.

The principle of the frozen spin target is illustrated in Fig.4.5. The particular high energy physics experiment for which this target was developed imposed several extreme design conditions, notably a high mean proton polarization in a target to which there was a very high angular access confined within a cylindrical region of relatively large length to diameter ratio. The only practical way of achieving high proton polarization together with a large solid angle of access to the target is by separating the functions of polarizing the target material and its subsequent use in the incident particle beam.

The target material is propanediol, doped with Cr.V complexes. This material is formed into several thousand small spheres of 1·5 mm diameter, and loaded into a metallic cavity which is cooled to temperatures below 0·8K by means of a He3 refrigerator. To polarize the free protons in the hydrogen of the propanediol the cavity is moved into a uniform magnetic field of 2·5 tesla produced by a superconducting magnet and simultaneously irradiated by microwaves of about 70 GHz. After the polarization has risen to an acceptable value the microwave irradiation is stopped, the temperature of the target material is lowered to below 0·5K and then the cavity is moved downwards through 55 cm into the beam line, where it experiences a magnetic field of 2·5 tesla strength provided by a second superconducting magnet. After about 40 minutes in this lower holding position the target is raised back into the centre of the polarizing magnet where the residual polarization is measured prior to re-polarization to restore the initial high polarization. Alternatively the direction of polarization can be reversed at this stage.

An important operational feature of this target is the addition of a hydrogen free duplicate target below the proper target. Since these two targets can be moved separately into the beam line the HEP experiment can be conducted in four different modes: no target in the beam, hydrogen free dummy target in the beam, unpolarized proper target and polarized proper target in the beam line. These different operational modes facilitate the setting up and tuning of the beam and the study of systematic changes in the HEP experiment.

The target and dummy target arrangement is shown in Fig.4.7a. To minimise the heat load to the cavity it is suspended via the microwave guide at the top and expands into a simple horn at the transition from guide to cavity. Directly above the region containing the target material the cavity is expanded laterally, within the limitations imposed by the requirement of high angular access, to form a reservoir for storing He3 liquid in the cavity above the top surface of the target material, but giving the lowest hydrostatic pressure at the centre of the target material. During build-up of polarization the cavity is continuously fed with liquid He3 and boiling occurs throughout the body of the target so that significant detrimental vertical temperature gradients do not become established. In the holding position, however, the target is cooled by evaporation from the free surface of the liquid contained only within the cavity, the system acting as a single-shot refrigerator which is refilled each time the target is raised to the polarizing position.

Since the entire cavity system, in moving from the polarizing to holding positions, passes through regions of intense field gradients of up to 0·8 tesla/cm, the limitation of heating by eddy currents was a severe design problem which necessitated the construction of the cavity from thin stainless steel foil coated with a thin surface layer of copper where required for electrical conductivity. Consequently, the body of the cavity contributes little to the maintenance of a uniform temperature throughout the depth of the contained liquid by thermal conduction in the cavity walls. The dummy cavity, containing carbon fibre to simulate the non-hydrogenous part of the target material, is suspended 7 cm below the proper cavity. The cavity also contains a coil for the measurement of the polarization of the target material by nuclear magnetic resonance (NMR) techniques.

The magnetic system of the target consists of three discrete superconducting magnet elements which are strongly coupled together, both electrically and mechanically, and contained in a separate cryostat within the main vacuum tank. The complete arrangement is shown in Fig.4.7a.

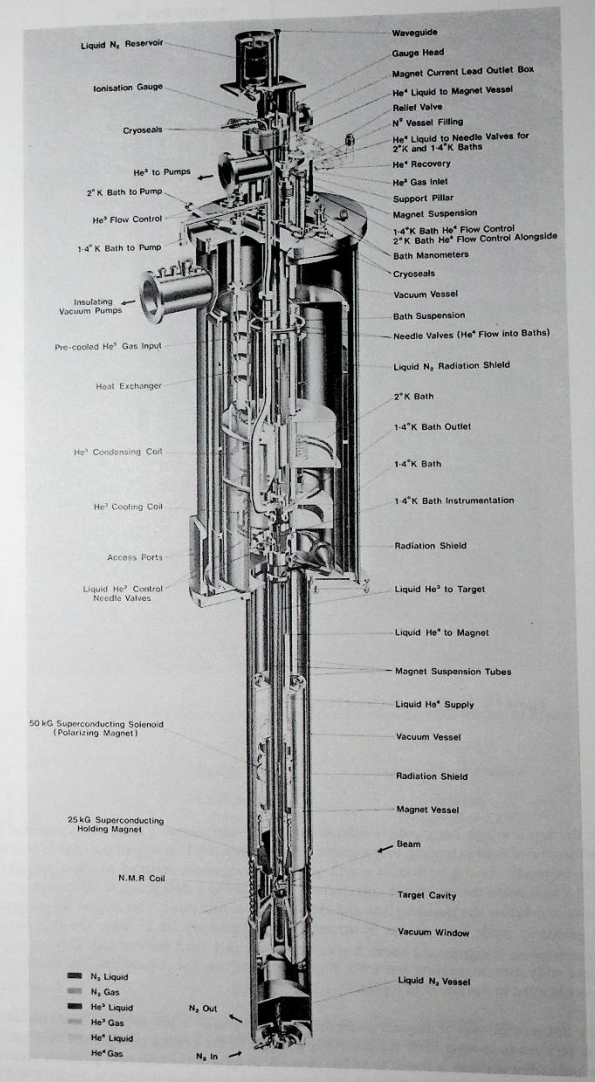

Figure 4.5. A cut-away drawing of the frozen spin polarized target apparatus: (10110)

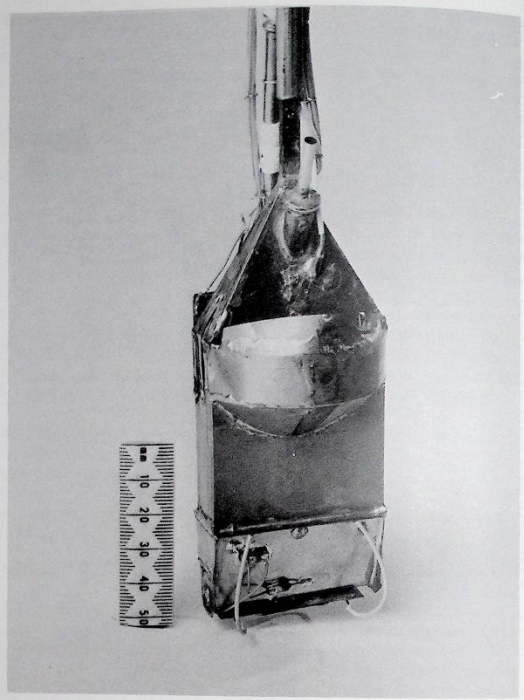

Figure 4.6. The frozen spin target cavity: (18879)

At the top is a high homogeneity magnet capable of operation at 5 tesla, with a region of high uniformity of field extending over a sphere of 5 cm diameter. This magnet operates in persistent current mode. At the bottom is a split pair coil arrangement designed to give a central field of 2·8 tesla when the cryostat is operated at 3 K, and giving a clear access to the centre of ± 45° above and below the median plane and almost 360° in that plane. This magnet is not operated in persistent mode since it was constructed from filamentary Nb.Ti. wire. The field between these magnets is maintained above 2 tesla by the use of a third booster coil. This not only reduces eddy current heating but more importantly reduces the polarization loss which would have obtained in the low field region.

With this arrangement of magnets giving the axial field profile shown in Fig.4.7b, the depolarization suffered in moving from the polarizing position to the holding position and back again to the polarizing position is found to be less than 1%, in spite of the high field gradients present in the region of the holding position. At the present time the magnet cryostat is operated at 4·2 K with the polarizing and holding fields both at 2·5 tesla. Since the target became operational it has functioned with an efficiency > 80%.

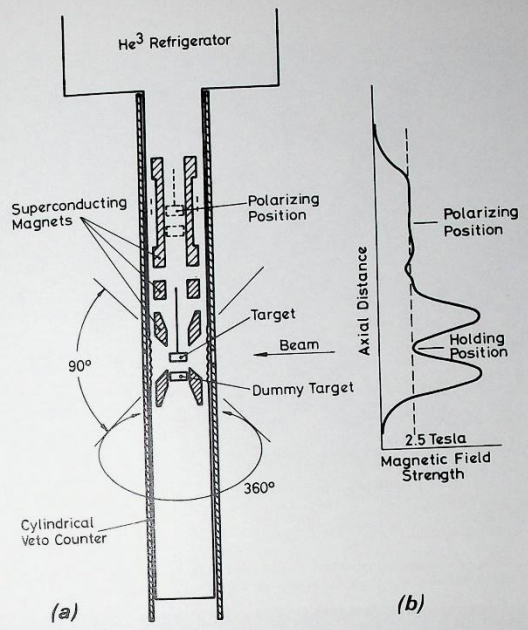

Figure 4.7. (a) Schematic of the target, dummy target and magnets in the frozen spin polarized target apparatus. (b) Profile of the axial magnetic field in the frozen spin polarized target apparatus: (18851)

In the Table below the present performance and parameters are compared with the initial design parameters.

Parameter	Design Value	Actual Performance
Target Material	LMN, organic if possible	Organic, Propanediol, Cr.V
P, initial	60%	70% - 72%
P, final	50%	65% - 67%
Target volume (cm^3)	15·6	18·7
Holding time† (mins)	120	45
H, polarizing (tesla)	2·5,5·0	2·5,5·0
H, holding† (tesla)	2·8	2·5
Magnet temperature† (K)	2·2	4·2
T, holding (K)	0·3	<0·5
Mark space ratio*	0·73	0·73

* Ratio of time target available for HEP use to total time, at constant polarization sign.
† Magnet operated at reduced ratings for economic and operational reasons

Since the mark space ratio is similar to that initially specified and the mean polarization significantly exceeds the design value the frozen spin polarized proton target has performed well above the design specification.

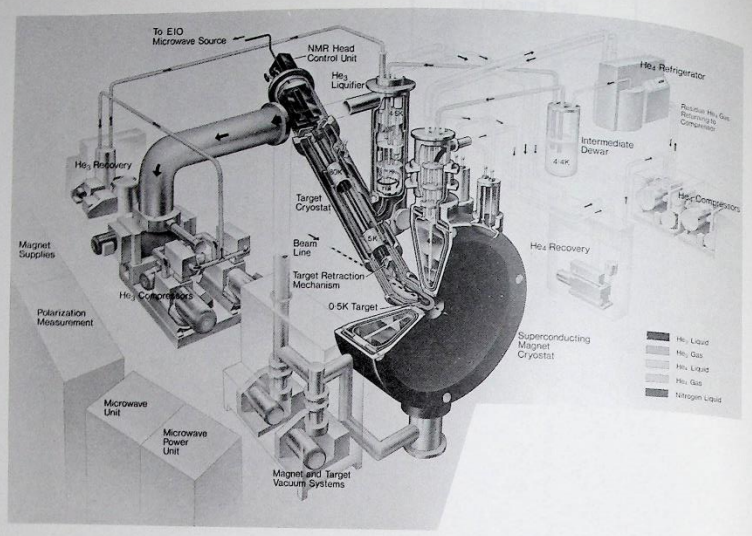

Figure 4.8. Above: A schematic layout of the polarized target PT55 system: (17961)
Below: Assembly of the component systems: (16259)

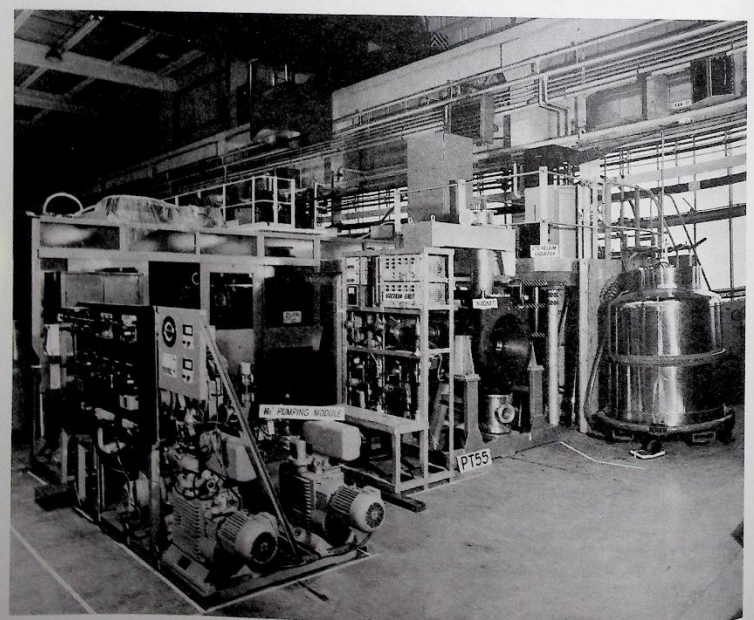

Polarized target PT 55

A polarized proton target is being constructed to investigate the interaction $\pi^- + p \rightarrow \Lambda^\circ + K^\circ$. A schematic diagram of the system is shown in Fig.4.8. Most of the major systems are nearing completion and the commissioning of individual systems has started.

All components for the magnet have been manufactured. The coil system has been assembled and tested in a large cryostat. The coils were operated first at 1·5 tesla and a field survey carried out over the target volume (5 cm long x 3 cm diameter) yielding a homogeneity of ± 2 parts in 10^4. After a quench at 2·48 tesla the system was operated at 2·62 tesla and 4·2 K. This was repeated a number of times without quenching for periods of up to 30 minutes. A spot check at 2·5 tesla showed the homogeneity to be within the required tolerances. A final test was carried out at 4·45 K and 2·62 tesla (corresponding to 5% over the operating currents) for 30 minutes. These tests show the system to be capable of meeting all the design parameters.

Polarized deuteron target for Experiment 14 (K20)

A deuteron target is to be used to measure the polarization in:

$$K^\pm n \rightarrow K^\pm n$$
$$K^+ n \rightarrow K^\circ p$$
$$K^- p \rightarrow \bar{K}^\circ n$$
$$K^\pm p \rightarrow K^\pm p$$

The available kaon fluxes dictate a fairly large target volume (30 to 80 cc) with neutron polarizations in excess of 25% while good angular access to the target is required. Background measurements will be particularly important because within the deuteron the neutron is not stationary.

Figure 4.9. Layout for a polarized deuteron target for Experiment 14 (K20): (18898)

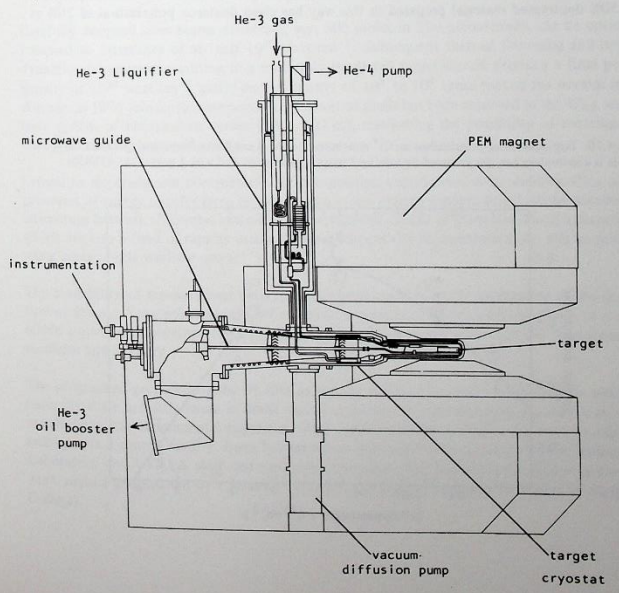

These requirements can be met by the design shown schematically in Fig.4.9. The PEM C-type magnet (M 1601) used in Experiment 3, has been modified to allow beam entry through the yoke. A continuous flow He-3 refrigeration system is used to cool the target material and several of the cryogenic components are the same as in PT 55, particularly the vertical He-3 liquefier. A separate horizontal cryostat contains the target itself. The demands of the highest possible polarizations imply large pumping speeds and an oil booster pump will be used as the primary He-3 pump. The cryostats and He-3 and He-4 pumping systems are under construction.

For the target material either deuterated propanediol or butanol will be used, while for background measurements the equivalent non-deuterated material will be loaded in the target, thus providing the opportunity to simultaneously obtain data on $K^{\pm}p$ channels.

The NMR detection system will have a single deuteron coil and several small proton coils to monitor the polarization of the residual free protons. Both NMR and microwave systems are designed and components are on order.

Polarized Target Research and Development

(ref.RL-74-147)

An existing Helium-3 refrigerator has been refurbished and equipped with a microwave source, superconducting solenoid and nuclear magnetic resonance spectrometers to undertake R and D for future polarized targets. The facility has been used a) to perform small sample polarization tests and relaxation time measurements on material prepared for the frozen spin target and b) in the development of a material suitable for the polarized deuteron target. The materials were prepared using an electron spin resonance spectrometer which was completed early in the year.

The material studies included preparation of propanediol with high concentrations of Cr.V, produced by lengthening the reaction process. As expected, the polarization was poor, but subsequent dilution to the optimum concentration produced good polarization (Fig.4.10). It had been generally believed that highly concentrated material was poor because of the Cr.III end product and that the reaction was irreversible. Our results showed this to be purely a Cr.V concentration effect and enabled us to produce deuterated material by dilution with deuterated propanediol. 50% deuterated material prepared in this way has given deuteron polarization of 26% at 0·5K.

Figure 4.10. Dependence of polarization on Cr^{V} concentration. A, B and C are the primary samples. $A_{2:1}$ for example is a secondary sample prepared by mixing 2 parts of unreacted diol with 1 part of A: (18850)

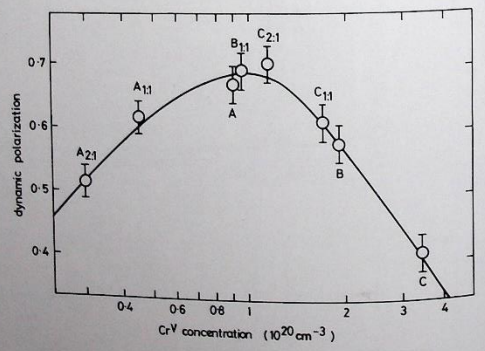

The preparation of highly concentrated D-6 (75% deuterated propanediol which must be used for the chemical reaction with potassium dichromate giving Cr.V) and its subsequent dilution with D-8 (100% deuterated propanediol) should allow the production of material with > 90% deuteration.

The material prepared for the frozen spin target had a low spin concentration of $1{\cdot}2 \times 10^{20}$ cm^{-3} which resulted in an increase in relaxation time of some 50% over previously published results thus contributing to the success of that target.

High Power Laser Facility

At its meeting on 30 May 1974 the Science Board endorsed proposals in a report from its Physics Committee which made a case for the provision of central high power laser facilities for the use of university groups. In July, Council gave approval in principle and asked the Rutherford Laboratory to prepare costed proposals on how best to proceed for consideration at its December 1974 meeting. These proposals were to take into account the plans of the UKAEA which also wished to embark on work using high power lasers.

Objectives

The principal scientific objectives to be met for university research are:

a) to create and study in the laboratory superdense plasmas generated by the laser compression of matter;

b) to study non-linear interactions of very intense laser radiation with matter;

c) to develop more efficient and new high power lasers for future experiments in laser compression and other fields.

Carefully designed laser beams delivering, say, 500 joules in 300 picoseconds, can be optically focussed to intensities of at least 10^{15} watt cm^{-2}. Subsequent thermal focussing and hydrodynamic compression occurring in a uniformly irradiated target should produce a final power density of 10^{19} watt cm^{-2} and a matter density of 10^{3} to 10^{4} times that of the normal solid. Already in 1974 substantial compression of spherical shells has been achieved in the USA with a laser system of intermediate power (50 J, 300 ps), confirming the possibility of entering this field with existing laser technology.

Crucial to the study and interpretation of compression experiments is an understanding of the processes of energy transfer from the laser beam to the plasma produced, and of the detailed relationships between absorptive and radiative mechanisms. Study of these non-linear interactions, which are also a field of rapidly increasing scientific activity in their own right, will be possible using lasers of intermediate power.

The availability of terawatt laser pulses will also open the way to the exploration of the generation of intense X-ray point sources and to the development of XUV and X-ray lasers, of considerable potential importance for other branches of physics, and with possible applications in medicine and industry.

The programme proposed by the UKAEA is broadly similar to the one outlined above although naturally there are differences in detail and in emphasis. In formulating proposals for the laser installations, the experimental apparatus, the buildings and the resources required to establish and operate a central facility, there has therefore been close consultation between Rutherford Laboratory and UKAEA staff and university scientists. The Rutherford Laboratory has also been advised and assisted by a Steering Committee chaired by Professor D. J. Bradley (Imperial College).

Initial Facilities

It was concluded that the requirements of both the AEA and the SRC could be satisfied by the same laser installations and by a common development programme for new and improved lasers. It was therefore proposed to Council that the SRC and the AEA should embark on a Joint Project at an annual cost to each party of about £1M. To launch the research programme it is proposed to provide two neodymium-glass lasers, each giving high quality beams capable of achieving power densities of 10^{15} watt cm^{-2} on targets. In its most straightforward form the main compression laser could produce a total of 500 joules in two beams with a tailored pulse of 300 picoseconds duration to irradiate a 100 μm diameter sphere with a power density exceeding 4·5 x 10^{15} watt cm^{-2}.

The second, intermediate energy, single beam laser would produce at least 10 joules in 100 picoseconds and could be focussed to power densities in excess of 10^{15} watt cm^{-2}. This laser would also be used for component testing, diagnostic development, and as a driver for the development of higher energy systems. It is also proposed to provide an electron beam generator capable of delivering a 30 ns, 100 kA electron pulse of energy at least 1 MeV for use in the development programme. Its function will be to trigger chemical lasers (eg HF) or to excite quasi-molecular lasers, high power CO_2 and exotic gas mixtures.

A purpose designed building will be required to house the complete activity of the laser centre. It is planned to locate this between AERE and the Rutherford Laboratory. This building will take at least 2 years to construct, so the lasers and the project team will be housed initially in temporary accommodation. It is envisaged that the direct staff of the joint project team will rise to about 70 by the end of the second year.

Council accepted the Rutherford Laboratory recommendations at its December meeting and has sought government approval to proceed.

NEUTRON BEAM RESEARCH

The reactor building at Institut Laue-Langevin, Grenoble

5. Neutron Beam Research

The Neutron Beam Research Unit (NBRU) is active mainly in three broad areas – research and development of neutron beam techniques and instrumentation, support of the UK neutron beam programme both at home and abroad, and participation in neutron beam science projects.

Amongst major projects, of the instruments being developed in collaboration with the Institut Laue-Langevin (ILL) at Grenoble, the polarized beam diffractometer D3 has now been installed and is undergoing commissioning experiments, and the diffuse scattering apparatus D11B is at an advanced stage of construction. The polarization analysis filter is under construction and components are already under test. In the development programme neutron beam tests have been carried out on a neutron beam "bending" device, on a new small-divergence Soller collimator, on magnetic mirrors and on the channel-plate position detector, and prototypes are under construction. As part of the Unit's programme concerned with future neutron sources and their utilization, there is active collaboration with AERE Harwell in developing pulsed source instrumentation on the AERE linac.

INSTRUMENTATION AND TECHNIQUES

Polarizing Filters

(ref.RL-74-036)

A polarizing filter containing polarized ^{149}Sm nuclei which are introduced as the dope into a cerous magnesium nitrate single crystal, is now under construction. The filter operates by selective spin capture and will initially be used for spin analysis of diffracted beams at wavelengths ∼ 1Å. High ^{149}Sm nuclear polarizations (∼ 85%) are achieved using a static process (Rose-Gorter Method) by holding the filter temperature near ·020K in the mixing chamber of a ^{3}He - ^{4}He dilution refrigerator, and applying a steady 0·3T horizontal magnetic field in the direction of the crystal unique symmetry axis which is common with the neutron beam direction. In the present design the applied magnetic field can be raised to ∼ 1·5T so as to enable a partial adiabatic demagnetisation of the paramagnetic crystal to be performed, thus facilitating its cooling. Large single crystals of cerous magnesium nitrate ($Ce_2Mg_3(NO_3)_{12}$ $24H_2O$) doped with Sm^{3+} ions have been successfully grown from aqueous solutions. The % doping measured in the crystals is critically dependent on the (samarium)/(cerium) ion concentrations in solution, and the precise conditions required in order to grow a crystal of the desired doping (5 to 8%) have been ascertained. The problem of mounting the crystal in the dilution refrigerator mixing chamber so as to minimise or exclude having ^{3}He in the neutron beam path (^{3}He has a very large thermal neutron absorption cross-section) has been investigated, and a suitable design suggested. The low temperature thermometry will be carried out by measuring the paramagnetic susceptibility of powdered cerous magnesium nitrate, which is calibrated at higher temperatures (0·3 to 4·2K) against a germanium primary standard resistor.

Possible metallic polarizing filter materials containing polarized ^{149}Sm nuclei have been investigated with the aim of easing the absorption heating problems that might occur in a paramagnetic salt filter with large beam intensities. The desired properties of a metallic material are firstly that the hyperfine magnetic field at the ^{149}Sm nucleus should be sufficiently large, and secondly that it should be possible fully to polarize the 4f electrons of the Sm^{3+} ions. It was demonstrated that ferromagnetic metals such as Sm_2Fe_{17} or $SmAl_2$ might provide the most suitable filter materials, since both satisfy the above conditions. It was further shown that neutron depolarization effects in these materials are likely to be negligibly small compared to the selective capture polarizing process. It is intended to test certain ferromagnetic samarium-containing metals when the neutron calibration measurements on the polarizing filter take place around the middle of 1975.

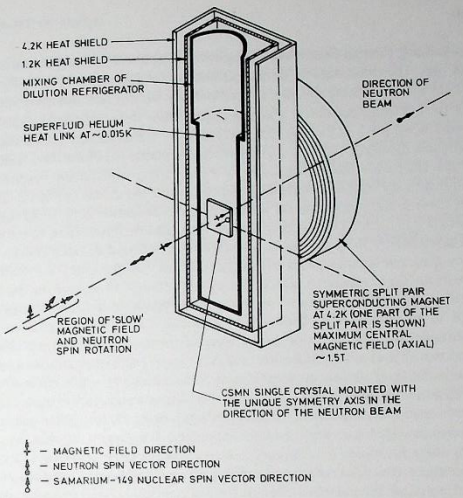

Figure 5.1. Schematic diagram of the temperature and magnetic field environment around the CSMN polarizing filter, and showing the principle of operation of the filter: (18849)

Figure 5.2. Proposed layout of the polarizing filter on the 6HGR10 beam hole at the AERE reactor DIDO: (18848)

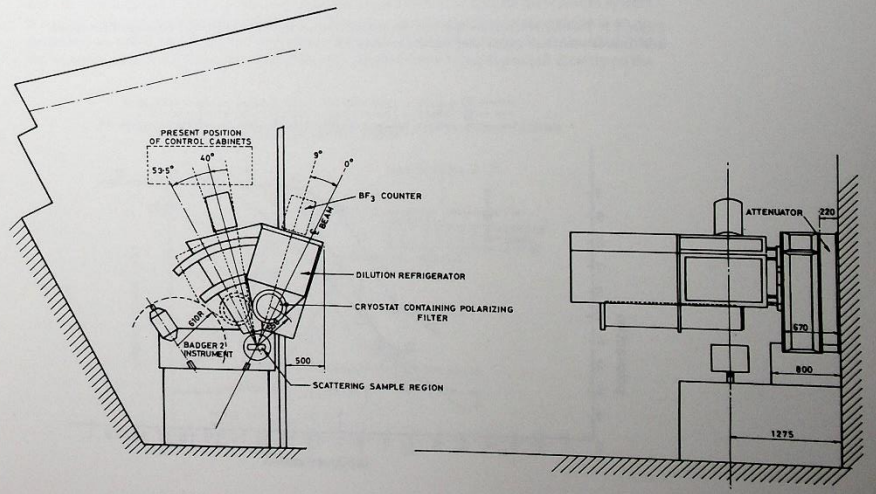

Polarizing Mirrors

The method of polarizing thermal neutron beams by total reflection from magnetized mirrors is a well-established one. The most suitable mirror material so far found seems to be Permendur (Fe(50)Co(48)V(2)) which theoretically has zero reflectivity for (−) spin neutrons and almost 100% reflectivity for (+) spin neutrons at glancing angles θ less than the critical glancing angle θ_{crit} (mrad) $\sim 1{\cdot}92\ \lambda$, where λ is the neutron wavelength in Å. Preliminary polarization measurements on thin films of cobalt:iron (50:50) deposited on plastic foils have been made in collaboration with the ILL, with the eventual aim of constructing a polarizing neutron bender similar to the non-polarizing bender described below; our results are shown in Fig.5.3. The main conclusions from these initial measurements are that a) the polarization at (θ/λ) values close to the critical value $(\theta/\lambda)_{crit(+)}$ for (+) spin neutrons on the magnetic film is close to unity, ie the magnetic film behaves ideally, b) the decrease in polarization observed at lower (θ/λ) values for films deposited on glass and Melinex occur at values consistent with the onset of (−) spin reflection taking place from these substrate layers, and c) our attempt to extend the useful (θ/λ) range by depositing the magnetized film on polypropylene (which should theoretically be non-reflecting) proved to be unsuccessful. During later discussions with the manufacturer of the polypropylene film we learnt that the uppermost layer of this film was in fact a dichloroethylene polymer, and this acts as a good reflecting substrate for (−) spin neutrons. We now intend to deposit the magnetic layer on to a polymer film of composition $(CH_2)_n$, since in theory this should be non-reflecting, and should give high polarizations over a large (θ/λ) range. The results so far suggest that it may now be possible to construct a polarizing mirror system using Melinex foils of the substrate provided it is designed to accept beams at angles close to $\theta_{crit(+)}$ over the whole wavelength range for which it is required, however for the polarizing bender application it is necessary to extend the (θ/λ) range. A polarizing mirror operating near wavelengths ~ 5Å would be a useful polarizer for polarized beam diffuse scattering, polarization analysis or spin echo spectroscopy instruments.

Figure 5.3. Polarization measurements on thermal neutron beams totally reflected from magnetized cobalt-iron films as a function of (glancing angle)/(wavelength): (18847)

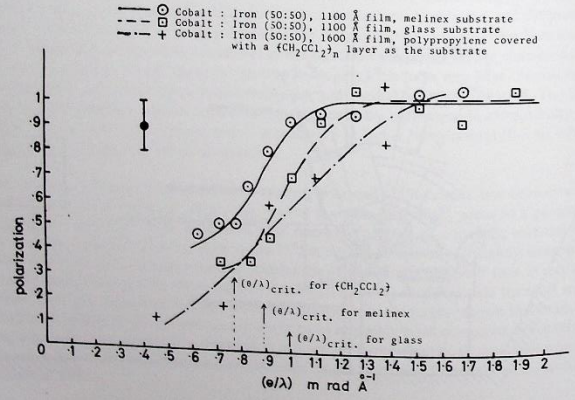

Stern-Gerlach Polarimeter

The (−) and (+) spin neutrons in a cold or thermal beam are spatially separated when the beam passes an inhomogeneous magnetic field whose gradient is perpendicular to the beam; this is the basis of the Stern-Gerlach polarizing method. Design studies are being carried out on the use of a conventional permanent or electromagnet assembly to spin analyse a low cross-section (∼ 5mm x 0·2mm) beam of neutrons in the wavelength range 3·5 to 12Å. Both magnet assemblies would be necessarily long (∼ 1m) and a further drift distance ∼ 2m allowed before the detector; with such an arrangement a spatial separation ∼ 2mm is predicted for the faster neutrons (3·5Å). It is intended to use a simple linear position sensitive detector of the type described below to determine the beam deflection, and with such a device we expect to achieve a spatial resolution ∼ 0·2 to 0·3mm. Despite the fact that a Stern-Gerlach device has to be physically large and heavy, it is unique in that it allows a method of directly measuring the beam polarization, and furthermore it is easily used with a 'white' beam.

Superconducting Hexapole Solenoid

Development work has begun on a hexapole solenoid for the production of long wavelength neutron beams with a polarization approaching 100% and a high overall transmittance. The hexapole produces an image of the input aperture by focusing (+)spin neutrons and defocusing (−)spin neutrons. Because of the weakness of the interaction, fields of ∼ 40kG must be achieved necessitating the use of a superconducting solenoid. In collaboration with the Superconducting Magnet Applications Group of the Applied Physics Division, a 1 metre prototype hexapole, with a bore of 5cm, is being developed. It is anticipated that a transmission for (+)spin neutrons of ∼ 12% (zero for (−)spin) of 10Å neutrons will be achieved. Increasing the length of the hexapole to, say, 3 metres causes the transmission to be enhanced to ∼ 65%.

Position Sensitive Detectors

Work has continued throughout the year on the linear PSD utilising a channel plate electron multiplier. A 20-channel experimental detector with a ± ½mm resolution was successfully demonstrated in October 1973. In this device, the stack of 1mm wide strips of lithium loaded glass scintillator was placed inside the vacuum envelope along with the photocathode, channel plate and electron collector. Clearly, a detector in which the scintillator is outside the vacuum system is a much more practical and versatile device. Work has concentrated on producing such an arrangement in which light from scintillations in the stack of scintillator strips is transmitted into the vacuum system via a fibre optic face plate, the photocathode being deposited directly on the

Figure 5.4. Tests of 23-channel position sensitive detector (PSD): (18846)

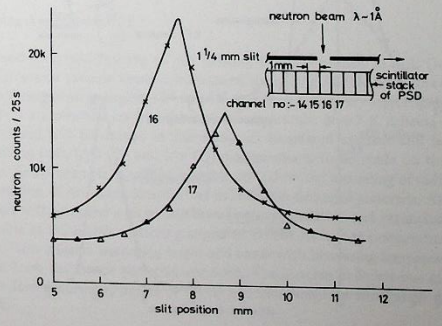

vacuum side. Progress was delayed due to a technical problem, eventually shown to be associated with the method of making electrical contact with the channel plate. This has now been resolved and a 20-channel device has been successfully demonstrated. A typical result is illustrated in Fig.5.4 which shows the signals from two adjacent channels when the detector is traversed behind a 1mm wide slit in a cadmium plate. A 100-channel electronic system for data collection and display has been commissioned. This is based on a multi-channel analyser using a small computer (PDP 11-105) with CAMAC interface. Work is now proceeding to produce a 100-channel module, several of which can be placed side by side to create a detector of any desired length.

For two-dimensional detectors, using a scintillator optically coupled to a photocathode channel plate electron collector assembly, methods of making the two-dimensional electron collector array have been investigated and a feasible solution found. Studies have been made of methods of making two-dimensional PSD's of rather coarser resolution (say 5mm rather than 1mm). The concept of a mosaic of small areas of scintillator, each corresponding to a 'picture element', coupled to a common, two-dimensional channel plate electron multiplier assembly by flexible light pipes has been examined. Preliminary measurements of light output from the light guide are very encouraging.

The possibility of using a relatively coarse resolution two-dimensional detector in a single-crystal diffractometer is being investigated. This type of detector requires a fast data collection and storage system, and the design of the data collection system has now started.

Figure 5.5. Tests of 5° bender on the 4H5 beam hole at DIDO: (18845)

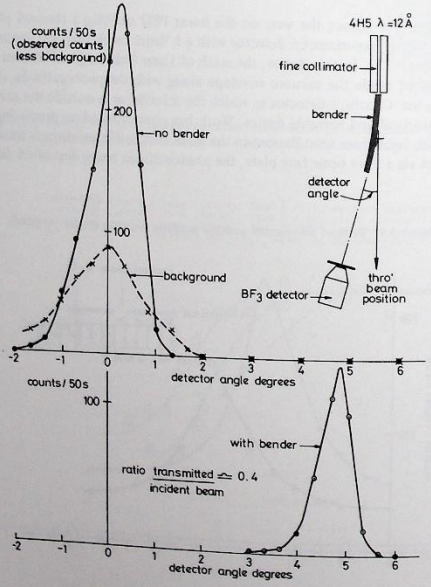

Neutron Guide Tubes

An experimental neutron beam bender has been completed for use with long wavelength neutrons (∼ 10Å). It consists of 11 Melinex films, ·025mm thick, spaced ·25mm apart on a former curved to a radius of 1880mm. The films are coated on each side with copper and the length of the device in the neutron beam direction (∼ 160mm) is such as to produce a beam deflection of 5°. The device was tested on the 4H5 beam hole at DIDO with a 12Å input beam defined by a collimator so that its divergence was approximately equal to the theoretical acceptance angle of the bender. Approximately 40% of the beam was transmitted through the device and successfully deflected through 5°. This result is illustrated in Fig.5.5. A Monte Carlo computer model of the bender has been made which takes into account, in a simple way, the distribution of surface slopes of the foils. Using measured values of surface quality, the model gives predictions of transmission efficiency which can be compared with neutron beam measurements. For example, the predicted transmission efficiency in the above bender experiment is 56% compared to the measured value of 40%. The difference is probably due to the tendency of the foils to curl slightly at the input and output of the device, where the foils are unsupported. The effect is difficult to take into account theoretically and results in the obscuration of the neutron beam being larger than that given simply by the ratio of foil thickness to inter-foil spacing.

Polarized Neutron Diffractometer, D3

The D3 Diffractometer was delivered to ILL in July. The monochromator installation was completed by the Institut in August and the whole system is undergoing its acceptance tests. It is expected that it will be scheduled for routine use early in 1975.

Superconducting Magnet and Cryostat for use on D3 and D5

A 4·8T magnet and cryostat is being provided for use on the two polarized beam diffractometers D3 and D5 at the ILL. A new diffractometer circle, with the necessary hardware and software accessories, will also be provided to control the specimen rotation angle within the asymmetric Helmholtz magnet when it is being used on D3.

Diffractometer Control

Several new units have been developed and used in the D3 diffractometer system. A Flipper Control Unit has been designed for use with a polarized neutron diffractometer. This is a CAMAC unit, and can be programmed into either an alternate or continuous mode of operation. The unit selects the state of the incident beam spin flipper and routes the detected neutron counts to the appropriate scaler. It selects either clock or monitor pulses to define the total measurement time. In alternate mode, the spin flipper is switched on and off with a period of about one second, thus avoiding the effects of longer term intensity fluctuations in the neutron beam. The ratio of time spent in the two states is preset from the data-way and can therefore be adjusted to optimise the measurement statistics. The flipper may be set either on or off in the continuous mode of operation.

Diffuse Scattering Apparatus, D11B

The D11B project is a modification to the existing D11 instrument at ILL (now known as D11A) by which a new vacuum vessel is introduced containing 32 ^{3}He detectors arranged so as to measure scattering at large angles (19° to 143° in 2θ). A helium cryostat capable of supporting and aligning 5 samples and cooling them to a temperature of 4·2 K is being provided. The complete instrument will be unique in the study of disordered systems and large molecular structures, enabling both high (Q) and low (Q) measurements to be made on the same sample simultaneously. As an example it will be possible to follow the annealing of radiation-induced defects as a function of annealing temperature in radiation-damaged materials. At low temperatures the defects will comprise a large number of point interstitials and vacancies which will be readily observable at the higher scattering angles of D11B. At higher temperatures the defects can migrate to form clusters becoming larger and larger with increasing temperature eventually disappearing to leave the lattice perfectly annealed. The increase in defect size can be followed by utilising the lower scattering angles of D11B and eventually the small angle scattering spectrometer D11A.

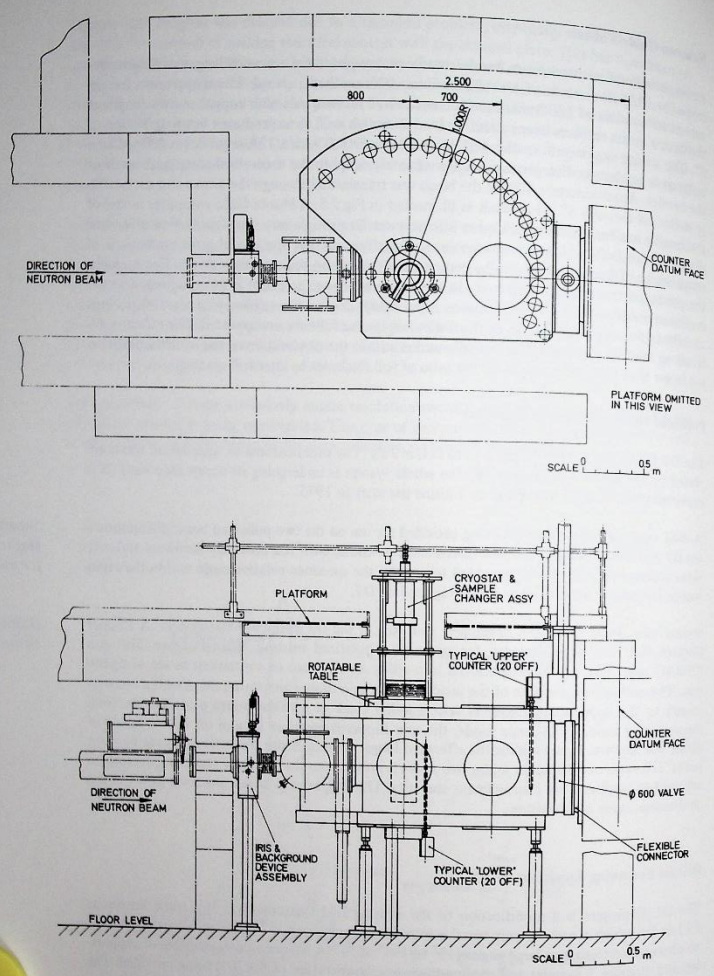

Figure 5.6. The D11B diffuse scattering apparatus which is being constructed for the Institut Laue-Langevin: (18494A)

Design work has proceeded throughout the year and all the major components of the RL part are now finalised. The main vacuum vessel and the cryostat have been ordered along with the electronic shaft positioning systems. A large vacuum gate valve, which isolates the main vacuum vessel from the rest of the existing D11A vacuum system has already been delivered to ILL. Apart from the three-shaft positioning systems, all the electronic control and data acquisition is being provided by the ILL. The system will allow four modes of preparation:—

(i) D11A alone
(ii) D11B alone
(iii) D11A and D11B working in parallel with the same sample
(iv) Preliminary time-of-flight studies (to determine the elastic width when using time-of-flight separation of elastic scattering).

The whole instrument (D11A plus D11B) will be controlled by a dedicated PDP-11 computer which will enable complete automation of control and data analysis to be performed on-line.

Instruments at AWRE Aldermaston

Development work has continued during the period of the HERALD reactor at AWRE. In collaboration with Birmingham University, modifications have been made to the chopper, counter array and blockhouse shielding of the Graphite-Monochromator-Chopper spectrometer. Three detectors at 100°, 110° and 120° give the largest range of momentum transfer available on any cold neutron spectrometer of comparable resolution in this country. The two-slot rotor has been installed providing an increase of flux of 2·5 with negligible worsening of the resolution.

Additional counters have been purchased for the small-angle scattering development of the defect scattering instrument G1. The Vanessa powder diffractometer, whose operation had ceased as from April 1973, was removed to storage.

SUPPORT OF THE UK NEUTRON BEAM PROGRAMME

The NBRU has a major role in the SRC support of United Kingdom university teams in the field of neutron beam scattering. Over 200 university staff, research associates and research students are involved in this programme which is carried out mainly on reactors in the UK and the high flux reactor at Grenoble, with the occasional use of reactors in Denmark and Canada.

Proposals for Experiments on Reactors

Proposals for SRC supported experiments, on reactors at home or abroad, are made bi-annually through the NBRU. A total of 212 proposals were submitted during the year, 104 for the UK and 108 for Grenoble. The Unit is responsible for processing these proposals for presentation to the appropriate SRC committees and, in the case of UK proposals for the Grenoble reactor, for their submission to the ILL for their selection processes.

Funding of Approved Experiments

Funds for approved experiments at home or abroad, ie travel/subsistence and material/equipment, are made available to university teams through the NBRU. Most of the funding under the heading of Materials/Equipment is made through Rutherford Laboratory/University agreements, in other cases purchases are made on behalf of the university team. Items which could have a general use, eg separated isotopes, ancilliary equipment, are purchased by the Unit and loaned to experimenters for the period of their measurements. Sixteen RL/University agreements are now in operation, 10 of these were set up in 1974.

Support of University Teams at Grenoble

With more instruments becoming available for routine use on the high flux reactor during the year, UK university teams are making increased use of the Grenoble facilities. Members of the Unit maintain close contacts with ILL staff and provide a liaison service for UK users. Visits, to use the Grenoble reactor, have been arranged for 115 members of university teams during 1974. Assistance has been given with the transport of equipment and samples on 32 occasions.

Technical Secretariat

Members of the Unit are involved in the preparation of technical reports and papers for SRC Boards, Committees and Sub-Committees, and for joint SRC/Establishment Committees at AERE Harwell and AWRE Aldermaston.

A special effort this year was devoted to support of the SRC Domestic Reactors Facilities Review Panel, the Unit providing a member, an adviser, and one of the secretaries. The Panel set up eight working parties to review future requirements at UK reactors in the following fields:–

(i) Single crystal diffraction
(ii) Powder diffraction
(iii) Inelastic scattering (Physics)
(iv) Inelastic scattering (Chemistry)
(v) Polarized neutron techniques
(vi) Diffuse scattering
(vii) Liquids
(viii) Biology

The NBRU provided secretaries for six of the working groups and members for three.

NEUTRON BEAM SCIENCE

Magnetic Studies

In collaboration with the University of Cambridge a study has been made of the neutron magnetic scattering by a single crystal of ferrous carbonate, $FeCO_3$, in the antiferromagnetic phase at 4·2K. Polarization analysis has been used to determine the absolute direction of the magnetic interaction vector for several low angle (hkℓ) reflections. The presence of equal proportions of the two 180° domain types in the crystal used prevented a direct observation of deviations in the directions of the interaction vectors due to spin-orbit coupling. However, an indirect measure of these deviations can be obtained from the degree of depolarization introduced by scattering. The results obtained in the experiment gave values for these deviations in qualitative agreement with theoretical predictions. Uncertainties intrinsic to the technique used and the sample under investigation prevented a quantitative comparison, but the experience gained suggests that more precise results can be obtained using a development of the present technique.

The magnetic structures of $TbZn_{12}$ and $Cu_{0\cdot5}Ga_{0\cdot8}Cr_2S_4$ have been determined in collaboration with Queen Elizabeth College, London University. Neutron powder measurements on $TbZn_{12}$ at ambient and 4·2K confirm that antiferromagnetic ordering exists at the lower temperature. The magnetic scattering indicated the presence of a non-commensurate structure with a propagation vector, $\underline{\tau}$, not lying parallel to a principal zone axis. A computer program has been developed to locate any $\underline{\tau}$ and was used to determine $|\tau|$ as 0·932Å^{-1} with a direction making approximately equal angles with the x, y and z axes of the tetragonal unit cell. The observed intensities correspond in all cases to groups of reflections and a helical spin model has been proposed which gives good agreement with the group intensities. The model is being refined by a least squares fitting procedure which compares the calculated intensities with the diffraction profile. $Cu_{0\cdot5}Ga_{0\cdot5}Cr_2S_4$ has the spinel structure and has been shown to be antiferromagnetic at 4·2K. An analysis of the neutron powder diffraction pattern, using the same technique as for $TbZn_{12}$, gives $|\tau| = 0{\cdot}0827 \pm 0{\cdot}0005$Å^{-1} with τ making a direction of $76 \pm 1°$ to x in the xz plane of the cubic unit cell. The non-commensurate magnetic structure is an elliptical spiral with an average chromium magnetic moment of $2{\cdot}3 \pm 0{\cdot}1\ \mu$B.

A magnetic structure determination of dysprosium manganate, $DyMn_2O_5$, and a study of the intermetallic compound FeGe in its cubic modification have been started using the high-flux facilities available at the ILL. Both investigations are also in collaboration with QEC, London University. The structure determination has begun with powder diffraction measurements in symmetrical transmission through a 2·3mm slab of highly-absorbing dysprosium compound. The magnetic scattering has been derived from comparison of the patterns obtained at 4·2 and 60K. The temperature dependence of the strongest magnetic peak indicates an ordering temperature of $8{\cdot}3 \pm 0{\cdot}2$K. The scattering angles for the magnetic peaks can be indexed in terms of a unit cell in which the a-axis is doubled with respect to that in the chemical cell of a = 7·29, b = 8·55, c = 5·68Å; space group Pbam. The commensurate nature of the structure contrasts with that of the isomorphous Lu, Er, Y, Ho, Tb and Nd compounds in which the magnetic structure arising from ordering of the manganese moments is helical with a propagation vector of the form (½ 0 τ), τ being in the range 0·24 to 0·36. The large unit cell dimensions make a precise determination of the structure difficult from powder measurements alone and a single crystal study is planned.

The cubic phase of FeGe a = 4·70Å, is known to be ferromagnetic in fields greater than some 0·2T, but its low field susceptibility, almost complete lack of hysteresis and complicated microwave magnetic resonance spectra have suggested a model in which the spins describe helices about <111> in zero external field. In the presence of a field the helices are supposed to go over into a crucial structure with its axis along the field direction. Confirmation of this model was sought using the powder neutron diffraction technique. No additional magnetic lines, such as would result from a non-commensurate helical structure, could be detected in measurements at 4·2K and zero field. Subsequently, careful measurements were made at this temperature, first in zero field and then in a field of 0·5T oriented parallel to the neutron scattering vector. These showed that, of the nuclear reflections, only the (110) contained an appreciable contribution from the zero-field magnetic scattering. This result and the intensity of the scattering are in good agreement with a simple ferromagnetic model for the 1μB moment on each Fe atom. Similar conclusions have been reached by other workers from neutron data obtained from a related material, MnSi, which also exhibits anomalous low-field magnetization behaviour. A satisfactory explanation has yet to be found for the origin of the observed bulk behaviour.

DATA ANALYSIS STUDIES

Neutron diffraction data from isotropic systems require techniques for estimating multiple scattering to obtain accurate results. If the structure factor modulates considerably in scattering vector, Monte Carlo methods are required. For pulsed sources, however, the diffraction experiment uses a continuous distribution of neutron wavelengths, and is analysed by time-of-flight techniques to give the scattered intensity as a function of wavelength. It would be necessary to perform the monochromatic simulation many times for the large range of wavelengths available to the diffractometer, but at only one or perhaps a small number of scattering angles. This operation is both formidable and wasteful, and a method is required by which time-of-flight diffraction data may be simulated to obtain these multiple scattering corrections.

An optimized algorithm has been devised which selects collision points and scattering directions within the specimen from cumulative distribution functions which represent all the particular wavelengths being considered, and computes scores into detector directions in such a way as not to bias the results. Though a somewhat larger number of paths needs to be studied in the pulsed source simulation than in the reactor case to obtain the required statistical accuracy, this increase is not nearly a factor equal to the number of wavelengths used in the simulation. This algorithm will be developed into a correction program which will be useful for data of liquids and amorphous materials taken on the time-of-flight diffractometer.

COMPUTING SERVICES

Data preparation area, central computer

6. Computing Services

(ref.RL-74-072, RL-74-111, RL-74-143)

The only major hardware change made to the IBM System 195 Central Computer during 1974 was the addition in March of a third megabyte of main core. The system has now given consistently high performance for a period of three years and from this experience it is now possible to predict its maximum capability when fully loaded. After deducting time lost through faults, maintenance, machine development, etc., just over 8,000 hours of good time were available to users in 1974. Central processor utilisation averaged 83%. After deduction of overheads this provided users with 5,412 hours of accountable computer time, which might increase to 6,000 hours under full pressure.

Remote computing has continued to develop, and about 50% of all jobs were loaded at remote stations. At the end of the year there were nineteen operational remote batch stations, most of which are equipped with a group of ELECTRIC terminals – VDUs, typewriters and graphics. The number of ELECTRIC identifiers active during any one week rose from 200 to 300 in 1974, and by the end of the year accounted for over 60% of the total number of jobs submitted, with a peak of 8,000 jobs one week.

Development work in remote computing is now directed towards networks, in collaboration with the Post Office's Experimental Packet Switching Service (EPSS). A link to the Advanced Research Projects Agency (ARPA) network via Professor Kirstein's nodal processor in London is operational.

Work is proceeding, based on GEC 4080 computers, to combine some local requirements (data collection, graphics, etc.) with RJE facilities. The work on graphics is directed towards removing local 'core-resident' interactive activities from the central computer. It also has wider application for remote users of interactive graphics.

Work is well advanced on coupling HPD1 and HPD2 in tandem mode. During 1974, HPD2 measured a total of 500,000 events. CYCLOPS, used previously for the measurement of spark chamber film, was taken out of service in May.

CENTRAL COMPUTER

The configuration of the central computer and its remote RJE stations is shown in Fig.6.1. Over 100 terminals communicate with the central computer, of which about half are attached to RJE stations.

Operations

A statistical summary of operations is shown below in the Tables showing machine utilisation and a breakdown of compute time between categories. The machine was scheduled for a total of 8,309 hours. Machine availability was 98% (8,133 hours) and the time available to users was 8,046 hours. The total number of jobs ran in 1974 (532,950) showed an increase of 18.4% over the 1973 figure. The average CPU utilisation was 83% corresponding to 6,709 hours. After deduction of overheads the compute time accounted to users was 5,412 hours.

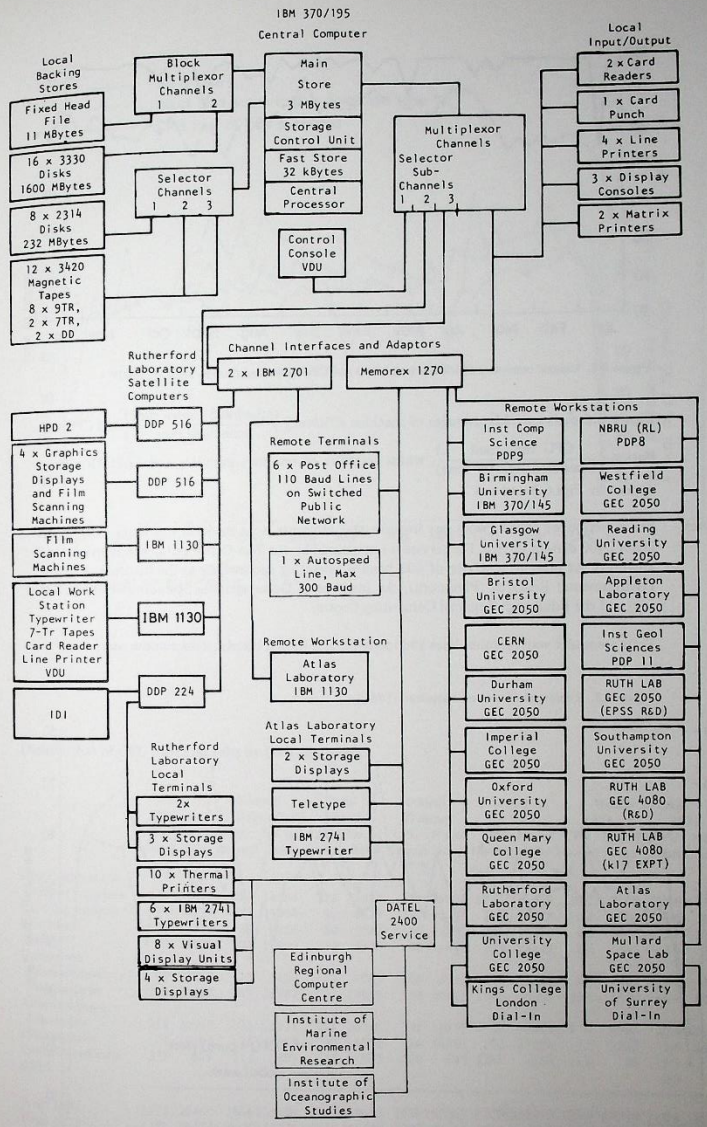

Figure 6.1. Organisation of the central computer, peripheral devices and remote work stations: (18856)

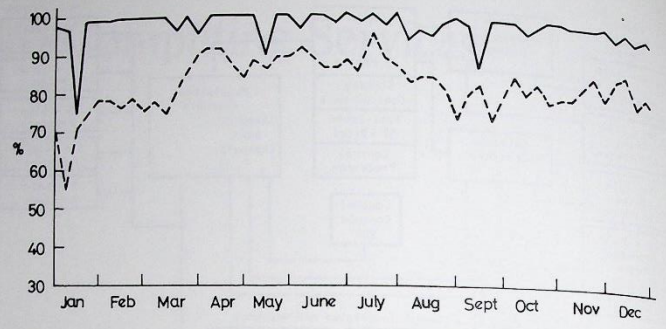

Figure 6.2. Central computer efficiency (solid line) and CPU utilisation (dotted line): (18860)

Figure 6.2 shows weekly averages of machine efficiency $\frac{\text{(scheduled - down time)}}{\text{(scheduled time)}}$ and CPU utilisation $\frac{\text{(CPU time used)}}{\text{(scheduled - down time)}}$, whilst statistics of remote computing and ELECTRIC usage appear in Figs.6.3 and 6.4.

Post Office Lines

For a period of about two years unsuccessful attempts were made to utilise the Post Office Datel 2400 dial-up service. The service is not assured by the Post Office but depends on terminal locations. At present, a service of 600 baud is operating successfully to the Institute of Marine Environmental Research (Plymouth), the Institute of Oceanographic Sciences (Wormley, Surrey) and the Edinburgh Regional Computing Centre.

Tests are under way on other lines and modems, and should benefit some remote users.

Figure 6.3. Remote work-station statistics: (18855)

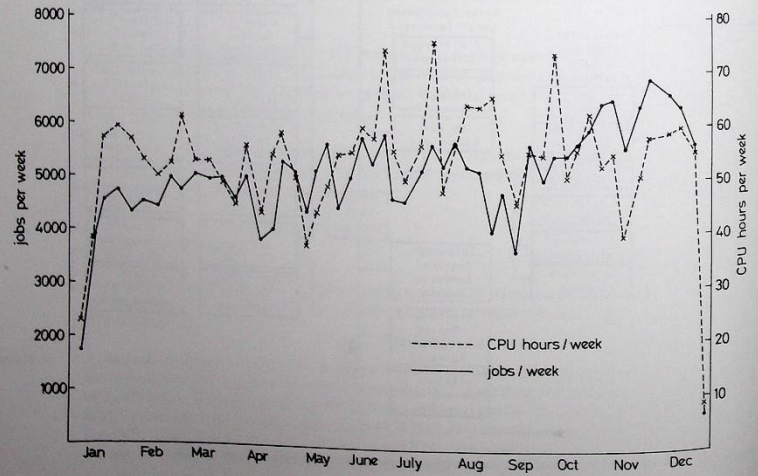

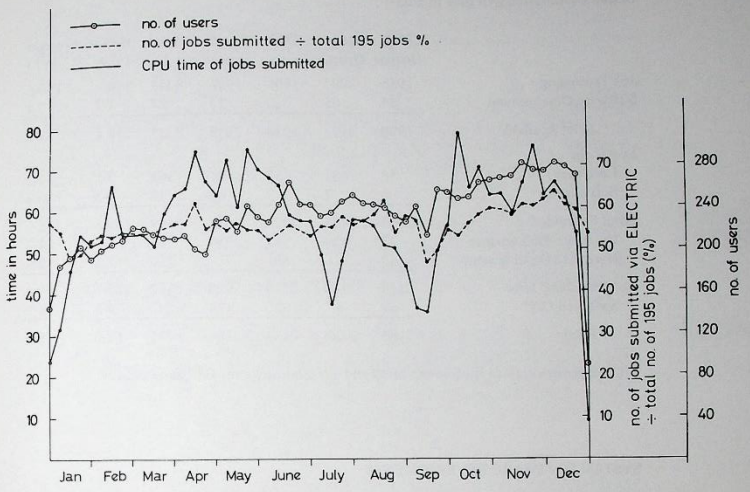

Figure 6.4. Use of ELECTRIC: (18854)

Distribution of CPU time and Jobs by User category

	First Quarter		Second Quarter		Third Quarter		Fourth Quarter		Total for Year		Weekly Average 1974		Weekly Average 1973	
	CPU (hours)	No. of Jobs	CPU (hours)	No. of Jobs	CPU (hours)	No. of Jobs	CPU (hours)	No. of Jobs	CPU (hours)	No. of Jobs	CPU (hours)	No. of Jobs	CPU (hours)	No. of Jobs
HEP Counters and Nuclear Structure	315	30044	381	33583	323	33023	343	36898	1362	133548	26·2	2568	30·6	2265
RL-Film Analysis	93	8717	198	9004	90	8639	159	10228	540	36588	10·4	704	6·6	640
RL-Other	94	19972	89	17654	58	17581	85	15087	326	70294	6·3	1352	5·9	1593
Theory	70	5870	91	10409	30	5420	48	6418	239	28117	4·6	541	5·3	391
Universities Nuclear Structure	69	5230	113	5400	67	4953	86	5313	335	20896	6·4	402	8·1	396
Film Analysis	269	20167	311	21987	303	19058	182	17055	1065	78267	20·5	1505	16·9	1024
Atlas Computer Laboratory	318	20936	325	21721	421	26226	359	30173	1423	99056	27·4	1905	20·0	1140
Miscellaneous	24	14695	25	15019	39	16957	34	16403	122	63074	2·3	1213	1·6	1085
System Overheads	271	829	333	807	333	832	360	642	1297	3110	25·0	60	15·7	70
DNPL	–	–	–	–	–	–	–	–	–	–	–	–	0·2	3
Total 1974	1523	126460	1866	135584	1664	132689	1656	138217	6709	532950	129·0	10249	110·9	8607
Total 1973	1386	96157	1606	114275	1460	118498	1344	121174	5796	450104	110·9	8607		
INCREASE	137	30303	260	21309	204	14191	312	17043	913	82846	18·1	1642		

Machine Utilisation (All time in hours)

	First Quarter	Second Quarter	Third Quarter	Fourth Quarter	Total for Year	Weekly Averages 1974	1973
Job Processing	1955	2097	1998	1996	8046	154·7	150·6
Software Development	25	25	20	17	87	1·7	2·4
Total Available	1980	2122	2018	2013	8133	156·4	153·0
Lost Time:							
Hardware	56	31	55	21	163	3·1	2·5
Software	6	2	3	2	13	0·3	0·4
Total Scheduled	2042	2155	2076	2036	8309	159·8	155·9
Hardware Maintenance	23	29	17	14	83	1·6	1·3
Hardware Development	49	–	61	–	110	2·1	2·6
Total Machine Time	2114	2184	2154	2050	8502	163·5	159·8
Switched Off*	69	–	30	134	233	4·5	8·2
Total	2183	2184	2184	2184	8735	168·0	168·0

* These figures include shut-downs of 69 and 131 hours over the Christmas periods.

SYSTEM SOFTWARE DEVELOPMENTS

The basic software for the central computer operating system is the IBM-OS/MVT/HASP, with some local additions, and on-line activities are supported by the locally-written MAST/DAEDALUS/ELECTRIC programs.

OS/360

Late in 1973 IBM provided version 21.7 of OS/360, which was introduced early this year and was expected to be the final version of OS to be issued. However, at the end of 1974 version 21.8 was received and is being studied. Both versions show only minor changes and corrections from their predecessors.

The main change during the year was the enlargement of certain supervisor work-areas, to cope with the increasing load following installation of the third megabyte of main memory. The increases were –

System Queue Area	40 kbytes	(work space for OS)
HASP	40 "	(more buffers, improved overlays)
ELECTRIC	30 "	(improved overlaying)
Link-Pack Area	20 "	(more resident SVC modules)
MAST	30 "	(to maintain response with more users)

HASP and COPPER

The HASP work space was increased to cope with the faster flow of jobs submitted remotely as work station usage increased. HASP can now be instructed by operators to select only jobs with priorities in a prescribed band, a facility of particular value during prime shift to avoid low priority jobs jumping the queue while others are waiting for disc or tape mounts. Further moves towards no-class input were made, the internal class being computed from the job parameters such as core and time requests. A 'no-restart' facility has been made available for jobs which should not be restarted after a system failure.

A new extended version of the COPPER control program has been introduced to help users cope with the near-saturation conditions existing on the central computer from time to time. It allows up to 8 levels of time allocation, of which most users currently see 5, viz priorities 12,8, 4,3 and 1 for express work, day-shift and urgent long overnight jobs, bulk production, and two levels of non-urgent background work. Individual user's requirements often fluctuate from week to week, so it was made possible for several accounts to pool their time allocation; this proved much more satisfactory than giving each user the same small allocation each week. The overall COPPER allocations are agreed with the 195 Advisory Committee, and each category of users are now enabled to allocate CPU time within their own field.

Data sets can now be mentioned on SETUP cards by symbolic references to the system catalogue. To give more information in response to status enquiries from users, a file has been introduced to hold information about jobs for as long as possible after their completion. The System Management Function has been allocated more space for recording and examining job turnround time.

MAST and DAEDALUS

In most respects the MAST and DAEDALUS system for on-line applications was unaltered, but changes were made to allow handling of lower-case text in messages as well as upper-case, and to allow a terminal to be used in conversational mode. In this mode input and output messages can alternate, whereas previously a terminal or program could send any number of messages before being required to receive a reply.

ELECTRIC

Documentation facilities in ELECTRIC have been extended considerably during the year. It is now possible for lower-case alphabetic characters to be entered at terminals and held in ELECTRIC files. In conjunction with a documentation processor and page layout instructions, this new facility allows text stored in files to be printed on a local line-printer specially equipped with upper and lower case characters. It has been used extensively, for example to produce manuals (including the Supplement to the ELECTRIC Users' Manual).

A user can now send a one-line message to another user (or to several simultaneously) by means of the MESSAGE command. The message will be received immediately if the user is logged-in, or stored for him if not. A longer message can be sent as a file by the MAIL command to a single user, providing his main directory includes a MAIL area.

An archiving scheme was introduced to ease the considerable pressure on filing space. It enables users to transfer ELECTRIC files to a mountable 3330 disc overnight and restore them again as required.

Other developments include automatic routing of line-printer output to remote workstations for jobs submitted via ELECTRIC, improvements to file security, and a scheme (not yet implemented) to allow transfer of ELECTRIC files to and from OS data sets.

GEC 2050 Workstations (ref.RL-74-042)

Only limited changes were made to the software for the standard GEC 2050 workstations. This is maintained by the Laboratory, and has been consolidated into a bootstrap loading system. All stations now load a bootstrap program from their cassette loader. This submits a job to the central computer which in turn picks up the current production version of the workstation RJE program with the necessary configuration from disc on the central computer. This control program is transmitted to the station, over-writes the contents of core in the GEC 2050 and is then automatically initialised.

This technique ensures all stations use the same level of RJE program and greatly eases the introduction of modifications and correction of faults. The current program is version 3.1 of the multi-leaving emulator, which allows upper and lower case characters to be used. Software was developed to allow users of low-speed terminals to dial-in to those workstations suitably equipped with the necessary hardware, instead of directly to the Rutherford Laboratory. Full ELECTRIC facilities were made available in this way to King's College, London and the University of Surrey.

GEC 4080 Satellite Computer

A GEC 4080 computer is being set up to replace the ageing DDP-224 computer, which is now becoming difficult to maintain. The initial system comprises 128 kbytes of core, one 9-track tape unit and two 2.4 Mbyte disc drives. Basic system software is being developed, and a link (initially at 9.6 kbaud) to the 370/195 central computer is being provided. It is intended to at-

tach the 4080 as a HASP workstation, with ELECTRIC and MUGWUMP facilities available from interactive terminals and disc-to-disc file transfer. There will be a variety of VDUs and graphics terminals connected, including a new large Tektronix 4014 storage tube display and a fast Hewlett-Packard refreshed display (see below).

The initial applications software in the 4080 for both patch-up and magnet design will follow the existing system closely. It will be written in Fortran, using the compiler provided by GEC. A new interactive graphics package is planned for the 4080, to replace the IDI package on the 370/195 and the DDP-224 graphics terminals. One possibility being examined is the standard GINO-F system, extensively used elsewhere and available from the Computer-Aided Design Centre at Cambridge.

Migration and Archiving

The IBM standard system management of libraries of users' load-modules leaves unusable gaps in the disc space reserved for them, and the 'clean-up' process for recovering space is not automatically initiated when needed. Space recovery is made harder by scattered modules which are still in use but rarely change and by others which are not in use, these latter wasting space as long as they remain undetected.

To deal with these problems, some changes to the standard system were started in 1973 and have been completed and brought into full operation during 1974. The new locally-modified system is believed to be the first practical version of automatic migration and archiving. Briefly, modules still under development are separated from unchanging members, while those not used for a long time are transferred to magnetic tape, whence they can now be retrieved by the users themselves. Ordinary libraries are listed weekly, and archived libraries monthly, as a public service. About one full 3330 disc has been saved by this work, with a gain in convenience.

Paper economy

Shortage of supplies of standard computer output paper, and its rapid rise in price, led to serious efforts to cut consumption. Some compiler changes were made to reduce paper output, and default options were modified in some cases so that users have to make specific requests for printed output they would previously have had automatically.

Printing at 8 lines per inch (instead of 6) will be tried out soon, using the same type-font, but in all these economy measures the biggest single factor is the cooperation of users.

Other developments

Some minor improvements were made to the Linkage Editor and to extended precision division.

Programs are being developed to enable Rutherford users to benefit from the new FR80 graphics hardware due at the Atlas Computer Laboratory next year.

Rutherford staff have continued to take an active part in the organisations of IBM machine users (SEAS and SHARE), particularly in the OS, HASP, Performance Evaluation and Fortran committees and in the new Future Requirements Project.

USER SUPPORT

Libraries

Each major group using the 370/195 has a disk-based user library of compiled programs. During the year each of these 40 libraries has been put into the automatic migration/archiving/cleanup system mentioned above. There are in addition six libraries of commonly used routines now available.

They are:

i) AERE Library, of which a new version was introduced during the year.

ii) CERN Library, providing routines mainly for HEP users. The CERN 7600 library was received recently.

iii) Computational Physics Communications (CPC) Library, of which twenty issues have been received already.

iv) Numerical Algorithms Group (NAG) Library, which is increasingly used at Universities.

v) Rutherford Library, of useful routines mostly written locally.

vi) Scientific Subroutine Package (SSP) Library, which was provided by IBM but is no longer supported by them and is falling into disuse.

Some track chamber members of the CERN Library joined the Rutherford Library RHELIB on autocall, i.e. the programmer need take no action to have them supplied. The long-established CERN statistical package SUMX was brought up to date and made more generally available: it is heavily used by the HEP community. *(ref.RL-74-061)*

Accounting

It is vital to keep track of usage of various parts of the computer system so that, for example, future requirements can be forecast and problems of individuals or groups identified. Accounting of jobs processed is regularly done, and facilities have been extended to monitor, for example, the turn-round time for jobs, the usage of disk data sets and tapes, and utilisation of I/O channels.

Databases

The High Energy Physics database obtained from the Stanford Linear Accelerator Center was adapted for use with the IBM-supplied STAIRS information retrieval system, instead of the SPIRES software with which it was originally associated. At present STAIRS relies on another package (CICS) for many support functions, but local software is being written so that STAIRS facilities can be accessed through the Laboratory's standard MAST/DAEDALUS system.

Utilities

The Administrative Terminal System (ATS) is an IBM-supplied program for document preparation. It was made available, at one terminal only, and its facilities will be compared with those recently added to ELECTRIC. It was used by Atlas Laboratory Staff for preparing a user manual.

A general utility package OSDITTO was obtained from IBM, with a view to replacing several diverse utilities by a single-package. An early application was to provide a utility for copying multi-file tapes, which had previously been a cumbersome procedure. The STACKER facility was introduced for compressing experimental data on 7-track magnetic tapes into high-density 9-track tapes. This was applied to several experiments run at Rutherford and CERN.

Advice and Information

With the increased number of remote users the majority of queries handled by the Program Advisory Office now come from such users, either by telephone or via their terminals. Considerable effort goes into keeping them informed and discovering their plans and problems.

Documentation has concentrated on re-writing the Computer Introductory Guide and Reference Manual (CIGAR). This has proved much more laborious than anticipated because of the very considerable changes to the computer system and its interface with users which have taken place since the last edition. However, parts of the new CIGAR are now available.

COMPUTER NETWORKS

With the installation of the IBM 370/195 computer late in 1971 the Rutherford Laboratory accepted the obligation to provide a computing service to a large number of users authorised by the 195 Advisory Committee. Provision of remote facilities began in 1971 with work stations at the Institute of Computer Science in London (based on a PDP9) and the Universities of Birmingham (IBM 360/44) and Oxford (IBM 2780). As shown above, the number of workstations, the facilities available at them and the use made of them have all increased enormously within the last four years. Clearly it is popular and convenient for users to access the powerful central computer at the Laboratory from their local terminal.

As a further step in providing more flexible remote facilities, interest in computer networks developed here rapidly during 1974. Networks in which several major computers are linked together and can be accessed from remote terminals appear to offer significant potential advan-

tages to the user. Firstly, networks greatly increase the amount of terminal equipment through which a particular central computer can be accessed. For example, if the CERN and Rutherford computer systems were joined in a network, access to the Rutherford 370/195 could be gained from all terminals at CERN, instead of only from the single Rutherford workstation there. Secondly, a user may have special demands such as access to large data bases or special program packages, which are best met on one particular computer. Thirdly, physics groups in scattered localities collaborating on experiments will each have work for their local main computer but may all prefer to process collaboration data on one computer, to avoid problems such as different word-lengths.

The first experience was obtained by connecting the Rutherford 370/195 to the ARPA (Advanced Research Projects Agency) network, which links a wide range of 'HOST' computers in the United States. Access is made via the PDP-9 at the Institute of Computer Science (at University College London), which functions as a 'HOST' computer on the network but appears to the 370/195 as a HASP workstation. Through these links terminal users on the 370/195 or any of its UK workstations can log into any HOST computer on ARPA to which they have authorised access, and terminal-type access to the 370/195 here (including full use of ELECTRIC) is possible for authorised users anywhere else on the network.

The Post Office is developing its EPSS (Experimental Packet Switched Service) of fast lines and exchanges for a UK network. The Laboratory is actively collaborating in designing protocols for terminal usage, remote job entry and file transfer across this network.

FILM ANALYSIS

HPD2

HPD2 completed its spark chamber measuring programme in the first half of the year, and was heavily used for production measuring of bubble chamber film. Tests were also carried out on film from BEBC and a track-sensitive target chamber. Hardware and software changes were, in the main, made only as operational weaknesses appeared.

Operations

Spark chamber measuring comprised 35,000 events for the ISR experiment (Proposal 72) and 115,000 for the S104 experiment (Proposal 93), all on 70mm reverse-developed film. Both figures include remeasurements where preliminary analysis showed them to be necessary.

Nearly all of the bubble chamber film came from the CERN 2-metre chamber. Measurements were made for four experiments in it, as follows (figures are for 3-view events, and include remeasurements) :

Low energy K^-p (~1 GeV/c) (Proposal 108)	238,000 events
High energy K^-p (14 GeV/c) (Proposal 109)	17,000 events
π^+d (4 GeV/c) (Proposal 36)	64,000 events
$K^\circ p$ (<1 GeV/c) (Proposal 89)	16,000 events
	335,000 events

The 1 GeV/c K^-p events comprised 134,000 on film exposed in 1970 and 104,000 on 1972 film, including 19,000 scanned and pre-digitised by a collaborating group at Imperial College, The experiment will be extended into a range of lower energies with further film next year. The 17,000 high energy K^-p events were on film taken in 1972 and included 3,000 for Ecole Polytechnique. A group there is collaborating on the experiment, for which measuring is nearly finished. Film for the π^+d experiment was taken in 1970 and 1972, and measuring is nearly complete. Over 31,000 of the 64,000 events measured this year were pre-digitised at Durham University, one of the collaborators in this experiment. Five groups are collaborating in the $K^\circ p$ experiment, for which 500,000 frames were exposed late in 1972 and a similar number (with an improved K° beam) in 1974. Most of the 1972 film has been measured (there are rather few events) and a start has been made on the later exposure.

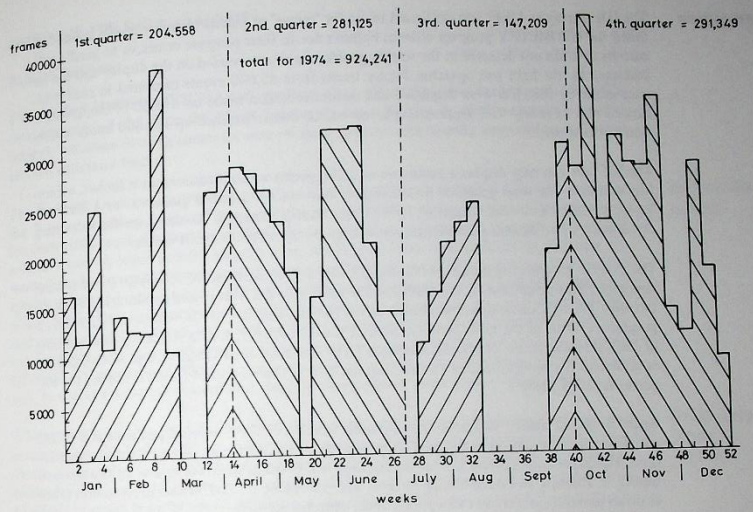

Figure 6.5. HPD2 statistics (weekly totals of frames measured): (18859)

A large sample of 9,000 events from the 1.5 metre chamber with track-sensitive target was measured in the first half of the year. The measurements were used to develop programs and gain experience in preparation for bulk processing of the film, expected next year. Pass rates through GEOMETRY are satisfactory for the complex events involved (which include at least two visible electron pairs), and 'patch-up' also appears to be satisfactory.

Several HPD records were set up this year. During October 20,000 events (on 42,000 frames) from the 2-metre chamber were measured in one week, and the year's total was nearly 345,000 bubble chamber events. The total of frames measured for all experiments in this year was 920,000. Weekly totals of frames measured appear in Fig.6.5. This intensive operation inevitably revealed some weaknesses, but despite two failures in the DDP-516 area and troubles with the laser illumination as the tubes neared the end of their nominal lives, only 16% of the 5,500 hours scheduled this year was lost for all causes of HPD2 failure.

Development

Some detailed hardware changes were made to improve operating efficiency, and a new display system was designed in preparation for operation of two HPDs in tandem. Measuring tests were made on BEBC film exposed in November 1973. There were problems in running the chamber at that time, and better film is expected in 1975. Further tests will be made when it becomes available.

Software in the DDP-516 and central computers was further developed, both for diagnosis purposes and to exploit some hardware features incorporated in HPD2. Error recovery procedures were improved so that faults in the hardware link to the central computer should require a minimum of corrective action by the HPD operator. Automatic accounting procedures were introduced at the beginning of the year and used to provide summaries of machine performance.

Tandem HPD complex

It is planned to upgrade HPD1 to HPD2 specification and operate the two machines in tandem on the DDP-516 computer. Most of the HPD1 reconstruction programme has been completed this year. The services and nearly all sub-systems of the machine were commissioned, and before the end of the year simulated data was passed through the DDP-516.

Light pen stations

The IDI display and light pen continued in use for 'rescue' of bubble chamber events which had failed the GEOMETRY program criteria. Failures due to filter program errors, or to small angle scatters or kinks not detected at the scanning table, are often revealed on the display and can be corrected by the light pen operator. Faulty tracks from 65,000 events measured in road guidance mode by the HPD were displayed and corrective action taken on 59,000 of them, with a success rate of nearly 75% representing some 40,000 events 'patched-up' in 1350 hours' operation of the system.

The IDI tube can only display a maximum of 2,000 points without unacceptable flicker, a number adequate for road guidance measurements but not for reduced guidance, so a Hewlett-Packard 1310A unit was bought in 1973. Using a small Interdata 70 computer for refreshing the display, up to 30,000 points have been written on the screen without flicker.

The present 'patch-up' system based on the IDI uses a fixed partition of 76 kbytes in the central computer, plus some core in the DDP-224 for refreshing the display and handling light-pen interrupts. The new patch-up station based on the Hewlett-Packard 1310A will be controlled by a program resident in the GEC 4080 (instead of the IBM 370/195), with refreshing and handling of the light-pen carried out by an Interdata 7/16 (instead of the DDP-224). The Interdata 7/16 is similar to the model 70 used for tests but has only the more limited facilities needed for this particular application.

Apart from the ability to display more points, which will cover reduced guidance and BEBC patch-up, the new station is designed to be much more flexible and suitable for other applications. Hardware zooming and windowing facilities will be available to the operator, also the possibility of rotating two-dimensional patterns and portraying three-dimensional structures (such as prism plots) from different viewpoints under operator control.

CYCLOPS

Measuring of film from the K13C Cambridge University/Rutherford Laboratory experiment was completed during the first half of the year. With the more flexible HPD2 available for measuring any further film from spark chambers, CYCLOPS was taken out of operation early in May and dismantled in July.

First measurements of K13C film were completed in 1973 and analysed by the spark-finding program. This showed some 27% of the 880,000 events required remeasuring, which was begun late in October 1973 and completed at the end of March 1974 after 90,000 events had been remeasured this year. Most rolls of film affected had originally been measured before all of the hardware and software improvements made to CYCLOPS last year were completed, and showed considerable benefit from remeasuring.

Calibration grids had been exposed at the start of each of the 260 rolls of film, and a large sample (generally 30 grid frames on every third roll of film) were measured, at several discriminator settings because of variable grid illumination levels.

CYCLOPS was built in 1965 to measure film from visual spark chamber experiments, and adapted subsequently to particular experimental requirements. After a slow start due to teething troubles, the change of central computer and troubles with one experiment, over two million events have been measured from four main experiments.

e-p scattering experiment (Glasgow/Sheffield) (1968-69)	100,000 events
$\Delta S=\Delta Q$ rule test in $K^\circ \to \pi e \nu$ (Cambridge/RL) (1968-70)	600,000 events
π° photoproduction (Glasgow/Sheffield) (1970-71)	400,000 events
$\pi^- p \to K^\circ \Lambda^\circ$ reaction study (Cambridge/RL) (1973-74)	1,125,000 events
TOTAL	2,225,000 events

These totals include remeasurements (eg some 27% of 880,000 events in the last experiment).

SOFTWARE FOR DATA ANALYSIS

Bubble Chambers

The standard HAZE-MATCH-EDGING program chain has continued in use for processing HPD measurements of film from the CERN 2-metre chamber. Not much program development was needed, but some filtering constants were re-tuned to give a significantly improved performance on film with faint tracks.

Reduced Guidance (ref.20)

The Reduced Guidance system was tested on a sample of film of 14 GeV/c K^-p interactions in the 2-metre chamber. In this system, one fiducial mark, all vertices and a point in a clear region for each track is pre-digitised on all views. It was sometimes found that the program established several tracks at 'clear points', and the track MATCH program was modified to eliminate unwanted duplicate tracks by comparing directions and curvatures on different views. Much of the trouble was attributed to one reference fiducial being inadequate on pre-digitising machines which do not maintain strictly reproducible film positions. The sample was accordingly re-digitised with three fiducials (allowing comparison of results with one, two or three) on two different machines. The new results will be compared with the earlier measurement (which showed a GEOMETRY pass rate of 70-75%). Improvements were also made to the track following routines, to detect small angle scatters and avoid confusion where tracks cross at small angles.

Track-sensitive target (ref.21)

A large sample of film from the Rutherford 1·5 metre chamber with track-sensitive target was measured on the HPD, and development of the chain of processing programs has continued. Tracks are pre-digitised in the Road Guidance mode, with the second of the three points per track placed where the track enters the target wall (for those which do so). Only the Rutherford EDGING program is being used for filtering, as the CERN HAZE was considered unsuitable for tracks passing through the target walls, and it has been modified to break the road into separate sections (before and after the walls) and search for a track in each. Short electron tracks are often very hard to filter, and if fewer than three master points are generated the pre-digitised points are substituted. The GEOMETRY pass rate at present is about 50% for events with an average of 9 constituent tracks.

HYDRA system and large chambers

The CERN programming system HYDRA (version 3.11) has been installed and tested on the central computer. There is no intention of changing the normal program chain used for 2-metre chamber film analysis but BEBC processing will make use of the CERN LBCG (Large Bubble Chamber Geometry) program in HYDRA.

No HPD measurement of BEBC film has been processed yet, but as a test two BEBC events were crudely measured on a Mangio-Spago pre-digitising table, using 20 fiducial marks on each of 3 views. Several changes, in the on-line control program for the pre-digitisers and elsewhere, were required to handle these events, which were then reconstructed by LBCG using appropriate HYDRA processors. There were problems with optical constants and distortions, as expected, whose solution awaits developments at CERN, but the results were reasonably promising.

Kinematics

The changes in treatment of convergence and hypothesis rejection in the Kinematics program have been completed, and the new version is in production use for several experiments. A new Kinematics manual is being prepared.

Spark Chamber and Electronic Experiments

The main work this year was the further analysis of measurements for the K13C multi-gap spark chamber experiment made on CYCLOPS during 1973-74. All measurements not already examined were processed by the spark-finding program, which showed some 75 rolls of film should be re-measured. This was done, usually with significant benefit.

Having established sparks in three dimensions, production processing with the track-finding program began and has run on 180 rolls so far (about 70%). It links sparks into linear tracks, and is usually found to need at least two passes. The first checks internal consistency of grid parameters and alignment of the chambers and establishes the clearing field correction, all on a roll-by-roll basis, and the second then finds tracks successfully. A program to check error parametrization of the tracks was developed. It fits pairs of lines to vee decays, and shows how the errors should be related to the angle and mean width of the lines.

Similar analysis programs are being developed for the π12 experiment, which uses optical chambers and some with magneto-strictive read-out.

Assistance has been given to two experimental groups (at CERN Omega spectrometer, Proposal 88 and ISR Proposal 72/129) in providing suitable versions of the tape indexing and general book-keeping system initiated by the K13C Group. Software for initial stages of data analysis has also been developed for the ISR experiment, and for the π9 polarized target experiment (Proposals 81/101).

The library building

TECHNICAL SERVICES AND ADMINISTRATION

7. Technical Services and Administration

RADIATION PROTECTION

Operations and Dosimetry

During 1974, as in previous years, the Laboratory has maintained standards of radiological safety well within the limits laid down by national and international bodies. In particular, the results of personal dosimetry show that no one working at the Laboratory exceeded the permitted levels for either external radiation or internal contamination.

Shielding

The Radiation Protection Group investigates and gives design advice on a wide range of shielding problems. During the year these have included studies of the protection required against neutrons, X-rays and gamma radiation that will be produced by the new 70 MeV injector, assistance in the design of the new high intensity beam line complex in Experimental Hall 1, the use of a directional detector system in investigating possible weakness in existing shielding, and computation of the muon shielding that would be required for extension of the EPIC project to 200 GeV protons.

Instrumentation

Accelerator developments and the obsolescence of existing equipment have led to detailed examination of improved techniques for the measurement of strong radiation fields and for handling the resultant data. In common with CERN and FNAL, we have found the combination of digitising electrometers with ionisation chambers attractive for use with pulsed accelerators and particularly suitable for modern methods of data transmission and presentation.

Induced radioactivity

The gamma spectrometry service has continued to operate for straightforward identification and quantification of radio-isotopes. It also provides the reference standard for the measurement of Nimrod beam intensities by the foil activation method and has been applied to beam distribution studies which relate to the efficient operation of Nimrod in terms of beam control and the reduction of radiation damage.

GENERAL SAFETY

In research the ideas pursued often require the design of special apparatus or the unusual application and modification of standard equipment. In many instances safety can be achieved in the design of apparatus, however, where this is not possible, for example with experimental high voltage apparatus, calculated and acceptable risks can be taken after thorough assessment by using carefully controlled working procedures. The publication of guide lines in the form of safety Codes of Practice plays an important part, hence the series of Codes on many subjects which have been developed over the years, are very necessary at the Laboratory.

Vigilance in looking for potential hazards and minimising them is the responsibility of staff concerned with the work. The Laboratory's Safety Group have an important role in assessing such hazards and communicating information about dangerous substances and activities as well as in controlling the safety aspects of standard plant and apparatus in conventional situations. During the year special attention was given to the requirements for the safe use of isobutane and methylal in spark chambers and proportional counters. Information on the hazards of these two substances was published and discussions with users initiated modifications which resulted in improved standards of safety. The safety aspects of mechanical handling in the new 70 MeV Injector and also with the hydrogen and electrical safety of the project were studied.

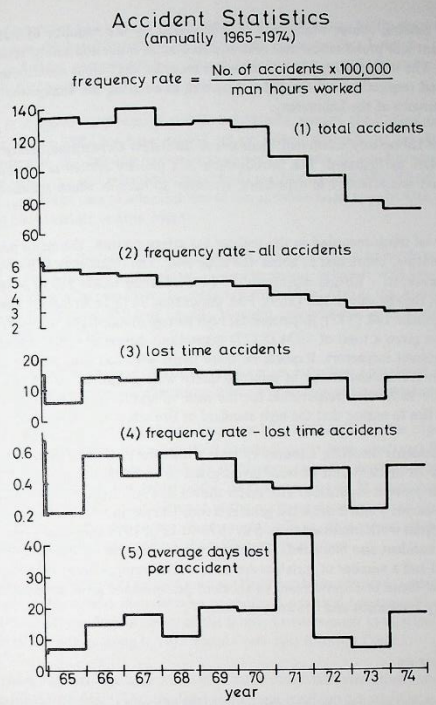

Figure 7.1. Review of Laboratory accident statistics: (18858)

A paper was presented at a safety conference for member states of CERN at Geneva in September and the Laboratory continue to be represented on the committee of the Oxford and District Accident Prevention Group. A seminar on fire precautions was organised by this group at the Laboratory. New health and safety legislation was published towards the end of the year and was being studied to consider its impact upon the work of the Laboratory. Safety services for the adjacent Atlas Computer Laboratory were continued.

The established methods of communicating safety requirements and information by means of mandatory Safety Notices, Safety Displays and Safety News sheets continued during the year. One new Safety Code was issued and two were revised. Sections of the Safety Handbook were also revised and re-issued.

The basic safety training course which had been attended by the majority of staff has been modified in content and presentation and re-introduced as an induction safety training course for new entrants. The new course utilises a videotape recorder and colour monitor and includes practice in artificial respiration and fire fighting as well as covering the emergency procedures and safety arrangements of the Laboratory.

Safety tours of the Laboratory continued; members of the Safety Committee, Safety Group and Fire Prevention staff participated. The introduction of a priority system in conjunction with local administration was effective in expediting attention to hazards which required urgent attention.

The total number of items recorded in the register for safety control, the major part of which was required by statute, continued at about the same level. The totals were as follows with the 1973 figures in brackets:– Lifting machines 375 (405); Lifting tackle 2535 (2448); Pressure vessels 939 (889); Safety valves 309 (289); Fire prevention 56 (52); Breathing apparatus and other safety equipment 148 (147); Experimental high voltage installations 381 (420). These registered items were given a total of 7974 (8377) inspections during the year, either by Safety Group staff or contract inspectors. Reports on these items were recorded and remedial action on defects and on recommendations to improve safety were progressed as necessary. Liaison continued with the authorities responsible for the issue of statutory certificates for means of escape in event of fire to ensure that the high standard of fire safety was being maintained.

The number of accidents involving Laboratory staff which were reported during the year was 73 compared with 78 in 1973 and all were investigated to ascertain the cause and to make recommendations to prevent repetition. The graph shown in Fig.7.1 provides statistics over the past ten years and curves 1 and 2 show the general trend. The number of accidents which resulted in loss of time from work increased from 6 in 1973 to 13 in 1974 and the average number of days lost for each accident also increased. These latter figures are a measure of severity of injury, the sample is small and a number of variables are involved, however, a fairly stable average is apparent. The general trend of improvement in accident performance gives no grounds for complacancy and safety assessment and control continues.

CHEMICAL SERVICES

General on-site chemical services are provided in the fields of water treatment, corrosion control, chemical analysis, the chemical coating and cleaning of components and electroplating work that cannot be done economically by commercial platers.

The many high purity water circuits, associated with cooling of the Nimrod magnets and ancillary equipment, require a frequent routine test programme to ensure that the high quality required is being maintained. Notwithstanding this control, problems still arise from the deposition of copper on the inside surfaces of rubber tubing included in the circuit and this eventually results in unacceptably high earth leakage currents. Tests are being conducted to understand the cause and mechanism of this problem. Corrosion problems arising in any cooling water circuit are also fully investigated.

Chemical identification techniques are applied to many substances, as a means of quality control checks on metals or to analyse contaminants in vacuum systems and oils.

SCIENCE RESEARCH COUNCIL WORKS UNIT

During 1974 the Council Works Unit extended its field of operation and it now includes the Royal Observatory Edinburgh. It has also continued with its responsibilities for work on design, construction and maintenance items at the Atlas and Appleton Laboratories, the Chilbolton and Winkfield Observatories, the Royal Greenwich Observatory, the London Office and the Rutherford Laboratory.

Atlas Computer Laboratory

At the Atlas Computer Laboratory the successful completion has taken place of a new extension. This consists of a building linking the two main buildings with a Lecture Theatre, Entrance Hall, offices and toilet accommodation. This extension is on two floors and covers an area of approximately 600 square metres.

Appleton Laboratory, the Chilbolton and Winkfield Observatories

Design work at Appleton Laboratory and its outstations, namely the Chilbolton and Winkfield Observatories, during 1974 has been carried out on several schemes. At the Appleton Laboratory an extension to the existing computer facilities for a new air conditioning unit was completed. Diesel generator sets were installed at both the Appleton and Winkfield Sites to guarantee electrical supplies in case of a breakdown in the main electrical supply. One of these was for the successful UK5 satellite control room.

A new heating plant, including boilers, pumps and individual building heating control systems was installed at the Appleton Laboratory. This scheme was designed with energy conservation in mind, employing weather sensitive, temperature controllers. Also at the Appleton Laboratory an extension to the Balloon Payload Facility is under construction. This work is due for completion in the Spring of 1975.

The Chilbolton Observatory near Andover will have an extension completed in the Spring of 1975. This consists of additional laboratory, office and storage accommodation.

A design for a new computer building to house an ICL 1904A Computer together with roadworks, associated landscaping and a new SEB Substation has been produced for the Appleton Laboratory. The building consists of a single storey structure, 'T' shaped in plan for ease of extension. The area of the building is just under 1000 square metres. It is attached to the existing buildings by a link entrance and it is situated at the north west corner of the site. The accommodation consists of a computer room, plant rooms, offices, data preparation areas, terminal rooms, engineers and tape store rooms and ancillary support areas.

The Integrated Environmental Design Concept (IED) has been adopted. This is a process of design applied to buildings and their services providing a practical approach to optimising three factors: (i) The quality and consistency of the internal environment in relation to the functions and the needs of the people using it. (ii) Capital Costs. (iii) Running Costs.

The construction consists of cavity walls with brick outer skin and blockwork inner skin, the cavities being filled with foam. The anodised aluminium windows are small in area recessed back to the inner face of the brickwork to reduce the direct solar gain and double glazed to reduce the heat loss. The roof is concrete with a thick layer of polystyrene under an asphalt finish. Great attention has been given to the thermal properties of the building resulting in low thermal gains in the summer and low losses in the winter with good thermal inertia to act as a stabilizing influence. The type of construction used also assists in the reduction of aircraft noise which is a problem on the site.

For the computer room and its associated areas air conditioning is required to meet the specified levels of temperature and relative humidity. With the fact also that the total energy input in the form of electrical power to the computer exceeds the heat losses from the whole building for most of the year, heat recovery forms the basic part of the design. The recovered heat will be used for re-heat purposes on the computer air conditioning and for heating the office area air conditioning. Separate air conditioning systems are used for the computer and office areas to comply with fire regulations and to allow for smoking in the offices. Electricity is the only energy source used on this building, and the heat recovery system can be shown to give an annual saving in the running costs compared with conventional systems.

A new transformer will be erected adjacent to the computer building to supply the computer via a new motor alternator set. Fluorescent lighting will provide illumination levels to the current IES guide. Emergency lighting is also incorporated where needed by means of self-contained automatic units.

Fire detection is also an important factor in the design of a computer building and this is integrated with an automatic fire extinguishing system using a Halon 1301 installation in the computer room. The design also incorporates a vacuum cleaning system which covers the computer room.

The computer building is now under construction and it will be completed in early 1976.

Work has now commenced at the design stage on further development on the Appleton Laboratory Site. This will consist of offices, laboratories, conference rooms, lecture theatre, entrance foyer and a Balloon Integration Area. The total development covers an area of approximately 4000 square metres.

The Royal Greenwich Observatory

At the Royal Greenwich Observatory, Herstmonceux, a new car park is planned together with preparations for their Tercentenary celebrations.

An interesting structure designed for the Observatory was a thermal shield wall round the Coude Room of the Isaac Newton Telescope. This was to prevent solar gain reaching the interior and affecting the optical equipment structure. In parallel with this thermal wall design, which was to be built in either brick or concrete, was an experiment insulating the structure of the optical equipment with polystyrene. The experiment showed that there would still be considerable thermal movement affecting the equipment.

The Royal Observatory Edinburgh

At the Royal Observatory, Edinburgh, it is planned to replace the existing heating in the main building consisting of electrode boilers with gas fired boilers to achieve greater efficiency, economy in running costs and continuity of heating in case of interrupted electrical supply. Also planned are extensions to their workshops and to their temporary office accommodation and the installation of a diesel generator set to give a guaranteed electrical supply.

London Office

Plans are now being prepared for major alterations to a building in Swindon to house a number of London Office staff.

Rutherford Laboratory

At the Laboratory the formal opening took place in November of the new library. This is a building which spans the roadway, linking buildings R1 and R25. It is essentially a concrete structure with arched beams faced with exposed aggregate. The windows, on the east side, are of solar control glass and the roof has a shallow pitch and is metal decked.

The year also saw completion of the new building to house the 70 MeV Injector for Nimrod.

Figure 7.2. The East side of the new library building: (18072)

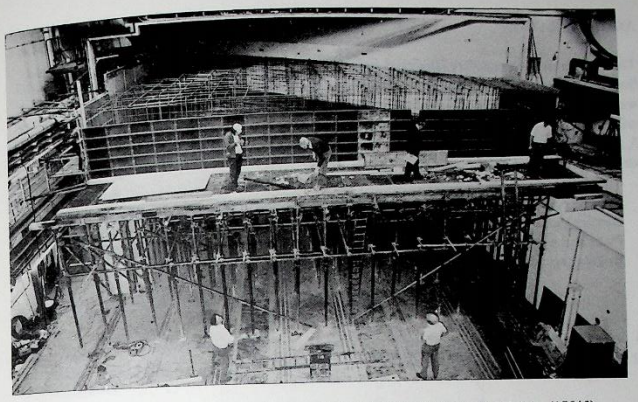

Figure 7.3. Construction work in progress on the concrete blockhouse in Experimental Hall 1: (17545)

An interesting structure to be erected at the Laboratory during the year was a concrete blockhouse in building R6. This consisted of two concrete walls and a flat concrete slab, simply supported on the walls approximately 5 metres above ground level. The slab consisted of approximately 250 cubic metres of concrete in one continuous pour. This is believed to be one of the largest ever pours of its type in this country.

During the year some preliminary design work has been carried out on the EPIC Project.

The Coseners House at Abingdon has major alterations planned. These mainly consist of an extension to the main house to provide additional conference, storage and toilet facilities.

In 1974, for the first time since being set up in 1972, the Council Works Unit work load on design and construction has exceeded £1 million per annum.

Figure 7.4. The West side of the new library building: (17747)

ADMINISTRATION

Finance

The Laboratory expenditure (financial year 1974/75) was £10·87 million, of which £1·37 million was for capital (including £0·53 million on the new injector for Nimrod) and £9·50 million was recurrent. Corresponding figures for 1973/74 were £9·48 million, £1·43 million and £8·05 million.

A brief analysis of the net expenditure is given below, with corresponding figures for the previous year shown in brackets.

	£ million
Staff expenditure (salaries and wages, insurance, superannuation, etc.)	4·35 (3·70)
Research and development (see below)	5·15 (4·35)
Plant and equipment	1·16 (1·18)
Building works	0·21 (0·25)
Total	10·87 (9·48)

A proportional representation of the breakdown of the research and development into divisional and other main components is shown in the pie chart.

Figure 7.5. Breakdown of the £5·15 Million R & D expenditure: (18857)

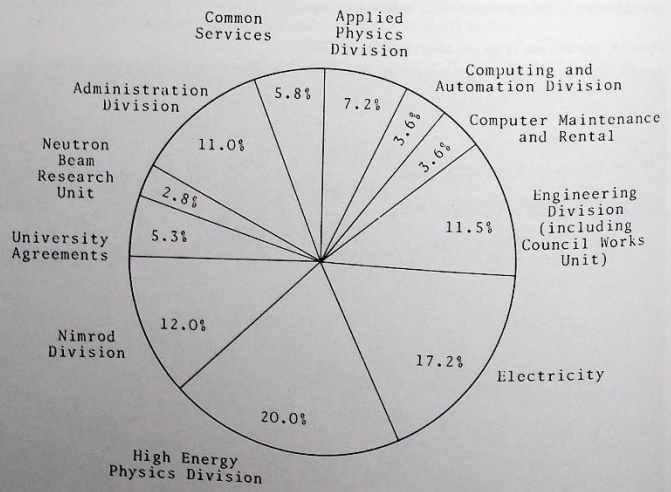

The staff position at the beginning and end of the year.

	Opening Strength 1.1.74	Changes during 1974: Gains	Changes during 1974: Losses	Closing Strength 31.12.74
NON INDUSTRIAL				
Senior and Banded Staff	27	4		31
Science Group	242·5	37	25·5	254
Professional and Technology Group	330·5	14·5	15	330
Administration Group	74	17·5	16	75·5
Research Associates	55	19	29	45
Non-Techs and Stores	37	1	2	36
Librarian	1	0	0	1
Secretarial and Typing	30	12	12	30
Photographers	3	0	0	3
Photoprinters	5	0	0	5
Machine Operators	58·5	13	18	53·5
Hostel Manageresses	2	0	0	2
Telephone Operators	2	1	1	2
Total Non Industrial	867·5	119	118·5	868
INDUSTRIAL				
Craft	167	22	34	155
Non-Craft	109	27	22	114
Apprentices	20	7	7	20
Total Industrial	296	56	63	289
GRAND TOTALS	1163·5	175	181·5	1157

Staff Numbers

The figures listed under "changes" include new entrants, resignations and promotions. Staff on sandwich courses, and those working part-time are counted as half.

Staff numbers continued to decline; the net decrease since 31 December 1970 has been 95 (7·5% of those in post at that date).

Staff Relations

Regular communication between the local Staff Side and management was maintained by quarterly meetings of the local Whitley Committee, including the Annual Meeting chaired by the Director. Additional joint working parties and meetings with management were convened to deal with such subjects as accommodation, fuel economy and the use of contract staff, thus providing further opportunities for full and frank discussions on staff conditions. Staff Side expressed dissatisfaction at certain aspects of the use of contract staff at a meeting with management and the Staff Side members continued to monitor the situation.

Staff Side members continued to take a keen interest in the EPIC Project and the proposal to set up with AERE a joint Laser Laboratory.

Staff Side showed great interest in the progress and commissioning of the new library, injector building and the Atlas Computer Laboratory extensions and welcomed the opportunity of participating in discussions on the accommodation provided by these schemes.

The Staff Side continued to provide members on the Restaurant, Safety and Staff Suggestions Committees and also to participate in the management of the Laboratory Death Benefit Scheme.

Regular three monthly meetings of the Local Joint Consultative Committee continued to provide communications between management and industrial staff. Special meetings of this body were held to discuss the use of contract labour at the Laboratory; a "failure to agree" was recorded and the matter referred to the Council's Joint Negotiating Committee.

Shop stewards representing the various Trade Unions recognised at the Laboratory continued to participate on tne Restaurant, Safety and Staff Suggestions Committees, thus providing further opportunities for exchanges of ideas between staff and management.

Trade Union representatives also participated in the management of the Laboratory Death Benefit Scheme.

Training

The academic year 1973-74 showed another decline in the level of day-release and evening training in the Laboratory, the total number of concessions being 64 compared with 76 last year. However concessions for Open University courses in technical subjects rose to 9 and the Open University is now an important source of training for Laboratory staff.

The success-rate in examinations has remained high; the overall success-rate for the 55 students taking day-release, and Open University courses was 89%. The 25 Craftsmen who sat Higher National Certificate and CGLI examinations achieved a pass-rate of 96%. Three members of staff received day-release concessions for specialist post-graduate courses and two are registered research students.

Only one member of the permanent staff of the Laboratory is now attending a sandwich course at a University. This student has an SRC Bursary to attend the Honours Degree course in Mechanical Engineering at Brunel University.

Two hundred and twenty three members of staff attended short courses on various technical and management subjects, 50% of these courses being run by AERE, 15% by SRC or CSD and 35% by a variety of other educational, professional and commercial bodies.

The Laboratory has continued its arrangements for oral French tuition for staff who have to visit ILL and CERN. The original group, now somewhat depleted by transfers and resignations, continued its studies two mornings a week at the Abingdon College of Further Education. A second group started at South Berkshire College of Further Education in September 1973 and a third group started at Abingdon after Easter 1974. In addition 3 senior members of the Laboratory staff were provided with French instruction at the Laboratory by a local private organisation specialising in this type of training.

The Laboratory has continued to collaborate with AERE in the recruitment and training of Craft Apprentices. There were 18 craft apprentices in training at the end of the academic year 1972-73, 4 completed their "time", 4 were recruited and 3 resigned during the period so the total at the end of the year 1973-74 was 15. All 4 craft apprentices who completed their training joined the Laboratory. The two Student Engineers who joined the training scheme in January 1973 went to University in October 1973 and both satisfactorily completed their first year studies. A third Student Engineer joined the scheme in January 1974 and completed 5 months of basic craft training in the AERE Apprentice School, followed by 4 months of practical training in the Rutherford Laboratory, preparatory to going to University in October 1974.

There were comparatively few internal training activities within the Laboratory during the year. In February 1974 a half day Management Seminar was attended by 13 Senior Staff and a similar seminar was attended by 16 staff who report directly to Division Heads and Group Leaders. The Laboratory was host establishment to SRC Senior and Junior Induction Courses.

The Laboratory provided industrial training during the year for 45 college-based sandwich course students, bringing the total over the last 14 years to 461. In addition Administration Division provided the usual two weeks of practical office training for 9 Business Studies Students from Abingdon College of Further Education.

General Administration

There has been a continuing increasing demand for administrative services during the year. With the high cost of housing in the area, full use was made of the Laboratory's furnished and unfurnished property.

The Neutron Beam Research Unit and part of Engineering Division were re-accommodated in Building R20 following the re-housing of the library in Building R61 thus continuing the process of more effective grouping of Laboratory staff.

In early July, Administration Division staff were heavily involved in the supplying of services to the XVII International Conference on High Energy Physics, held at Imperial College, London. An attempt was made to spread staffing needs across the whole of the Division so as to cause the least disruption of work at the Laboratory.

Approval was obtained from Council for major alterations to be carried out at The Cosener's House to enable it to be used more effectively as an SRC conference centre.

Meetings and Schools

The Cosener's House has been well used during the year to provide conference facilities, particularly for Council and Board meetings, week-end Conferences, Summer Schools and Training Courses.

Figure 7.6. View of the reading room in the new library: (18455)

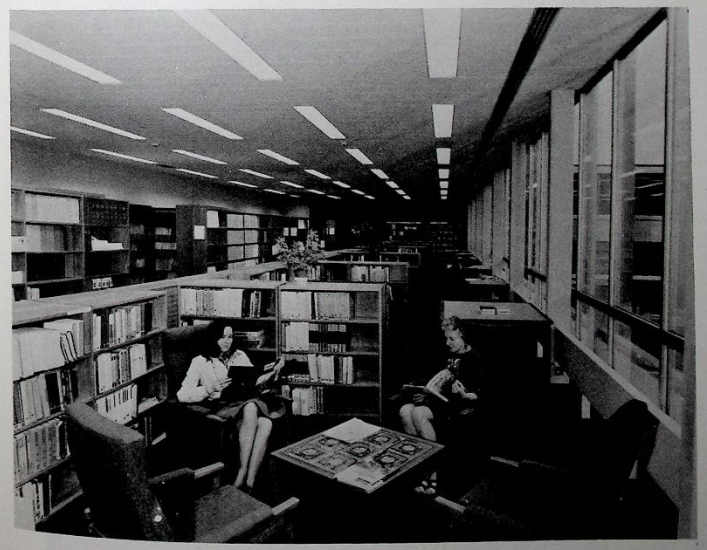

Meetings were held at the Laboratory on: Theoretical Physics-Annual Conference (2–4 January); Conference on Quantum Mechanics (15–16 February); NBRU Meeting on Neutrons and Biology (18 April); Exotic Atoms – Institute of Physics Meeting (19 June); EPIC – Town Meeting (18 July); Summer School for Experimental Physicists (9–27 September); the Laboratory also provided financial support for the Summer School for Theorists held at Durham University (8–12 September); HPD Annual Conference (1–2 October); Meeting of the Nuclear Physics Board (26 November).

Meetings were held at The Cosener's House on: Council Meeting (19–20 March); Deep Inelastic Phenomena (4–5 May); SEAS Working Party (30 September – 4 October); EPIC (2–6 December).

Visits

The Nuclear Physics Board visited the Laboratory on 25 – 26 November. During the visit the new Library was officially opened by Dr T G Pickavance, CBE, the first Director of the Rutherford Laboratory. The Chairman of the Nuclear Physics Board, Professor W E Burcham, FRS, presented Dr Pickavance with an inscribed tray as a momento of the occasion and Mrs Pickavance with a bouquet of flowers.

Parties of visitors taken on conducted tours of the Laboratory during the year totalled 660.

International Conference

The Laboratory organised the XVII International Conference on High Energy Physics, this being the first occasion that a conference in this series has been held in this country. The conference took place from 1 to 10 July at Imperial College, London with approximately 800 delegates, from more than forty countries. Administrative staff were provided by the Laboratory. The Proceedings of the Conference were published by the Laboratory in November 1974.

Figure 7.7. Dr T G Pickavance CBE opening the new library: (18060)

Appendix A: Publications

RUTHERFORD LABORATORY PUBLICATIONS AND REPORTS

Proceedings of the XVII International Conference on High Energy Physics, London, 1 to 10 July 1974.

Rutherford Laboratory Annual Report 1973.

RL-73-016 Study of narrow mesons near their thresholds. D M Binnie, L Camilleri, N C Debenham, A Duane, D A Garbutt, J R Holmes, W G Jones, J Keyne, M Lewis, I Siotis, P N Upadhyay, I F Burton, J G McEwan

RL-73-037 Pion-nucleus coupling constants for ^{7}Li and ^{9}Be. G T A Squier, M E Cage, G J Pyle, A S Clough, G K Turner, B W Allardyce, C J Batty, D J Baugh, W J McDonald, R A J Riddle, L H Watson

RL-73-045 High transverse momentum hadron jet production in a gluon-exchange model. I Montvay

RL-73-048 Search for superheavy elements and actinides produced by secondary reactions in a tungsten target. C J Batty, A I Kilvington, J L Weil, G W A Newton, M Skarestad, J D Hemingway

RL-73-100 Gauge models without charmed hadrons. G G Ross, R K P Zia

RL-73-138 HASP multileaving workstation support in the GEC 2050. C J Adams, A G Waters

RL-73-146 The use of physics literature: chapter on nuclear physics. A P Banford, E Marsh

RL-73-155 Tests of ππ phase determinations. D Morgan

RL-73-159 Nimrod operation and development - quarterly report - July 1 to September 30 1973. D E Gray

RL-74-001 Calculation of energy loss figures for a twin detector telescope system, using a Wang 363 desk calculator. D C Adams

RL-74-002 Dosimetry by charge decay of polymer Thermoelectrets. M D A King

RL-74-003 The 10.5" diameter scintillation detector. R Simpson

RL-74-004 Line control procedures for asynchronous and synchronous serial communications links. J F MacEwan

RL-74-006 The high speed serial data link for the IBM terminal computer. J MacEwan

RL-74-007 Character multiplexors for satellite computers attached to the 370/195 computer. J MacEwan

RL-74-012 Computing and automation division quarterly report: 1 October 1973 - 30 December 1973. W Walkinshaw, A T Lea

RL-74-013 Pion nucleus total cross-sections from 88 to 360 MeV. A S Clough, G K Turner, B W Allardyce, C J Batty, D J Baugh, W J McDonald, R A J Riddle, L H Watson, M E Cage, G J Pyle, G T A Squier

RL-74-014 EPIC updated: variable damping and tunes in the $e^{\pm}$ ring. G H Rees

RL-74-015 EPIC transfer lines. B D Jones

RL-74-016 Polarisation measurements in $\pi^{+}p$ elastic scattering from 0.60 to 2.65 GeV/c. J F Martin, J C Sleeman, R M Brown, P J Duke, W M Evans, E S Groves, R E Hill, W R Holley, D P Jones, J J Thresher, M W Tyrrell

RL-74-017 The inclusive reaction $K^{-}p \rightarrow pX$ at 14.3 GeV/c. S N Tovey, K Paler, T P Shah, R J Miller, J J Phelan, B Chaurand, B Drevillan. J M Gago, G Labrosse, R Lestienne, R Salmeron, R Barloutand, A Borg, D Denegri, F Pierre, M Spiro

RL-74-018 Some operational characteristics of the π12 1mm spaced MWPC beam chamber. J E Bateman, J F Connolly

RL-74-019 Preliminary results on the characteristics of a multiwire proportional chamber with 1mm wire spacing. J A Blissett, T A Broome, J C Hart, M L Mallary, N Middlemas, A G Parham, B T Payne, T W L Sanford, T G Walker

RL-74-020 Reports issued by the Rutherford Laboratory, 1960-1973. E Marsh

RL-74-021 Gas evolution from plastic materials by high energy radiation. J T Morgan, G B Stapleton

RL-74-022 Triple-Regge analysis of pp → pX and some related phenomena - a detailed study. D P Roy, R G Roberts

RL-74-023 Switching magnet profile and dimensions. A G A M Armstrong

RL-74-024 Hot or cold bore for a superconducting EPIC ring? J R J Bennett

RL-74-025 Vacuum requirements for the proton ring of EPIC. J R J Bennett

RL-74-026 Eddy currents in the vacuum chamber of the EPIC Electron ring. J R J Bennett

RL-74-027 Proceedings of a seminar on bookkeeping systems for high energy physics experiments. R A Rosner

RL-74-028 Nimrod operation and development - quarterly report - October 1 to December 31 1973. D E Gray

RL-74-029 1.5 Metre cryogenic bubble chamber operation 1973. T G Coleman

RL-74-030 Beam toroid current monitor system for Nimrod 70 MeV injector project. NPAG Design Specification No. 42. J F Connolly, A S Gilby

RL-74-032 Obtaining IBM 1130 disk monitor source coding from the IBM optional materials tape. B H Bracher, P C Thompson

RL-74-033 K17 - a seperated low momentum kaon beam at Nimrod - an interim report. C J Batty, M K Craddock, C J Reason, R A J Riddle, R E Walsh, D H Worledge, M Eckhause, N Berovic, G J Pyle, G T A Squier, A S Clough, G K Turner

RL-74-034 A dipole pomeron Ansatz. R J N Phillips

RL-74-035 A study of the variation of the neon concentration during an experiment with a track sensitive target. J G V Guy, J W G Wignall, C M Fisher

RL-74-036 Feasibility studies on the production of metallic thermal neutron polarizing filter materials containing polarized Samarium - 149 nuclei. W G Williams

RL-74-038 Proceedings of the 1973 School for Young High Energy Physicists - Rutherford Laboratory - July 1973. H Muirhead

RL-74-039 Mueller-Regge analysis in the central region. T Inami

RL-74-040 The third order correction to the binding energy of the He^4 nucleus. I Ulehla, N T Nguyen

RL-74-041 The work of the Rutherford Laboratory in 1973. J R Smith, F M Telling (editors)

RL-74-042 A Bootstrap loader for HASP multileaving workstations. A G Waters, C J Adams

RL-74-043 An interface to connect a CMD disk drive to an IBM 1130 computer. J G Watson

RL-74-044 Communications between programmers and computer operators on the system 195. A R Mayhook

RL-74-045 SPINE: A multiprocessing data acquisition system for a high energy physics experiment. R P Hand, D Maden

RL-74-046 S-channel models for the Pomeron R D Peccei

RL-74-047 High energy electron selection by means of X-ray transition radiation. J E Bateman

RL-74-048 The proton duoplasmatron ion source for the preinjector of the new injector for Nimrod. R G Fowler, R Sidlow, G Soulby, N D West

RL-74-049 Programming the formula evaluator. C MacLean, G McPherson, P Wilde

RL-74-050 Solvable one dimensional models of particle production. R D Peccei

RL-74-051 Condensed matter research using pulsed neutron sources. A C Wright, R N Sinclair (editors)

RL-74-052 Design study for beam line dipoles (Superconducting). A D McInturff

RL-74-053 Longitudinal instabilities in EPIC ($e^{\pm}$). H G Hereward

RL-74-054 Reference numbering system for EPIC lattice components. B G Loach

RL-74-055 New injector for Nimrod, Beam diagnostics, energy ramping measurements. F J Swales

RL-74-056 $|\eta+-|$ and the reaction $e^+e^- \to K^oK^o$ at the ϕ -resonance. G V Dass

RL-74-057 The feasibility and applications of a 60Å time of flight spectrometer. B C Haywood, J B Hayter, J W White

RL-74-058 Vacuum outgassing in the electron ring of EPIC. J R J Bennett

RL-74-059 MNLISTPR: a list processing package for flexible storage of data. M J Newman

RL-74-060 Rough digitising system: Introduction to 1130 software. B H Bracher, J F MacEwan, A G Waters

RL-74-061 SUMX on the Rutherford Laboratory central computer. P J Hemmings, G R Donaldson

RL-74-062 Longitudinal head-tail effect by the bunch length variation method. H G Hereward

RL-74-063 Is the O^+ nonet respectable? D Morgan

RL-74-064 EPIC main ring: the cheapest current density. A G Armstrong

RL-74-065 Deep inelastic structure functions of the photon. R P Worden

RL-74-066 HENRY: a program for computing self and mutual inductances of an array of solenoids. D Barlow

RL-74-067 Development and testing of a prototype superconducting RF separator. A Carne, R G Bendall, J R J Bennett, B G Brady, J A Hirst, J V Smith

RL-74-068 What a dominating ρ and weak exotics can do for ππ scattering near threshold. M R Pennington

RL-74-069 CRYSTAL operators' guide, W S Chapman, R Bairstow, R Hatley

RL-74-070 CRYSTAL programmer's guide. W S Chapman, R Bairstow, R Hatley

RL-74-071 EPIC main ring quadrupoles. A G A M Armstrong

RL-74-072 Computing and Automation Division quarterly report, 31 December 1973 - 31 March 1974. W Walkinshaw, A J Oxley (editors)

RL-74-073 A study of the Q enhancement in the reaction $K^-p \to K^-\pi^-\pi^+p$ at 14.3 GeV/c. S N Tovey, J D Hansen, K Paler, T P Shah, J J Phelan, R J Miller, S Borenstein, B Chaurand, B Drevillon, G Labrosse, A Borg, D Denegri, Y Pons, M Spiro

RL-74-075 Design considerations for a rapid cycling bubble chamber suitable for operation at the CERN SPS. B R Diplock, W Turner, P R Williams

RL-74-076 Fortran programs for 3 saddle wound dipole magnets, for a Tokamak D-magnet and for the geometry of the constant perimeter end. H I Rosten

RL-74-077 A method for the calculation of the magnetostatic field from a wide class of current geometries. H I Rosten

RL-74-078 The scientific case for EPIC. G Manning, G Ringland, R L Sekulin, M R Harold, F Foster

RL-74-079 Sum rules for inverse ππ scattering amplitudes. A K Common, M R Pennington

RL-74-080 A method of testing multiwire proportional chambers by glow discharge/photographic techniques. J B Marsh, J E Boon, K H Souten, B O'Hagen

RL-74-081 New injector for Nimrod, Beam diagnostics - Pre injector emittance measuring equipment. F Swales

RL-74-082 A fixed sumrule in photon-photon scattering. R P Worden

RL-74-083 EPIC machine design study group of the Rutherford and Daresbury Laboratories: design and status of EPIC. J R J Bennett, H C Brook, M H R Donald, D A Gray, M R Harold, J D Lawson, J D Lewin, B G Loach, J R M Maidment, G H Rees, P F Smith, W A Smith, E A Hughes, N Marks, B E Poole, N W Poole, V P Suller, G Saxon, T Swain, K Tarry, D J Thompson

RL-74-084 Multiparticle production and the asymptotic behaviour. R D Peccei

RL-74-085 Water cooling for the 70 MeV injector. K H Roberts

RL-74-086 Users guide to Syncost (PRC 37-01) and EPICOS: a general purpose cost estimating programme for IBM 360/370 computers. P R Chadwick, B G Loach

RL-74-087 Differential cross-sections for elastic π^-p scattering at 16 momenta between 996 MeV/c and 1342 MeV/c. P C Barber, T A Broome, B G Duff, F F Heymann, D C Imrie, G J Lush, E N Mgbenu, K M Potter, L A Robbins, R A Rosner, S J Sharrock, A D Smith, R C Hanna, P R Pitts, E J Sacharidis

RL-74-090 EPIC main ring dipole magnets. A G A M Armstrong

RL-74-091 Argonne- CERN-Rutherford-TST-Colaboration: report on tests. J H Foster, E W Fitz-Harris

RL-74-092 Experimental limits to the $\pi^0 \rightarrow e^+e^-$ rates and their consequences for a direct electron-hadron coupling. J D Davies, J G Guy, R K P Zia

RL-74-093 Calculations of the performance of various 'cold neutron sources' for a high flux beam reactor. P Carter, P D Hey, R W Newport, G C Stirling

RL-74-094 A low mass cylindrical spark chamber with capacity read-out. G T J Arnison

RL-74-095 Rough digitising system: 1130 - 360 transfer programs. B H Bracher, J F MacEwan A G Waters

RL-74-096 Liquid hydrogen-deuterium targets: a guide for the design, manufacture and testing of target flasks. J R Stokoe, F Row

RL-74-097 Outline of EPIC cooling systems. P T J Goodyer, H C Brooks

RL-74-098 Physics with an electron positron storage ring of beam energy E = 14 GeV. EPIC working party 1

RL-74-099 Preliminary proposals for AC distribution system for EPIC. R Tolcher, H C Brooks

RL-74-100 A proposal to build a 14 GeV electron-positron colliding beam facility - EPIC.

RL-74-101 Outline proposals for EPIC magnet power supplies. A G Wheldon, H C Brooks

RL-74-102 Resonance method to produce a polarisation asymmetry in electron-positron storage rings. W T Toner

RL-74-103 Spectrum correction factors for sample holder and self-shielding effects for planar samples in thermal neutron scattering studies. C J Carlile

RL-74-104 Basque superconductor solenoid; operation and instruction handbook. G Gallagher-Daggitt, C Micklewright, J Dawson, J Brown

RL-74-105 Critical potentials, leptons and weak currents. P F Smith, J D Lewin

RL-74-106 Backward production of meson resonances in 4 GeV/c π^+d interactions. M J Emms, J B Kinson, B J Stacey, M F Votruba, P L Woodworth, I G Bell, M Dale, D Evans, J V Major, K Neat, J A Charlesworth, R L Sekulin

RL-74-107 Test of the vector dominance model by forward and backward ρ^0 and ω^0 production. J A Charlesworth, R L Sekulin, M J Emms, J B Kinson, B J Stacey, M F Votruba, P L Woodworth, I G Bell, M Dale, D Evans, J V Major, K Neat

RL-74-108 GFUN mesh generator: status on 15 July 1974. J F Marshall

RL-74-109 Description of the modified DEEEES motor encoder control system used to position the D3 diffractometer shafts. K M Knight

RL-74-110 A contention system for CCITT/V24 ansynchronous devices to gain access to multiplexors/computers. K W Taylor

RL-74-111 Computing and Automation Division quarterly report, 1 April - 30 June 1974. W Walkinshaw, A T Lea (editors)

RL-74-112 Two component analysis of the inelastic overlap function. T Inami, R J N Phillips, R G Roberts

RL-74-113 High energy elastic scattering. R J N Phillips

RL-74-114 Flipper control unit. J B Forsyth, K M Knight, J Penfold, P W Saunders

RL-74-117 Rough digitising system: 1130 control blocks, files and codes. B H Bracher, J F MacEwan, A G Waters

RL-74-118 Diffractive scattering in the dual model. Chan Hong-Mo, J E Paton, Tsou Sheung Tsun

RL-74-119 Diffraction and multiparticle unitarity in the dual model. Chan Hong-Mo

RL-74-120 The construction and calibration of a strip line prototype phase comparator for use on the 70 MeV injector. J E Ellis, N Perera, E G Sandels

RL-74-121 Glauber model and unitarity condition. J Formanek

RL-74-123 Kinematic fitting: an improved method for convergence, D J Crennell, D E Hall

RL-74-124 A feasibility report for a colliding beam facility, EPIC.

RL-74-125 Output display units Type A and Type B. J B Forsyth, K M Knight, P E Smith

RL-74-126 Phase-shift analysis of the reaction $\pi^-p \rightarrow \Lambda^0K^0$. R D Baker

RL-74-127 π-deuteron scattering. D V Bugg

RL-74-128 How crossing affects the analytic relationship between low energy $\pi\pi$ amplitudes and their asymptotic behaviour. M R Pennington

RL-74-129 Preliminary EPIC site investigation. D A Gray

RL-74-130 Magnetic diffuse scattering with polarized thermal neutrons. W G Williams, B D Rainford

RL-74-131 Design notes on the tank and debuncher auto tuning system for the 70 MeV injector. R W Mann, E G Sandels

RL-74-132 An improved method for the numerical solution of the magnetic field integral equation. C J Collie, C W Trowbridge

RL-74-133 Computer aided design at the Rutherford Laboratory. C W Trowbridge

RL-74-134 A thermally switched flux pump. G J Homer, P J Houzego, C A Scott, M N Wilson

RL-74-135 Multifilamentary niobium tin magnet conductors. D C Larbalestier, P E Madsen, J A Lee, M N Wilson, J P Charlesworth

RL-74-136 Multifilamentary niobium tin solenoids. D C Larbalestier, V W Edwards, J A Lee, C A Scott, M N Wilson

RL-74-137 The control of 'training' in 'race-track' shaped superconducting magnets. V W Edwards, C A Scott, M N Wilson

RL-74-138 Rutherford Laboratory instrument loan pool catalogue.

RL-74-139 Particle exchange in K^+p scattering. W N Cottingham, A C Davis, D I Giddings,

RL-74-140 Collision broadening of resonances D V Bugg

RL-74-141 70 MeV injector: the basic control system for the low and high energy drift space (LEDS & HEDS) triplet power supplies. R J Baker

RL-74-142 Investigation into the use of thyristors in place of the present mercury-arc converters in the excitation equipment of the alternators of the Nimrod magnet power supply plant. T J Packer

RL-74-143 Computing and Automation Division - quarterly report - 1 July 1974 to 29 September 1974. W Walkinshaw, T Lea

RL-74-144 Efficiencies of long thermal neutron detectors. B H Mearden

RL-74-145 Epic transfer lines - preliminary beam design. B D Jones.

RL-74-146 Simple tests of quark-nucleon reciprocity. Y Zarmi

RL-74-147 Research and development for polarized targets (1973/74). S F J Cox

RL-74-148 Nimrod operation and development - quarterly reports: January 1 to March 31 1974; April 1 to June 30 1974. D E Gray (editor)

RL-74-150 An investigation of the characteristics of a negative pion beam by means of induced chromosome aberrations in human peripheral blood lymphocytes. D C Lloyd, R J Purrott, G W Dolphin, D H Reading

RL-74-151 Some notes on the separation of e^+e^- beams in the interaction regions. M R Harold

RL-74-152 EPIC sextupoles: status report. M R Harold

RL-74-153 Improvements to injection into EPIC. A Carne

RL-74-154 A brief summary of beam loading effects expected in EPIC. M H R Donald

RL-74-155 Spin of leading clusters and slope of the overlap function. A Bialas, N Sakai

RL-74-156 Do extensive air shower data provide a reliable information on proton-proton total cross section? J Formanek, B Franek

RL-74-159 The Gould 5000 electrostatic printer/plotter. D S Greenaway

RL-74-160 70 MeV injector: earth bonding in the EHT area. A G Wheldon

---

OTHER REPORTS ; JOURNAL ARTICLES:; CONFERENCE PAPERS (not published elsewhere)

1 K Abe, T DeLillo, B Robinson, F Sannes, J Carr, J Keyne, I Siotis
Measurements of p + p → p + X between 50 and 400 GeV. Phys. Rev. Lett. 31 (1973) 1527

2 K Abe, T DeLillo, B Robinson, F Sannes, J Carr, J Keyne, I Siotis, A Pagnamenta
Determination of Triple Regge Couplings from a study of the reaction p + p → p + X between 50 and 400 GeV. Phys. Rev. Lett. 31 (1973) 1530

3 B Alper, H Bøggild, P Booth, L J Carroll, G von Dardel, G Damgaard, B Duff, J N Jackson, G Jarlskog, L Jonsson, A Klovning, L Leistam, E Lillethun, S Ølgaard-Nielsen, M Prentice, J M Weiss
The production of charged particles with high transverse momentum in proton-proton collisions at the CERN ISR. Nucl. Phys. B (to be publshed)

4 B Alper, H Bøggild, P Booth, L J Carroll, G von Dardel, G Damgaard, B Duff, K H Hansen, J N Jackson, G Jarlskog, L Jonsson, A Klovning, L Leistam, L Lee Chi Kwong, E Lillethun, G Lynch, S Ølgaard-Nielsen, M Prentice, S Sharrock, D Quarrie, J M Weiss
Correlations between charged particles emitted at large angles in high-energy proton-proton collisions. Lett. Nuovo Cim. 11 (1974) 173

5 D Aschman, C Caverzasio, L Dick, A Gonidec, K Green, A Gsponer, K Kuroda, A Michalowicz, P Phizacklea, M Poulet, G L Salmon, M Werleu
Spin effects in the inclusive reactions $\pi^{\pm} + p (\uparrow) \rightarrow \pi^{\pm}$ + anything at 8 GeV/c.
XVII International Conference on High Energy Physics, London, July 1974

6 A Astbury
"The formation of high mass mesons"
Nucleon-Antinucleon Symposium. Prague June 1974 (CERN 74.18)

7 S L Baker, K W J Barnham, P J Dornan, S L Glickman, G P Gopal, W A C Mier-Jedrzejowicz, R A Stevens, J R Carter, S Norton, J E Allen, V A Bull, A P White
Isobar model analysis of $\pi^+p \rightarrow p\pi^+\pi^o$ and $\pi^+p \rightarrow n\pi^+\pi^+$ around 1 GeV/c. XVII International Conference on High Energy Physics, London, July 1974

8 M Bardadin-Otwinowska, R Barloutaud, A Borg, D Denegri, F Pierre, M Spiro, B Chaurand, B Drevillon, G Labrosse, R Lestienne, D Linglin, R A Salmeron, R J Miller, K Paler, J J Phelan, T P Shah, S N Tovey
Determination of the $K^-\pi^-$ inelastic cross sections for C.M. energy up to 2.8 GeV. Nucl. Phys. B72 (1974) 1

9 M Bardadin-Otwinowska, A Borg, F Pierre, R Barloutaud, C Louedec, M Spiro, B Chaurand, B Drevillon, J Gago, G Labrosse, R Salmeron K Paler, S N Tovey, T P Shah, R J Miller, J J Phelan
Inclusive production of charged and neutral sigma hyperons in K^-p interactions at 14.3 GeV/c. Saclay preprint D.Ph.P.E. 74.07

10 V Barger, R J N Phillips
Quark parton model relations in deep inelastic lepton scattering. Nucl. Phys. B73 (1974) 269

11 V Barger, R J N Phillips
Compatibility of old and new πN charge-exchange results. Phys. Lett. 53B (1974) 195

12 V Barger, J Luthe, R J N Phillips
Tests of geometrical scaling and generalizations. Wisconsin preprint December 1974

13 V Barger, R J N Phillips
The derivative rule for helicity-flip amplitudes. Wisconsin preprint October 1974

14 C J Batty, G T A Squier, G K Turner
Forward pion-nucleus scattering amplitudes. Nucl. Phys. B67 (1973) 492

15 D F Baxter, I D Buckingham, I F Corbett, P A Dunn, J McL.Emmerson, J Garvey, F Hart, G Hughes, C M S Jones, R Maybury, N Middlemas, P R Norton, T W Quirk, J A Scheid, A M Segar
A Study of neutral final states in K^-p interactions in the range 690 to 934 MeV/c. Nucl. Phys. B67 (1973) 125 (Oxford preprint 63-67)

16 D E Baynham, J H Coupland, J Simkin
High Field Iron Magnets. Nucl. Instrum. & Meth. 114 (1974) 169

17 A Berthon, G Tristram, J Vrana, T C Bacon, A A Brandsetter, I Butterworth, G Gopal, P S Jones, P J Litchfield, M Mandelkern, J Meyer, G Poulard, B Tallini, W Wojcik, J Zatz, R Strub
Cross sections for quasi two body reactions formed in K^-p interactions between 1263 and 1843 MeV/c. Nuovo Cim. 21A (1974) 149

18 D M Binnie, L Camilleri, J Carr, N C Debenham, A Duane, D A Garbutt, W G Jones, J Keyne, I Siotis, J G McEwan
Search for neutral mesons near 1 GeV/c^2.
Phys. Rev. Lett. 32 (1974) 392

19 A Borg, M Bardadin-Otwinowska, R Barloutaud, C Louedec, L Moscoso, F Pierre, M Spiro, B Chaurand, B Drevillon, G Labrosse, R Lestienne, A Rouge, R Salmeron, H Videau, R Miller, K Paler, J J Phelan, T P Shah, S Tovey
Inclusive production of Lambda and neutral Kaon in K^-p interactions at 3.93 and 14.3 GeV/c.
Nuovo Cim. 22A (1974) 559

20 A D Bryden
Reduced guidance filtering. HPD Annual Conference, Rutherford Laboratory, October 1974

21 A D Bryden
Measurement of film from a bubble chamber with track-sensitive target. HPD Annual Conference, Rutherford Laboratory, October 1974

22 C J Carlile, D K Ross
An experimental verification of the Chudley-Elliott model for the diffusion of hydrogen in α-phase Pd/H. Solid State Communications, 15 (1974) 1923

23 C J Carlile, K H Krebs
Quasielastic neutron scattering and orientational motions in liquid crystals. Vth International Conference on Liquid Crystals, Stockholm, June 1974

23A R J Cence, F A Harris, B D Jones, R E Morgado, M W Peters, L M Shiraishi, D E Yount, B Gauld, V Perez-Mendez, D B Clarke, D B Cline, R Frommer
Search for the rare decay $K^+ \to \pi^+ e^+ e^-$. Phys. Rev. 10D (1974) 776

24 Y A Chao, R K P Zia
Magnetic moment of Δ^{++} in a bootstrap model. Nuovo Cim. 19A (1974) 651

25 B J Charles, T R M Edwards, W M Gibson, R S Gilmore, C M Hughes, J Malos, A C McPherson, J C Sleeman, V J Smith, R J Tapper, B McCartney, P D Wroath, G C Oades, G A Beck, M Coupland, S G F Frank
K^+p scattering between 0.7 and 1.9 GeV/c. Baryon Resonances Conference, Purdue University, 1973

26 J A Charlesworth, R L Sekulin, M J Emms, J B Kinson, B J Stacey, M F Vortruba, P L Woodsworth, I G Bell, M Dale, D Evans, J V Major, K Neat
Test of the vector dominance model by forward and backward ρ^0 and ω^0 production. Nucl. Phys. B79 (1974) 375 (RL-74-107)

27 B S Chaudhary, S N Ganguli, A Gurtu, P K Malhotra, U Mehtani, R Raghavan, A Subramanian
"Neutral pion production in $\bar{p}p$ annihilations at 2 GeV/c" presented at (a) Vth International Conference on Many Particle Hadrodynamics, Eisenach-Leipzig, June 1974, (b) IIIrd Int. Symposium on Antinucleon-nucleon Interactions, Prague, June 1974 and (c) XVII International Conference on High Energy Physics, London, July 1974

28 N M Clarke
Target spin effects in the scattering of composite particles. J. Phys. 7 (1974) 16

29 E F Clayton, T C Bacon, R M Waters, I Butterworth, G P Gopal, R T Ross, A J Van Horn
$K^-p \to \Lambda\pi^0$ partial wave amplitudes from 1550 to 2150 MeV. XVII International Conference on High Energy Physics, London July 1974

30 E F Clayton, T C Bacon, I Butterworth, R M Waters, B Conforto, G P Gopal, G E Kalmus, P J Litchfield, R T Ross, A J Van Horn
A high statistics determination of the Λ^0 mean lifetime. XVII International Conference on High Energy Physics, London, July 1974

31 A S Clough, G K Turner, B W Allardyce, C J Batty, D J Baugh, W J McDonald, R A J Riddle, L H Watson, M E Cage, G J Pyle, G T A Squier
Pion-nucleus total cross-sections from 88 to 860 MeV. Nucl. Phys. B76 (1974) 15 (RL-74-013)

32 J E Coggle, J Shewell, M Y Gordon, P J Lindop
Some in vivo effects of π^- mesons in mice. XI International Cancer Congress, Florence, 1974

33 T G Coleman, C M Fisher, E W Fitzharris, J H Foster, J G V Guy, P R Williams, H Leutz, M Thevenon, J Tischlauser, H Wenninger
Physics run with an all plexiglas track sensitive target. Nucl. Instrum. Meth. 114 (1974) 381

34 J H Coupland
The calculation of the field integral of magnet coils. Nucl. Instrum. Meth. 117 (1974) 491

35 J H Coupland
High field (5 T) pulsed superconducting dipole magnet. Proc. Instn. Elect. Engrs. 121 (1974) 771

35A J T Dakin, G J Feldman, F Martin, M L Perl, W T Toner
Measurement of inclusive hadron electro production in hydrogen and deuterium. Phys. Rev. D5 (1974) 1401

36 G V Dass
$|\eta_{+-}|$ and the reaction $e^+e^- \to K^0\bar{K}^0$ at the ϕ-resonance. Phys. Lett. 51B (1974) 247 (RL-74-056)

37 G V Dass, H Fraas
Time-reversal-invariance-like relations for spin effects in elastic and inelastic reactions; vector meson photoproduction versus Compton scattering from nucleons. Ann. Phys. N.Y. December 1974
Pomeron factorization and the reaction $\gamma N \to \phi N$. DESY preprint 74/58

38 J D Davies, J G Guy, R K P Zia
Experimental limits to the $\pi^0 \to e^+e^-$ rate and their consequences for a direct electron-hadron coupling. Nuovo Cim. 24A (1974) 324 (RL-74-092)

39 D Denegri, R Barloutaud, A Borg, C Louedec, F Pierre, M Spiro, B Chaurand, B Drevillon, G Labrosse, R Lestienne, D Linglin, R A Salmeron, T P Shah, K Paler, R J Miller, J J Phelan
Search for a Double-Pomeron-Exchange contribution in the reaction $K^-p \to K^-\pi^+\pi^-p$ at 14.3 GeV/c. Nuovo Cim. 21A (1974) 556

40 D Denegri, Y Pons, R Barloutaud, A Borg, C Louedec, M Spiro, K Paler, T P Shah, S N Tovey, B Chaurand, B Drevillon, G Labrosse, R Lestienne, R A Salmeron
Evidence for double dissociation in K^-p interactions at 14.3 GeV/c. Saclay preprint D.Ph.P.E. 74-06

41 J Dowell, J Garvey, M Jobes, I R Kenyon, J Mawson, T McMahon, I F Corbett, R J Esterling, M R Jane, N H Lipman, R S Orr, K C T O Sumorok, S Dagan, Y Gnat, J Grunhaus, J R Arch, E H Bellamy, M G Green, J B Lister, P V March, A R Robertson, J A Strong, D H Thomas, G Alexander
Preliminary analysis of $\pi^-p \to \pi^+\pi^-n$ at 12 GeV/c from Omega. XVII International Conference on High Energy Physics, London July 1974

42 A Duane, D M Binnie, L Camilleri, J Carr, N C Debenham, D A Garbutt, W G Jones, J Keyne, I Siotis, J G McEwan
New upper limit on the width of the X^0 (958) Phys. Rev. Lett. 32 (1974) 425

43 Ecole Polytechnique, Paris-Rutherford Laboratory-CEN, Saclay Collaboration
Momentum transfer distributions of various diffractive enhancements in K^-p interaction at 14.3 GeV/c. Comparisons with K^+p interactions at 12 GeV/c. XVII International Conference on High Energy Physics, London July 1974

44 Ecole Polytechnique, Paris-Rutherford Laboratory-CEN, Saclay Collaboration
Inclusive production of antilambdas in K^-p interactions at 14.3 GeV/c. XVII International Conference on High Energy Physics, London July 1974

45 Ecole Polytechnique, Paris-Rutherford Laboratory-CEN, Saclay Collaboration
Inclusive $K^{*-}(890)$ and $K^{*0}(890)$ production in 14.3 GeV/c K^-p interactions. XVII International Conference on High Energy Physics, London, July 1974

46 J A Edgington, B J Howard, I M Blair, B E Bonner, F P Brady, M W McNaughton.
A measurement of neutron proton bremsstrahlung near 130 MeV. Nucl. Phys. A218 (1974) 151

47 E Eisenhandler, W R Gibson, C Hojvat, P I P Kalmus, L C Y Lee Chi Kwong, T W Pritchard, E C Usher, D T Williams, M Harrison, W H Range, M A R Kemp, A D Rush, J N Woulds, G T J Arnison, A Astbury, D P Jones, A S L Parsons
"Differential cross-sections for $\bar{p}p \to \pi^-\pi^+$, K^-K^+ between 0.8 and 2.4 GeV/c" Phys. Lett. 47B (1973) 531 (RL-73-123)

48 E Eisenhandler, W R Gibson, C Hojvat, P I P Kalmus, L C Y Lee Chi Kwong, T W Pritchard, E C Usher, D T Williams, M Harrison, W H Range, M A R Kemp, A D Rush, J N Woulds, G T J Arnison, A Astbury, D P Jones, A S L Parsons
"Interpretations of the differential cross-sections for $\bar{p}p \to \pi^-\pi^+$" Phys. Lett. 47B (1973) 536 (RL-73-124)

49 E Eisenhandler, W R Gibson, C Hojvat, P I P Kalmus, L C Y Lee Chi Kwong, T W Pritchard, E C Usher, D T Williams, M Harrison, W H Range, M A R Kemp, A D Rush, J N Woulds, G T J Arnison, A Astbury, D P Jones, A S L Parsons
"Some observations on the differential cross-sections for $\bar{p}p \to K^-K^+$" Phys. Lett. 49B (1974) 201

50 E Eisenhandler, W R Gibson, C Hojvat, P I P Kalmus, L C Y Lee Chi Kwong, T W Pritchard, E C Usher, D T Williams, M Harrison W H Range, M A R Kemp, A D Rush, J N Woulds, G T J Arnison, A Astbury, D P Jones, A S L Parsons
"Antiproton-proton elastic scattering from 0.69 to 2.43 GeV/c" XVII International Conference on High Energy Physics, London July 1974

51 E Eisenhandler, W R Gibson, C Hojvat, P I P Kalmus, L C Y Lee Chi Kwong, T W Pritchard, E C Usher, D T Williams, M Harrison, W H Range, M A R Kemp, A D Rush, J N Woulds, G T J Arnison, A Astbury, D P Jones, A S L Parsons
"A comparison of $\bar{p}p$ and pp elastic scattering at 90^{o}" Nucleon-Antinucleon Symposium. Prague June 1974

52 M J Emms, J B Kinson, B J Stacey, M F Vortruba, P L Woodworth, I G Bell, M Dale, D Evans, J V Major, K Neat, J A Charlesworth, R L Sekulin
Backward production of meson resonances in 4 GeV/c $\pi^{+}d$ interactions. Phys. Lett. 51B (1974) 195 (RL-74-106)

53 E J Emms, J B Kinson, B J Stacey, M F Vortruba, P L Woodworth, I G Bell, M Dale, J V Major, J A Charlesworth, D J Crennell, R L Sekulin
A search for spectator isobars in deuteron collisions. Phys. Lett. 52B (1974) 372

54 M J Emms, G T Jones, J B Kinson, B J Stacey, M F Vortruba, P L Woodworth, I G Bell, M Dale, J V Major, J A Charlesworth, D J Crennell, R L Sekulin
A Spin-parity analysis of the $\pi^{-}\pi^{+}\pi^{+}$ system produced coherently in 4 GeV/c $\pi^{+}d$ interactions. XVII International Conference on High Energy Physics, London July 1974

55 M J Emms, J B Kinson, B J Stacey, M F Vortruba, P L Woodworth, I G Bell, M Dale, D Evans, J V Major, K Neat, J A Charlesworth, R L Sekulin
The forward production of the ω^{o}- meson in the reaction $\pi^{+}d \rightarrow p_{s}p\omega^{o}$ at 4 GeV/c. XVII International Conference on High Energy Physics, London July 1974

55A EPIC Machine Design Study Group: "Design & Status of EPIC". Proc. IX International Conference on High Energy Accelerators, SLAC, (May 1974)

56 C M Fisher, J G V Guy, J W G Wignall
The geometrical reconstruction of events from track sensitive targets. Nucl. Instrum. Meth. 118 (1974) 171

57 C M Fisher
Review of some techniques for experiments in the late 1970s. HPD Annual Conference, Rutherford Laboratory, October 1974

58 I S K Gardner
Second harmonic RF acceleration on Nimrod. 9th International Conference on High Energy Accelerators, SLAC, California May 1974

59 J Garvey
Status of the Omega Camera System. Conference on Computer Scanning, Oxford, 1974

60 W R Gibson, E Eisenhandler, C Hojvat, P I P Kalmus, L C Y Lee Chi Kwong, T W Pritchard, E C Usher, D T Williams, M Harrison, W H Range, M A R Kemp, A D Rush, J N Woulds, G T J Arnison, A Astbury, D P Jones, A S L Parsons
"Antiproton-proton elastic scattering from 0.69 to 2.43 GeV/c" Elementary Particles and Nuclear Structure Conference (Institute of Physics) Glasgow, March 1974

61 P M Girard, I H Rose, D B Scott,
Implementation of a graphics and text output retrieval system. Software Practice and Experience 4 (1974) 279

62 R Golub, J M Pendlebury
Method of studying surface properties relevant to ultra-cold neutrons. Phys. Lett. A50 (1974) 177

63 E E Gross, N M Clarke, C B Fulmer, M L Halbert, D C Hensley, C A Ludemann, D Martin, A Scott, J G Cramer, M Zisman, R Devries
Scattering of ^{16}O ions from ^{28}Si ^{59}Co and ^{60}Ni at 142 Mev. 1974 Fall Meeting of the Division of Nuclear Physics, Pittsburgh, Pennsylvania October 1974

63A M R Harold et al. (SPEAR Storage Ring Group) "SPEAR Status and Improvement Programme" Proc. IX International Conference on High Energy Accelerators, SLAC, (May 1974)

64 D C Hensley, C B Fulmer, N M Clarke, R Eagle, R J Griffiths
53.4 MeV ^{3}He scattering from the samarium isotopes. ORNL Report No 4937 (1973) 70

65 G J Homer, P J Houzego, C A Scott, M N Wilson
A thermally switched flux pump. Applied Superconductivity Conference, 1974

66 B J Howard, J A Edgington, S S das Gupta, I M Blair, B E Bonner, F P Brady, M W McNaughton, N M Stewart
Differential cross-sections for np and nd elastic scattering near 130 MeV. Nucl. Phys. A218 (1974) 140

67 T Inami
Mueller-Regge analysis in the central region Nucl. Phys. B77 (1974) 337 (RL-74-039)

68 T Inami, R J N Phillips, R G Roberts
Two-component analysis of the inelastic overlap function. Phys. Lett. 53B (1974) 355 (RL-74-112)

69 K Jaegar, A Thomas, H Leutz, E Fitzharris, J H Foster, P R Williams
Neon-hydrogen mixture run with the 12 foot bubble chamber. ANL-BBC-158

70 M R Jane, B D Jones, N H Lipman, D P Owen, B K Penney, T G Walker, M Gettner, P Grannis, H Uto, J Anderson, E H Bellamy, M G Green, J Kirkby, P E Osman, J A Strong, D H Thomas, C M Solomonides
A measurement of the charge asymmetry in the decay $\eta \rightarrow \pi^{+}\pi^{-}\gamma$. Phys. Lett. 48B (1974) 265 (RL-73-140)

70A M R Jane, B D Jones, N B Lipman, D P Owen, B K Penney, T G Walker, M Gettner, P Grannis, H Uto, J Anderson, E H Bellamy, M G Green, J Kirkby, P E Osman, J A Strong, D H Thomas, C M Solomonides
A measurement of the charge asymmetry in the decay $\eta \rightarrow \pi^{+}\pi^{-}\pi^{o}$". Phys. Lett. 48B (1974) 260 (RL-73-139)

71 G E Kalmus
Review of the BEBC programme and its implications on automatic film measuring equipment. HPD Annual Conference, Rutherford Laboratory, October, 1974

72 N F Kember, F A Smith
An approach to microdosimetry in a π meson beam using nuclear emulsions. 5th International Conference of Radiation Research, Seattle, Radiation Research 59 (1974) 115

72A N M King et al
"Performance Study on pp Storage Rings at Several Hundred GeV/c: Injectors Working Group Report". CERN/ISR-AS/74-51

72B N M King, M Cornacchia
"Sextupolar Tune Shifts in the SPS". CERN Lab-II-DI-PA/74-1

73 W S Lam, J Tran Than Van, J Uscherssohn
Inclusive electroporduction in the photon fragmentation region. Nucl. Phys. B74 (1974) 59

74 G A Lambert
195 Computer Bulletin no. 14. Archive Magnetic Tape Library

75 R A Lawes
Prelinimary production of BEBC digitisings by the HPD2 at the Rutherford Laboratory. HPD Annual Conference, Rutherford Laboratory, October 1974

76 M Le Bellac, H I Miettinen, R G Roberts
Structure of two-body correlations in high energy hadron production. Phys. Let.. 48B (1974) 115

76A H Lynch, R Schwitters, W T Toner
"Background Sources at PEP". SLAC-LBL PEP 137

77 P J Litchfield
Baryon Resonances. XVII International Conference on High Energy Physics, London, July 1974

78 W J McDonald, A I Kilvington, C J Batty, J L Weil
Identification of fission activity using thin film detectors. Nucl. Instrum. Meth. 115 (1974) 185

78A J R M Maidment et al (DESY Storage Ring Group) "DORIS Present Status and Future Plans" Proc. IX International Conference on High Energy Accelerators, SLAC, (May 1974)

78B J R M Maidment et al (DESY Storage Ring Group) "The First Operational Experience with the Double Storage Ring DORIS". Proc. VI USSR National Accelerator Conference, Moscow, (Nov, 1974)

79 A J Mill, J D Lewis
Radiation response of mammalian cells after irradiation with a beam of negative pi-mesons 5th International Conference of Radiation Research, Seattle. Radiation Research 59 (1974) 60

80 D Morgan
Tests of ππ phase determinations Phys. Rev. D9 (1974) 3210 (RL-73-155)

81 D Morgan
Is the O^+ nonet respectable? Phys. Lett. 51B (1974) 71 (RL-74-063)

82 D Morgan
ππ and Kπ scattering - special topics. XVII International Conference on High Energy Physics, London, July 1974

83 A H W Nias, D Greene, D Major, D R Perry, D H Reading
Determination of RBE values for fast neutrons and negative π-mesons using frozen HeLa cells Brit. J. Radiology 47 (1974) 800

84 M J O'Connell
Multivariate least squares fitting program using modified Gram-Schmidt transformations. Comput. Phys. Commun. 8 (1974) 56

85 M J O'Connell
Search program for significant variables. Comput. Phys. Commun. 8 (1974) 49

86 K Paler, T P Shah, S N Tovey, R J Miller, J J Phelan, N M Cason, P H Stuntebeck, N N Biswas, V P Kenney, W D Shephard, B Chaurand, B Drevillon, G Labrosse, R Lestienne, R A Salmeron, M Bardadin-Otwinowska, A Borg, C Louedec, Y Pons, H Spiro
Factorisation in the inclusive reactions $\pi^{\pm}p \to \Lambda + X$ and $K^-p \to \Lambda + X$. Phys. Lett. 48B (1974) 151

87 F Palou
A simple lower bound for the $\pi^o\pi^o$ total cross section. Lett. Nuovo Cim. 9 (1974) 615

88 R D Peccei
Solvable one-dimensional models of particle production. Nucl. Phys. B81 (1974) 301 (RL-74-050)

89 R D Peccei
Multiparticle production and the asymptotic behaviour of form factors. Phys. Lett. 51B (1974) 279

90 R D Peccei
Crossing symmetry and coherent states. Phys. Rev. D10 (1974) 759

91 R J N Phillips
Comment on real parts of KN and $\bar{K}N$ elastic amplitudes. Nucl. Phys. B72 (1974) 481

92 R J N Phillips, D P Roy
Duality. Rep. Progr. Phys. 37 (1974) 1035

93 F Pierre, M Bardadin-Otwinowska, R Barloutaud A Borg, Y Pons, M Spiro, B Chaurand, B Drevillon, J M Gago, G Labrosse, R Lestienne, R A Salmeron, K Paler, T P Shah, S Tovey
Inclusive γ production in K^-p interactions at 14.3 GeV/c. Nucl. Phys. B77 (1974) 45

94 H D Politzer, G G Ross
Scaling behaviour in a class of massive non-Abelian gauge theories. Nucl. Phys. B75 (1974) 269

94A G H Rees
"The Design of a 14 GeV Electron-Positron Colliding Beam System, - EPIC" Proc. VI USSR National Accelerator Conference, Moscow, (Nov, 1974)

95 G G Ross, R K P Zia
Gauge models without charmed hadrons. Nuovo Cim. 24A (1974) 61

96 R T Ross, A J Van Horn, G P Gopal, G Kalmus, T C Bacon, E F Clayton, I Butterworth
$K^-p \to \Sigma^{\pm}\pi^{\mp}$ partial wave amplitudes from 1540 to 2170 MeV. XVII International Conference on High Energy Physics, London, July 1974

97 D P Roy, R G Roberts
Tripple Regge analysis of pp → pX and some related phenomena - a detailed study. Nucl. Phys. B77 (1974) 240

98 F Sannes, T de Lillo, M Lieberman, J Mueller, B Robinson, I Siotis, G Cvijanovich, A Pagnamenta, R Stanek
Study of the inclusive reaction p + p → p + X between 40 and 260 GeV/c using an internal H_2 jet target. Phys. Rev. Lett. 30 (1973) 766

99 B C Sinha
A nucleus-nucleus optical potential using a density dependent two-body interaction. Phys. Rev. Lett. 33 (1974) 600

100 B C Sinha, F Duggan
A three parameter nucleon-nucleus optical model on the energy shell. Nucl. Phys. A226 (1974) 31

101 B C Sinha, F Duggan
The Thomas-Fermi approximation and the imaginary part of the optical potential. Phys. Lett. 47B (1973) 389

102 P F Smith, F F Heymann, D Imrie, N R Daly, N J Freeman
The lifetime of the proton and possible higher mass meta-stable particles. Nuovo Cim. 21A (1974) 567

103 D B Thomas
Superconducting Magnets. IX International Conference on High Energy Accelerators, Stanford, 1974

104 D B Thomas
Superconductivity. Meeting on Technology arising from High Energy Physics, CERN, Geneva, 1974

104A W T Toner
"British Plans for a Future Accelerator". Inst. Phys. Conference on Physics at Very High Energies, Westfield College, London (September, 1974)

104B W T Toner
"Status of EPIC". Topical Meeting on Phys. of Colliding Beams, ICTP, Trieste, (June 1974)

104C W T Toner
"A first look at a polarisimeter for EPIC or PEP". SLAC-LBL PEP 137

105 S N Tovey, K Paler, T P Shah, R J Miller, J J Phelan, B Chaurand, B Drevillon, J M Gago, G Labrosse, R Lestienne, R Salmeron R Barloutaud, A Borg, D Denegri, F Pierre, M Spiro
The inclusive reaction $K^-p \to pX$ at 14.3 GeV/c. Nucl. Phys. B76 (1974) 290 (RL-74-017)

106 P Turowski, J H Coupland, J Perot
Pulsed Superconducting Magnets of the GESSS Collaboration. IX International Conference on High Energy Accelerators, Stanford, 1974

107 A J Van Horn, G P Gopal, R T Ross, B Conforto T C Bacon, E F Clayton, I Butterworth
$K^-p \to \bar{K}N$ partial wave amplitudes from 1540 to 2170 MeV. XVII International Conference on High Energy Physics, London July 1974

108 C R Walters
Magnetization and design of multistrand superconducting conductors. Applied Superconductivity Conference, 1974

109 W G Williams
Instrumentation for Polarization Analysis. Neutron Crystallography, Institute of Physics and Chemical Society, Sheffield, December 1974

110 G Wilquet, W L Knight, J G Guy, S N Tovey, E Gelfand, T Mann, J Schenps, F R Stannard, D J Miller
The ΛΛ mass spectrum produced by 2.2 GeV/c K^- interactions on nuclei. (Submitted to Nuovo Cimento).

111 B M Winston, R J Berry, D R Perry, D H Reading
Effects of the radiation at the entrance point of a negative π-meson beam. Brit. J. Radiology 47 (1974) 201

112 R P Worden
Deep inelastic structure functions of the photon. Phys. Lett. 51B (1974) 57

113 R P Worden
A fixed pole sum rule in photon-photon scattering. Phys. Lett. 52B (1974) 87

THESES

J Carr (Imperial College, London)
Search for neutral mesons with masses near 1 GeV/c^2.

J K Davies (University of London)
An experiment to measure the high energy coherent scattering of partons on helium nuclei. (HEP/T/51)

G Hall (Imperial College, London)
K$\pi\pi$ states in K^+d interactions (HEP/T/52)

N J D Jacobs (University of London)
A study of two and three body final states in K^+p interactions between 2 and 3 GeV/c. (HEP/T/48)

D R Jeremiah (University of London)
The π^-d scattering length from a measurement of the (π^-d) mesic X-rays. (HEP/T/50)

J A Jones (Oxford University)
The $\pi\pi$ interaction as observed in $\pi^-p \to \pi\pi N$ at low energies. (HEP/T/46)

J C Sleeman (Oxford University)
An experiment to study polarisation effects in π^+p elastic scattering in the momentum range 600-2700 MeV/c. (HEP/T/49)

C M Solomonides (University of Sussex)
Experimental measurement of the charge asymmetry in the decay $\eta \to \pi^+\pi^-\pi^o$. (HEP/T/47)

G K Turner (University of Surrey)
Pion-nucleus total cross-sections from 86 to 860 MeV.

S A Weisrose (Kings College, London)
Composite Particle Interactions on ^{56}Fe near 85 MeV.

PROPOSALS FOR HEP EXPERIMENTS (submitted during 1974)

Proposal

140 Experiments with high-energy charged hyperons at the SPS.
Geneva, University, Heidelberg University, Lausanne University, Orsay, Strasbourg University, Rutherford Laboratory

141 Inelastic neutrino interactions at the SPS using a counter set-up.
CERN, Hamburg, Karlsruhe, Oxford University, Westfield College, Bristol University, Rutherford Laboratory

142 K^+p interactions at 14 GeV/c using the Omega spectrometer.
Birmingham University, Glasgow University

143 Magnetic recoil spectrometer for the gas jet target at FNAL.
Rochester University, Rutgers University, Imperial College, London

144 Search for heavy long-lived integrally charged particles.
Rutherford Laboratory

145 Exclusive reactions in πp and Kp interactions in the energy range up to 80 GeV.
Amsterdam, CERN, Munich MPI, Oxford University, Rutherford Laboratory

146 Continuation, with increased sensitivity, of the search for e, e^+e^- pairs, high transverse momentum π^{+-o}, and multiple pion correlations in collisions with high transverse momentum.
CERN, Columbia, Rockefeller, Oxford University

147 Y^* production from π^+p and K^-p incident states at 6.7 GeV/c using the SLAC hybrid facility.
Imperial College, London

148 π^+ and π^- total cross sections on deuterium and the total cross section for the production of neutral particles in the π^-d interaction for π energies from 50 to 350 MeV at SIN.
SIN, Karlsruhe University, Neuchatel University, Oxford University, Heidelberg, University College London

Proposals continued

149 A Ξ^* experiment at the BNL multiparticle spectrometer.
Imperial College, London, Southampton University

150 Exchange mechanisms in quasi two-body final states, using the RMS facility.
Rutherford Laboratory, Wesfield College London, University of Edinburgh

151 Exclusive hadronic processes at large P_T.
CERN, Genova, Oslo, University College, London

152 The negative pion dose-response curves for frozen HeLa cells at various positions along the depth dose profile.
Glasgow Institute of Radiotherapeutics, Rutherford Laboratory

153 Three experiments to study π^- induced chromosome aberrations in human lymphocytes.
National Radiological Protection Board

154 The relationship of π^- beam dosimetry, and the radiobiological effects on mammalian systems in vitro and in vivo.
St. Bartholomew's Hospital

155 Dosimetry experiments to back up biological work with π^-.
Rutherford Laboratory, St. Bartholomew's Hospital, Leeds

156 X-rays from K^-p atoms.
Birmingham University, Surrey University, Rutherford Laboratory

157 Search for the electric dipole moment of the neutron using bottled neutrons.
University of Sussex, Harvard University, Oak Ridge National Laboratory, Technical University, Munich, University of Oxford, ILL, Grenoble, CENG, Grenoble

158 Rare meson systems produced in $K^\pm p$ collisions at 18 and 32 GeV/c using the RF separated beam and the Omega spectrometer at the SPS.
University of Birmingham

159 K^-p interactions between 450 and 900 MeV/c.
Rutherford Laboratory, Imperial College, London

160 High energy ν and $\bar{\nu}$ interactions at the CERN SPS using a hydrogen filled track sensitive target in BEBC and a wide band beam.
University of Bari, Free University, Brussels Rutherford Laboratory, University College, London

Appendix B: Lectures and Meetings

NIMROD LECTURES ON PARTICLE PHYSICS

M Albrow (CERN, 7 January): Inelastic proton scattering at the ISR.

L M Seghal (Aachen, 14 January): Neutrino electron scattering in theories with neutral currents.

S Wojcicki (Stanford and CERN, 21 January): K^{o}_{L} Decay.

G Preparata (Rome, 28 January): A possible way to look at deep inelastic phonemena - the massive quark model.

M Pennington (RL, 4 February): $\pi\pi$ scattering: how crossing and analyticity can ruin your phase shift analysis.

R D Peccei (RL, 11 February): Quark imprisonment scheme.

I Halliday (Imperial College, 18 February): A model for fixed angle pp scattering.

G Goldhaber (Berkeley, 19 February): New data from SPEAR.

D P Roy (RL, 26 February): Diffraction 73.

W Allison (Oxford, 4 March): Identifying secondary particles at SPS energies: a new approach (ISIS).

N F Ramsey (Oxford & Harvard, 11 March): Search for a neutron electric dipole moment.

T K Gaisser (Bartel, USA, 15 March): Cosmic-ray air showers and Feynman scaling above 2,000 GeV.

D Websdale (CERN & Imperial College, 18 March): $K^{-}p$ and pp charge exchange.

W Kienzle (CERN, 25 March): Results from CERN ITEP collaboration at Serpukhov.

R Cashmore (Oxford, 1 April): Baryon resonances below 2 GeV: their poles, their classification and their decays.

L Foa (CERN & Pisa, - ril): Correlation data from Pisa/Stonybrook collaboration at ISR.

B Grayor (CERN, 22 April): ω-ρ interference and other results from $\pi^{-}p \to \pi^{-}\pi^{+}n$ at 17.2 GeV/c.

J Illiopoulos (Orsay, 29 & 30 April, 1 & 3 May): An introduction to gauge theories for experimentalists.

R F Schwitters (SLAC, 6 May): New $e^{+}e^{-}$ results from SPEAR.

D Schildknecht (DESY, 13 May): New results on generalized vector dominace.

G V Dass (RL, 20 May): Why study decays of the $(K^{o}\bar{K}^{o})$ pair-state?

D H Saxon (RL, 30 May): Inclusive lepton production by 300 GeV protons.

D H Wilkinson, FRS (Oxford, 3 June): Second class currents.

W H Range (Liverpool, 10 June): Polarisation measurements in pseudo-scalar meson photoproduction.

R Thun (CERN, 17 June): Recent measurements of correlations associated with photons at large P_{T}.

R Rubenstein (FNAL, 12 July): FNAL total cross-section data.

A Bassetto (Padua, 12 August): Review of many-particle production models.

G G Ross (RL, 23 September): Asymptotic freedom.

D Cundy (CERN, 30 September): ν physics (London Conference Review Talk).

R J N Phillips (RL, 7 October): High energy elastic scattering.

A Astbury (RL, 14 October): $\bar{p}p$ formation experiments.

G Manning & W T Toner (RL, 21 October): SPEAR Summer School.

A L Sessoms (CHLM, CERN, 28 October): Correlation measurements in proton-proton interactions at ISR energies.

A J G Hey (Southampton, 4 November): $SU(6)_W$ is alive and well.

C de Tar (CERN and MIT, 11 November): s-channel structure of Reggeon diagrams.

R M Brown (RL, 25 November): The physics programme at FNAL.

S Tovey (RL, 2 December): A Partial wave analysis of the $K\pi\pi$ system in K^-p interactions at 14.3 GeV/c.

J Kirkby (SLAC, 9 December): The Lamb Shift in π-μ atoms.

A Van Horn (RL, 16 December): Y^* spectroscopy.

SEMINARS IN HIGH ENERGY PHYSICS

G Thompson (Oxford, 16 January): An Ascoli analysis of 3π data in the A_3 region.

D Weingarten (Orsay, 24 January): Density correlations of the hadron gas as the origin of early multiplicity scaling.

J L Cardy (Daresbury, 30 January): A self-consistent pomeron.

J Dias de Deus (Niels Bohr Inst., 5 February): Geometric scaling and the pp elastic differential cross-section at the ISR.

W N Cottingham (Bristol, 6 February): The periphery of the proton.

M Teper (Westfield College, 13 February): Unitarity and large transverse momenta.

C Sachrajda (Imperial College, 14 February): Perturbation theory approach to fixed angle scattering.

W Zakrzewski (Durham, 20 February): Some ambiguities of the multi-Regge model.

H Danskin (Imperial College, 27 February): The mystery of the disappearing masses: accidental symmetries and pseudo-Goldstone bosons.

B Read (Daresbury, 6 March): Progress in vector dominance.

T W Quirk (Oxford & FNAL, 13 March): The FNAL muon spectrometer experiment.

J C Collins (Cambridge, 20 March): The renormalisation group.

D K Choudhury (Oxford, 27 March): Approach to asymptopia in electron-positron annihilation into hadrons.

P Estabrooks (Durham, 3 April): Tests of duality in reggeon-particle scattering.

M Rubinstein (CERN, 9 April): Deep inelastic scattering.

N Sakai (Max Planck Inst., 24 April): Multiplicity distributions in impact parameter space.

G Guralnik (Brown University & Imperial College, 1 May): Permanently bound quarks - new solutions to old field equations.

R K P Zia (Southampton, 8 May): Scaling in critical phenomena.

H Burkhardt (Birminham, 16 May): Serious ambiguities in inelastic phase shift analysis.

A Love (Sussex, 23 May): Improved renormal group equations and critical phenomena.

F E Elvekjaer (CERN, 29 May): Is tensor exchange peripheral?

M G Olsson (Wisconsin, 12 June): Resonance and background addition re-examined with applications to pole models of low energy photoproduction and πN elastic scattering.

J L Rosner (Minnesota, 7 July): How to find charmed particles.

K Igi (Tokyo, 24 July): A resonance model of baryons based on duality and the quark model.

P Kabir (Virginia, 7 August): Possible variation of the gravitation constant.

Y Oyanagi (NLHEP, Japan, 14 August): $\pi\pi$ finite energy sum rules.

A Schwimmer (Weizmann Inst., 19 August): S-channel absorbtive models of the pomeron.

C Rosenzweig (Weizmann & U C Berkeley 21 August): Making the dual photon massive: a new kind of Higgs-Schwinger mechanism?

M Bishari (Weizmann Inst., 28 August): Exchange degeneracy, unitarity & multiparticle production.

G Carl (Guelph, 2 September): Weak & electromagnetic annihilations at high energy.

A Bassetto (Padua, 3 September): Multiperipheral factorization & the bootstrap idea.

J Formanek (RL & Charles University, 18 September): High energy processes with nuclear targets.

L Schroeder (LBL California, 24 September): Physics with high energy nuclei at Berkeley - a general survey of the Bevalac Project.

S Yasumi (NLHEP, Japan 1 October): Some experiments done with the 1.3 GeV Electron Synchrotron of INS in Tokyo.

E Lehman (Daresbury, 9 October): Reggeon calculus approach to high energy hadronic scattering in nuclei.

Y Zarmi (Weizmann Inst., 16 October): Hadron-parton reciprocity.

D V Nanopoulos (CERN, 23 October): The question of non-leptonic interactions of leptons.

P Estabrooks (Durham, 29 October): The use of zeros in $\pi\pi$ phase shift analysis.

W N Cottingham (Bristol, 6 November): Particle exchange in exotic channels at low energies.

H Muirhead (Liverpool, 13 November): Anti-proton interactions.

J E Paton (Oxford, 20 November): Reggeon parameters from duality and unitarity.

G Cohen-Tannoudji (Saclay, 27 November): Reggiometry.

G V Dass (RL, 4 December): Pomeron factorisation and ϕ production.

F T Ezawa (DAMPT, 18 December): Asymptotically scale-free theory of the large transverse momentum processes.

RUTHERFORD LABORATORY LECTURES

(on subjects of general scientific interest)

K V Roberts (Culham, 7 February): Thermonuclear fusion by laser compression.

P D Dunn (Reading, 7 March): Energy and the future.

A C Hastings (Clerk to the Committee, 17 April): The work of the Select Committee on Science and Technology.

G Manning (RL, 23 May): What's happening in High Energy Physics and is it exciting?

D Michie (Edinburgh, 20 June): Chess, Robotics and North Sea Oil.

I Maddock (DTI, 15 October): The R and D Dilemma.

R L Mössbauer (ILL, 24 October): Application of anomalous dispersion of X-rays, neutrons and γ-rays in crystallography.

S A Tobias (Birmingham, 7 November): R and D in high speed bulk forming.

Sir John Gray (MRC, 28 November): Fundamental science and the solution of health problems.

G Manning (RL, 18 December): What are the new particles and why the fuss?

E H Cooke-Yarborough (AERE, 19 December): Thermo-mechanical oscillators.

APPLIED PHYSICS LECTURES

N M King (RL, 20 February): Progress on the 400 GeV European Synchrotron (SPS)

W Smart (NAL, 13 May): Progress on the 15 foot Bubble Chamber at FNAL.

A Rogers (SLAC, 29 May): The SLAC Hybrid Bubble Chamber and Streamer Chamber

SEMINARS IN COMPUTING

J W Burren (RL, 18 January): Relational data-base systems.

(25 January): Seminar on book-keeping systems.

H J Down (London Computer Centre, 1 February): The ULCC as a Regional Centre.

J W Burren, T G Pett, D B Scott (RL, 14 February): Getting the best out of the ELECTRIC system.

C Adams and A Bell (RL, 1 March): High level assemblers.

J A Baker (Berkeley, 15 March): Computing at the Lawrence Berkeley Laboratory.

D Maden (RL, 22 March): A user's experience of the GEC 4080.

(17 May): Progress reports on various aspects of the C & A Division's work.

R A Lawes (RL, 7 June): Progress with HPD machines at the Rutherford Laboratory.

(20 June): Trends in data acquisition at CERN.

A Bryden (RL, 5 July): HPD reduced guidance measurement systems.

J W Burren (RL, 19 July): Introduction to computer networks.

J Zoll (CERN, 4 October): The HYDRA system.

C Adams (RL, 11 October): High level network protocols.

B G MacGowan (IBM(UK) Ltd., 25 October): A brief introduction to the use of computers in Air Traffic Control.

R Rosner (RL, 1 November): Computing facilities at high energy laboratories in the USA.

(7 November): Progress reports on various aspects of the C & A Division's work.

(22 November): Report from SEAS 1974.

R E Thomas (ACL, 6 December): Atlas Computer Laboratory future graphics facilities.

D M Sendall (CERN, 20 December): Small computers in data acquisition at CERN.

ELECTRONICS SEMINARS

E G Murphy (Culham Laboratory, 26 November): Data acquisition from fusion experiments at Culham.

A C Peatfield (DL, 3 December): The use of CAMAC at Daresbury Laboratory.

NEUTRON BEAM RESEARCH MEETINGS

(April 18): Neutrons and Biology (in association with the British Biophysical Society and the Neutron Scattering Group of The Institute of Physics and The Chemical Society).

(April 24): Condensed Matter Research Using Pulsed Neutron Sources (at The University of Reading, in association with the Neutron Scattering Group of The Institute of Physics and The Chemical Society, and AERE Harwell).

CONFERENCES AND MEETINGS

Theoretical Physics Meeting (2 to 4 January)

Quantum Gravity Conference (15, 16 February, Coseners House)

Council meeting (19, 20 March, Coseners House)

GESS meeting (8, 9 April, Coseners House)

Pulsed neutron sources meeting (21 to 26 April, Coseners House)

Meeting on Deep Inelastic Phenomena (4, 5 May, Coseners House)

"Exotic Atoms" - A half-day meeting of the Particle Nuclei Interactions Group of the Institute of Physics (19 June)

$\pi\pi$ phenomenology meeting (23, 24 June, Coseners House)

XVII International Conference on High Energy Physics (1 to 10 July, Imperial College)

EPIC meeting (18 July)

Summer School for Theorists (8 to 12 September, Durham University)

Summer School for Experimentalists in High Energy Nuclear Physics (9 to 27 September)

HPD Annual Conference (1, 2 October)

ILL sub-committee meeting (24, 25 October, Coseners House)

NBRC meeting (28, 29 October, Coseners House)

Nuclear Physics Board meeting (26 November)

EPIC meeting (2 to 6 December, Coseners House)

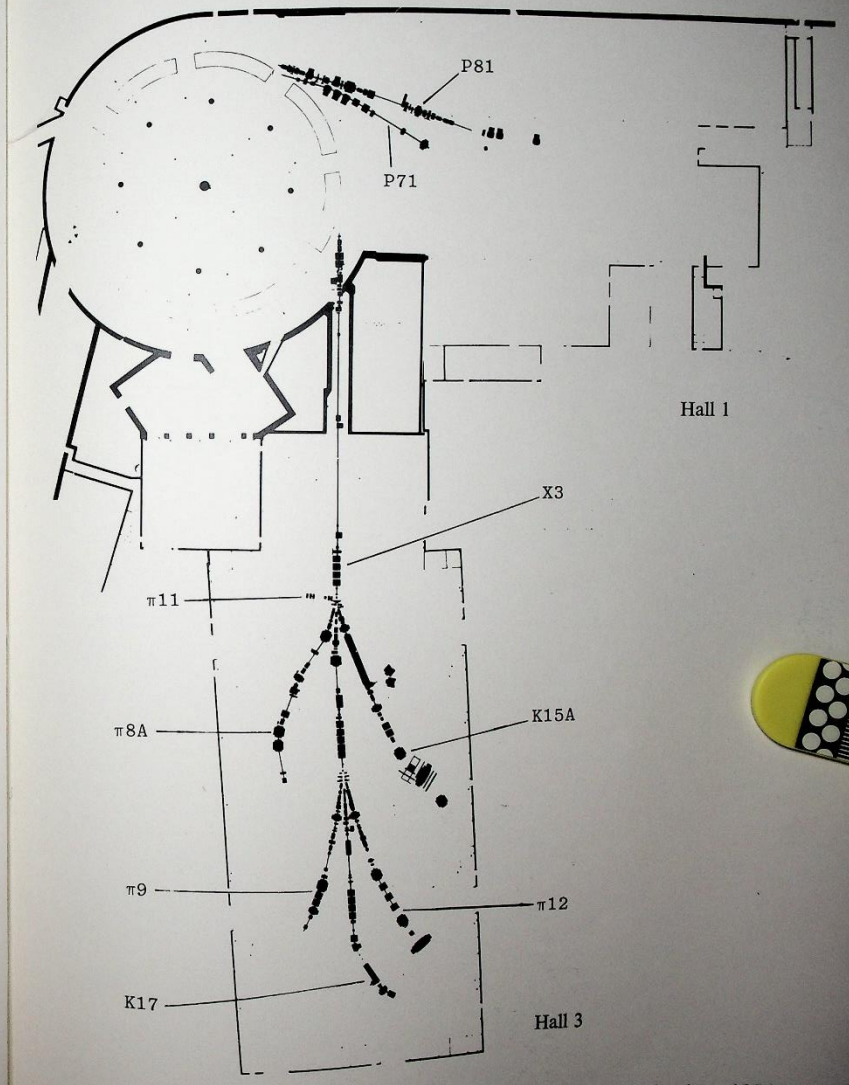

Beam lines in the experimental halls at Nimrod during 1974